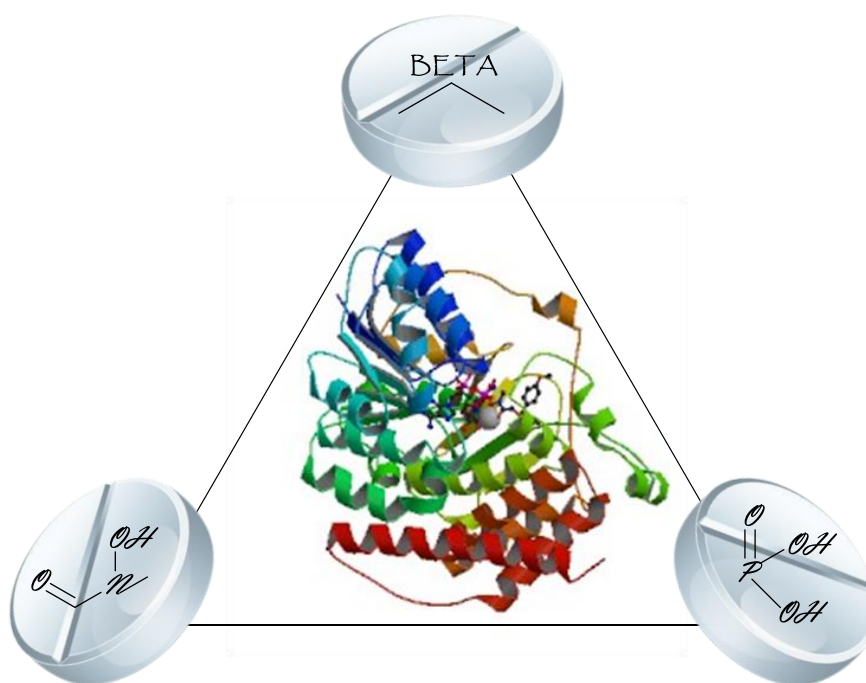


Synthesis and Evaluation of 1-Deoxy-D-xylulose 5-phosphate reductoisomerase Inhibitors as Antimalarial and Antituberculosis Agents



René Chofor

Promoter: Prof. dr. apr. S. Van Calenbergh

Academic year 2015 – 2016

Synthesis and Evaluation of 1-Deoxy-D-xylulose 5-phosphate reductoisomerase Inhibitors as Antimalarial and Antituberculosis Agents

René Chofor

Thesis submitted to the Faculty of Pharmaceutical Sciences in fulfilment of the
requirements for the degree of Doctor in Pharmaceutical Sciences

Promoter: Prof. dr. apr. S. Van Calenbergh

Academic year 2015 – 2016

TABLE OF CONTENTS

	Page
Summary	v
Overview of synthesized compounds	xv
List of abbreviations and notations	xvi
CHAPTER	
I. INTRODUCTION	1
I.A. Malaria	1
I.A.1. Epidemiology	1
I.A.2. Biology of <i>Plasmodium</i>	2
I.A.3. Current malaria management options	4
I.A.4. The necessity for new antimalarials	10
I.B. Tuberculosis	13
I.B.1. Pathogenesis, diagnosis and treatment	13
I.C. Isoprenoid biosynthesis as a drug target	16
I.C.1. Target-based drug design	18
I.C.2. The mevalonate versus the non-mevalonate pathway for isoprenoid biosynthesis	19
I.C.3. The non-mevalonate pathway in <i>P. falciparum</i> and <i>M. tuberculosis</i> as a drug target	22
I.C.4. 1-Deoxy-D-xylulose-5-phosphate reductoisomerase	23
I.D. Fosmidomycin	26
I.D.1. Discovery, antibacterial and antiplasmodial activity	26
I.D.2. Binding mode and kinetics of Dxr inhibition	27
I.E. Fosmidomycin as a lead in drug design	29
I.E.1. Modifications of the retrohydroxamate moiety	32
I.E.2. Modifications of the propyl spacer	39
I.E.3. Modifications of the phosphonate functionality	48
I.E.4. Overview of fosmidomycin SAR and conclusions	53

REFERENCES	56
II. SCOPE AND STRATEGIES	81
III. HYDROXAMATE-MODIFIED ANALOGUES OF FOSMIDOMYCIN	89
III.A. Introduction	89
III.B. Synthesis	90
III.C. Biological evaluation	91
III.D. Conclusions	93
III.E. Experimental details	93
REFERENCES	105
IV. GENERAL CONSIDERATIONS ON PHOSPHONATE CHEMISTRY	109
IV.A. Formation of the C-P bond in phosphonates	109
IV.A.1. The Michaelis-Arbusov reaction	109
IV.A.2. Phosphonylation by Michael addition	110
IV.B. Phosphonate deprotection strategies	111
REFERENCES	113
V. BETA-SUBSTITUTED ANALOGUES OF FOSMIDOMYCIN	117
V.A. Introduction	117
V.B. β -(Alkyl)aryl analogues	117
V.B.1. Synthesis	118
V.B.2. Biological evaluation	122
V.B.3. X-ray structures of PfDxr in complex with four inhibitors	125
V.B.4. Molecular modeling on MtbDxr	129
V.B.5. Conclusions	131
V.B.6. Experimental details	133
V.C. β -Arylpropyl- analogues of fosmidomycin	148
V.C.1. Synthesis	149
V.C.2. Biological evaluation	150
V.C.3. X-ray structures of PfDxr in complex with seven inhibitors	151
V.C.4. Conclusions	155

V.C.5. Experimental details	156
REFERENCES	171
VI. PHOSPHORAMIDE ANALOGUES OF FOSMIDOMYCIN	177
VI.A. Introduction	177
VI.B. Synthesis	178
VI.C. Conclusions	180
VI.D. Experimental details	181
REFERENCES	186
VII. CYCLIC PHOSPHONATE PRODRUGS OF FR900098.....	191
VII.A. Introduction	191
VII.B. Synthesis	193
VII.C. Conclusions	197
VII.D. Experimental details	197
REFERENCES	204
VIII. BROADER INTERNATIONAL CONTEXT, RELEVANCE AND FUTURE PERSPECTIVES.....	209
VIII.A. Global socio-economic impact of malaria	209
VIII.B. The global burden of tuberculosis	210
VIII.C. The potential for Dxr inhibitors to contribute to the global antimalarial and/or antituberculosis armamentarium	212
VIII.C.1. Desired qualities for new antimalarial drugs	212
VIII.C.2. Desired characteristics of new antituberculosis drugs	217
VIII.D. Future perspectives	218
VIII.E. The broader malaria prevention outlook: Vector control	220
REFERENCES	222

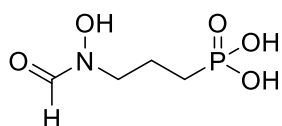
APPENDIX

Curriculum vitae

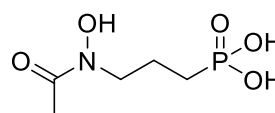
Acknowledgements

SUMMARY

Against the backdrop of an increasing need for new drugs to fight both malaria and tuberculosis, the enzyme 1-deoxy-D-xylulose-5-phosphate reductoisomerase (Dxr), which is involved in the non-mevalonate pathway for isoprenoid biosynthesis, has emerged as a promising drug target. In apicomplexan parasites (including *Plasmodium species*), most Gram-negative and some Gram-positive bacteria (including *Mycobacterium tuberculosis*), Dxr catalyses the first committed step of isoprenoid synthesis via the non-mevalonate pathway, which is absent in humans. Inhibitors of Dxr can therefore be anticipated to display activity against a variety of bacterial and protozoan pathogens. Fosmidomycin (**1.1**) and its methyl homologue FR900098 (**1.2**), both natural antibiotics extracted from *Streptomyces* in the 1970s, are established inhibitors of Dxr. Despite its remarkable human safety record and promising clinical antimalarial performance, fosmidomycin unfortunately, does not meet all the requirements for new antimalarial and/or antituberculosis drugs, by reason of its unfavorable pharmacokinetic profile.



Fosmidomycin (**1.1**)

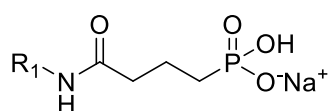


FR900098 (**1.2**)

Fosmidomycin is structurally characterized by a retrohydroxamic acid group (which chelates the bivalent metal ion Dxr depends on), a phosphonate group (which mimics the phosphate in DOXP, the natural substrate of Dxr) and a propyl spacer linking these moieties. The work covered in this thesis constitutes part of an extensive effort to increase our understanding of the structure-activity relationship of fosmidomycin analogues as Dxr inhibitors, and to develop new antimalarial and/or antituberculosis agents based on the fosmidomycin or FR900098 scaffold. Taking into account reported structural modifications and the prevailing SAR (covered in Chapter I), this thesis describes our efforts to introduce modifications at three different parts of this lead: the retrohydroxamic acid group, the phosphonate group and the propyl linker. Synthetic routes to these analogues were elaborated and the products were tested for their ability to inhibit Dxr (our primary attention was focused to PfDxr, but

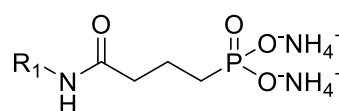
isozymes from other species were also considered), *M. smegmatis* growth and the proliferation of a *P. falciparum*-K1 Strain.

Chapter III is dedicated to our attempts to replace the hydroxamate group of fosmidomycin with alternative bidentate ligands. Although the chelating ability of hydroxamates often makes them potent metalloenzyme inhibitors, most hydroxamic acids suffer from poor oral bioavailability and significant binding to other metals (e.g., Zn^{2+} , Cu^{2+} , etc.) besides Mn^{2+} and Mg^{2+} . In addition, hydroxamic acids may be rapidly degraded *in vivo* by hydrolysis, glucuronidation and sulfation and may suffer from poor pharmacokinetic and toxicological profiles. Surprisingly, the prepared compounds (**3.1a-i**, **m-q**) were essentially inferior in activity when compared to the lead compound. This outcome reinforces the view that an intact hydroxamate or retrohydroxamate group is imperative for ligating the divalent metal in Dxr.



3.1a-i, m-p

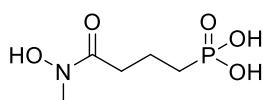
- a:** Ph
- b:** (2-Me)Ph
- c:** (2,6-diMe)Ph
- d:** (2-MeO)Ph
- e:** (2,6-diMeO)Ph
- f:** (2-F)Ph
- g:** (2-Ac)Ph



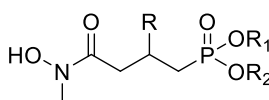
3.1q

- h:** (2-MeSO₂)Ph
- i:** (2-NMe₂)Ph
- m:** SO₂CH₃
- n:** (2-COOH)Ph
- o:** (2-OH)Ph
- p:** (2,6-diOH)Ph
- q:** (2-CN)Ph

Chapter V describes our efforts to perform the first systematic exploration of substituents, introduced at the β -position of the propyl backbone of **1.6** (the equipotent hydroxamate analogue of FR900098).



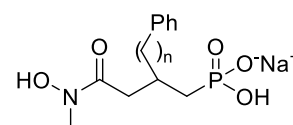
1.6



5.1a-c, f

- a:** R = Ph
- b:** R = (4-Me)Ph
- c:** R = (4-MeO)Ph
- d:** R = (4-Cl)Ph
- e:** R = (3,4-diCl)Ph
- f:** R = Me

$R_1/R_2 = H/Na^+$ for **5.1a-c, f**; $R_1 = R_2 = NH_4^+$ for **5.1d, e**

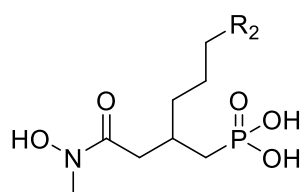


5.2a-d

- a:** n = 1
- b:** n = 2
- c:** n = 3
- d:** n = 4

While direct introduction of aromatic rings at the β -carbon (a modification earlier found promising when performed at the α -position) afforded moderate PfDxr inhibitors and poor EcDxr and MtbDxr inhibitors, introduction of a propyl linker between the β -carbon and the phenyl ring resulted in optimal *E. coli* and *M. tuberculosis* Dxr inhibition. Both a phenylpropyl (**5.2c**) and a phenylbutyl (**5.2d**) substituent afforded potent PfDxr inhibition. Crystallographic studies of the complexes of PfDxr with **5.1a**, **5.1b**, **5.2c** and **5.2d** (section V.B.3.) showed two different, novel modes of binding to PfDxr. The compounds showing the best enzyme inhibition (and best *in vitro* activity against the parasite, i.e., **5.2c** and **5.2d**) mimic the favorable interactions between the indole ring of the conserved tryptophan in the flap with the fosmidomycin backbone that have been seen in a number of antibiotic-bound ternary complexes. However, this mimicry is achieved by intramolecular interactions within each inhibitor (**5.2c** and **5.2d**), such that the phenyl ring common to this series spatially overlaps the usual position of the indole ring. Rearrangement of the flap results in favorable interactions between the phenyl ring of the inhibitors and the tryptophan.

In a follow-up study aiming at exploring the influence of lipophilicity, electronic and steric properties of the phenylpropyl side chain of **5.2c**, we prepared compounds **5.24**. Evaluation of these derivatives indicated that it is not trivial to increase the affinity for PfDxr by subtle modifications of the phenyl ring anticipated to occupy the aromatic 'hotspot'.

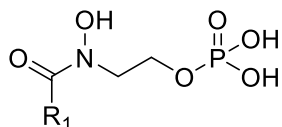


- | | |
|--------------------------------------|---|
| a: R ₂ = (4-Me)Ph | f: R ₂ = (3-F)Ph |
| b: R ₂ = (3-Me)Ph | g: R ₂ = (4-CF ₃)Ph |
| c: R ₂ = (4-MeO)Ph | h: R ₂ = 1-naphthyl |
| d: R ₂ = (3-MeO)Ph | i: R ₂ = 2-naphthyl |
| e: R ₂ = (4-F)Ph | j: R ₂ = biphenyl |

5.24

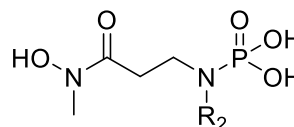
In Chapter VI, we tried to increase the acidity of the phosphonic acid group by incorporating a nitrogen atom into the α -position of the three-carbon chain of compound **1.6**. The introduction of electron withdrawing aryl or halogen substituents in α -position of the phosphonate group of fosmidomycin is known to increase the acidity of the phosphonic acid group, thereby leading to a stronger interaction with the phosphate binding site of Dxr. With the anticipation that amide derivatives of phosphoric acid (**6.1**) are chemically and

metabolically more stable than the corresponding esters (e.g., **1.35** and **1.36**, highly potent but metabolically unstable Dxr inhibitors), attempts to prepare the phosphoramides stalled due to the surprisingly high lability of the target compounds under synthesis conditions.



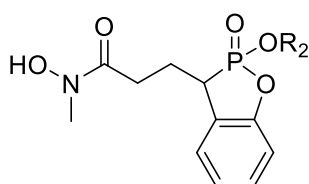
1.35: R₁ = H

1.36: R₁ = CH₃



6.1: R₂ = H, alkyl, aryl, alkylaryl...

The development of a cyclic prodrug scaffold (**7.7**), which would temporarily lock one of the phosphonate O in a cycle with an α substituent as a way of improving the oral bioavailability of analogues while reducing toxicity from *in vivo* activation, was attempted in Chapter VII. Unfortunately, high sensitivity of the formed ring to hydrolysis during synthetic manipulation of other groups in the intermediates, blocked access to the desired targets.



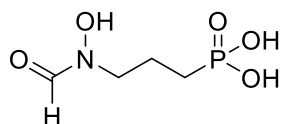
7.7 R₂ = H, acyloxy, alkoxy carbonyl, alkyl, aryl, alkylaryl...

Finally, in Chapter VIII, a critical reflection is made on the broader international context of this thesis, the relevance and future perspectives.

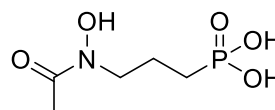
Overall, during this doctoral study, new analogues of fosmidomycin/FR900098 were prepared, which add girth on the current SAR of Dxr inhibition. Specifically, the data on the β -substituted analogues improve our knowledge of the behavior or interactions of the conserved tryptophan residue in the Dxr active site. This serves as a clarion call for further exploration of substituents on the propyl spacer, as this has thus far yielded the most promising Dxr inhibitors.

SAMENVATTING

In het kader van een toenemende behoefte aan nieuwe geneesmiddelen voor de bestrijding van zowel malaria als tuberculose, geldt 1-deoxy-D-xylulose-5-phosphate reductoisomerase (Dxr), een enzyme betrokken in de non-mevalonaatweg voor de biosynthese van isoprenoïden, als een veelbelovende drug target. In apicomplexe parasieten (waaronder *Plasmodia*), de meeste Gram-negatieve en enkele Gram-positieve bacteriën (waaronder *Mycobacterium tuberculosis*), katalyseert Dxr de eerste differentiërende stap van de isoprenoïdsynthese via de, in de mens afwezige, non-mevalonaatweg. Het ligt derhalve in de lijn der verwachting verwacht dat inhibitoren van Dxr activiteit vertonen tegen verschillende bacteriële en protozoïsche pathogenen. Van de natuurlijke antibiotica fosmidomycine (**1.1**) en het methylhomoloog FR900098 (**1.2**), welke omstreeks 1970 voor het eerst werden geïsoleerd uit *Streptomyces*, is vastgesteld dat het inhibitoren van Dxr zijn. Ondanks een uitstekend humaan veiligheidsprofiel en veelbelovende klinische anti-malaria eigenschappen, voldoet fosmidomycine helaas niet aan alle eisen voor nieuwe anti-malaria en/of antituberculose geneesmiddelen, als gevolg van een ongunstig farmacokinetisch profiel.



Fosmidomycin (**1.1**)



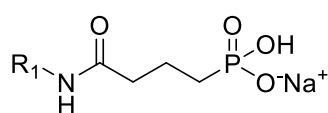
FR900098 (**1.2**)

De structuur van fosmidomycine wordt gekenmerkt door een retrohydroxamaat-groep (de werking van Dxr is afhankelijk van de chelatie van tweewaardige metaalionen), een fosfonaatfunctie (welke de fosfaatgroep van DOXP, het natuurlijke substraat van Dxr, nabootst) en een propyleenlinker welke deze twee functionaliteiten verbindt. Het werk beschreven in dit proefschrift maakt deel uit van een uitgebreide studie naar de structuur-activiteitsrelatie van fosmidomycine analogen als Dxr inhibitoren en om nieuwe anti-malaria- en/of anti-tuberculosemiddelen op basis van het fosmidomycine of FR900098 skelet te ontwikkelen. De reeds gepubliceerde structurele aanpassingen en de heersende SAR (uiteengezet in hoofdstuk I) in ogenschouw nemend, beschrijft dit proefschrift onze inspanningen om variaties aan te brengen in de drie verschillende delen van dit molecuul: de

(retro)hydroxamaatgroep, de fosfaatgroep en de propyleenlinker. De syntheserouten naar deze analogen werden uitgewerkt en de producten werden niet alleen getest op hun vermogen om Dxr te remmen (onze aandacht ging hierbij in de eerste plaats uit naar PfDxr, maar isozymen uit andere organismen werden later ook beschouwd) maar ook om de groei van *M. smegmatis* alsook de verspreiding van een *P. falciparum*-K1 stam te onderdrukken.

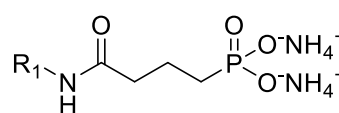
Hoofdstuk III beschrijft onze pogingen om de hydroxamaatfunctie van fosmidomycine door alternatieve bidentate liganden te vervangen. Hoewel het sterke chelerende vermogen van hydroxamaten vaak resulteert in potente metallo-enzym-inhibitoren vertonen de meeste hydroxamaten een slechte orale biologische beschikbaarheid en een niet te verwaarlozen binding aan andere metalen (zoals Zn^{2+} , Cu^{2+} , etc.) naast Mn^{2+} en Mg^{2+} .

Bovendien kunnen hydroxamaten *in vivo* snel worden afgebroken door hydrolyse, glucuronidatie en sulfatatie en worden ze vaak in verband gebracht met een slechte farmacokinetisch en toxicologisch profiel. Helaas vertoonden de gesynthetiseerde verbindingen (**3.1a-i**, **m-q**) een inferieure activiteit vergeleken met de lead verbinding. Dit resultaat onderstreept de visie, dat een intacte hydroxamaat- of retrohydroxamaatfunctionaliteit cruciaal is voor het binden van het tweewaardige metaalion in Dxr.



3.1a-i, m-p

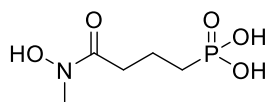
- a:** Ph
- b:** (2-Me)Ph
- c:** (2,6-diMe)Ph
- d:** (2-MeO)Ph
- e:** (2,6-diMeO)Ph
- f:** (2-F)Ph
- g:** (2-Ac)Ph



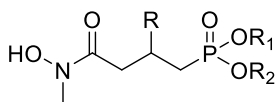
3.1q

- h:** (2-MeSO₂)Ph
- i:** (2-NMe₂)Ph
- m:** SO₂CH₃
- n:** (2-COOH)Ph
- o:** (2-OH)Ph
- p:** (2,6-diOH)Ph
- q:** (2-CN)Ph

Hoofdstuk V beschrijft onze inspanningen in het kader van het eerste systematische onderzoek naar de invoering van substituenten op de β -positie van de propyleenlinker van **1.6** (het equipotente hydroxamaat analogoog van FR900098).



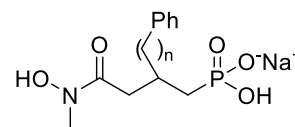
1.6



5.1a-c, f

- a: R = Ph
- b: R = (4-Me)Ph
- c: R = (4-MeO)Ph
- d: R = (4-Cl)Ph
- e: R = (3,4-diCl)Ph
- f: R = Me

$R_1/R_2 = H/Na^+$ for **5.1a-c, f**; $R_1 = R_2 = NH_4^+$ for **5.1d, e**

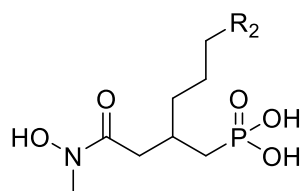


5.2a-d

- a: n = 1
- b: n = 2
- c: n = 3
- d: n = 4

Terwijl de directe invoering van arylgroepen op het β -koolstofatoom (een modificatie die uit eerdere studies succesvol bleek te zijn indien uitgevoerd op de α -positie) slechts aanleiding gaf tot matige PfDxr en slechte EcDxr en MtbDxr inhibitoren, bleek de invoering van een propyleenlinker tussen het β -koolstofatoom en de arylgroep te resulteren in een optimale *E. coli* en *M. tuberculosis* Dxr remming. Zowel een fenylpropyl (**5.2c**) als een fenylbutyl (**5.2d**) substituent resulteerde in sterke PfDxr inhibitie. Kristallografische studies van de complexen van PfDxr met **5.1a**, **5.1b**, **5.2c** en **5.2d** (sectie V.B.3.) brachten twee verschillende bindingswijzen met PfDxr aan het licht. De analogen met de beste enzyminhibitie (en de beste *in vitro* activiteit tegen de parasiet, te weten **5.2c** en **5.2d**) bootsen de gunstige interactie tussen het fosmidomycineskelet en de indoolring van het geconserveerde tryptofaan uit de lus na, die reeds eerder werden waargenomen in een aantal ternaire complexen waarin het antibioticum gebonden is. Intramoleculaire interacties binnen de remmers (**5.2c** en **5.2d**) zorgt ervoor dat de fenylring de positie bezet die normaal ingenomen wordt door de indoolring van het eerder vermelde tryptofaanresidu. Heroriëntatie van de lus resulteert in gunstige interacties tussen de fenylring van de remmers en tryptofaan.

In het kader van een vervolgstudie waarbij het effect van het variëren van het lipofiele, elektronische en sterische karakter van de fenylpropyl zijketen uit **5.2c** werd onderzocht, werden de analogen **5.24** gesynthetiseerd. Het bleek echter niet triviaal om de affiniteit voor PfDxr te verhogen door middel van subtiele veranderingen van de fenylring die een aromatische 'hotspot' bezet.

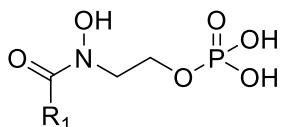


- a:** R₂ = (4-Me)Ph **f:** R₂ = (3-F)Ph
b: R₂ = (3-Me)Ph **g:** R₂ = (4-CF₃)Ph
c: R₂ = (4-MeO)Ph **h:** R₂ = 1-naphthyl
d: R₂ = (3-MeO)Ph **i:** R₂ = 2-naphthyl
e: R₂ = (4-F)Ph **j:** R₂ = biphenyl

5.24

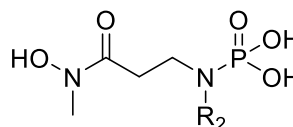
Hoofdstuk VI beschrijft onze pogingen om de pKa van de fosfonzuurgroep te verlagen door de introductie van een stikstofatoom op de α -positie van de drie-koolstof-keten van verbinding **1.6**. Het is bekend dat de invoering van elektronenzuigende aryl- of halogeensubstituenten op de α -positie van de fosfonaatgroep in fosmidomycine resulteren in een verlaging van de pKa deze fosfonzuurgroep, wat op zijn beurt weer leidt tot een sterkere interactie met de fosfaatbindingsplaats van Dxr.

Hoewel vooraf de verwachting heerste dat amidederivaten van fosforzuur (**6.1**) chemisch en metabool stabiel zouden zijn dan de overeenkomstige esters (fosfaatesters **1.35** en **1.36**, zijn zeer potente maar metabool instabiele Dxr remmers), bleek de verrassend hoge labiliteit van de doelverbindingen onder de syntheseomstandigheden fnuikend voor de voortgang van dit deelproject.



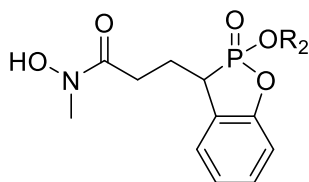
1.35: R₁ = H

1.36: R₁ = CH₃



6.1: R₂ = H, alkyl, aryl, alkylaryl...

De ontwikkeling van een cyclisch prodrug motief (**7.7**), waarbij tijdelijk één van de fosfonaatzuurstoffen in een ring met een α -substituent wordt vastgezet, staat beschreven in hoofdstuk VII. Deze modificatie beoogde zowel de verhoging van de orale biologische beschikbaarheid als het reduceren van de toxiciteit ten gevolge van bioactivatie. Als gevolg van de hoge hydrolysegevoeligheid van de gevormde ring tijdens de nodige manipulaties van de overige functionele groepen tijdens de synthese, bleken, jammer genoeg, de geplande doelmoleculen niet haalbaar.

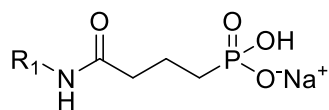


7.7 $R_2 = \text{H, acyloxy, alkoxy, carbonyl, alkyl, aryl, alkylaryl...}$

In Hoofdstuk VIII wordt een kritische beschouwing gegeven waarbij wordt ingegaan op de bredere internationale context van dit proefschrift, de wetenschappelijke relevantie en de toekomstperspectieven.

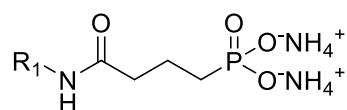
Globaal beschouwd, werden tijdens dit doctoraatstraject nieuwe analogen van fosmidomycine/FR900098 ontwikkeld, die de huidige SAR-kennis van Dxr inhibitie verder uitdiepen. De gegevens verkregen met de β -gesubstitueerde analogen dragen, in het bijzonder, bij aan onze kennis over het gedrag en de interacties van het geconserveerde tryptofaanresidu in het actieve centrum van Dxr. Dit rechtvaardigt een roep om verder onderzoek naar analogen met substituenten op de propyleenlinker aangezien deze strategie tot nu toe de meest veelbelovende Dxr inhibitoren opleverde.

OVERVIEW OF SYNTHESIZED COMPOUNDS



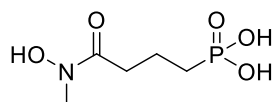
3.1a-i, m-p

a: Ph
b: (2-Me)Ph
c: (2,6-diMe)Ph
d: (2-MeO)Ph
e: (2,6-diMeO)Ph
f: (2-F)Ph
g: (2-Ac)Ph

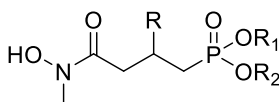


3.1q

h: (2-MeSO₂)Ph
i: (2-NMe₂)Ph
m: SO₂CH₃
n: (2-COOH)Ph
o: (2-OH)Ph
p: (2,6-diOH)Ph
q: (2-CN)Ph



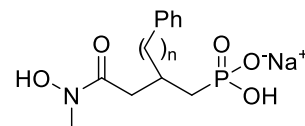
1.6



5.1a-c, f

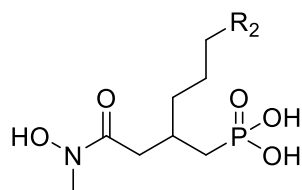
a: R = Ph
b: R = (4-Me)Ph
c: R = (4-MeO)Ph
d: R = (4-Cl)Ph
e: R = (3,4-diCl)Ph
f: R = Me

$R_1/R_2 = \text{H}/\text{Na}^+$ for **5.1a-c, f**; $R_1 = R_2 = \text{NH}_4^+$ for **5.1d, e**



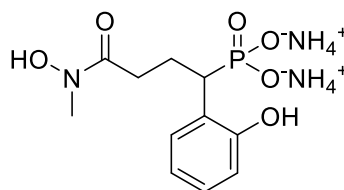
5.2a-d

a: n = 1
b: n = 2
c: n = 3
d: n = 4



5.24

a: R₂ = (4-Me)Ph **f:** R₂ = (3-F)Ph
b: R₂ = (3-Me)Ph **g:** R₂ = (4-CF₃)Ph
c: R₂ = (4-MeO)Ph **h:** R₂ = naphthalen-1-yl
d: R₂ = (3-MeO)Ph **i:** R₂ = naphthalen-2-yl
e: R₂ = (4-F)Ph **j:** R₂ = biphenyl



7.8

LIST OF ABBREVIATIONS AND NOTATIONS

ACT	Artemisinin-based Combination Therapy
ADME	Absorption, Distribution, Metabolism, and Excretion
Ar	Aryl
BAIB	(Diacetoxyiodo)benzene
BCG	Bacille Calmette-Guérin
Bn	Benzyl
Boc	<i>tert</i> -Butoxycarbonyl
br	Broad
BSTFA	<i>N,O</i> -Bis(trimethylsilyl)trifluoroacetamide
CoA	Coenzyme A
d	Doublet
DIPEA	<i>N,N</i> -Diisopropylethylamine
DMAP	4-(Dimethylamino)-pyridine
DMAPP	Dimethylallyl Diphosphate
DNA	Deoxyribonucleic Acid
DOXP	1-Deoxy-D-xylulose-5-phosphate
Dxr	1-Deoxy-D-xylulose-5-phosphate reductoisomerase
FV	Food Vacuole
EcDxr	<i>Escherichia coli</i> 1-deoxy-D-xylulose-5-phosphate reductoisomerase
EC ₅₀	Half Maximal Effective Concentration
EDC.HCl	<i>N</i> -(3-Dimethylaminopropyl)- <i>N'</i> -ethylcarbodiimide hydrochloride
EMB	Ethambutol
Equiv.	Equivalence
<i>et al.</i>	Et Alii (and others)
Et ₃ N	Triethylamine
GlpT	Glycerol-3-phosphate Transporter
GPCRs	G protein-coupled receptors
GSK	GlaxoSmithKline
h	Hour

HIV	Immunodeficiency Virus
(HP)LC	High Pressure/Performance Liquid Chromatography
HTS	High-throughput screening
Hz	Hertz
IC ₅₀	50% Inhibitory Concentration
IFN- γ	Interferon-gamma
INH	Isoniazid
ip	Intraperitoneal
IPP	Isopentenyl Diphosphate
IPTp	Intermittent preventive treatment in pregnancy
m	Multiplet
Mtb	<i>Mycobacterium tuberculosis</i>
MDR	Multidrug-resistant
MEP	2-C-methyl-D-erythritol-4-phosphate
Min	Minute
MOM	Methoxy methyl
MS	Mass Spectrometry
MVA	Mevalonic acid
NADPH	Nicotinamide Adenine Dinucleotide Phosphate (reduced form)
nd	not determined
NCS	<i>N</i> -chlorosuccimimide
NMP	Non-mevalonate Pathway
NMR	Nuclear Magnetic Resonance Spectroscopy
PAS	Para-aminosalicylic Acid
PCR	Polymerase Chain Reaction
PDB	Protein Data Bank
PfDxr	<i>Plasmodium falciparum</i> 1-deoxy-D-xylulose-5-phosphate reducto- isomerase
PfEMP1	<i>P. falciparum</i> Erythrocyte Membrane Protein 1
POM	Pivaloyloxymethyl
ppm	Parts Per Million

PZA	Pyrazinamide
quant.	Quantitative
RBCs	Red Blood Cells
RIF	Rifampicin
RNA	Ribonucleic Acid
rt	Room temperature
s	Singlet
SAR	Structure Activity Relationship
SM	Streptomycin
TB	Tuberculosis
TEMPO	2,2,6,6-Tetramethyl-1-piperidinyloxy, free radical
TFA	Trifluoroacetic Acid
THF	Tetrahydrofuran
TLC	Thin Layer Chromatography
TMSBr	Bromotrimethylsilane
TNF- α	Tumor-necrosis Factor-alpha
WHO	World Health Organization
δ	Chemical Shift

Chapter I

INTRODUCTION

I. INTRODUCTION

I.A. Malaria

I.A.1. Epidemiology

Malaria, a preventable and treatable disease, is caused by protozoan parasites of the genus *Plasmodium*. Four *Plasmodium* species are traditionally responsible for malaria in humans:

Plasmodium falciparum, which causes malaria tropica;

Plasmodium malariae, which causes malaria tertiana;

Plasmodium ovale, which causes malaria quartana; and

Plasmodium vivax; which causes malaria tertiana.

Recently, some human cases of malaria have been reported with *Plasmodium knowlesi*, a species that is morphologically similar to *P. malariae* and causes malaria in primates in certain forested parts of South-East Asia where its vector thrives.^{1,2} *P. falciparum* and *P. vivax* are the two species of greatest economic importance since the former is the most virulent (accounting for the majority of all clinical cases), while the latter has the ability to form a dormant liver stage (hypnozoites) in infected patients, which may lead to relapse of clinical malaria symptoms months or even years after initial infection. Additionally, *P. falciparum* and *P. vivax* have the shortest development cycles and are therefore more common than other *Plasmodium* species. *P. vivax* is geographically the most widespread and the most common species observed in the temperate regions of the world, due to its ability to mature in mosquitoes within a broad temperature range.^{3,4} Because malaria transmission rates are low in most regions where *P. vivax* is prevalent, the human populations affected achieve little immunity to this parasite; as a result, in these regions, *P. vivax* infections affect people of all ages. Mixed infections of *P. falciparum* and *P. vivax* are rarely reported, but polymerase chain reaction (PCR) detection methods have shown that these can be as high as 30% of all *Plasmodium* infections.⁵

The epidemiology of malaria is complex and may vary considerably even within relatively small geographical regions. The disease is most prevalent in the tropical and sub-tropical regions. In many malaria-endemic zones (parts of Asia, Africa, Central and South America, Oceania, and certain Caribbean Islands) occurrence depends on the following factors: the availability of competent vectors, parasite development, vector biting habits (anthropophilic or zoophilic), and the behavior of infected people. The vector for malaria is the female *Anopheles* mosquito; *A. gambiae* and *A. funetus* being the most effective and efficient vector species.⁶ The highest transmission is in sub-Saharan Africa and in parts of Oceania such as Papua New Guinea, where nearly all infections are caused by the dreaded *P. falciparum*. Massive eradication campaigns led to elimination of malaria in temperate areas such as Europe and the United States but the presence of the anopheles mosquitoes that can transmit malaria in some of these areas presents a re-introduction threat.⁷

I.A.2. Biology of *Plasmodium*

Plasmodium species belong to the phylum *Apicomplexa*: parasitic protists, which harbor a plastid-like organelle called apicoplast and a unique apical secretory structure, mediating locomotion and host cell invasion. All species are obligate endoparasites. These unicellular eukaryotes obtain nutrients from the cells of their hosts; meanwhile, eluding the immune response in these cells. The *Apicomplexa* have complex life cycles that are characterized by three distinct processes: sporogony, merogony and gametogony. The natural ecology of human malaria involves *Plasmodium* species infecting successively two types of hosts: humans where the parasite multiplies asexually and female *Anopheles* mosquitoes, where its sexual reproductive cycle occurs.

Malaria is transmitted through the bite of an infected female *Anopheles* mosquito by which inoculation of plasmodial sporozoites into the human host takes place (Figure I.1). The sporozoites infect liver cells and mature into schizonts, which rupture to release merozoites into the bloodstream (merogony). In case of *P. vivax* and *P. ovale*, some sporozoites turn into the aforementioned hypnozoites that persist in the liver. The liberated merozoites access and multiply asexually (within 48 to 72 hours) in erythrocytes. Some merozoites differentiate into male and female gametocytes (gametogony), which are ingested by a female *Anopheles* mosquito during a blood meal, marking the onset of the sporogonic (sexual) cycle. This culminates in the release of sporozoites, which migrate to the mosquitoes salivary glands for

inoculation into a new human host. Fever paroxysms, the hallmark of malaria, and other clinical manifestations occur when infected red blood cells (RBCs) rupture and release parasite-derived molecules that stimulate the production of pro-inflammatory cytokines by the host.

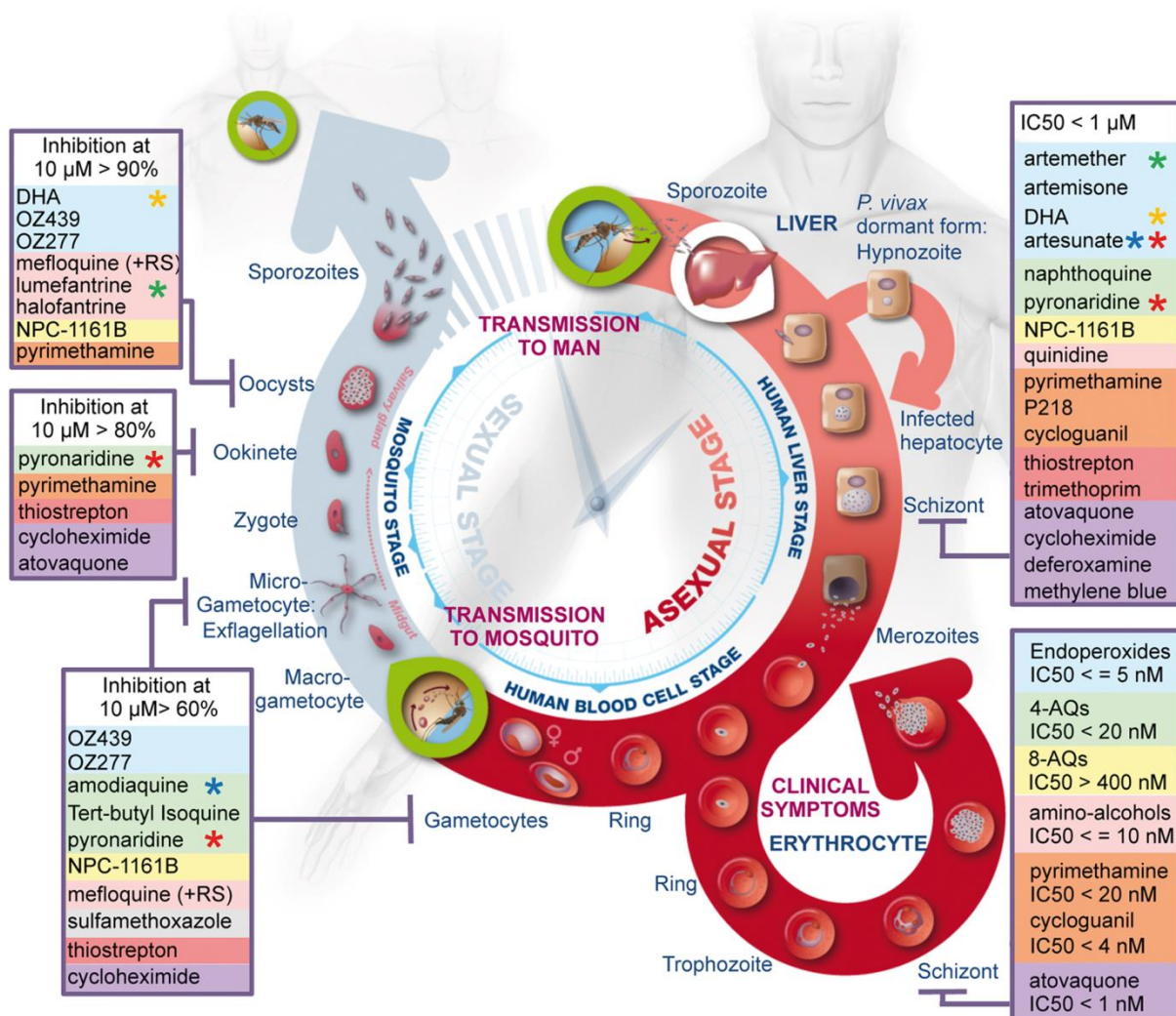


Figure I.1: The life cycle of *Plasmodium* species depicting the point of action of various antimalarials.⁸

All *Plasmodium* species studied so far utilize antigenic variation on the surface of infected RBCs as a strategy to avoid antibody recognition.⁹ *P. falciparum* expresses the *var* genes, which encode proteins known as *P. falciparum* erythrocyte membrane protein 1 (PfEMP1), so-called because they are exported from the parasite and end up in the membrane of the infected RBC (Figure I.2). PfEMP1 is key to the lethality of *P. falciparum* infection, because the PfEMP1 molecules on the erythrocyte surface cause the cell to stick to capillary walls. In

this way, the infected cells are prevented from circulating through the spleen where they would be recognized by immune cells and removed from the circulation. By switching the *var* gene expressed, the parasite changes the PfEMP1 on the host-cell surface before the host immune system can mount a full response to it. Capillaries become clogged, resulting in the severe symptoms of tropical malaria.¹⁰

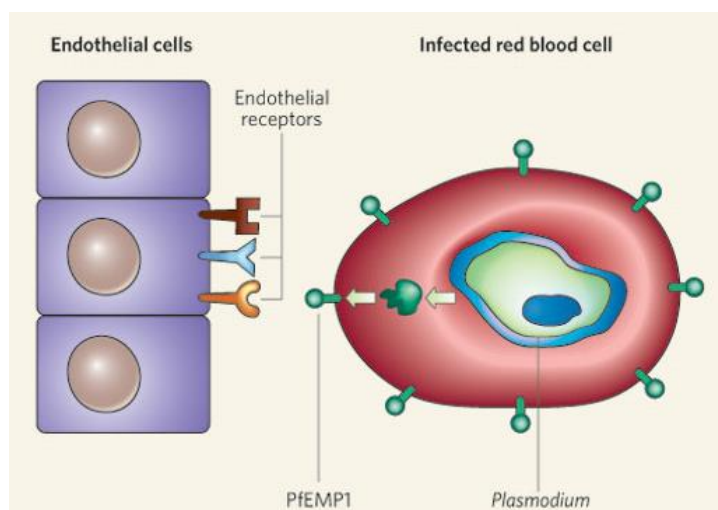


Figure I.2: A red blood cell infected with *Plasmodium falciparum*. The surface of the infected cell is studded with proteins of the PfEMP1 family, encoded by *var* genes. The various PfEMP1 molecules can bind to one of a series of receptors on the endothelial cells that line the capillary walls.¹⁰

Besides eluding the human immune response, as *P. falciparum* grows within its host erythrocyte it induces an increase in the permeability of the erythrocyte membrane to a range of low-molecular-mass solutes including Na^+ and K^+ .¹¹ This results in a Na^+ concentration gradient between the erythrocyte cytosol and the parasite cytosol, which causes a large inward movement of Na^+ across the parasite plasma membrane.¹² The parasite exploits the Na^+ electrochemical gradient to energize the uptake of inorganic phosphate (assisted by a Na^+ -dependent transporter), an essential nutrient for cell metabolism, which is also required for the synthesis of DNA, RNA and numerous phosphorylated metabolic intermediates.¹³

I.A.3. Current malaria management options

Clinical illness is caused by the intra-erythrocytic stage of the parasite but also, other stages assure the survival and mass dispersion of disease and are thus legitimate targets in malaria

eradication efforts (see Figure I.1). In addition to personal protective measures such as sleeping under insecticide-impregnated bed nets, use of insecticides against mosquitoes and the disruption of mosquito breeding grounds, continuous effort towards a viable treatment of infected persons is necessary. An ideal antimalarial drug should accomplish a radical treatment of infected persons within a short time frame, so that onwards transmission of the parasites is also interrupted.

I.A.3.1. Prevention of infection and/or clinical disease

Innate and acquired protective immunity both constitute the natural human arsenal for fighting malaria. Innate immunity consists of various traits of erythrocytes that discourage infection: The sickle-cell trait protects against the development of severe *P. falciparum* malaria.¹⁴ Furthermore, entry of merozoites into erythrocytes is believed to be mediated by a crucial RBC surface binding receptor, the Duffy glycoprotein. The Duffy-blood-group-negative genotype found predominantly in West-African and African-American populations, has long been known to confer complete resistance to *P. vivax* infection,¹⁵ although recent studies show that this immunity may be fading.^{16,17}

Adolescents and adults in malaria endemic regions are often clinically immune; they remain free of malaria symptoms despite maintaining low-grade infection throughout the transmission season, whereas children under 5 years of age suffer severe disease and risk death. Immunity may be essentially strain-specific and a long period is required to 'see' the local repertoire of strains.^{18,19} The principal features of naturally acquired immunity to *P. falciparum* are understood but little is known about the underlying mechanisms.²⁰ Clinical immunity is usually lost during pregnancy, especially among primigravid women, or after migration to areas where the disease is not endemic. Acquired immunity does not prevent re-infection but does reduce the severity of disease. Long-term prophylaxis by vaccination has been promoted but especially challenging since parasite devices such as the PfEMP1 (*P. falciparum*), assure avoidance of the host immune system. Currently, RTS,S/AS01 (Mosquirix), a vaccine developed by GlaxoSmithKline (GSK) and backed by the Bill & Melinda Gates Foundation, for children, is the most advanced vaccine candidate against *P. falciparum*. Results from phase III trial data released in April 2015, show that the vaccine prevented a substantial number of cases of clinical malaria over a 3-4 year period in young infants and children when administered with or without a booster dose.²¹ Efficacy was

enhanced by the administration of a booster dose in both age categories. An efficacy of 55% reduction in the frequency of malaria episodes during a 12 months follow-up had been reported for previous trials.^{22,23,24} This means that the vaccine has the potential to make a significant contribution to malaria control when used in combination with other effective control measures, especially in areas of high transmission. Very recently (July 24, 2015) the European Regulators (EMA) gave green light to this malaria vaccine candidate after assessing its safety and effectiveness and the WHO will consider recommending Mosquirix in the course of this year (2016).

I.A.3.2. Diagnosis and treatment

Malaria is most widely diagnosed by direct visualization of parasite intra-erythrocytic stages through light microscopy of thick and thin Giemsa-stained blood smears.²⁵ Alternative diagnostic methods include fluorescence microscopy of parasite nuclei stained with acridine orange, rapid dipstick immunoassays of various malaria antigens and polymerase chain reaction based assays.^{26,27} The most commonly used drugs for malaria treatment or chemoprophylaxis come from the following five compound classes:

Quinine and related compounds: Members of this group include quinine, chloroquine, amodiaquine, quinidine, mefloquine, halofantrine, primaquine, lumefantrine, piperaquine, pyronaridine (Figure I.3). The molecular basis of the action of these drugs is not completely understood, but they are thought to interfere with hemoglobin digestion by accumulating in the food vacuole (FV) of the plasmodium parasite during the erythrocytic stage of the life cycle.²⁸ In order to obtain essential nutrients, parasites digest haemoglobin within the FV, a process which generates toxic haem moieties as by-product. Chloroquine interrupts subsequent polymerization of haem to non-toxic haemozoin crystals by the parasite through the formation of drug-haemozoin complexes and/or binding of the drug to the growing face of the haemozoin crystals.²⁹ Other members of this group do not appear to be concentrated so extensively in the FV and may act on alternative targets in the parasite.

Antifolates: Folate synthesis is essential to the parasite as it is unable to scavenge pyrimidines from its host. Pyrimethamine, proguanil, chlorproguanil, trimethoprim and sulphadoxine affect the pre-erythrocytic and erythrocytic stages of the parasite's life cycle, by blocking of the folate biosynthetic pathway in the parasite. Combination drugs, such as

sulfadoxine + pyrimethamine, act through sequential and synergistic blockade of 2 key enzymes involved in folate biosynthesis. Pyrimethamine and related compounds inhibit dihydrofolate reductase, while sulfones and sulfonamides inhibit dihydropteroate synthase.^{30,31,32}

Artemisinin-type compounds: Artemisinins are among the most potent front-line antimalarial agents. Structural derivatives of artemisinin such as dihydroartemisinin, artemether, artesunate act rapidly throughout the phases of the asexual intra-erythrocytic cycle, and also act on young gametocytes.^{33,34} Due to the short plasma half-lives of artemisinin drugs, high rates of recrudescence infections are frequently reported when they are administered as mono-therapeutic agents. Recommended current practice is to combine an artemisinin drug with another effective long-acting anti-malarial partner (Artemisinin-based Combination Therapy, ACT). The mechanism of action of compounds in this group is incompletely understood, but the prevailing hypothesis is that the endo-peroxide bridge is essential for activity. Reductive cleavage of the endo-peroxide moiety through intra-parasitic interaction with ferrous iron (in the form of haem or Fe²⁺ salts) generates free-radical species, which alkylate various parasite membranes including the endoplasmic reticulum, mitochondrial and plasma membranes, leading to their destruction.^{35,36}

Hydroxynaphthaquinones: Atovaquone is used in a fixed combination with proguanil (Malarone™ GlaxoSmithKline) for malaria prophylaxis and clinical disease treatment. The drug is structurally similar to ubiquinone (also called coenzyme Q), which is an integral component of electron flow in aerobic respiration. The passage of electrons from ubiquinone to cytochrome bc1 (complex III) is inhibited by atovaquone.^{37,38} The collapse of the mitochondrial membrane potential has been associated with apoptosis.³⁹

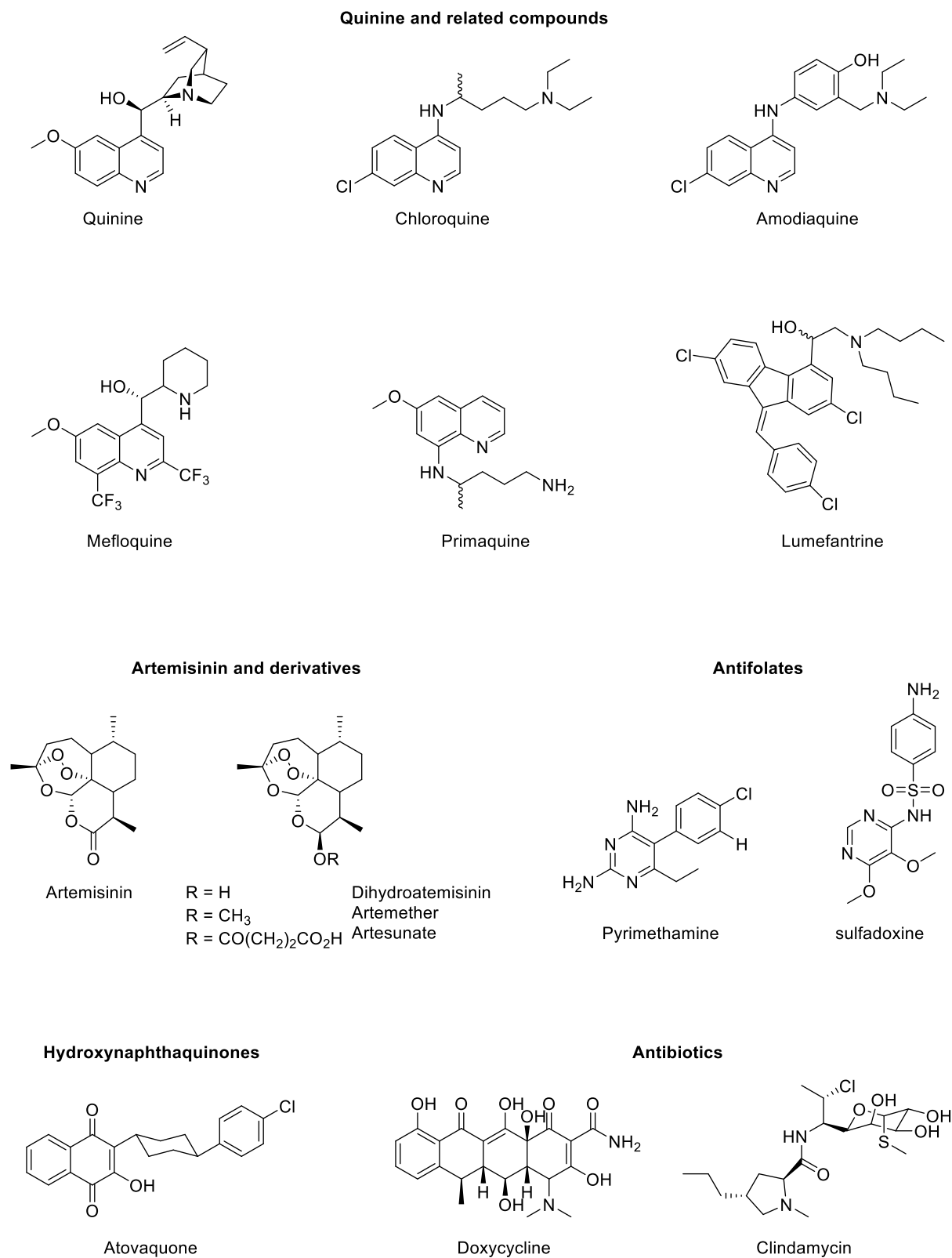


Figure I.3: Representative compounds from the five mainstream antimalarial drug classes.

Antibacterial drugs: Clindamycin, ciprofloxacin, azithromycin and doxycycline are antibiotics that also exert antimalarial activity. These drugs are weak and slow acting antimalarials and

should never be used in monotherapy to treat malaria. The anti-malarial activities of these compounds involve the inhibition of DNA replication and inhibition of protein synthesis inside the apicoplast of *Plasmodium species*.⁴⁰ Doxycycline is the most frequently used antibiotic for antimalarial therapy, either in combination with quinine, chloroquine, or as a prophylactic agent.^{41,42,43} Since doxycycline is contra-indicated in small children and pregnant women, clindamycin is a valuable alternative.⁴⁴

Currently, the WHO recommended first-line treatment for uncomplicated malaria caused by *P. falciparum* comprises the following combinations: artemether-lumefantrine (Coartem), amodiaquine-artesunate (Coarsucam), atovaquone-proguanil (Malarone). The combination of sulfadoxine and pyrimethamine (Fansidar) is also commonly used.⁴⁵ Severe malaria should be treated with injectable artesunate (intramuscular or intravenous) and followed by a complete course of an ACT as soon as the patient can take oral medicines. Intravenous quinine is also used for the treatment of severe or complicated malaria, which is caused almost exclusively by *P. falciparum*. In case the infecting species is uncertain (*P. malariae*, *P. vivax* or *P. ovale*) or in the event of resistance, clinicians should administer the same treatment as for complicated *P. falciparum* infection, since mixed infections are common. Parasitemia should decrease by 75% and clinical status improve within 48 hours after initiating therapy. If not, drug resistance, inadequate drug levels or the presence of clinical complications should be suspected. In this case, radical treatment with primaquine may be necessary after therapy of the blood-stage infection, to eradicate hypnozoites and prevent relapses.

Chloroquine-resistant *P. falciparum* is widespread and currently exists in all malarious areas of the world except Mexico, Central America, the Caribbean and parts of the Middle East. Yet, chloroquine remains highly effective against *P. malariae*, *P. ovale*, and *P. vivax* everywhere except Papua New Guinea and parts of Indonesia, where significant resistance has developed. For regions with chloroquine-sensitive *Plasmodium species*, chloroquine is the recommended chemoprophylactic. Otherwise, mefloquine (Lariam) is the drug of choice and doxycycline is an acceptable alternative.

I.A.4. The necessity for new antimalarials

Considering the persistently high annual death toll due to malaria, continuing effort towards a more efficient eradication plan is necessary. Antimalarial chemotherapy will play a central role in any new strategy since the history of undulating success in eliminating malaria has weighed mostly on the lapses in killing the human-borne forms of the parasite.

I.A.4.1. Mechanisms of antimalarial resistance

Antimalarial resistance is the ability of a parasite strain to survive and/or multiply despite the administration, absorption, entry into the parasite or infected RBC (for the appropriate time duration necessary for normal action), of a drug given in doses equal to or higher than those usually recommended, but within tolerance of the subject. Drug resistance is distinguished from treatment failure (failure to resolve clinical disease) since the former can cause the latter, but not all treatment failure is due to drug resistance. Incorrect dosing, non-compliance with duration of dosing regimen, low drug quality, poor or erratic absorption and misdiagnosis are factors that contribute to treatment failure in an individual.⁴⁶ The consequent exposure of parasites to suboptimal drug levels allows the selection of resistant parasite strains. Spontaneous single point or multiple mutations confer resistance to parasites, such that drug pressure removes susceptible parasites while resistant strains survive. Heterogeneous populations of parasites that can have widely varying drug susceptibility, from highly resistant to completely sensitive have been found in single malaria isolates.⁴⁷ Over time, resistance becomes established in the population and can be very stable, persisting long after specific drug pressure is removed. The mechanism of resistance has been well documented for chloroquine, the antifolate combination drugs, and atovaquone.

The global spread of chloroquine-resistant *P. falciparum* strains was actually the most devastating defeat in malaria control of the 20th century. Following this fall, successive antimalarial drugs have originally raised a glimmer of hope, just to later meet the same fate (Table I.1). The capacity for *P. falciparum* to expel chloroquine at a rate that does not allow this antimalarial drug to reach levels required for inhibition of haem polymerization is believed to be the cause of resistance.⁴⁸ It is unclear whether parasite resistance to other quinoline antimalarials (amodiaquine, mefloquine, halofantrine, and quinine) occurs via similar efflux mechanisms. Specific gene mutations encoding for resistance to both

dihydrofolate reductase and dihydropteroate synthase have been identified and combinations of these mutations have been associated with varying degrees of resistance to antifolate combination drugs such as sulfadoxine + pyrimethamine. Resistance to atovaquone, a hydroxynaphthaquinone, is conferred by single-point mutations in the cytochrome-b gene. Polymorphisms in the *P. falciparum* multidrug resistance protein-1 gene, which localizes to the membrane of the food vacuole, the site of action of a number of drugs, impacts on sensitivity to multiple antimalarial drugs by enhancing efflux of the drugs from cells (including resistance to increasingly used components of ACTs).⁴⁹

Taking into account the realities of multidrug resistance, the mild-to-severe and/or sometimes fatal toxicity issues associated with antimalarials,⁵⁰ shortcomings on the cost effectiveness of currently available therapy, the increasing need for more orally bio-available drugs that can be administered in a nonhospital setting (preferably single-daily dosing, and short curative regimens), there is broad consensus on the urgent need to accelerate research towards new antimalarial entities.

Table I.1: Chronology of resistance against common antimalarials.

Antimalarial	Introduced in	First case of resistance
Quinine	1632	1910
Chloroquine	1945	1957
Proguanil	1948	1949
Sufadoxine-Pyrimethamine	1967	1967
Mefloquine	1977	1982
Atovaquone	1996	1996

I.A.4.2. Feeding the antimalarials pipeline

Multiple strategies are being explored in the current pipeline for antimalarial drug discovery, the most pursued of which are:

- The piggyback approach is to explore classes of drug molecules as antimalarials that have already been thoroughly evaluated as drug leads for other diseases addressed by major pharma. One example is the protein farnesyltransferase inhibitors that

have been extensively developed over the past decade as anti-cancer agents.⁵¹ After *P. falciparum* was shown to contain protein farnesyltransferase, piggybacking of the tetrahydroquinoline class of protein farnesyltransferase inhibitors led to the cure of malaria-infected rodents, although further work is needed to reduce the metabolic instability of this class of drug leads.^{52,53}

- Recycling of known malaria drugs is being pursued by performing synthetically affordable chemical modifications on classical antimalarials, or development of new suitable combination partners for existing monotherapy drugs. Indeed since halofantrine use is limited by toxicity, the more tolerated analogue lumefantrine was developed and is now a component of the co-artemether combination (artemether/lumefantrine).⁵⁴ Re-introduction of drugs after a period of non-use has been considered as a strategy to combat malaria. This has been demonstrated in Malawi, which halted chloroquine use in 1993 due to resistance. Chloroquine was demonstrated to have 99% clinical efficacy a decade later, presumably due to the re-expansion of susceptible parasites.^{55,56}
- Arguably, the most innovative approach to chemotherapy is the identification of new targets and subsequent discovery of compounds that act on these targets. Ideally, new drug combinations should contain both fast acting and long-lasting schizonticides combined with transmission-blocking partners.

Piggybacking or recycling drugs has been promoted as a way to lower overall costs in antimalarial drug development but in the latter approach, the risk of fast induction of resistance through the lack of structural diversity with predecessors, or by targeting the same enzyme or pathway is not to be underestimated. In an effort to catalyze the development of new antimalarials, the Medicines for Malaria Venture and Scynexis, Inc., assembled the Malaria Box, an open library composed of 400 compounds spanning a 50% inhibitory concentration (IC₅₀) range of 30 nM to 4 μM.⁵⁷ Compounds featured in the Malaria Box are also filtered based on druglike properties. The discovery of novel therapeutics, hinging especially on structurally different chemical entities and targets that as yet are unexplored, remains an attractive approach towards an end game malaria containment scenario.

I.B. Tuberculosis

I.B.1. Pathogenesis, diagnosis and treatment

Human tuberculosis is caused principally by *Mycobacterium tuberculosis* (Mtb), a member of the *Mycobacterium tuberculosis* complex that also includes *M. africanum*, *M. bovis*, *M. microti*, *M. canetti* and *M. pinnipedii*. *Mycobacterium tuberculosis* is contracted through inhalation of infectious saliva droplets or mucus expelled by someone with active pulmonary disease. The pathogen settles in the lungs where it targets macrophages, important effector cells in the immune system, as its preferred habitat as long as they are in their resting state.⁵⁸ For individuals with healthy immune systems, once inside the macrophage, the bacteria is encapsulated (phagocytosed) in an endocytic vacuole to form tiny capsules (granuloma) which can persist for several years, causing latent infection.^{59,60} Whereas resting macrophages fail to harm *M. tuberculosis*, activated macrophages can control the growth of the microbe, although sterile eradication is seldom achieved.⁶¹ Interferon-gamma (IFN- γ) and tumor-necrosis factor-alpha (TNF- α), produced by T cells, are important macrophage activators. Macrophage activation permits phagosome-lysosome fusion, thereby creating a lethal environment for the bacteria due to acidic pH, reactive oxygen intermediates, lysosomal enzymes, etc. *M. tuberculosis* evades this host defense strategy by arresting the phagosome at an early stage of maturation, and by preventing fusion of the phagosome with lysosomes.^{62,63,64} Latent infection can be reactivated in infected individuals triggered by a compromised immune system and may induce active TB characterized by coughing of blood, chest pain, shortness of breath and constitutional symptoms such as malaise, weakness and fever. Dissemination of the bacilli via the lymphatic system and bloodstream to other organs (kidneys, bone marrow, meninges, etc) is also possible.

The tuberculin skin test or the TB blood (IFN- γ) assays are commonly used to determine if a person has been infected with the TB bacteria but do not provide information on the nature of infection (latent or active disease).^{65,66} A false-positive tuberculin skin test result is possible for people who have received Bacille Calmette-Guérin (BCG), the vaccine for TB disease. For complete characterization, additional tests such as a chest x-ray, microscopic observation of Ziehl-Neelsen-stained sputum specimens, drug-susceptibility testing of cultures, and histopathological examination of biopsy samples supplement the

aforementioned tests. Invasive procedures to obtain samples like cerebral spinal fluid for testing of extra pulmonary TB makes that the diagnosis of tuberculosis remains clinically challenging and logistically difficult in resource-limited settings.⁶⁷

The discovery of streptomycin (SM, Figure I.4), a natural antibiotic isolated from *Streptomyces griseus* in the early 1940s, represented the first breakthrough in TB chemotherapy.^{68,69} Shortly afterwards, in 1946, *para*-aminosalicylic acid (PAS) was developed.⁷⁰ Following the addition of isoniazid (INH) to the antituberculosis arsenal in 1952, it was soon discovered that monotherapy of these drugs led to rapid development of resistance. Clinicians recognized that if all these drugs were given simultaneously, drug resistance did not emerge and lifetime cures of tuberculosis were finally achievable.^{71,72,73} With the drug resistance situation getting worse over the decades, a cocktail of drugs is the current practice in fighting TB. The recommended first line therapy against drug-sensitive active TB consists of four drugs: INH, rifampicin (RIF), pyrazinamide (PZA), and either ethambutol (EMB) or SM for two months, followed by an additional four months of treatment with RIF and INH. The WHO advises against the use of SM as part of first-line treatment regimens for children with pulmonary TB or tuberculous peripheral lymphadenitis.⁷⁴ Persons with latent *Mtb* infection who are at increased risk for active tuberculosis require preventive treatment.⁷⁵ The preferred regimen is INH alone for nine months or for a longer duration in HIV-infected persons, although a combination of INH and RIF has recently shown to be comparatively effective.^{76,77}

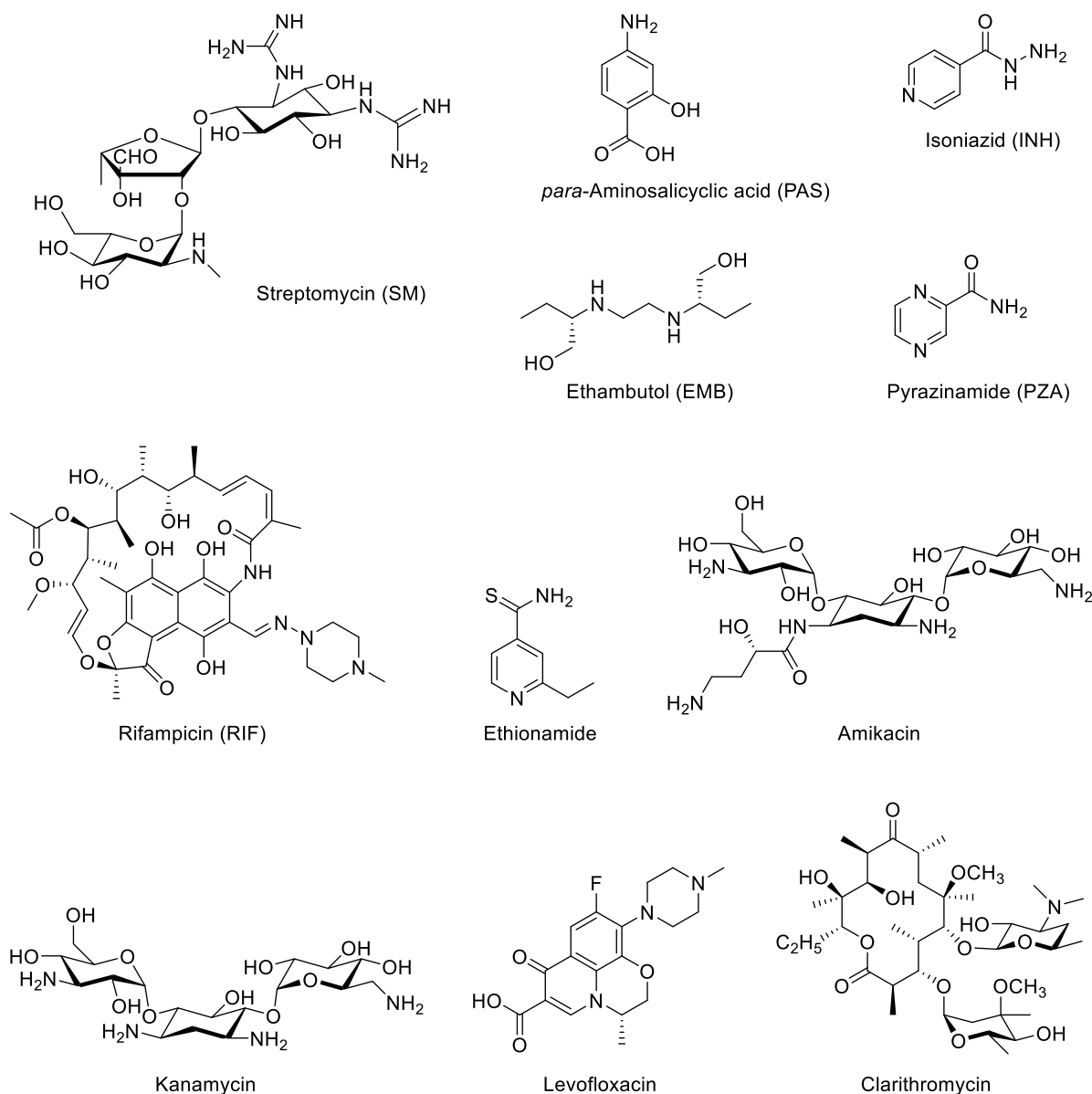


Figure I.4: Structures of first-line and example multidrug-resistant tuberculosis drugs.

While RIF inhibits DNA coiling and transcription, INH and EMB target cell wall synthesis by respectively inhibiting mycolic acid synthesis and arabinogalactan synthesis. The exact target of PZA is unclear, but it is thought to disrupt plasma membrane energy metabolism or inhibit fatty acid synthesis.⁷⁸ Streptomycin interferes with protein synthesis at the ribosome level.⁷³

Multidrug-resistant (MDR) TB, which started in the early 1990s as an emerging torpedo to antituberculosis efforts, occurs when a *Mycobacterium tuberculosis* strain is resistant to INH and RIF, the two mainstays of first-line TB therapy.⁷⁹ To cure MDR TB, healthcare providers administer a combination of second-line injectable drugs such as amikacin and kanamycin,

alongside selected fluoroquinolones (e.g. levofloxacin). Extensively drug-resistant TB and totally drug-resistant TB is terminology used nowadays to characterize complications with treatment. This necessitates the use of more complex combinations involving drugs like ethionamide and clarithromycin, as the last hope to solve the poor survival rates associated with these disease forms.⁸⁰ Improper diagnosis and/or drug prescription, occasional shortage in drug supply and the high stigma about TB, which results in unwillingness to seek early treatment, allow the development of a large bacteria population and escalate the acquisition of drug resistance.⁸¹ All first-line as well as other TB drugs have a number of adverse side effects including, but not limited to, hepatitis, gastrointestinal distress, peripheral neurotoxicity, disturbed vision and nephrotoxicity, which should be tolerated by the patient when not severe.⁸² However, the usually lengthy treatment, side effects, various socioeconomic factors, and the tendency for patients to feel well long before safe completion of the prescribed course, promote non adherence, thereby increasing the risk of resistance development.^{83,84}

It is worth noting that no new first-line antibiotics have been introduced into the TB pharmaceutical depository during the last fifty years. MDR TB has worse cure rates (40-80%) than for drug-susceptible strains (cure rates of >90%),⁸⁵ whereas the cost of second line drugs may be close to 100 times more than first-line therapy.⁸⁶ The BCG which is the only vaccine available, does not fully protect against Mtb, especially in adults.⁸⁷ Considering that the introduction of new, safe, effective and affordable drugs will avert millions of unnecessary deaths, the integration of both drug-susceptible and resistant TB into such a plan will be possible if the new generation drug strategy exploits unprecedented Mtb targets.

I.C. Isoprenoid biosynthesis as a drug target

Developing a new drug from original idea to the launch of a finished product is a complex process, which can take 10-12 years and cost in excess of \$1 billion.⁸⁸ Drug discovery for a given disease (Figure I.5) usually involves either target-based or phenotypic-based high-throughput (HTS) screening of a compound library. The former approach is frequently preferred when the underlying cause of the condition or biochemical pathways involved are understood, whereas the latter allows to identify leads without prior knowledge of the

molecular mechanisms or implicated target(s). In the past 25 years, molecular target-based drug screening has become the main drug discovery paradigm used in both the pharmaceutical industry and in academic biomedical research.⁸⁹ Yet, during the 10-year period between 1999 and 2008, the contribution of phenotypic screening to the discovery of first-in-class small-molecule drugs exceeded that of the target-based approach; the United States Food and Drug Administration approved 28 first-in-class small-molecule drugs developed through the former approach as opposed to 17 achieved through the target-based means.⁹⁰ Accordingly, the declining use of phenotypic screening over the past 25 years is thought to be a reason behind the recent dwindling in drug research and development breakthroughs. In actual fact, both approaches to drug discovery have advantages and shortcomings:

- The strengths of the target-based approach include the ease to optimize hits and the compatibility of both small-molecule screening strategies and biologic-based approaches such as identifying monoclonal antibodies. This drug discovery paradigm is however, not so innovative; often leading to (me-too) drugs with no new mechanisms of action.
- On the other hand, the ability to develop first-in-class drugs through phenotypic screening is an asset in drug discovery. Prior understanding of the molecular mechanism of action is not a requisite for the assays and the observed activity may translate into a therapeutic impact in a given disease state more effectively than that of target-based assays. Unfortunately, it may cost a lot of efforts to identify targets and to elucidate the mechanism of action of promising entities. This in turn slows the optimization of the molecular properties of drug candidates. Additionally, effective incorporation of new screening technologies into phenotypic screening with the aim of increasing the throughput is a challenge.

The work presented in this thesis focuses on the fifth step of the target-based approach to drug discovery, i.e. lead optimization, hence it is further reviewed here below.

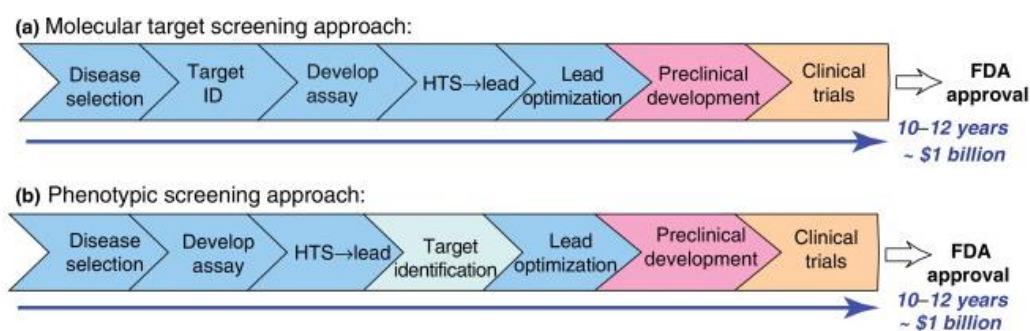


Figure I.5: The different phases of mainstream drug discovery approaches.⁸⁸

I.C.1. Target-based drug design

A target is usually a single gene, gene product or molecular mechanism that has been identified on the basis of genetic analysis or biological observations. Target validation is typically done at three levels: the molecular level (e.g., inhibition of a particular enzyme), the cellular level and the whole animal model level.⁹¹ A target is considered truly validated when a drug acting on it is in the clinic for treatment of human diseases. In 2006, Overington *et al.* carried out an extensive analysis of the different molecular targets modulated by registered drugs. Of the 1065 drugs reviewed, they estimated 324 targets: 266 human genome-derived proteins and 58 pathogenic organism targets.⁹² G protein-coupled receptors (GPCRs), kinases, proteases and ion channels are amongst the most explored drug targets, with GPCRs alone representing the target of some 50-60% of currently marketed drugs.⁹³

After the identification of a biological target of interest, the next challenge begins with the conversion of the target into a bioassay that allows a readout of target modulators. Following successful assay development, compounds can be screened using this bioassay. The basic requirement for a high throughput screening (HTS) assay is that it be sensitive, quick, highly reproducible, robust and suitable for screening thousands or even millions of samples. HTS affords 'hits', which then undergo more detailed profiling of physicochemical and *in vitro* absorption, distribution, metabolism, and excretion (ADME) properties. Since most initial 'hits' usually have low affinity towards their target, they need to be structurally modified in order to increase their potency and also to optimize other properties like solubility, toxicity, selectivity, etc. Ideally, hit optimization may be steered by the knowledge of the three dimensional structure of the biological target obtained through X-ray crystallography or nuclear magnetic resonance (NMR) spectroscopy. If an experimental

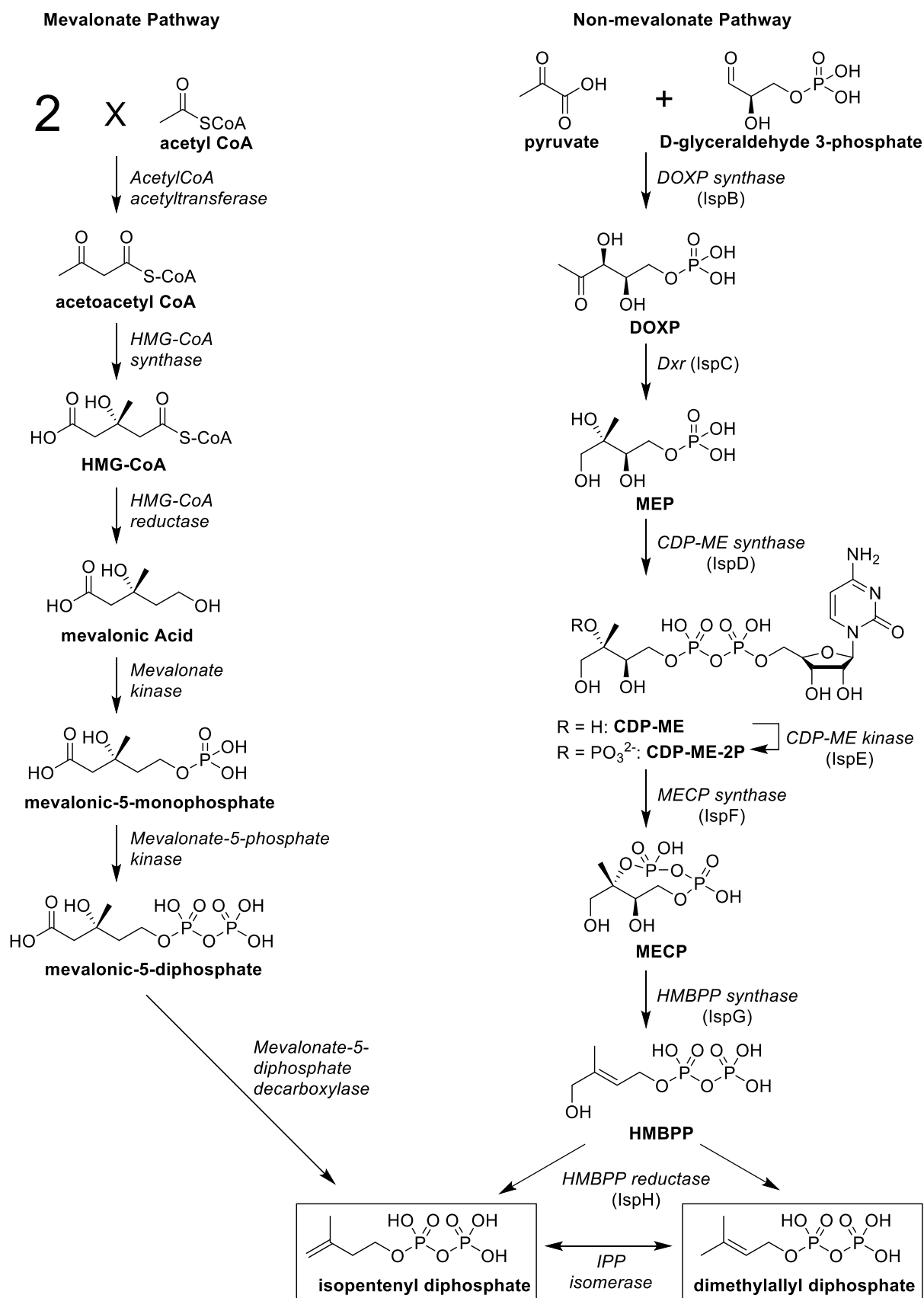
structure of a target is not available, it may be possible to create a homology model of the target based on the experimental structure of a related protein.⁹⁴ Likewise, structure-activity relationship (SAR) analysis may help in lead optimization. The objective of the lead optimization phase is to maintain favorable properties in lead compounds while synthetically improving on deficiencies in the lead structure. Only 10% of small molecule projects within industry might make the transition to pre-clinical candidate and since the attrition rate of compounds entering the clinical phase is also high, again only 1 in 10 candidates may reach the market.⁹⁵

I.C.2. The mevalonate versus the non-mevalonate pathway for isoprenoid biosynthesis

Isoprenoids (also referred to as terpenoids) represent the oldest known biomolecules^{96,97} and the largest group of contemporary natural products, encompassing over 30,000 known compounds.⁹⁸ Key biochemical functions in all aspects of life have been attributed to this family, including but not limited to roles in electron transport (quinones), as photosynthetic pigments (carotenoids, side chain of chlorophyll), regulation of growth and development (steroid hormones, cytokinins), signal transduction (prenylation of proteins), constituents of membranes, bile acids, mating pheromones and reproductive hormones.^{99,100} Despite their huge structural diversity, all isoprenoids are biosynthesized from the 5-carbon isoprene building units isopentenyl diphosphate (IPP, Scheme I.1) and dimethylallyl diphosphate (DMAPP), as proposed by Ruzicka.^{101,102}

Since its discovery in the 1950s, the mevalonate (MVA) pathway (Scheme I.1) was for several decades unanimously accepted as the unique source of isoprenoid building blocks IPP and DMAPP.^{103,104,105,106} By the early 1990s, the impossibility to reconcile certain biosynthetic observations with the MVA paradigm was independently recognized by different researchers. For instance, mevinolin, a highly potent competitive inhibitor of HMG-CoA¹⁰⁷ reductase was found to strongly inhibit sterol biosynthesis but unable to interrupt the accumulation of plastidial isoprenoids (including monoterpenes, carotenoids, and the prenyl moiety of chlorophylls, plastoquinone, and tocopherol) in higher plants.¹⁰⁸ Poor yields were also reported for the incorporation of ¹⁴C-labeled mevalonate into plant chloroplast isoprenoids (e.g., carotenoids).¹⁰⁹ Further labeling experiments with ¹³C-labeled precursors,

including ^{13}C -pyruvate, did not fit the MVA route, but did shed light on the role of pyruvate as the precursor of isoprene units in *Escherichia coli* (*E. coli*).¹¹⁰ Eventually, the groups of Arigony and Rohmer independently established the existence of a second pathway for isoprenoid biosynthesis, variously referred to as the non-mevalonate pathway (NMP), the 2-C-methyl-D-erythritol-4-phosphate (MEP) pathway, the 1-deoxy-D-xylulose-5-phosphate (DOXP) pathway or the Rohmer pathway.^{111,112}



Scheme I.1: Isoprenoid biosynthesis via the mevalonate and the non-mevalonate pathway.

As depicted in scheme I.1, the NMP commences with the condensation of pyruvate and D-glyceraldehyde 3-phosphate to form 1-deoxy-D-xylulose 5-phosphate (DOXP), catalyzed by DOXP synthase.¹¹³ In the second and most studied step of this pathway, DOXP reductoisomerase (IspC, Dxr), mediates the isomerization and reduction of DOXP using nicotinamide adenine dinucleotide phosphate (NADPH) as the hydride source, to yield MEP according to a mechanism that is reviewed below (section I.C.4).¹¹⁴ Subsequently, MEP is converted to 4-diphosphocytidyl 2-C-methyl-D-erythritol (CDP-ME) in a cytidine triphosphate (CTP)-dependent reaction governed by CDP-ME synthase (IspD, YgbP).¹¹⁵ CDP-ME kinase (IspE, YchB) mediates the phosphorylation of CDP-ME with ATP, to afford 4-diphosphocytidyl-2-C-methyl-D-erythritol-2-phosphate (CDP-ME-2P).¹¹⁶ Next, 2-C-methyl-D-erythritol 2,4-diphosphate (MECP) synthase (IspF, YgbB) uses CTP as a cofactor to cyclize and dephosphorylate CDP ME-2P, generating MECP.¹¹⁷ The latter is subsequently converted to 1-hydroxy-2-methyl-2-*cis*-butenyl 4-diphosphate (HMBPP) by HMBPP synthase (IspG, GcpE)¹¹⁸ before final conversion into a mixture of IPP and DMAPP by HMBPP reductase (IspH, LytB, IPP/DMAPP synthase).¹¹⁹ Unlike their MVA-pathway dependent counterparts, organisms using the NMP do not rely on IPP isomerase which interconverts IPP and DMAPP.

I.C.3. The non-mevalonate pathway in *P. falciparum* and *M. tuberculosis* as a drug target

Most eukaryotes (including mammals and fungi) use exclusively the MVA pathway to obtain IPP and DMAPP. In contrast, the overwhelming majority of eubacteria use the orthogonal NMP, including key pathogens such as some Gram-negative bacteria and *Mycobacteria*.^{120,121,122} Notable exceptions include several clinically important Gram-positive organisms, including staphylococci and streptococci, which have retained the MVA pathway.¹²³ Some eukaryotic microbes including the *Apicomplexan* protozoan pathogens *Plasmodium species* and *Toxoplasma gondii* utilize only the eubacteria-like NMP.^{124,125} In plants, both pathways are present with the NMP being operative in the chloroplast and the MVA pathway in the cytosol and mitochondria.¹²⁶ Both pathways are also conserved in certain *Streptomyces species*,^{127,128} while several obligate intracellular organisms such as rickettsiae and mycoplasmas, have lost *de novo* isoprenoid metabolism altogether.¹²⁹

Thus, a common denominator for both *P. falciparum* and *M. tuberculosis* is their exclusive dependence on the NMP to obtain vital isoprenoids. The fact that all enzymes of this pathway have no human homologues, creates a vulnerability for these pathogens. The respective enzymes constitute metabolic chokepoints and may be lucrative targets to feed the antimalarial and/or antituberculosis pipeline.^{130,131} All the enzymes involved in the NMP have been genetically validated as drug targets¹³² and the X-ray structure of each of the enzymes has been solved.^{133,134} In a recent systematic druggability assessment of the NMP enzymes, Hirsch and co-workers found that all substrate- or cofactor-binding pockets are druggable.¹³⁵ All intermediates of this pathway are phosphorylated and therefore highly polar. Correspondingly, the active sites are particularly polar, making the structure-based design of drug-like inhibitors for these enzymes challenging. Nevertheless, the promising results with fosmidomycin, stimulates the continuing search for inhibitors of the NMP enzymes. Fosmidomycin, an inhibitor of Dxr, has been the subject of phase II clinical trials as an antibiotic and is currently also being tested for the treatment of malaria (see I.D.1).

I.C.4. 1-Deoxy-D-xylulose-5-phosphate reductoisomerase

I.C.4.1. Structure

Dxr mediates the first committed step of the NMP¹²⁶ and until now, it is the most widely explored therapeutic target in this pathway.¹³⁵ Over thirty reported (co)crystal structures of Dxr from multiple organisms, including *P. falciparum* and *M. tuberculosis*, have provided key information on both the active site architecture and the binding mode of NADPH, DOXP and inhibitors.¹³⁶ The overall structure of PfDxr is essentially similar to that of other species.^{137,138,139} PfDxr is a homodimer; each monomer shows a V-like shape and consists of two large domains separated by a cleft containing a deep pocket, a linker region, and a small C-terminal domain (Figure I.6). One of the large domains, the N-terminal domain (amino acid residues 77 to 230), binds the NADPH cofactor. A basic element of the secondary structure of this domain is the seven-stranded β -sheet in the center of the domain that is sandwiched by two arrays of three α -helices. The other arm of the V-shape is the catalytic domain (residues 231 to 369) that comprises the binding site for the bivalent cation (usually Mg^{2+} , Mn^{2+} or Co^{2+}), for the inhibitor (fosmidomycin in Figure I.6) and also a flexible loop. It is an α/β -type structure consisting of five α -helices ($\alpha 7$ - $\alpha 11$) and four β -strands ($\beta 8$ - $\beta 11$).

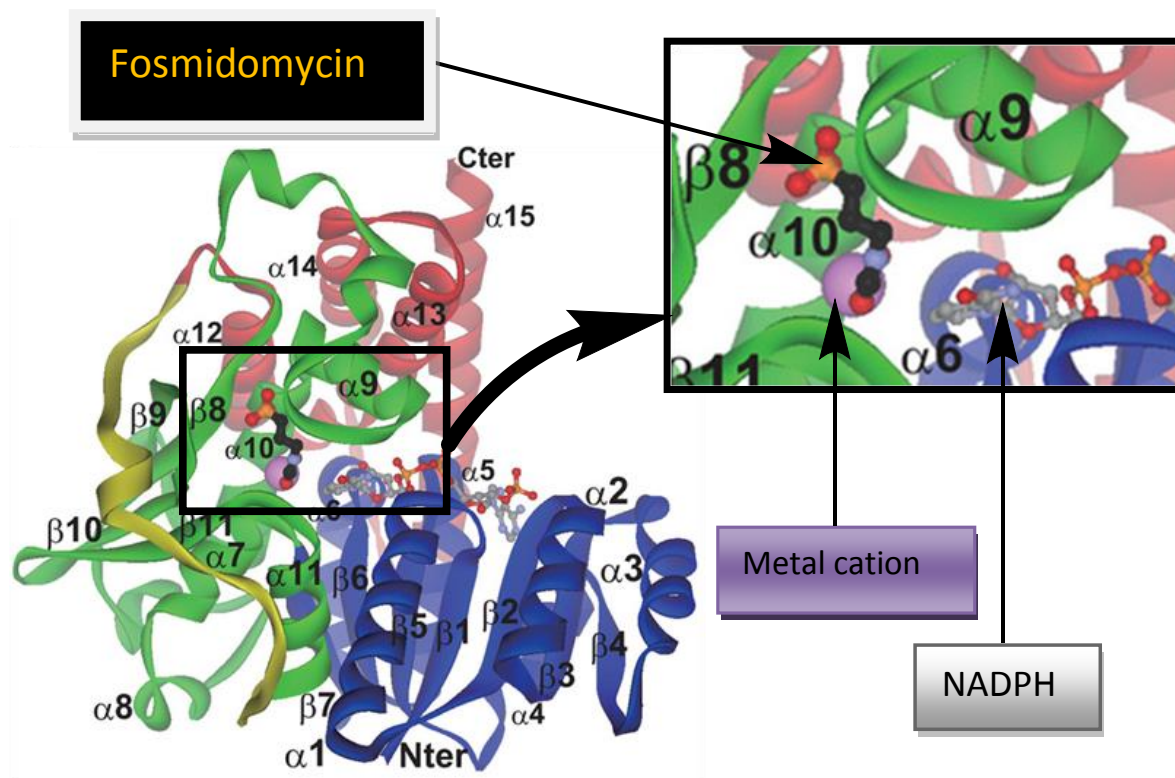


Figure I.6: The three-dimensional structure of fosmidomycin-bound quaternary complex of PfDxr. The NADPH-binding, catalytic, linker, and C-terminal domains are depicted in blue, green, yellow, and red, respectively. The bound fosmidomycin (black for carbon) and NADPH (gray for carbon) molecules are shown as ball-and-stick models (adapted from Umeda *et al.*, 2011).¹³⁹

The C-terminal α -helical domain (residues 396 to 486) is postulated to play mainly a structural role. The linker region connects the catalytic domain to the C-terminal domain while also contributing to dimer formation by interacting with the same region of the other Dxr subunit. Upon binding of the substrate or an inhibitor (the binding mode is presented below), the enzyme undergoes an induced-fit movement and the active site is covered by a flexible loop which caps it off from bulk solvent.

I.C.4.2. Mechanism of action

Most Dxr mechanistic studies have been performed on the *E. coli* isozyme, which is high yielding on the currently available recombinant expression system, provides comparative IC_{50} values as other isozymes and is also easier to handle than, for instance, the PfDxr.¹⁴⁰ As mentioned above, Dxr, a clinically validated target, steers the transformation of DOXP to

MEP in the first dedicated step of the NMP. The reaction proceeds via an isomerization of DOXP to 2-C-methyl-D-erythrose 4-phosphate, followed by an NADPH-mediated reduction to MEP.¹⁴¹ Although a concerted α -ketol rearrangement has long been under debate as a possible mechanism for the isomerization step,¹⁴² the current consensus is that a stepwise fragmentation-reassembly via a retro-aldol/aldol sequence (Figure I.7) is the most plausible mechanism.^{143,144,145} The evidence accumulated from experiments based on the kinetic isotope effect, points to an initial deprotonation of the C4-hydroxyl group of DOXP, followed by cleavage of the C3-C4 bond in a retro-aldol manner to afford two fragments, the enolate of hydroxyacetone and glyceraldehyde phosphate.^{146,147} These then reunite in an aldol reaction to produce a new C-C bond and generate the aldehyde intermediate, which is subsequently reduced by NADPH to yield MEP. Reduction of the aldehyde intermediate proceeds by transfer of the pro-*S* hydride ion from NADPH to its *RE* face, making Dxr a class B dehydrogenase.^{148,149}

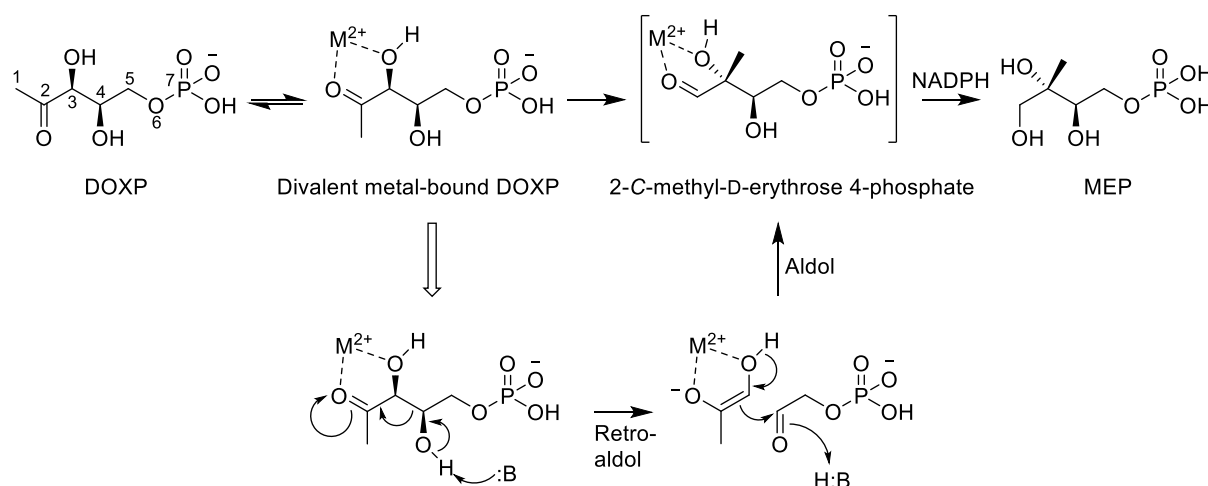


Figure I.7: Reaction mechanism for Dxr-catalyzed conversion of DOXP to MEP.

Recently, Sangari and collaborators identified a new family of enzymes designated Dxr-like (DRL) enzymes, which catalyze the transformation of DOXP to MEP in NMP-dependent organisms, like *Brucella abortus*, but have no overall homology to the Dxr.¹⁵⁰ *B. abortus* is an infectious, blood borne gram-negative bacterium, which causes brucellosis, manifesting in the form of premature abortion of a cattle fetus and can also infect humans.¹⁵¹

I.D. Fosmidomycin

I.D.1. Discovery, antibacterial and antiplasmodial activity

Research on fosmidomycin (**1.1**, Figure I.8), also known as FR31564 or 3-(*N*-formyl-*N*-hydroxyamino)propyl-phosphonate, started in the late 1970s when Fujisawa Pharmaceutical Co isolated this natural antibiotic from *Streptomyces*, alongside FR900098 (**1.2**), FR32863 (**1.3**) and FR33289 (**1.4**), all compounds characterized by a phosphonic acid and an *N*-acylhydroxamino function.^{152,153,154}

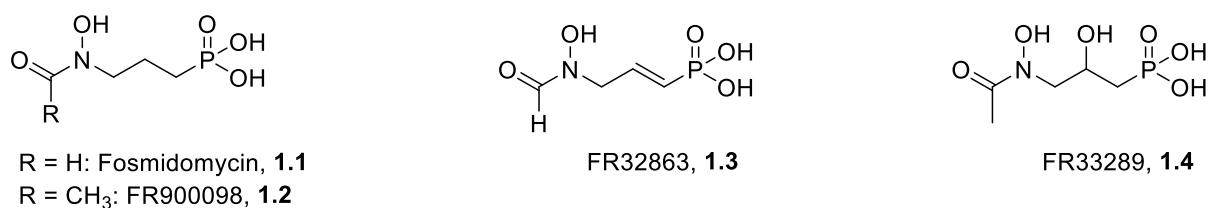


Figure I.8: Structure of fosmidomycin and related natural compounds originally isolated by the Fujisawa Pharmaceutical Co.

These extracts were found to exhibit antibacterial effects against most Gram-negative bacteria, but have minimal activity against Gram-positive bacteria. Fosmidomycin was evaluated in the 1980s in an early phase I study and a phase II study for the management of urinary tract infections.^{155,156,157} It proved to be effective and well tolerated; no major adverse effects were observed even when given in repeated doses of 8 g/day intravenously for 7 days, 4 g/day intramuscularly for 5 days, and 4 g/day orally for 7 days. Unmetabolized fosmidomycin was the only bioactive substance found in the urine of volunteers and mild outcomes like diarrhea and flatulence was attributed to gut biota alteration.¹⁵⁸ However, with the emergence of more potent antibiotics at that time, further development of fosmidomycin and its congeners was discontinued.

Seto and coworkers discovered that fosmidomycin inhibits purified recombinant EcDxr activity in a dose-dependent manner with an IC₅₀ value of 8.2 nM.¹⁵⁹ In 1999, Jomaa and coworkers¹²⁴ provided evidence for the presence of the NMP in the apicoplast of *P. falciparum* and revealed that both fosmidomycin and FR900098 were able to:

- inhibit the enzymatic activity of recombinant PfDxr,

- suppress the growth of *P. falciparum* in culture, and
- cure mice challenged with *Plasmodium vinckei*.

Different groups have since also demonstrated that fosmidomycin potently inhibits Dxr of other organisms and kills multiple pathogens reliant on this enzyme.^{160,161,162,163} Using mass spectrometry to profile NMP metabolites, Zhang *et al.* revealed that IspD is a second *in vivo* target for fosmidomycin within isoprenoid biosynthesis in *P. falciparum* and *E. coli*.¹⁶⁴ The absence of the NMP in humans combined with its essentiality in *Plasmodium* species garnered impetus for the development and use of fosmidomycin as an antimalarial. Indeed, in a clinical study conducted in Gabon and Thailand, orally administered fosmidomycin led to a fast parasite clearance in subjects with acute uncomplicated *P. falciparum* malaria, albeit with a high rate of recrudescence, thereby precluding its use in monotherapy.^{165,166} The combination of fosmidomycin with most antimalarial agents in clinical use has been investigated and successful combination partners, including artesunate and clindamycin, tested clinically.^{167,168,169,170} Although initially very promising, the development of a fosmidomycin-clindamycin combination therapy has recently stalled due to inadequate efficacy in clearing uncomplicated malaria in Mozambican children less than three years old.¹⁷¹ Results from an ongoing clinical Phase II trial of a fosmidomycin-piperaquine combination sponsored by Jomaa Pharma GmbH are awaited.¹⁷²

I.D.2. Binding mode and kinetics of Dxr inhibition

Fosmidomycin inhibits the Dxr-catalyzed reaction by mimicking the binding mode of Dxr's substrate, as revealed by X-ray crystal structures of fosmidomycin/FR900098-bound complexes of EcDxr,¹⁷³ PfDxr¹³⁹ and MtbDxr.¹⁷⁴ The fosmidomycin molecule lies in a crevice of the Dxr catalytic domain where the phosphonate functionality occupies the phosphate binding site, the carbon backbone of the inhibitor interacts with a hydrophobic patch, while the hydroxamate chelates the active site bivalent metal. Since cellular concentrations of Mg²⁺ are much higher than Co²⁺ or Mn²⁺, it is often considered to be the physiologically relevant cofactor.¹⁷⁵ In PfDxr (Figure I.9b), the phosphonate group of fosmidomycin forms a tight hydrogen-bound network with Ser270, Asn311, two water molecules, and His293, while the three-carbon backbone lies parallel to the indole ring of Trp296 and also interacts with Met298. The hydroxamate group coordinates a Mg²⁺ ion that is bound by residues Asp231, Glu233, and Glu315. A *cis* (Z) arrangement of the oxygen atoms of the hydroxamate

group is essential for tight binding of the inhibitor to the active site metal. The binding mode of FR900098 to MtDxr (Figure I.9a), is similar to that of fosmidomycin to PfDxr, but with the acetylhydroxyamino group additionally involved in van der Waals contacts with the indole ring of Trp203.

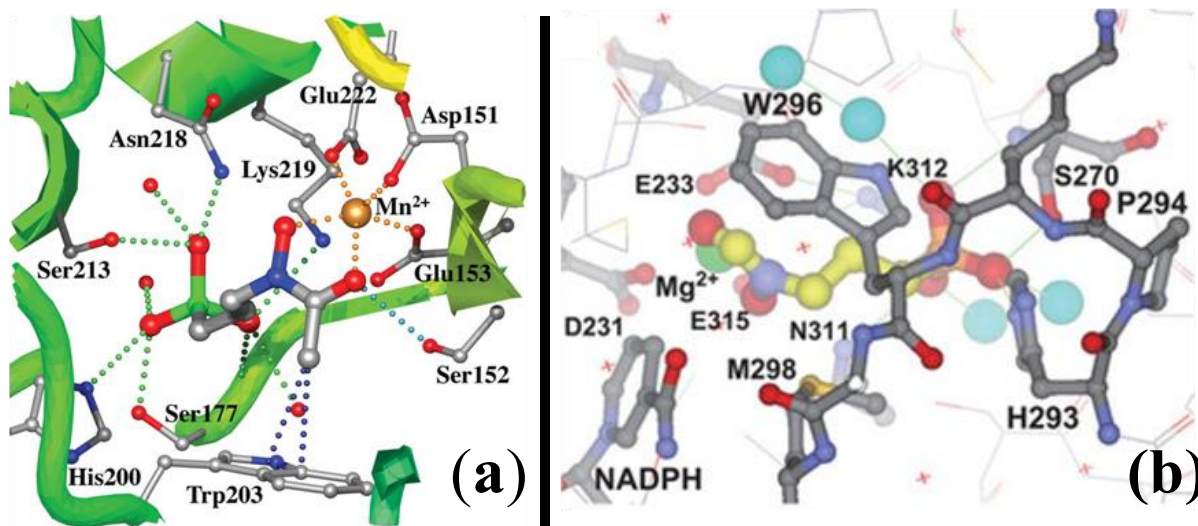


Figure I.9: Inhibitor complex with Dxr: **(a)** Interactions of FR900098 with MtDxr.¹⁷⁴ The interactions of the acetylhydroxyamino group are indicated in navy blue for the closest van der Waals contacts with the indole ring of Trp203 and in sky blue for the hydrogen bond to the hydroxyl group of Ser152. **(b)** Fosmidomycin complex with PfDxr.¹³⁹ The carbon atoms of fosmidomycin, the four buried water molecules, and the bound Mg^{2+} ion are shown in yellow, cyan, and green, respectively.

The kinetics of inhibition by fosmidomycin have been characterized to different extents for Dxrs of various species. Fosmidomycin was initially described as a mixed inhibitor of the EcDxr¹⁵⁹ and later, as a competitive inhibitor against *Z. mobilis*¹⁶⁰ and *A. thaliana*¹⁷⁶ Dxr. More detailed investigations of the pre-steady-state phase of inhibition revealed that fosmidomycin is actually a slow-onset, tight-binding inhibitor often described as following a two-step binding mechanism (Figure I.10).^{177,178} In the first phase, a conformational change is induced after fosmidomycin binds to Dxr according to a competitive inhibition pattern characterized by the constant K_i . This conformational change is essential for tight binding and requires prior formation of a Dxr-NADPH complex. Next, a tighter complex (Dxr-inhibitor*) is formed, consonant with a non-competitive inhibition profile described by the constant K_i^* where $K_i^* < K_i$. By pre-incubating the enzyme with NADPH and fosmidomycin

and then adding DOXP, the slow-onset phase is avoided and therefore, the observed inhibition constant represents K_i^* . Thus, the slow tight-binding property of fosmidomycin is a reason for the difference in measured inhibition constants when the same enzyme/inhibitor complex is evaluated; depending on whether the inhibitor was added to an enzyme-substrate mixture or rather was pre-incubated with the enzyme before substrate addition and activity measurement. Most publications do not detail what order was employed. Enzyme concentration, pathogen strain (in whole-cell assays), substrate and inhibitor are other factors that may influence the measured value thereby complicating the comparison of results reported by different research groups.¹⁷⁹ Although studies have shown that Dxr has a preference for NADPH over nicotinamide adenine dinucleotide (NADH), the Dxr maximum turnover numbers using both cofactors are similar, suggesting that the 2'-phosphate of NADPH contributes predominantly to binding and not to catalysis.¹⁸⁰ It is considered to interact with active-site residues before DOXP (or the inhibitor) binds and induces folding of the flexible loop over the active site.

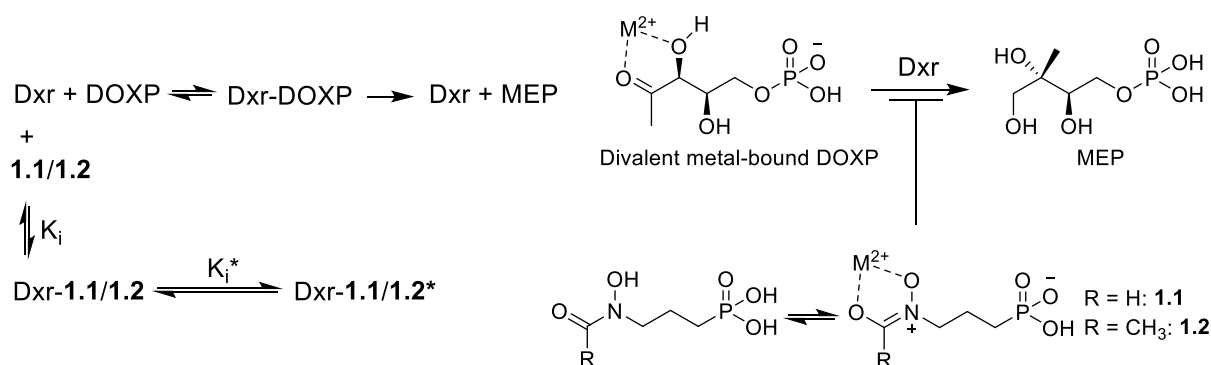


Figure I.10: Analogy between DOXP and Fosmidomycin/FR900098.

I.E. Fosmidomycin as a lead in drug design

The clinical validation of Dxr as a drug target and the use of fosmidomycin to treat malaria patients, raised the stakes on blocking the NMP as a drug discovery venture. Although fosmidomycin is a remarkably safe antimalarial agent, poor pharmacokinetic properties such as moderate bioavailability (with an absorption of approximately 30% after oral dosing), short serum half-life (1.6 hours) and the consequent malaria recrudescence limit its therapeutic use.^{181,158,182} Similarly, while fosmidomycin effectively inhibits purified recombinant MtbDxr, this highly hydrophilic antibiotic cannot penetrate the notoriously

thick and lipophilic mycobacterial cell wall (Figure I.11) and lacks significant activity against intact bacteria.^{161,183}

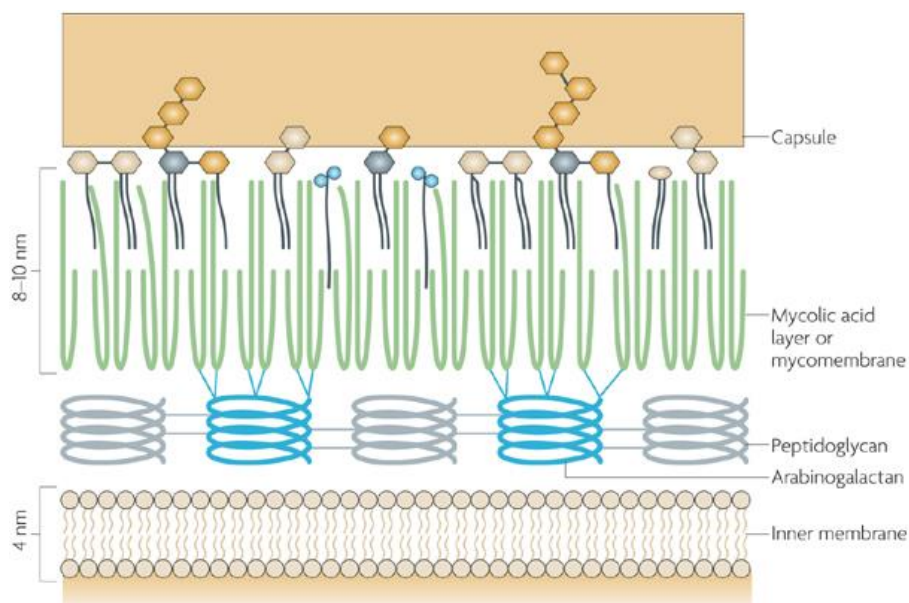


Figure I.11: Current view of the mycobacterial cell wall. The cell wall is mainly composed of a large cell-wall core or complex that contains three different covalently linked structures (peptidoglycan (grey), arabinogalactan (blue) and mycolic acids (green)). The covalent linkage of mycolic acids results in a hydrophobic layer of extremely low fluidity. The outer part of the mycomembrane contains various free lipids, such as phenolic glycolipids etc, which are intercalated with the mycolic acids. The outer layer, which is generally called the capsule, mainly contains polysaccharides (glucan and arabinomannan).¹⁸⁴

Fosmidomycin comprises three main structural parts: a phosphonic acid group, a retrohydroxamate and a three-carbon spacer connecting these two moieties. Its phosphonate group is highly ionized at physiological pH, which is the main reason for its limited capacity to passively diffuse through cell membranes and, consequently, its moderate bioavailability. While this does not preclude efficient uptake in *P. falciparum*, other organisms like *Mtb*, are not sensitive to fosmidomycin because they lack a glycerol-3-phosphate transporter (GlpT) that is known to actively transport fosmidomycin across the hydrophobic cell membranes of bacterial pathogens such as *E. coli* and some apicomplexan parasites like *Plasmodium*.^{185,186,187} Furthermore, for *Plasmodium* and some other species, it has been shown that a so-called parasite-induced new permeability pathway accounts for selective uptake of fosmidomycin and FR900098 into infected erythrocytes.¹⁸⁸ Although the

chelating ability of hydroxamates often makes them potent metalloenzyme inhibitors, most hydroxamic acids suffer from poor oral bioavailability and significant binding to other metals (e.g., Zn²⁺, Cu²⁺, etc.) besides Co²⁺, Mn²⁺ and Mg²⁺.^{189,190,191} In addition, hydroxamic acids may be rapidly degraded *in vivo* by hydrolysis, glucuronidation and sulfation and may suffer from poor pharmacokinetic and toxicological profiles.¹⁹²

Despite these limitations, a subtle switch of the (*N*-formyl-*N*-hydroxy)amino group in fosmidomycin to the (*N*-acetyl-*N*-hydroxy)amino in FR900098, affords a two-fold increase in potency against *P. falciparum in vitro* and against *P. vinckei* in a mouse model of infection.¹²⁴ Indeed, FR900098 has shown superior activity to fosmidomycin in many assays and these two compounds are the most studied Dxr inhibitors. Notably, in the FR900098-PfDxr co-crystal structure, the *N*-methyl group is situated in a hydrophobic pocket flanked by Met298 and Met360, and engages in a favorable van der Waals contact with the indole ring of Trp296.^{139,193} This implies that based on the fosmidomycin/FR900098 scaffold, structural modifications leading to more lipophilic Dxr inhibitors, which may better passively permeate into cells and display improved pharmacokinetic properties, could yield more efficacious agents. Towards this end, extensive medicinal chemistry efforts have yielded various synthetic analogues of fosmidomycin/FR900098 with interesting activity profiles that are reviewed below.

Even with the abundance of crystallographic information about Dxr from several organisms, its dramatic conformational change upon ligand binding renders the structure-based design of improved inhibitors challenging. Owing to the extremely flexible Dxr active site, some fosmidomycin analogues have been proposed to bind in a "reversed" fashion by docking studies, with the phosphonate moiety binding to the Mg²⁺ cation and the hydroxamate located in the phosphonate-binding site, further demonstrating the challenges to rationally optimize this lead.¹⁹⁴ In order to circumvent the limitations associated with the phosphonate and hydroxamate moiety of fosmidomycin, two strategies have been widely exploited in the design of potent analogues: masking of the polar phosphonate group as prodrugs and/or substituting the hydroxamate of fosmidomycin with an alternative metal binding group. Alteration of the three-carbon scaffold has also been probed and analogues combining any of these modifications have been updated. Therefore, in this overview, analogues are classified according to the modifications of the fosmidomycin/FR900098 frame. The activity

of analogues is most often tested either against live parasites or the reductoisomerase enzymes PfDxr, MtbDxr and EcDxr. Inhibitory activities are commonly reported as percentual inhibition for a given concentration of inhibitor, as a K_i -value or as an IC_{50} -value, while *in vivo* results are typically reported as graphic representations of mice survival, relative reduction in infected red blood cells etc. The activity data of analogues reported by different groups have contributed unequivocally towards a better understanding of the structure activity relationships, although they do not allow numerical comparison *sensu stricto*. For a thorough understanding of the SARs, the activity trends rather than specific numerical comparisons are discussed.

I.E.1. Modifications of the retrohydroxamate moiety

I.E.1.1. Hydroxamate reversal

The retrohydroxamate moiety of fosmidomycin coordinates the vital divalent cation in the active site in essentially the same manner as the β -hydroxyketone function of DOXP. The Rohmer group was the first to demonstrate that **1.5** and **1.6** (Figure I.12), the reverse hydroxamate counterparts of respectively fosmidomycin and FR900098, elicit a slow tight-binding inhibitory activity against *E. coli* Dxr, comparable to the natural inhibitors.¹⁹⁵ The *N*-methylated analogue **1.6** is a stronger EcDxr inhibitor than the *N*-H analogue **1.5**, which performs equally well as fosmidomycin. Woo *et al.* later resynthesized compound **1.5** alongside other analogues (see below) and showed that it is a slower binder, needing more time than fosmidomycin to form the tightly bound Dxr-inhibitor complex with *Synechocystis* Dxr.¹⁷⁸

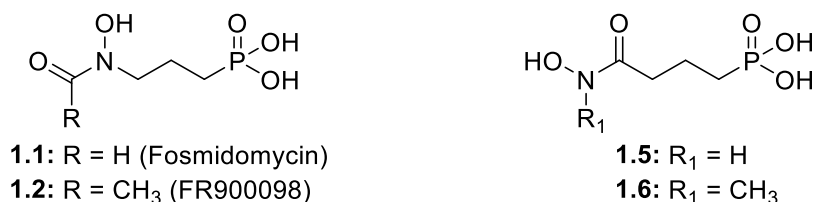


Figure I.12: Reversal of the retrohydroxamate function of fosmidomycin or FR900098.

Zinglé *et al.* noted that the *N*-methylated compound (**1.6**) outperformed its nonmethylated homologue **1.5** due to a hydrophobic interaction between the *N*-methyl group and indole

ring of Trp212 (EcDxr), analogous to the acetyl residue of FR900098 or the terminal methyl group of DOXP.¹⁹⁶

With this blueprint in mind, multiple fosmidomycin/FR900098 analogues comprising a reverse hydroxamate moiety have been prepared by various groups, some of which show sub-micromolar IC₅₀ values. The following sections feature such analogues alongside those bearing the retrohydroxamate moiety, discussed within the context of other relevant modifications.

I.E.1.2. Alteration of the acyl moiety

Flexible docking experiments conducted by different groups suggest that pliable spacious acyl derivatives of fosmidomycin have the potential to bind in an alternative lipophilic pocket.^{197,198,199} This information, along with the observation that the stability of the acetyl group in **1.2** or the *N*-methyl in **1.6** contributes to the superior activity of these analogues, suggests that further extension of the inhibitor into the hydrophobic pocket could introduce additional favorable van der Waals interactions and would improve binding affinity. The Rohmer group also tested the *N*-ethylated analogue **1.7** (Figure I.13) but concluded that this substituent is too bulky to fit in the apparently narrow active site around the metal ion.¹⁹⁵

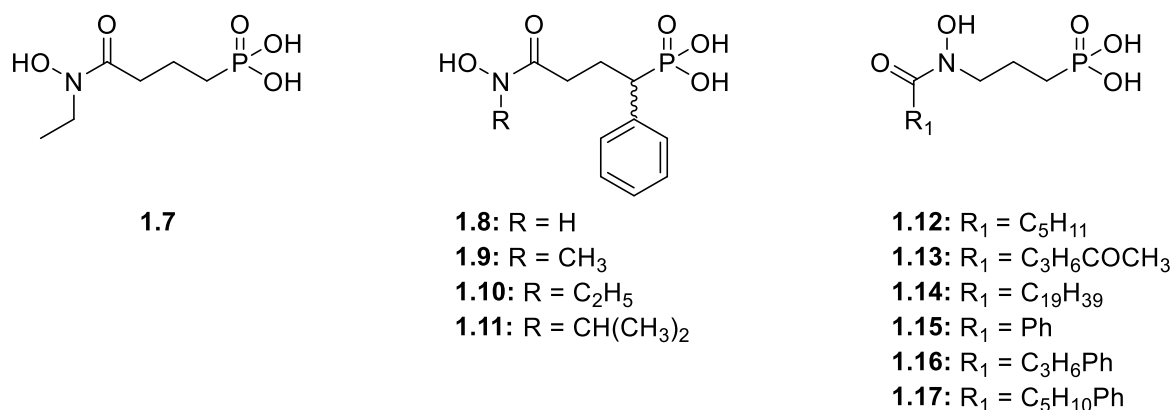


Figure I.13: Dxr inhibitors with different *N*-substituted moieties.

Later, Kurz and co-workers combined the reoriented hydroxamate with favorable α -phenyl substituent (see below) to generate a series of *N*-substituted analogues like **1.8-1.11**. They found that **1.10** and **1.11** perform poorly (with respect to **1.8**) as EcDxr and PfDxr inhibitors (Table I.2a).^{200,201} The *N*-methylated analogue **1.9** is the best of the series, outperforming both fosmidomycin and FR900098 on PfDxr inhibition. Generally, PfDxr shows to be more

susceptible to the activity of the tested compounds than EcDxr. Ortmann *et al.* synthesized compounds **1.12-1.14**, **1.17** (Table I.2b) and showed that introduction of a carbonyl group into the acyl chain of **1.13** results in a two fold increase in activity, compared to **1.12**, which has the same acyl chain length but lacks this functionality. The authors presumed that a hydrogen bond formation to a Met214 (EcDxr) N-H of the Dxr flexible loop located over the active site is responsible for this observation.¹⁹⁸ Even so, none of the compounds in this group elicits EcDxr inhibition comparable to that of fosmidomycin and FR900098.

Table I.2: Biological evaluation of hydroxamate-based fosmidomycin/FR900098 derivatives.

(a)			(b)	
Compound	Enzyme inhibition		Compound	Enzyme inhibition
	IC ₅₀ (μM)			IC ₅₀ (μM)
	EcDxr	PfDxr		EcDxr
Fosmidomycin (1.1)	0.221	0.144	Fosmidomycin (1.1)	0.035
FR900098 (1.2)	0.131	0.015	FR900098 (1.2)	0.035
1.8	0.592	0.012	1.12	10
1.9	0.243	0.003	1.13	5.4
1.10	15	0.015	1.14	inactive
1.11	inactive	inactive	1.17	5.1

Replacement of the formyl group of fosmidomycin by a benzoyl group in **1.15** leads to submicromolar inhibition of *E. coli* and *P. falciparum* Dxr, albeit with half the potency of fosmidomycin.¹⁴⁰ The length of the acyl substituent, however, proved important as insertion of a spacer between the carbonyl group and the phenyl ring (as in **1.17**) leads to a significant loss of activity. This demonstrates that the steric limitation around the metal ion applies for analogues with a retrohydroxamate or a hydroxamate moiety alike. There is approximately 1-3 orders of magnitude difference in activity between EcDxr and PfDxr inhibition values, which is noteworthy since EcDxr is often used in place of PfDxr to assess the antimalarial potential of compounds. As a general finding, the introduction of large acyl residues prevents the formation of the desired hydroxamate-metal interaction geometry and leads to

a significant loss of Dxr inhibitory activity compared to the lead compounds **1.1** and **1.2**, or their reverse hydroxamate counterparts.

Notwithstanding these failings, the Dowd group recently waded into acyl chain modifications by using the Mtb Dxr-fosmidomycin co-crystal structure to design bisubstrate ligands, capable of binding to both the DOXP and NADPH sites.²⁰² They observed a more efficient coordination of the metal cation by *N*- versus *O*-linked substituents on the retrohydroxamate of fosmidomycin. While highlighting the importance of having an aromatic group in the inhibitor, they also suggested that an alkyl chain between the retrohydroxamate and the aryl group is required for accessing an alternate binding pocket. The best result was obtained for **1.16**, which inhibits MtbDxr with an IC₅₀ of 17.8 μM in a competitive manner with respect to DOXP, but in a noncompetitive manner with respect to NADPH, in disagreement with the modeled binding mode. The adenosine-binding pocket gave a good score on a druggability test conducted by Hirsch and co-workers,¹³⁵ so the possibility to explore it for the development of alternative bisubstrate analogues remains open.

I.E.1.3. Essence of the *N*-hydroxyl function

The bivalent nature of the Dxr active site metal demands an intact (retro)hydroxamate group in any (potential) inhibitor, for full coordination to this ion. As seen above, acyl chain modifications have not resulted in significantly improved activity of fosmidomycin/FR900098 analogues, even though they retain a carbonyl vicinal to an N-OH group, a feature that favors metal complexation. Hence it seems obvious that deleting the essential carbonyl and/or the N-OH will be detrimental for Dxr inhibitory activity.

Giessmann *et al.* synthesized a series of amidopropylphosphonates (**1.18**, Figure I.14), but none of these showed detectable *E. coli* Dxr inhibition when tested up to 30 μM, indicating the importance of the N-OH group for Dxr inhibition.¹⁴⁰ This was further proven by Woo *et al.* following the evaluation of compounds **1.19** wherein the N-OH was replaced with N-CH₃.¹⁷⁸ During the synthesis of α-substituted fosmidomycin analogues, Haemers *et al.* observed that benzyl removal from the retrohydroxamate moiety by catalytic hydrogenation typically resulted in the formation of the desired compound, but also significant amounts of the corresponding deoxygenated derivative, i.e., the amide, due to competitive “full” reduction.²⁰³ Deprotection of the phosphonate moiety of these deoxygenated products

afforded analogues such as **1.20**, which are moderately potent in inhibiting *E. coli* Dxr (**1.20**; $IC_{50} = 2.39 \mu\text{M}$, versus $0.030 \mu\text{M}$ for fosmidomycin and $0.31 \mu\text{M}$ for the corresponding *N*-acetyl retrohydroxamate) and capable of inhibiting the growth of a Dd2 *P. falciparum* strain at submicromolar concentrations. Merklé *et al.* showed that the propylphosphonate **1.21a**, aminopropylphosphonate **1.21b** and 3-acetamidopropylphosphonate **1.21c** inhibit EcDxr by at least a factor of 10^6 weaker than fosmidomycin, with the primary amine surprisingly emerging the best of all three compounds.¹⁷⁹

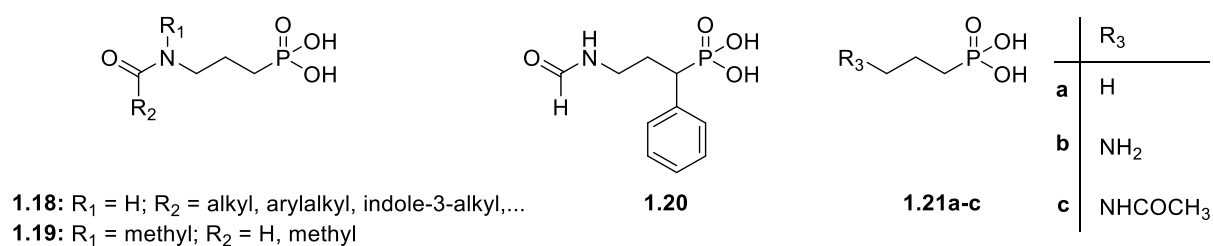


Figure I.14: *N*-hydroxyl-free fosmidomycin analogues.

Recently, the Rohmer group compared the EcDxr inhibition of compounds **1.22-1.24** (Figure I.15) to that of fosmidomycin (**1.1**) or the reverse hydroxamate counterpart of FR900098 (**1.6**) under two conditions: with and without pre-incubation of inhibitor and the enzyme before substrate addition and measurement of activity (Table I.3).²⁰⁴



Figure I.15: Hydroxamate modified fosmidomycin analogues.

They found that replacing the hydroxamate chelating group with a hydrazide as in **1.22** is detrimental for activity. A plausible explanation for this observation is that the hydrazide group is protonated at the pH of the enzymatic assays (pH 7.5) thereby reducing the chelating potency of the N-H with the Mg^{2+} ion. The *O*-methylated hydroxamate **1.23**, is similarly inactive against EcDxr. Contrary to the previously noted Dxr-inhibition superiority of *N*-methylated compounds over the non-methylated ones,¹⁹⁵ the interaction of the *O,N*-dimethylated compound **1.24** with Dxr is worse than that of its N-H hydroxamate analogue

1.23, probably by cause of the *O*-methyl group which is bulky enough (when present together with the *N*-methyl) to prevent binding by steric hindrance.

Table I.3: Inhibition of recombinant *E. coli* Dxr by fosmidomycin (**1.1**), reverse *N*-methylated phosphonohydroxamate (**1.6**) and chelating analogues **1.22-1.24**.

Compound	IC ₅₀ (μM) without pre-incubation	IC ₅₀ (μM) with pre-incubation (2 min)
1.1	0.25	0.032
1.6	0.5	0.048
1.22	1800	1000
1.23	11500	930
1.24	6900	3800

I.E.1.4. Isosteric replacement of the hydroxamate

In view of the aforementioned limitations associated with the hydroxamate moiety of **1.1** and **1.2**, many research groups have ventured the replacement of this pharmacophore with more lipophilic hydroxamate bioisosteres possessing improved bioavailability and/or metal-binding properties. Dxr is a metalloenzyme containing hard divalent metal ions (e.g., Mg²⁺) which are relatively nonpolarizable and have high charge-to-radius ratios. The active site ion therefore goes for hard ligands with oxygen being the most preferred coordinating atom, followed by nitrogen or sulfur, although the latter tend to coordinate to soft and more polarizable ions like zinc.²⁰⁵ Nakamura and co-workers showed that a *cis* arrangement of the two oxygen atoms of the hydroxamate group is required for effective metal chelation.¹³⁹ Furthermore, they suggested that alternative functional groups containing *cis* oxygen atoms might have comparable metal coordination ability.

Catechols **1.25a** and **1.25b** (Figure I.16) show IC₅₀ values of 24.8 μM and 4.5 μM, respectively, when tested for inhibition of EcDxr, indicating a preference for a 3,4- (**1.25b**) over a 2,3-substitution (**1.25a**) pattern.²⁰⁶ In search for lipophilic fosmidomycin analogues, Andaloussi *et al.* resynthesized **1.25b** alongside other hydroxamate modified compounds with a bulky heteroaryl moiety such as **1.25c** and the oxazolopyridinones **1.25d-e**.²⁰⁷ Compound **1.25b** displays a double-digit micromolar activity against MtbDxr (IC₅₀ = 41 μM),

but fails to show any activity against intact *M. tuberculosis*. Overall, tests conducted with these compounds revealed that steric constraint in the vicinity of the Dxr active site is deleterious to inhibitory potency. Other attempts to substitute the hydroxamate group of fosmidomycin with similar sterically demanding chelating moieties led to the conclusion that the Dxr active site is very narrow around the metal cation.^{208,209} Dithiocarbamates are well-known metal-complexing compounds.²¹⁰ However, compounds **1.25f** and **1.25g** were found unable to inhibit the activity of EcDxr ($IC_{50} > 1000 \mu M$),²⁰⁴ probably because in addition to the bulky nature of the supposed metal chelating group, the soft-base character of the sulfur atoms does not allow efficient coordination of hard cations such as Mg^{2+} .

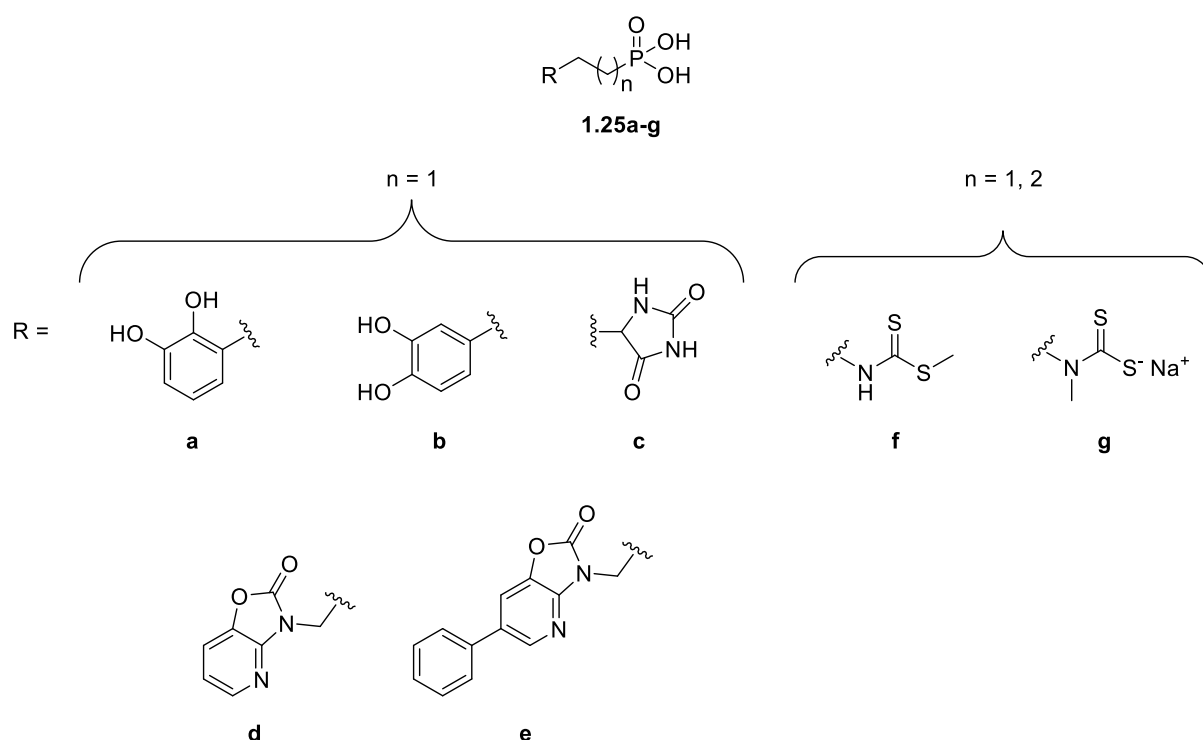


Figure I.16: Different chelating groups as hydroxamate substitutes.

Substituted phosphinic acids (e.g., **1.26** and **1.27**, Figure I.17)²¹¹ and the phosphonic acid group (as in **1.28**)²¹² have also been proposed as surrogates for the hydroxamic moiety of fosmidomycin. The former compounds are still to be tested for Dxr inhibition, but tests on different weed plants in a green house demonstrated insignificant *in vivo* activity. Installation of the phosphonic acid in **1.28** for metal chelation proved deleterious for Dxr inhibitory activity (IC_{50} PfDxr $> 300 \mu M$; IC_{50} EcDxr $> 500 \mu M$ versus $0.003 \mu M$ (PfDxr) and $0.12 \mu M$ (EcDxr) for its *N*-methyl hydroxamate counterpart (see below)).

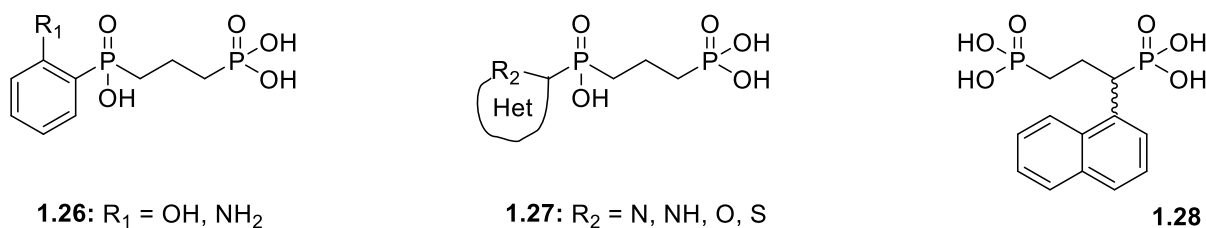


Figure I.17: Structures of fosmidomycin analogues bearing alternative metal chelating groups.

In sum, the above findings illustrate the importance of the hydroxamate group as the most effective bidentate metal binding group in Dxr inhibitors. Even if modifying this group is a delicate venture fraught with pitfalls, the door is not fully closed. Notably, the potential to increase lipophilicity through surrogate chelators and by designing bisubstrate ligands and the moderate activity of the catechol derivatives all suggest that exploiting chemical diversity could ultimately afford Dxr inhibitors that do not suffer from the liabilities of a hydroxamate group.

I.E.2. Modifications of the propyl spacer

Unlike the hydroxamate group of fosmidomycin and FR900098, the three-carbon chain has shown to be more suitable for derivatization and till date, analogues modified in this part are amongst the most potent Dxr inhibitors known. Modifications at the level of the carbon backbone might involve alteration of the chain length as well as introduction of substituents at different positions on the linker. Herewith, we present a synopsis of the main outcomes, with emphasis on the most promising analogues published.

I.E.2.1. Chain length variation

Although it has taken some time to arrive at this conclusion, a three-carbon chain is now universally accepted as the ideal length for linking the phosphonate warhead to the (retro)hydroxamate moiety in fosmidomycin analogues. Already in the 1980s, the research laboratories of Fujisawa reported changes in the carbon backbone. Ethylene analogues **1.29a-b** (Figure I.18) were synthesized and tested on a bacteria panel (*Staphylococcus aureus*, *Bacillus subtilis*, *Proteus vulgaris*, *Escherichia coli* and *Pseudomonas aeruginosa*) but show no antibiotic activity.²¹³ Zinglé *et al.* later attempted to adopt a two-methylene spacer for reverse hydroxamate analogues (**1.30a-b**) but this resulted in drastically decreased

inhibitory activity against EcDXR, whereas lengthening the spacer (**1.31a-b**) moderately decreased activity.¹⁹⁶ The group of Nakamura corroborated this finding with crystal structural analysis, which revealed that compounds with a shorter carbon chain cannot simultaneously occupy the phosphonate binding site and the hydroxamate binding site, while a longer carbon backbone in analogues prevents them from efficiently fitting into the active site.¹³⁹

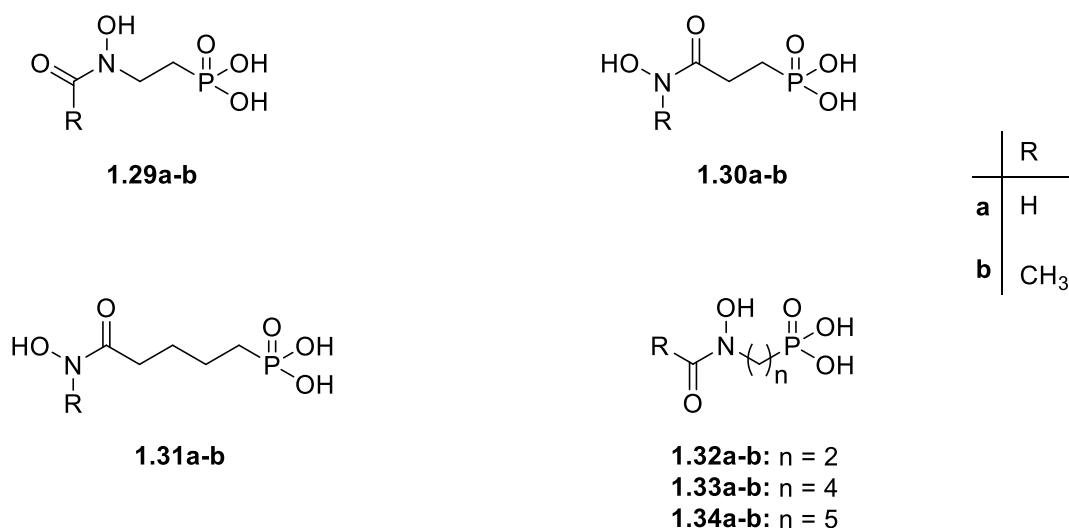


Figure I.18: Fosmidomycin analogues with different carbon chain lengths.

In an effort to examine what linker length was optimal, the Dowd group recently synthesized a series of compounds (amongst which **1.32a-b**, **1.33a-b** and **1.34a-b**) with two to five methylene units separating the nitrogen and phosphorus atoms.²¹⁴ When tested for the inhibition of MtbDxr, compounds with three methylene groups emerged as the most active (Table I.4). All compounds were unable to inhibit mycobacterial growth in nutrient-rich (7H9) or minimal (GAST) media, which was attributed to their high polarity, which diminishes penetration of the lipophilic mycobacterial cell wall.

Table I.4: Effect of chain length variation on MtbDxr inhibition and Mtb MIC.

Compound	R	n	MtbDxr IC ₅₀ , μ M
			(% inhibition at 100 μ M)
Fosmidomycin (1.1)	H	3	0.44
FR900098 (1.2)	CH ₃	3	2.39
1.32b	CH ₃	2	(74%)
1.33b	CH ₃	4	(80%)
1.34b	CH ₃	5	(86%)

I.E.2.2. Introduction of substituent(s) at the phosphonate α -carbon atom

Several studies have shown that the introduction of (preferably electron withdrawing) substituents to the α position of the phosphonate of fosmidomycin/FR900098 can significantly increase Dxr inhibitory activity. The hypothesis is that electron withdrawing substituents in α position decrease the pK_{a2} of the phosphonate group, which for that reason appears in its double-ionized form. The dianion species has been shown to act as an acceptor in the H-bond network, which is favorable for binding to and potent inhibition of Dxr.^{196,215} Fosfoxacin (**1.35**, Figure I.19), a natural antibiotic that was extracted for the first time in 1990 from *Pseudomonas fluorescens*, contains a phosphate group in place of the phosphonate in fosmidomycin.²¹⁶ Woo *et al.* showed that fosfoxacin and its acetyl congener (**1.36**) are significantly more potent inhibitors of *Synechocystis sp.* PCC6803 Dxr than fosmidomycin (K_i of 19 nM (**1.35**) and 2 nM (**1.36**) versus 57 nM for fosmidomycin).¹⁷⁸ Since the metabolic liability of the phosphate precludes its *in vivo* use as a Dxr inhibitor, α -substituents that tune the pKa of the more stable phosphonate in fosmidomycin/FR900098 analogues, to approximate that of a phosphate would be beneficial for activity.

**Figure I.19:** Phosphate analogues of fosmidomycin and FR900098.

Apart from influencing the acidity of the phosphonate, some (α -)substituents may also increase the overall lipophilicity, thereby possibly enhancing cellular uptake. Additionally, such substituents may form favorable interactions with Dxr residues possibly improving the anchoring of the inhibitor in the active site. The majority and most promising analogues known in this category bear α -aryl substituents, while a small set of α -halogenated analogues have also been reported, typically prepared and tested as racemates.

Groundwork by Haemers *et al.*²¹⁷ and subsequently by Devreux *et al.*²¹⁸ in our research group involved the synthesis of analogues such as **1.37** and **1.38** (Figure I.20), bearing a (substituted) phenyl ring in α -carbon. The potency of these compounds was related to the electron-withdrawing potential of groups introduced on the phenyl ring.

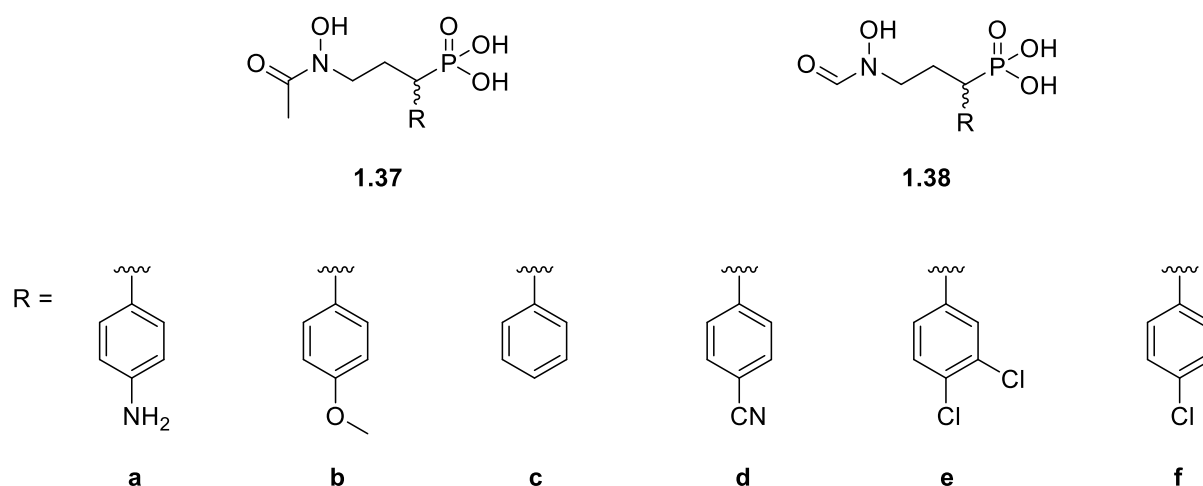


Figure I.20: Alpha-aryl substituted analogues of FR900098 and fosmidomycin.

The IC_{50} values of **1.37a** (3.60 μ M), **1.37b** (0.459 μ M), **1.37c** (0.311 μ M), **1.37d** (0.119 μ M), **1.37e** (0.119 μ M), and **1.37f** (0.099 μ M) against EcDxr illustrate this trend, although these compounds all show inferior potency compared to the parent compound FR900098 (0.030 μ M). Generally, the activity of the *N*-formyl analogues outperformed that of the *N*-acetyl counterparts, but also the *N*-formyl analogues (**1.38**) showed weaker activity against EcDxr than fosmidomycin and FR900098, except **1.38d** which was equipotent to fosmidomycin ($IC_{50} = 0.056 \mu$ M). Interestingly, when tested for their *in vitro* inhibition of *P. falciparum* growth, compounds **1.37b-f** all surpassed fosmidomycin's activity and among their *N*-formyl counterparts, **1.38e** performed best with a 12-fold increased inhibition with respect to

fosmidomycin. The dichloro derivatives **1.37e** (*N*-acetyl) and **1.38e** (*N*-formyl) were later evaluated against MtbDxr and displayed IC₅₀ values of 0.7 μM and 0.15 μM respectively, compared to fosmidomycin (0.08 μM) and FR900098 (0.16 μM).^{219,220}

Behrendt *et al.* synthesized and evaluated a series of reverse hydroxamate derivatives **1.39** (Figure I.21), with different substitution patterns at the α position.^{200,201} Once more, an inhibition discrepancy was observed between EcDxr and PfDxr, with the compounds performing inferior in the former compared to fosmidomycin, but surpassing the activity of this lead against PfDxr. The *N*-methylated compound bearing a (3,4-diF)Ph substituent outperformed both fosmidomycin and FR900098, displaying the most potent PfDxr inhibition (IC₅₀ = 3.0 nM versus 15 nM for FR900098) and *in vitro* *P. falciparum* (K1 strain) growth inhibition (IC₅₀ = 0.29 μM against 1.48 μM for FR900098).

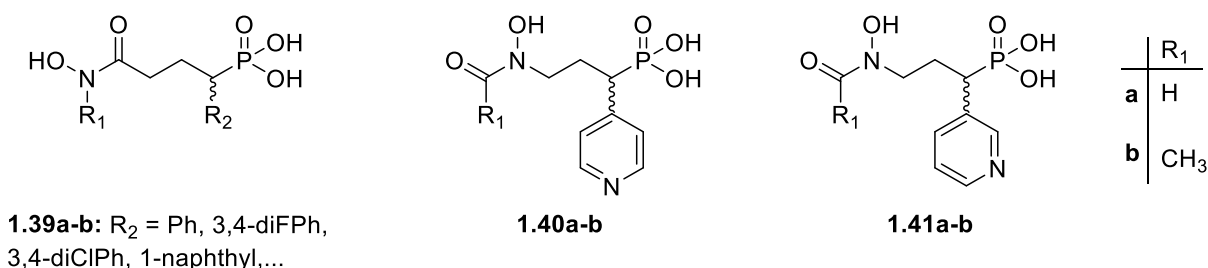


Figure I.21: Alpha-aryl substituted analogues of FR900098 and fosmidomycin, bearing a reverse hydroxamate.

As an extension of their work on a series of lipophilic, pyridine- or quinoline-containing phosphonates,^{194,221} the group of Song synthesized and tested analogues **1.40** and **1.41**, in anticipation that electron-deficient pyridines will do better than a (decorated) phenyl ring in modifying the phosphonate acidity.²²² Expectedly, the pyridine-containing fosmidomycin derivatives were found to be highly potent inhibitors of PfDxr (K_i values of 1.9-13 nM versus 21 nM for fosmidomycin), with the best one (**1.41b**) being approximately 11 times more active than fosmidomycin. However, except for **1.40a**, which was equipotent to fosmidomycin, these compounds showed an inferior EcDxr inhibition than the lead. These derivatives consistently outperform their phenyl counterparts (**1.37** and **1.38**) in the inhibition of both enzymes, and also potently block the proliferation of multidrug resistant *P. falciparum* with half maximal effective concentration (EC₅₀) values as low as 170 nM. The crystal structure of a quaternary complex with PfDxr shows that the pyridine moiety of **1.40b** is hosted in a rather hydrophobic cavity formed by the flexible loop, where the pyridine

nitrogen atom is also favorably engaged in a hydrogen bond with a thiol group of a cysteine residue.

Extensive crystallographic studies of various α -aryl derivatives in complex with EcDxr,²⁰¹ MtbDxr,^{219,221,223} and PfDxr²²² show that the active-site flap becomes disordered in these structures and the enzyme maintains an open conformation. This prevents the interaction of the indole ring of a highly conserved tryptophan residue (Trp211 in EcDxr, Trp203 in MtbDxr, and Trp296 in PfDxr) with the fosmidomycin backbone, as observed in earlier antibiotic-NADPH-active-site metal containing ternary complexes.^{139,163,174} The changes to the flap are a direct consequence of the mode of binding of these analogues to the Dxr active site, since extensive clashes would otherwise result with the indole ring's placement in the ternary complexes. Recent complexes of various α -aryl derivatives with PfDxr,^{212,224} however, show quite well-defined flaps (including the tryptophan); the substrate-binding site undergoes less drastic changes but has opened up sufficiently to accommodate the inhibitors. The major conformational changes make it difficult to pinpoint the precise cause of the enhanced potency of these α -aryl derivatives. This is further complicated by the low overall sequence homology between Dxrs from different pathogens, which makes that the activity of a particular compound can vary when tested on different enzymes.

Following the revelation that introduction of one or two fluorine atoms in the α -carbon (Figure I.22a) can enhance the potential of phosphonates as hydrolytically stable phosphate mimics,²²⁵ Verbruggen *et al.* ventured exchanging the bulky α -aryl substituents discussed above for sterically less demanding and electron-withdrawing halogens, to generate **1.42-1.44** (Figure I.22b) as analogues of FR900098.²²⁶ These compounds were evaluated *in vitro* against *P. falciparum* and *in vivo* in the *P. berghei* mouse model. *In vitro* (Table I.5), all three analogues showed submicromolar activity on two *P. falciparum* strains and appeared to be 5-to 6-fold more active than the parent compound fosmidomycin and slightly superior to FR900098 on the K1 strain. The promising *in vitro* activity of the α -fluorinated analogues **1.43** and **1.44** resonated in the *P. berghei* (GFP ANKA strain) acute mouse model, where the α -aryl fosmidomycin analogue **1.38e** failed to show significant *in vivo* activity despite its promising *in vitro* performance. These findings consolidate the view that electron withdrawing substituents, causing a decrease in phosphonate pKa, may favor the antimalarial activity of fosmidomycin analogues.

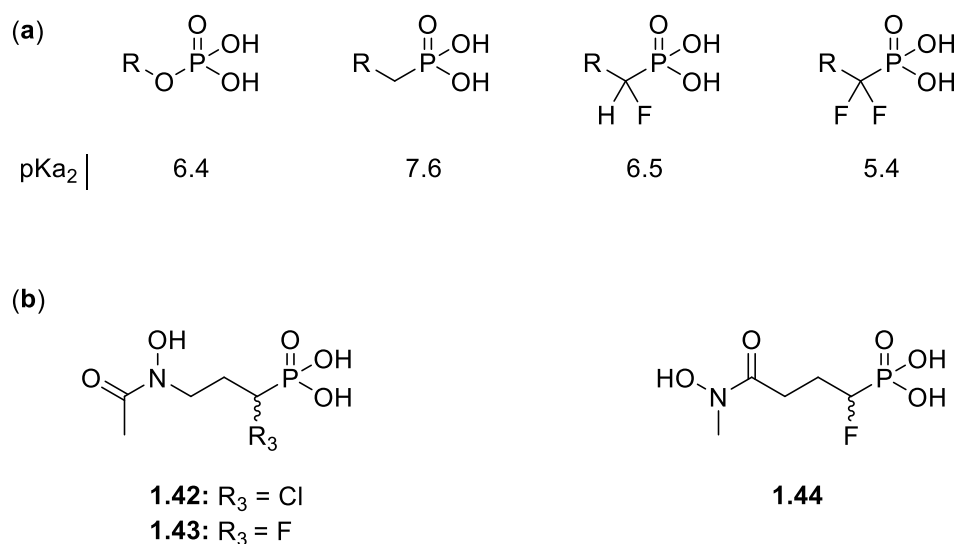


Figure I.22: Phosphonates as phosphate mimics in FR900098 analogues.^{225,226}

Table I.5: *In vitro* growth inhibition of the *P. falciparum* strains GHA and K1.

Compound	IC ₅₀ (μM)	
	Pf-GHA	Pf-K1
fosmidomycin (1.1)	nd	1.73 ± 0.89
FR900098 (1.2)	nd	0.42 ± 0.17
α-(3,4diCl)Ph analogue (1.38e)	0.60 ± 0.01	0.16 ± 0.01
1.42	0.82 ± 0.10	0.30 ± 0.06
1.43	0.70 ± 0.08	0.29 ± 0.06
1.44	0.73 ± 0.11	0.31 ± 0.07

nd = not determined

Alternatively, attempts to introduce alkyl substituents in the α-position of fosmidomycin or FR900098 have not been so rewarding. Analogues characterized by (hydroxy)alkyl **1.45**²²⁷ and arylmethyl **1.46**²²⁸ (Figure I.23) substituents in the α-position were synthesized and evaluated as bis-pivaloyloxymethyl (POM) ester prodrugs. When tested for their inhibition of *P. falciparum* 3D7 growth, a considerable loss of antimalarial activity was observed with the hydroxymethyl, ethyl, propyl, isopropyl, and dimethyl substituted bis-POM analogues (**1.45a-b**). Only the formyl- and acetyl-retrohydroxamate α-monomethyl analogues were

equipotent (97% growth inhibition at 25 μM) to the α -phenyl prodrug of fosmidomycin (**1.47**) and FR900098 (**1.49**).

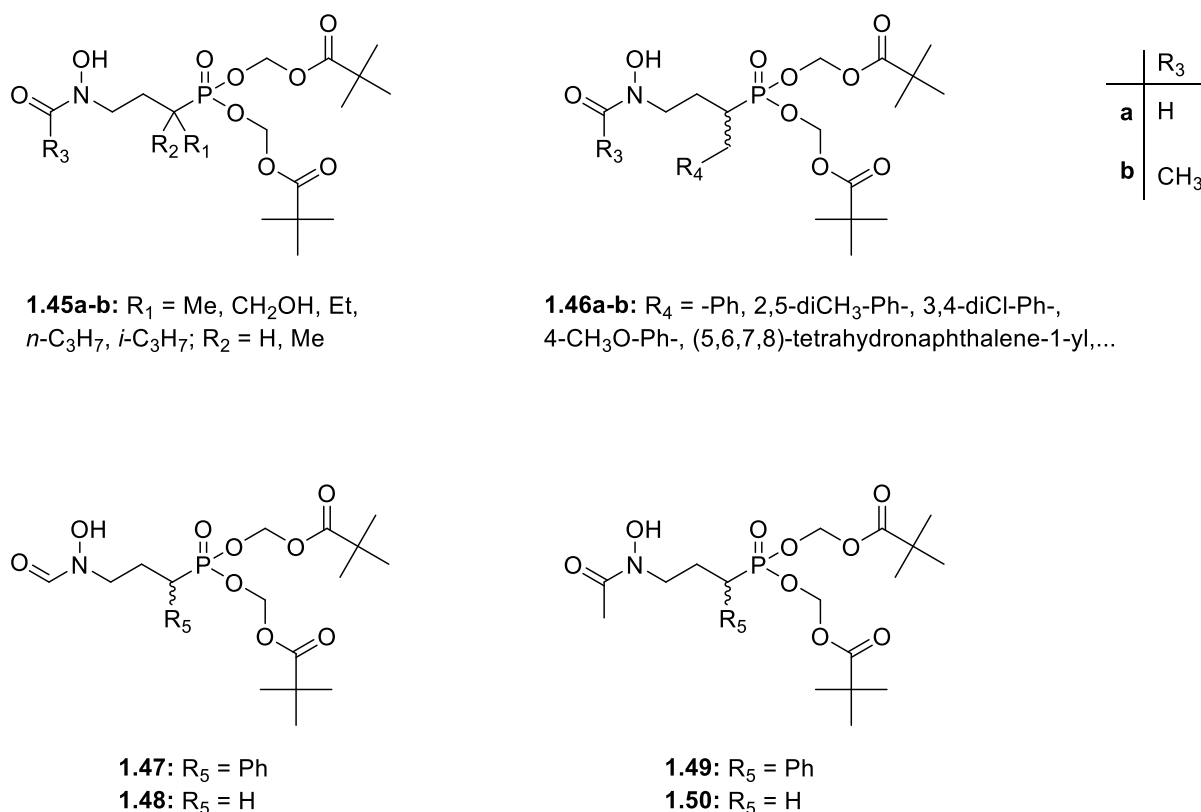


Figure I.23: (α -alkyl/aryl) prodrug derivatives of fosmidomycin and FR900098.

Electron-withdrawing substituents on the phenyl ring in analogues **1.46** improved the antiplasmodial activity, the *N*-formyl α -3,4-dichlorobenzyl derivative being the most potent of this series. With an IC₅₀ value of 0.9 μM , this compound was found to be about twice as active as the bis-POM ester of fosmidomycin (**1.48**, IC₅₀ = 2.1 μM), however, less active than the corresponding FR900098 prodrug (**1.50**, IC₅₀ = 0.4 μM). As observed before for α -aryl substituted analogues, electron-donating substituents lead to a significant reduction of antiplasmodial activity, while steric constraints probably impede the activity of the tetrahydronaphthyl derivative. Here again, the formyl derivatives were consistently more active than the corresponding acetyl derivatives.

I.E.2.3. Conformationally restricted analogues

In an effort to further explore SAR and to gain insight in the preferred conformation of fosmidomycin or to obtain more potent analogues, compounds **1.51-1.56** (Figure I.24) in

which a ring restricts the rotational freedom of the three-carbon chain in fosmidomycin or FR900098 have been synthesized. Locking of the spacer in a cyclopentyl ring revealed that the *trans*-isomer **1.51** is more potent (**a**, $IC_{50} = 0.20 \mu\text{M}$; **b**, $IC_{50} = 2.3 \mu\text{M}$) than its corresponding *cis*-isomer **1.52** (**a**, $IC_{50} = 2.3 \mu\text{M}$; **b**, $IC_{50} = 12 \mu\text{M}$), although inferior to both fosmidomycin ($IC_{50} = 0.029 \mu\text{M}$) and FR900098 ($IC_{50} = 0.035 \mu\text{M}$) with respect to EcDxr inhibition.²⁰³ The racemic formyl analogues outperformed their acetyl counterparts.

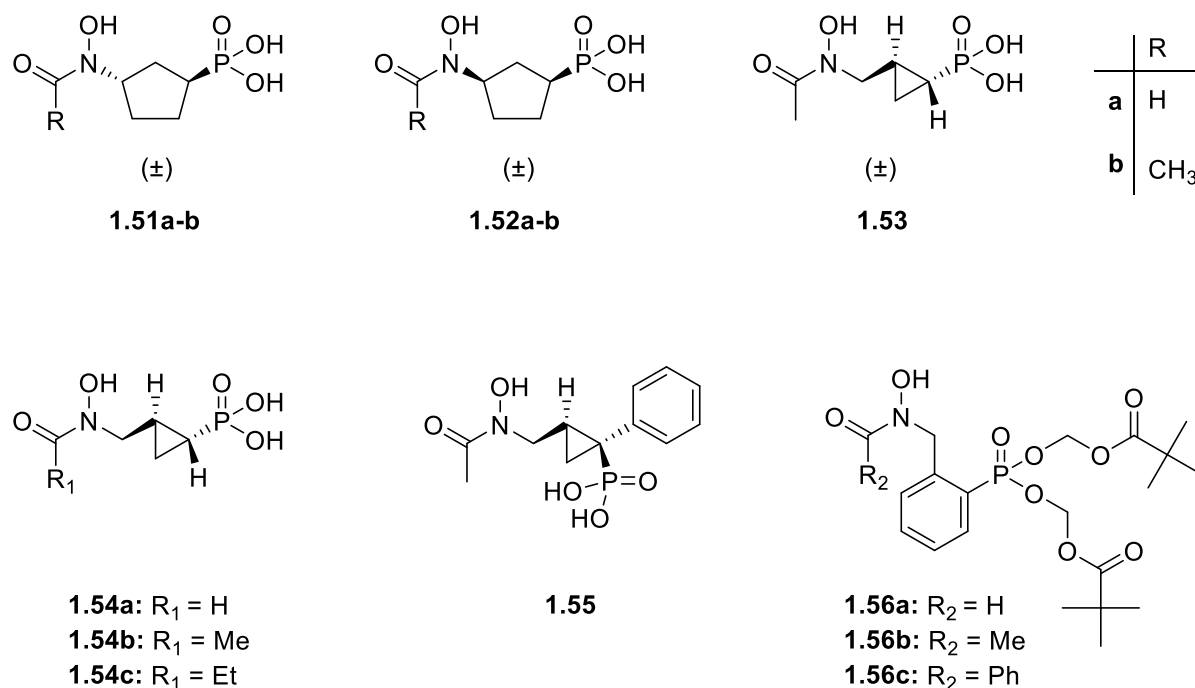


Figure I.24: Conformationally restricted fosmidomycin/FR900098 analogues.

Likewise, incorporation of the α,β -bond in a cyclopropyl unit and evaluation of EcDxr and *P. falciparum* growth inhibition,²²⁹ learned that the racemic *trans*-cyclopropane **1.53** inhibits EcDxr in the submicromolar range ($IC_{50} = 0.16 \mu\text{M}$). Interestingly, the enantiomerically pure (1*R*,2*S*)-analogue (**1.54b**) shows EcDxr inhibitory activity comparable to that of fosmidomycin and proves also equipotent as a *P. falciparum* inhibitor. Introduction of an *N*-formyl group (**1.54a**) leads to an 8-fold drop in activity, while the *N*-propionyl moiety (**1.54c**) performs even poorer. The superior activity of the *N*-acetyl **1.54b** with respect to the *N*-formyl derivative **1.54a** is consistent with the biological activity of fosmidomycin and FR900098, but contrary to the trend observed for the cyclopentyl-constrained analogues **1.51** and **1.52**. The *cis*-cyclopropane analogue **1.55**, featuring a phenyl ring in α -position fails to significantly inhibit EcDxr ($IC_{50} > 30 \mu\text{M}$). Kurz *et al.* prepared and tested the bis-POM analogues **1.56a-c**,

but unlike the 'flexible' α -aryl-substituted analogues discussed in section I.E.2.2., these conformationally restrained aromatic analogues exhibit only moderate *in vitro* antimalarial activity against the chloroquine-sensitive strain 3D7 of *P. falciparum*.²³⁰ The most active derivative **1.56c** displays an IC_{50} value of 47 μ M. The intrinsic flexibility of the Dxr active site seems to call for some degree of rotational freedom in potential inhibitors. In order to examine the effect of unsaturation within the propyl chain on MtbDxr inhibition and cell growth, Jackson *et al.*,²¹⁴ prepared and evaluated the α/β -unsaturated FR900098 analogues **1.57a-c** (Figure I.25).

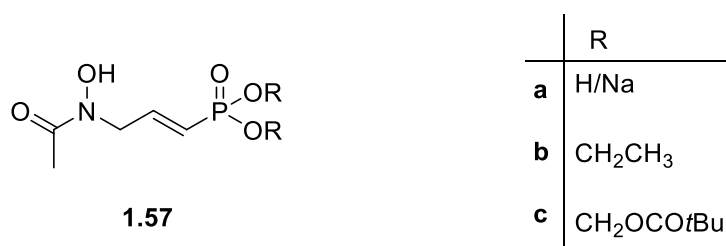


Figure I.25: Fosmidomycin analogues characterized by unsaturation within the propyl chain. They found that the free phosphonic acid (**1.57a**) and its more lipophilic pivaloyl ester (**1.57c**) show higher potency than the parent compound (FR900098) on Mtb Dxr inhibition and antitubercular activity.

I.E.3. Modifications of the phosphonate functionality

I.E.3.1. Phosphonate isosteres

Under physiological conditions, fosmidomycin's charged polar phosphonate group significantly contributes to its poor oral efficacy and prevents penetration across very highly lipophilic cell walls, such as that found in Mtb. With the aim of abating these shortcomings, numerous attempts have been made to replace this group with less polar alternatives, which can adopt the role of H-bonding-acceptor in the DOXP phosphate binding site of Dxr.

For the fact that rapid *in vivo* inactivation by phosphatases precludes the clinical development of fosfoxacin (**1.35**) and its acetyl congener (**1.36**), Woo *et al.* attempted to substitute the phosphonate moiety in fosmidomycin with a carboxylate (**1.58**, Figure I.26) or sulfamate (**1.59**).¹⁷⁸ The group of Rohmer later added the reverse hydroxamate analogues **1.60-1.61** and the sulfonates **1.62** to this list.¹⁹⁶ However, all these efforts resulted in a dramatic loss in Dxr inhibition compared to fosmidomycin. The H-bonding essential for Dxr

binding is possibly not conserved for these analogues since contrary to the phosphonate group which can potentially bind as a mono- or dianion, the carboxylate can only form a mono anion and the sulfamate is neutral. Furthermore, the planar carboxylic acid is not an effective mimic of the tetrahedral phosphonic acid. Attempts to address the geometric requirement in possible phosphonate isosteres resulted in analogues such as the (aryl)alkylsulfones (**1.63**) and the sulfonamides **1.64**,²¹⁵ but also, these compounds fail to show significant inhibitory activity against EcDxr.

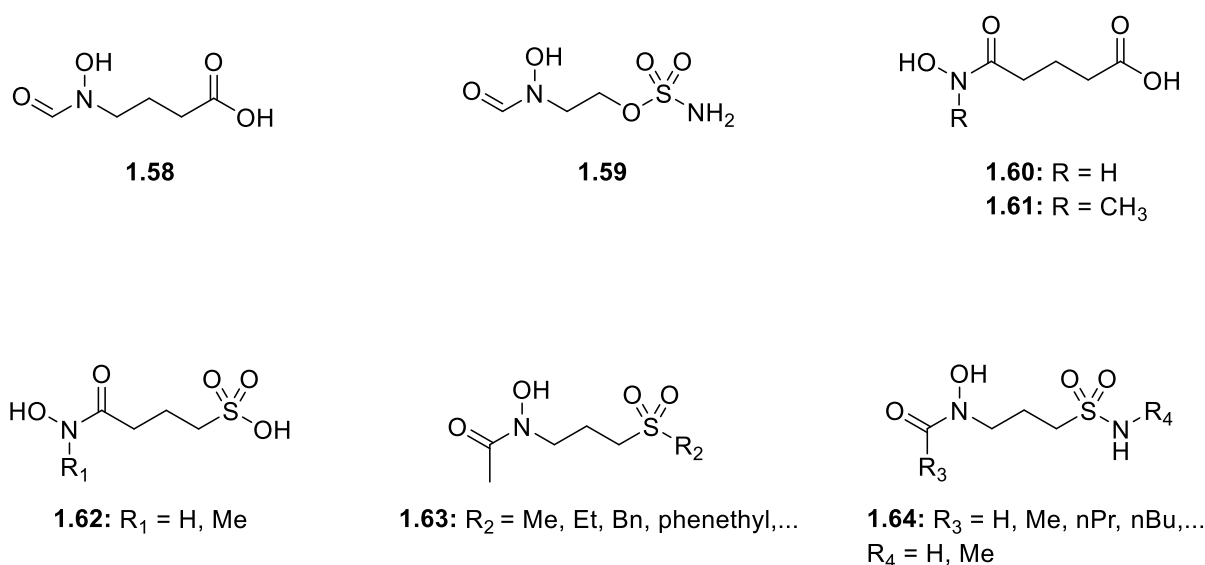


Figure I.26: Fosmidomycin and FR900098 analogues based on phosphonate omission.

Recently, Van Aerschot and coworkers reported analogues **1.65-1.66** (Figure I.27) in which the phosphonate of fosmidomycin/FR900098 is substituted with an *N*-acylated sulfonamide group.²³¹ They contended that the acidic N-H moiety of acylated sulfonamides (pK_a ≈ 2.5) will result in a negative charge *in vivo* and could thus at least partially restore interaction with Dxr in analogy with the activity noted for phosphonate monoesters,²¹⁵ while the uptake of these analogues could be improved.

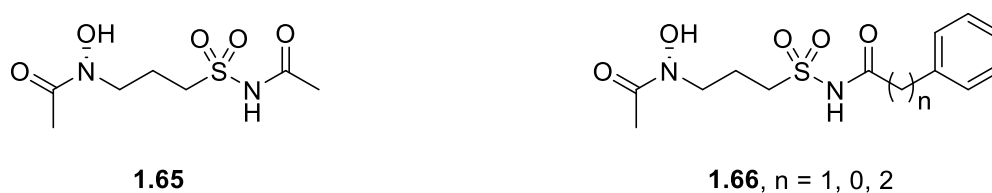


Figure I.27: *N*-Acylated sulfonamides as potential phosphonate isosteres.

Unfortunately, also this effort turned out fruitless as the residual EcDxr enzymatic activity remained $\pm 100\%$ for concentrations of **1.65-1.66** up to 100 μM . The compounds also failed to demonstrate antimicrobial activity at 64 μM . These findings make clear that there is little room for substituting the fosmidomycin phosphonate moiety.

I.E.3.2. Prodrug strategy

Extensive literature has accumulated on the attempts to mask the charged phosphonate group of fosmidomycin/FR900098 or analogues thereof, in an effort to achieve passive permeation through cellular membranes. This could avoid dependence on active transport systems such as the transporter used by apicomplexans like *P. falciparum*. Indeed, mutation of this carrier is a known mechanism of fosmidomycin resistance.¹⁸⁶ Additionally, passive diffusion would allow to target NMP-dependent organisms that lack such transport systems. For a successful application of this approach, the prodrug must be robust enough to survive the gastrointestinal tract milieu until absorption into the systemic circulation where, it must also remain intact long enough for intracellular distribution. Hydrolysis of the protective group by non-specific esterases inside the cell, would release the active inhibitor.

The first-generation prodrugs of FR900098 were structurally simple aryl phosphonates. Reichenberg *et al.* demonstrated that out of a series of aryl prodrugs **1.67a-c** (Figure I.28), the bis-(4-methoxyphenyl) diester **1.67c** was the best, outperforming FR900098 when both were administered orally in mice infected with *P. vinckei* and equipotent to this lead during intraperitoneal (ip) administration.²³² Hydrolysis of the phosphonic ester generates the desired phosphonate and the (substituted) phenol component. Concerns over the toxicity of the phenol derivatives, motivated the development of alternative protecting groups. Work on more functionalized lipophilic moieties including acyloxyalkyl- and alkyloxycarbonyloxyalkyl-ester analogues was introduced by Ortmann *et al.* and later expanded for fosmidomycin by the groups of Kurz and Dowd (**1.68**, Figure I.29).^{227,228,230,233,234,235,236}

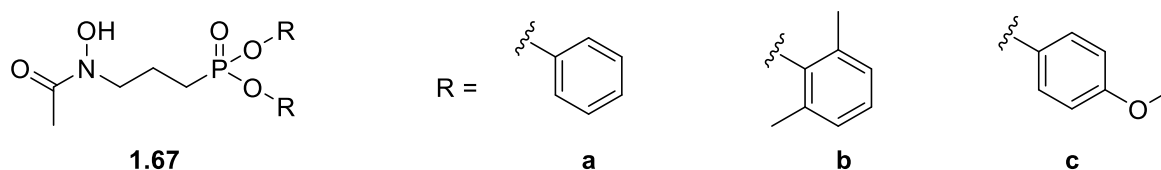
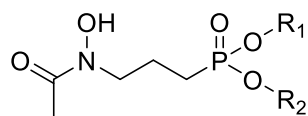


Figure I.28: Diaryl FR900098 prodrugs.

Generally, hydrolysis of such groups in the cell would release a hemiketal, which will spontaneously break down into an aldehyde and the active form of the inhibitor.²³⁷ In case the acyloxy group and the phosphonate O are connected via a methylene group, a hemiacetal of formaldehyde is formed upon esterase action, followed by rapid conversion to formaldehyde (Figure I.30). To avoid the formation of formaldehyde during hydrolysis, other analogues were prepared. Several of the lipophilic esters showed improved antimalarial activity relative to fosmidomycin and FR900098. The Dowd group tested some of these analogues against a panel of organisms, particularly Gram (+) bacteria including *M. tuberculosis* and found their activity to be enhanced, compared to the phosphonate leads. While diethyl fosmidomycin showed little antibacterial activity, activity against these organisms generally increased with increasing size of the lipophilic ester. Interestingly, analogs with a secondary ester did not outperform their primary counterparts possibly because the cellular esterase does not tolerate additional bulk adjacent to the phosphonate ester.

Recently Kurz and co-workers reported a systematic comparison of phosphonate and phosphonate-hydroxamate double prodrugs of reverse fosmidomycin derivatives.²³⁸ For the modification of the phosphonate motif, they used acyloxymethyl- and alkoxycarbonyloxymethyl ester groups while simple esters, carbonates, and carbamates were used to mask the hydroxamate (**1.70**, Figure I.31). When assayed for inhibition of PfDxr, none of the prodrugs caused detectable enzyme inhibition, understandably because all prodrugs appear too bulky to get accommodated at the Dxr active site. Moreover, the double prodrugs are unable to chelate the essential divalent metal ion of Dxr. Several phosphonate prodrugs and double prodrugs were found to inhibit the multiplication of *P. falciparum* blood stages with IC₅₀ values in the single-digit nanomolar range (IC₅₀ values versus Pf Dd2: 4-9 nM). Their inhibitory efficacy exceeds that of the parent free phosphonic acid **1.69** by about 1 order of magnitude. With few exceptions (e.g., **1.71** IC₅₀ = 4 nM, the most active compound from the study), they found that the additional derivatization of the hydroxamic acid group led to reduced antiplasmodial activity versus strain Dd2. The introduction of a morpholine-containing carbamate for instance, resulted in complete loss of antiplasmodial activity.



1.68

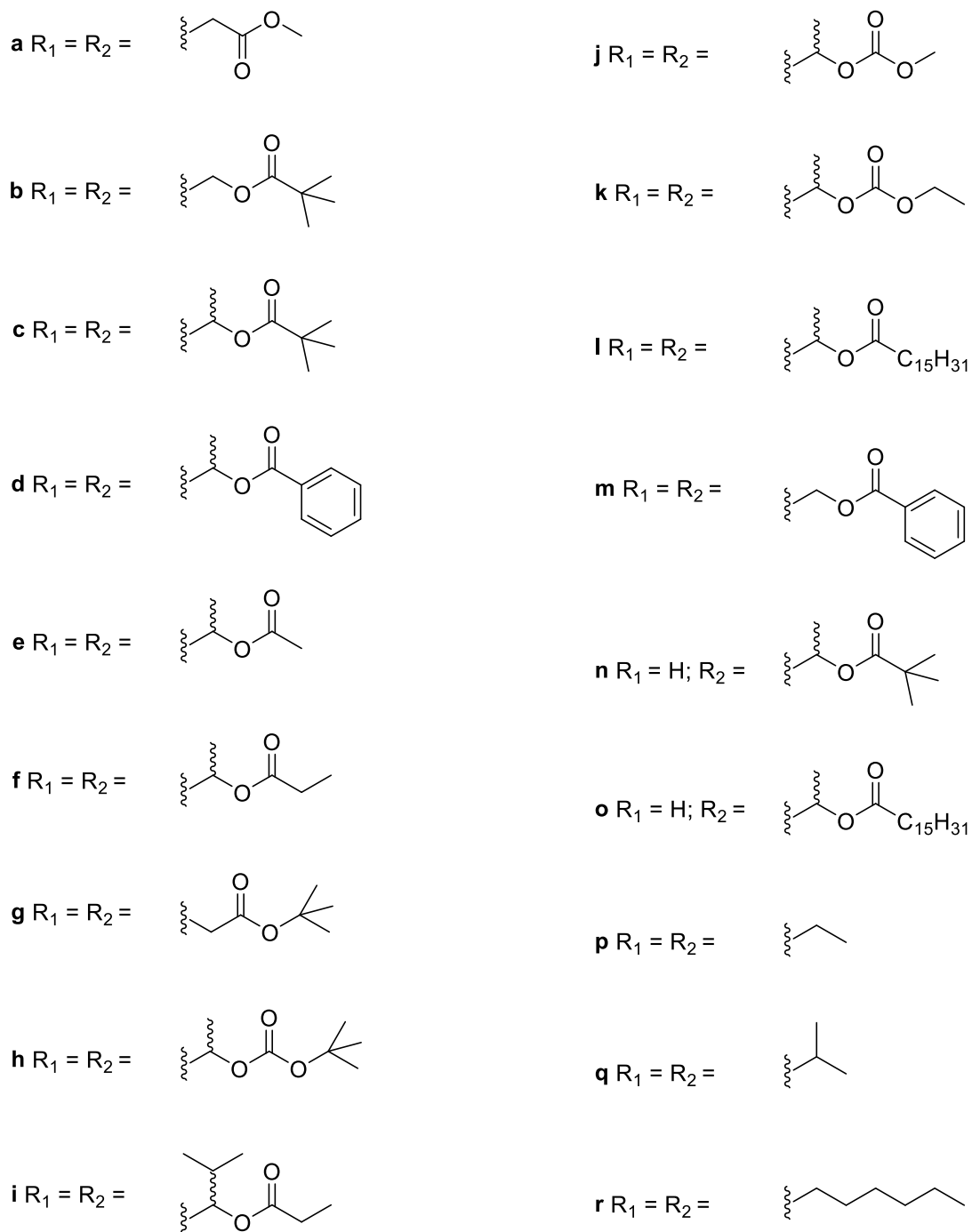


Figure I.29: Overview of reported acyloxyalkyl- and alkyloxycarbonyloxyalkyl-ester prodrugs of FR900098.

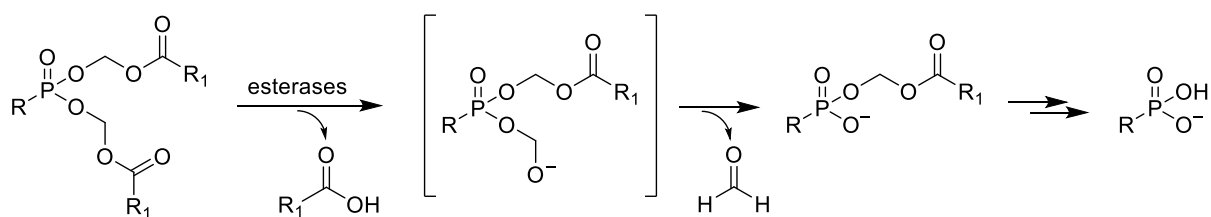


Figure I.30: Hypothetical sequence of reactions for bioactivation of phosphonate prodrugs.

Likely, hydrolytic cleavage is a limiting factor responsible for the observed reduction of antiparasmodial activity caused by several modifiers of the hydroxamate motif.

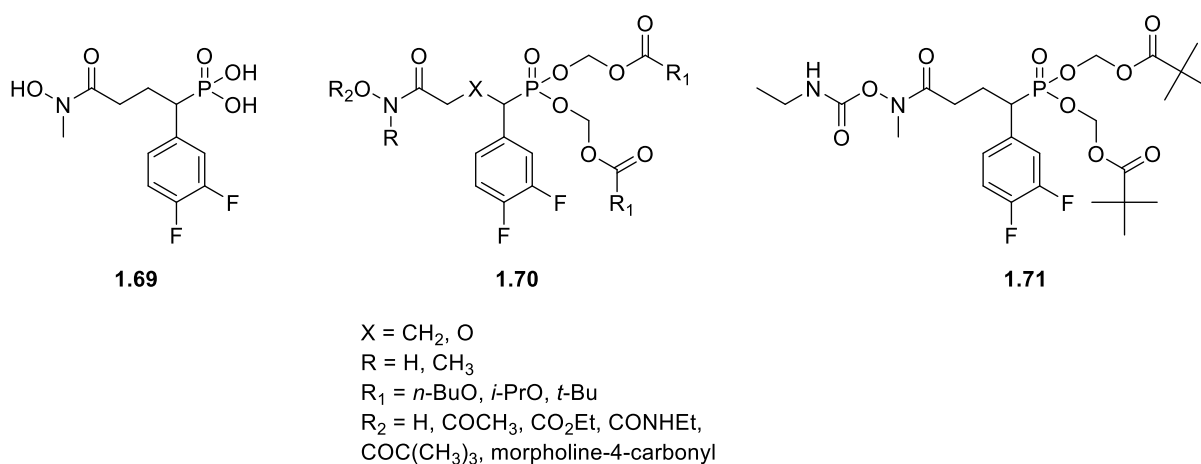


Figure I.31: Prodrugs of reverse fosmidomycin analogues.

I.E.4. Overview of fosmidomycin SAR and conclusions

The trends elaborated in the previous sections regarding the SAR of fosmidomycin and its analogues are summarized in Figure I.32. In spite of the many constraints that must be dealt with in designing new inhibitors, the biological activity of some published analogues still raises questions as to how far one may go into the venture. Notably, analogues such as **1.72-1.77** (Figure I.33), lacking either the hydroxamate or the phosphonate group have been reported to unexpectedly show interesting biological activity. Deng *et al.* used coordination chemistry and structure based design to access **1.72**, a strong, lipophilic Dxr inhibitor with broad antibacterial activity and structurally distinct from fosmidomycin.²⁰⁶ Even though **1.73** and **1.74** are fragments of one of the most potent known Dxr inhibitors (**1.38e**, EcDxr IC₅₀ = 0.059 μM), both show weak Dxr inhibition.¹⁹⁴

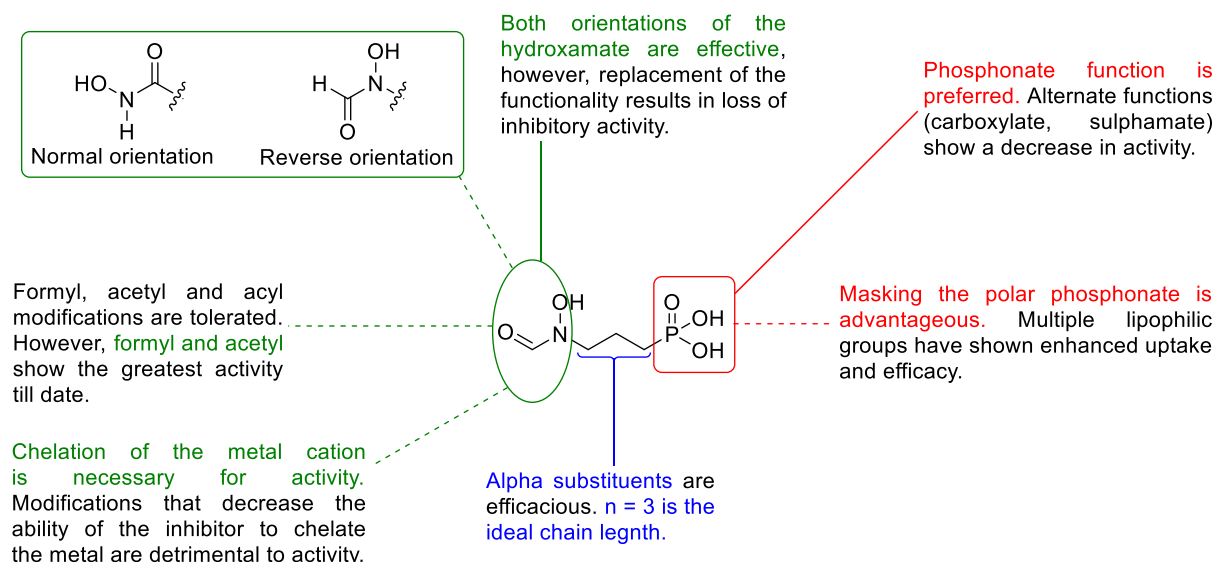


Figure I.32: Structure activity relationships of fosmidomycin analogues.

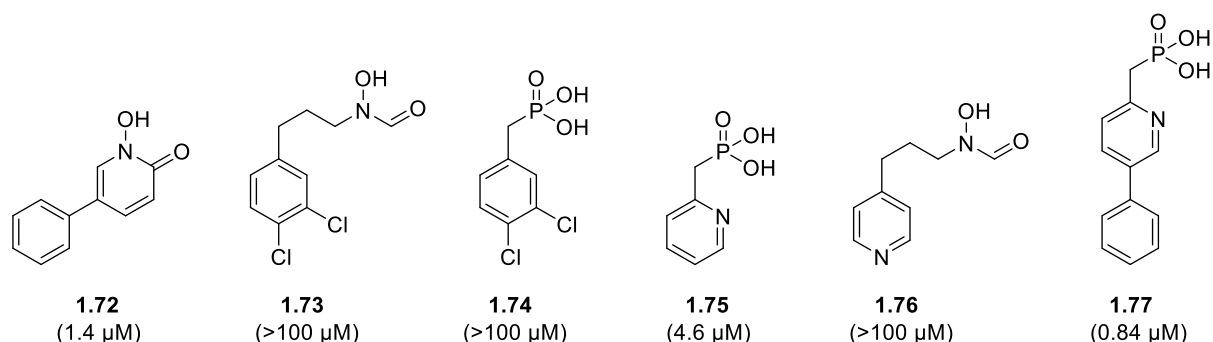


Figure I.33: Structures of Dxr inhibitors, together with their IC_{50} values against *E. coli* Dxr in Parentheses.

Crystallographic studies on the pyridyl analogue **1.75** revealed that its binding to EcDxr is sustained by π - π -stacking interactions between the pyridyl ring and the indole ring of Trp211 of the Dxr flexible loop. This is further strengthened by charge transfer, an event that does not occur with the 3,4-dichloro fragments **1.73** and **1.74**. A similar outcome is to be expected for **1.76**, but it seems the absence of the phosphonate group is deleterious to activity. X-ray studies on compound **1.77** showed that the conformation of Trp211 (EcDxr) in the Dxr/**1.77** complex is different (compared to fosmidomycin binding), with the indole ring flipped almost 180° . This orientation could allow the 5-phenylpyridine group of the inhibitor to undergo more π - π stacking and hydrophobic interactions with the indole, which might account for the enhanced activity of **1.77**. Even if some of the results trickled in

serendipitously, the activity of these 'unclassical' analogues suggests that there may be more gaps in the current SAR data of fosmidomycin and that there is much room for exploring new inhibitors. Amendment of the three-carbon spacer has so far proven to be beneficial but not exhaustive. Exploration of new analogues will mine more SAR information as well as offer the opportunity to access potent, druglike Dxr inhibitors.

REFERENCES

1. Singh, B.; Sung, K. L.; Matusop, A.; Radhakrishnan, A.; Shamsul, S. S.; Cox-Singh, J.; Thomas, A.; Conway, D. J. A large focus of naturally acquired *Plasmodium knowlesi* infections in human beings. *Lancet* **2004**, 363, 1017–1024.
2. Vythilingam, I.; Tan, C. H.; Asmad, M.; Chan, S. T.; Lee, K. S.; Singh, B. Natural transmission of *Plasmodium knowlesi* to humans by *Anopheles latens* in Sarawak, Malaysia. *Trans. R. Soc. Trop. Med. Hyg.* **2006**, 100, 11, 1087–1088.
3. Martens, P.; Kovats, R. S.; Nijhof, S.; De Vries, P.; Livermore, M. T. J.; Bradley, D. J.; Cox, J.; McMichael, A. J. Climate change and future populations at risk of malaria. *Global Environ. Chang.* **1999**, 9, S89–S107.
4. Mendis, K.; Sina, B. J.; Marchesini, P.; Carter, R. The neglected burden of *Plasmodium vivax* malaria. *Am. J. Trop. Med. Hyg.* **2001**, 64, 97–106.
5. Mayxay, M.; Pukrittayakamee, S.; Newton, P. N.; White, N. J. Mixed-species malaria infections in humans. *Trends Parasitol.* **2004**, 20, 5, 233–240.
6. Coetzee, M.; Fontenille, D. Advances in the study of *Anopheles funestus*, a major vector of malaria in Africa. *Insect Biochem. Molec. Biol.* **2004**, 34, 599–605.
7. Tanner, M.; Greenwood, B.; Whitty, C. J. M.; Anshah, E. K.; Price, R. N.; Dondorp, A. M.; Von Seidlein, L.; Baird, J. K.; Beeson, J. G.; Fowkes, F. J. I.; Hemingway, J.; Marsh, K.; Osier, F. Malaria eradication and elimination: views on how to translate a vision into reality. *BMC Medicine* **2015**, 13, 167.
8. Delves, M.; Plouffe, D.; Scheurer, C.; Meister, S.; Wittlin, S.; Winzeler, E. A.; Sinden, R. E.; Leroy, D. The activities of current antimalarial drugs on the life cycle stages of *Plasmodium*: A comparative study with human and rodent parasites. *PLoS Med* **2012**, 9, 2, e1001169.
9. Ferreira, M. U.; Da Silva, N. M.; Wunderlich, G. Antigenic diversity and immune evasion by malaria parasites. *Clin. Diagn. Lab. Immun.* **2004**, 11, 6, 987–995.
10. Borst, P.; Genest, P. A. Switching like for like. *Nature* **2006**, 439, 926–927.
11. Kirk, K. Membrane transport in the malaria-infected erythrocyte. *Physiol. Rev.* **2001**, 81, 2, 495–537.

12. Lee, P.; Ye, Z.; Van Dyke, K.; Kirk, R. G. X-ray microanalysis of *Plasmodium falciparum* and infected red blood cells: effects of qinghaosu and chloroquine on potassium, sodium, and phosphorus composition. *Am. J. Trop. Med. Hyg.* **1988**, 39, 2, 157–165.
13. Saliba, K. J.; Martin, R. E.; Broer, A.; Henry, R. I.; McCarthy, C. S.; Downie, M. J.; Allen, R. J. W.; Mullin, K. A.; McFadden, G. I.; Broer, S.; Kirk, K. Sodium-dependent uptake of inorganic phosphate by the intracellular malaria parasite. *Nature* **2006**, 443, 582–585.
14. Aidoo, M.; Terlouw, D. J.; Kolczak, M. S.; McElroy, P. D.; Kuile, F. O. T.; Kariuki, S.; Nahlen, B. L.; Lal, A. A.; Udhayakumar, V. Protective effects of the sickle cell gene against malaria morbidity and mortality. *The Lancet* **2002**, 359, 1311–1312.
15. Miller, L. H.; Mason, S. J.; Clyde, D. F.; McGinniss, M. H. The resistance factor to *Plasmodium vivax* in blacks. The Duffy-blood-group genotype, FyFy.N. *Engl. J. Med.* **1976**, 295, 6, 302–304.
16. Pasvol, G. Eroding the resistance of Duffy negativity to invasion by *Plasmodium vivax*? *Trans. R. Soc. Trop. Med. Hyg.* **2007**, 101, 953–954.
17. Ménarda, D.; Barnadasa, C.; Bouchier, C.; Henry-Halldin, C.; Gray, L. R.; Ratsimbaoa, A.; Thonier, V.; Carod, J. F.; Domarle, O.; Colin, Y.; Bertrand, O.; Picot, J.; King, C. L.; Grimberg, B. T.; Mercereau-Puijalon, O.; Zimmerman, P. A. *Plasmodium vivax* clinical malaria is commonly observed in Duffy-negative Malagasy people. *PNAS* **2010**, 107, 13, 5967–5971.
18. Day, K. P.; Marsh, K. Naturally acquired immunity to *Plasmodium falciparum*. *Parasitol. Today* **1991**, 7, 3, 68–71.
19. Pinkevych, M.; Petravic, J.; Chelimo, K.; Kazura, J. W.; Moormann, A. M.; Davenport, M. P. The Dynamics of naturally acquired immunity to *Plasmodium falciparum* infection. *PLOS Comput. Biol.* **2012**, 8, 10, e1002729.
20. Doolan, D. L.; Dobano, C.; Baird, J. K. Acquired immunity to malaria. *Clin. Microbio. Rev.* **2009**, 22, 1, 13–36.
21. RTS,S Clinical Trials Partnership. Efficacy and safety of RTS,S/AS01 malaria vaccine with or without a booster dose in infants and children in Africa: final results of a phase 3, individually randomized, controlled trial. *Lancet* **2015**, 385, 1581.
22. Alonso, P. L.; Sacarlal, J.; Aponte, J. J. *et al.* Efficacy of the RTS,S/AS02A vaccine against *Plasmodium falciparum* infection and disease in young African children: randomized controlled trial. *The Lancet* **2004**, 364, 9443, 1411–1420.

23. Alonso, P. L.; Sacarlal, J.; Aponte, J. J. *et al.* Duration of protection with RTS,S/AS02A malaria vaccine in prevention of *Plasmodium falciparum* disease in Mozambican children: single-blind extended follow-up of a randomized controlled trial. *Lancet* **2005**, 366, 9502, 2012–2018.
24. Sacarlal, J.; Aide, P.; Aponte, J. J. *et al.* Long-term safety and efficacy of the RTS,S/AS02A malaria vaccine in Mozambican children. *J. Infect. Dis.* **2009**, 200, 3, 329–336.
25. Kawamoto, F.; Kumada, N. Fluorescent probes for detection of protozoan parasites. *Parasitol. Today* **1987**, 3, 9, 284–286.
26. Kawamoto, F. Rapid diagnosis of malaria by fluorescence microscopy with light microscope and interference filter. *The Lancet* **1991**, 337, 8735, 200–202.
27. Pieroni, P.; Mills, C. D.; Ohrt, C.; Harrington, M. A.; Kain, K. C. Comparison of the ParaSight™-F test and the ICT Malaria Pf™ test with the polymerase chain reaction for the diagnosis of *Plasmodium falciparum* malaria in travellers. *Trans. R. Soc. Trop. Med. Hyg.* **1998**, 92, 2, 166–169.
28. Foley, M.; Tilley, L., Quinoline antimalarials: mechanisms of action and resistance and prospects for new agents. *Pharmacol. Ther.* **1998**, 79, 1, 55–87.
29. Loria, P.; Miller, S.; Foley, M.; Tilley, L., Inhibition of the peroxidative degradation of haem as the basis of action of chloroquine and other quinoline antimalarials. *Biochem. J.* **1999**, 339, 363–370.
30. Nzila, A.; Ward, S. A.; Marsh, K.; Sims, P. F. G.; Hyde, J. E., Comparative folate metabolism in humans and malaria parasites (part I): pointers for malaria treatment from cancer chemotherapy. *Trends Parasitol.* **2005**, 21, 292–298.
31. Olliaro, P. Mode of action and mechanisms of resistance for antimalarial drugs. *Pharmacol. Therapeut.* **2001**, 89, 207–219.
32. Saifi, M. A.; Beg, T.; Harrath, A. H.; Altayalan, F. S. H.; Al Quraishy, S. Antimalarial drugs: Mode of action and status of resistance. *Afr. J. Pharm. Pharmacol.* **2013**, 7, 5, 148–156.
33. Skinner, T. S.; Manning, L. S.; Johnston, W. A.; Davis, T. M. *In vitro* stage-specific sensitivity of *Plasmodium falciparum* to quinine and artemisinin drugs. *Int. J. Parasitol.* **1996**, 26, 5, 519–525.
34. Kumar, N.; Zheng, H. Stage-specific gametocytocidal effect *in vitro* of the antimalaria drug qinghaosu on *Plasmodium falciparum*. *Parasitol. Res.* **1990**, 76, 214–218.

-
35. Scott, M. D.; Meshnick, S. R.; Williams, R. A.; Chiu, D. T.; Pan, H. C.; Lubin, B. H.; Kuypers, F. A. Qinghaosu-mediated oxidation in normal and abnormal erythrocytes. *J. Lab. Clin. Med.* **1989**, 114, 401–406.
36. Meshnick, S. R.; Thomas, A.; Ranz, A.; Xu, C. M.; Pan, H. Z., Artemisinin (qinghaosu): the role of intracellular hemozoin in its mechanism of antimalarial action. *Mol. Biochem. Parasitol.* **1991**, 49, 2, 181–189.
37. Fry, M.; Pudney, M. Site of action of the antimalarial hydroxynaphthoquinone, 2 [trans-4-(4'-chlorophenyl)cyclohexyl]-3-hydroxy-1,4-naphthoquinone(566C80). *Biochem. Pharmacol.* **1992**, 43, 7, 1545–1553.
38. Vaidya, A. B.; Lashgari, M. S.; Polog, L. G.; Morrisey, J. Structural features of *Plasmodium* cytochrome b that may underlie susceptibility to 8-aminoquinolines and hydroxynaphthoquinones. *Mol. Biochem. Parasit.* **1993**, 58, 1, 33–42.
39. Srivastava, I. K.; Rottenberg, H.; Vaidya, A. B. Atovaquone, a broad spectrum antiparasitic drug, collapses mitochondrial membrane potential in a malarial parasite. *J. Biol. Chem.* **1997**, 272, 7, 3961–3966.
40. Fichera, M.; Roos, D. A plastid organelle as a drug target in apicomplexan parasites. *Nature* **1997**, 390, 407–409.
41. Kain, K. C.; Shanks, G. D.; Keystone, J. S. Malaria chemoprophylaxis in the age of drug resistance. I. currently recommended drug regimens. *Clin. Infect. Dis.* **2001**, 33, 226–234.
42. Ejaz, A.; Haq Nawaz, K.; Hussain, Z.; Butt, R. Awan, Z. I.; Bux, H. Treatment of uncomplicated *Plasmodium falciparum* malaria with quinine-doxycycline combination therapy. *J. Pak. Med. Assoc.* **2007**, 57, 10, 502–505.
43. © World Health Organization. Update on artemisinin resistance. April **2011**. [<http://www.who.int/malaria/publications/atoz/arupdate042012.pdf?ua=1>].
44. Lell, B.; Kremsner, P. G. Clindamycin as an antimalarial drug: review of clinical trials *Antimicrob. Agents Chemother.* **2002**, 46, 8, 2315–2320.
45. World Health Organization. WHO World Malaria Report **2014**; http://www.who.int/malaria/publications/world_malaria_report_2014/en/ (accessed on February 11, 2015).

46. Vestergaard, L. S.; Ringwald, P. Responding to the challenge of antimalarial drug resistance by routine monitoring to update national malaria treatment policies. *Am. J. Trop. Med. Hyg.* **2007**, *77*, 6, 153–159.
47. Thaithong, S. Clones of different sensitivities in drug-resistant isolates of *Plasmodium falciparum*. *Bull. World Health Organ.* **1983**, *61*, 4, 709–712.
48. Peter B. Bloland, P. B. Drug resistance in malaria. WHO/CDS/CSR/DRS/2001.4.
49. Cui, L.; Mharakurwa, S.; Ndiaye, D.; Rathod, P. K.; Rosenthal, P. J. Antimalarial drug resistance: Literature review and activities and findings of the ICEMR network. *Am. J. Trop. Med. Hyg.* **2015**, *93*, 3, 57–68.
50. Croft, A. M.; Whitehouse, D. P.; Cook, G. C.; Beer, M. D. Safety evaluation of the drugs available to prevent malaria. *Expert. Opin. Drug Saf.* **2002**, *1*, 19–27.
51. Cox, A. D.; Der, C. J. Ras family signaling: therapeutic targeting. *Cancer Biol. Ther.* **2002**, *1*, 6, 599–606.
52. Nallan, L.; Bauer, K. D.; Bendale, P.; Rivas, K.; Yokoyama, K.; Horney, C. P.; Pendyala, P. R.; Floyd, D.; Lombardo, L. J.; Williams, D. K.; Hamilton, A.; Sebti, S.; Windsor, W. T.; Weber, P. C.; Buckner, F. S.; Chakrabarti, D.; Gelb, M. H.; Van Voorhis, W. C. Protein farnesyltransferase inhibitors exhibit potent antimalarial activity. *J. Med. Chem.* **2005**, *48*, 3704–3713.
53. Eastman, R. T.; White, J.; Hucke, O.; Bauer, K.; Yokoyama, K.; Nallan, L.; Chakrabarti, D.; Verlinde, C. L.; Gelb, M. H.; Rathod, P. K.; Van Voorhis, W. C. Resistance to a protein farnesyltransferase inhibitor in *Plasmodium falciparum*. *J. Biol. Chem.* **2005**, *280*, 13554–13559.
54. Rosenthal, P. J. Antimalarial drug discovery: old and new approaches. *J. Exp. Biol.* **2003**, *206*, 3735–3744.
55. Laufer, M. K.; Thesing, P. C.; Eddington, N. D.; Masonga, R.; Dzinjalama, F. K.; Takala, S. L.; Taylor, T. E.; Plowe, C. V. Return of chloroquine antimalarial efficacy in Malawi. *N. Engl. J. Med.* **2006**, *355*, 19, 1959–1966.
56. Laufer, M. K.; Takala-Harrison, S.; Dzinjalama, F. K.; Stine, O. C.; Taylor, T. E.; Plowe, C. V. Return of chloroquine-susceptible falciparum malaria in Malawi was a re- expansion of diverse susceptible parasites. *J. Infect. Dis.* **2010**, *202*, 5, 801–808.

-
57. Spangenberg, T.; Burrows, J. N.; Kowalczyk, P.; McDonald, S.; Wells, T. N. C.; Willis, P. The open access Malaria Box: a drug discovery catalyst for neglected diseases. *PLoS One* **2013**, *8*, 6, e62906.
58. Kaufmann, S. H. E.; Hess, J. Impact of intracellular location of and antigen display by intracellular bacteria: implications for vaccine development. *Immunol. Lett.* **1999**, *65*, 81–84.
59. Schlesinger, L. S. Macrophage phagocytosis of virulent but not attenuated strains of *Mycobacterium tuberculosis* is mediated by mannose receptors in addition to complement receptors. *J. Immunol.* **1993**, *150*, 2920–2930.
60. Russell, D. G. Who puts the tubercle in tuberculosis? *Nat. Rev. Microbiol.* **2007**, *5*, 39–47.
61. Fenton, M. J.; Vermeulen, M. W. Immunopathology of tuberculosis: roles of macrophages and monocytes. *Infect. Immun.* **1996**, *64*, 683–690.
62. Armstrong, J. A.; Hart, P. D. Phagosome-lysosome interactions in cultured macrophages infected with virulent tubercle bacilli: reversal of the usual nonfusion pattern and observations on bacterial survival. *J. Exp. Med.* **1975**, *142*, 1–16.
63. Ferrari, G.; Langen, H.; Naito, M.; Pieters, J. A coat protein on phagosomes involved in the intracellular survival of mycobacteria. *Cell* **1999**, *97*, 435–447.
64. Meena, L. S.; Rajni. Survival mechanisms of pathogenic *Mycobacterium tuberculosis* H₃₇Rv. *FEBS Journal* **2010**, *277*, 2416–2427.
65. McNerney, R.; Maeurer, M.; Abubakar, I. *et al.* Tuberculosis diagnostics and biomarkers: needs, challenges, recent advances, and opportunities. *J. Infect. Dis.* **2012**, *205*, S147–S158.
66. Zumla, A.; Raviglione, M.; Hafner, R.; Von Reyn, C. F. Tuberculosis. *N. Engl. J. Med.* **2013**, *368*, 8, 745–755.
67. Hopewell, P. C.; Pai, M.; Maher, D.; Uplekar, M.; Raviglione, M. C. International standards for tuberculosis care. *Lancet Infect. Dis.* **2006**, *6*, 11, 710–725.
68. Schatz, A.; Waksman, S. A. Effect of streptomycin and other antibiotic substances upon *Mycobacterium tuberculosis* and related organisms. *Proc. Soc. Exp. Biol. Med.* **1944**, *57*, 2, 244–248.
69. Waksman, S. A. Streptomycin: Background, isolation, properties and utilization. *Science* **1953**, *118*, 259–266.

70. Lehmann, J. *para*-Aminosalicylic acid in the treatment of tuberculosis. *The Lancet* **1946**, 247, 15–16.
71. Cohn, M. I.; Middlebrook, G.; Russell, W. F. J. Combined drug treatment of tuberculosis. I. Prevention of emergence of mutant populations of tubercle bacilli resistant to both streptomycin and isoniazid in vitro. *J. Clin. Invest.* **1959**, 38, 8, 1349–1355.
72. Iseman, M. D. Evolution of drug-resistant tuberculosis: A tale of two species. *Proc. Natl. Acad. Sci. USA* **1994**, 91, 2428–2429.
73. Honore, N.; Cole, S. T. Streptomycin resistance in mycobacteria. *Antimicrob. Agents Chemother.* **1994**, 38, 2, 238–242.
74. Guidance for national tuberculosis programmes on the management of tuberculosis in children-2nd ed. World Health Organization **2014**. (Guidance_NTP_on_Management_of_TB_in_Children.pdf).
75. © World Health Organization. WHO policy on collaborative TB/HIV activities. Geneva, **2012** (http://whqlibdoc.who.int/publications/2012/9789241503006_eng.pdf).
76. Martinson, N. A.; Barnes, G. L.; Moulton, L. H.; Msandiwa, R.; Hausler, H.; Ram, M.; McIntyre, J. A.; Gray, G. E.; Chaisson, R. E. New regimens to prevent tuberculosis in adults with HIV infection. *N. Engl. J. Med.* **2011**, 365, 11–20.
77. Sterling, T. R.; Villarino, M. E.; Borisov, A. S.; Shang, N.; Gordin, F.; Bliven-Sizemore, E.; Hackman, J.; Hamilton, C. D.; Menzies, D.; Kerrigan, R. N.; Weis, S. E.; Weiner, M.; Wing, D.; Conde, M. B.; Bozeman, L.; Horsburgh, R.; Chaisson, R. E. Three months of rifapentine and isoniazid for latent tuberculosis infection. *N. Engl. J. Med.* **2011**, 365, 2155–2166.
78. Janin, Y. L. Antituberculosis drugs: Ten years of research. *Bioorg. Med. Chem.* **2007**, 15, 2479–2513.
79. Mitchison, D. A. Role of individual drugs in the chemotherapy of tuberculosis. *Int. J. Tuberc. Lung Dis.* **2000**, 4, 9, 796–806.
80. Caminero, J. A.; Sotgiu, G.; Zumla, A.; Migliori, G. B. Best drug treatment for multidrug-resistant and extensively drug-resistant tuberculosis. *Lancet Infect. Dis.* **2010**, 9, 621–629.
81. Chen, S.; Huai, P.; Wang, X.; Zhong, J.; Wang, X.; Wang, K.; Wang, L.; Jiang, S.; Li, J.; Peng, Y.; Ma, W. Risk factors for multidrug resistance among previously treated patients with tuberculosis in eastern China: a case–control study. *Int. J. Infect. Dis.* **2013**, 17, e1116–e1120.

-
82. American Thoracic Society/Centers for Disease Control and Prevention/Infectious Diseases Society of America: Treatment of tuberculosis. *Am. J. Respir. Crit. Care Med.* **2003**, 167, 603–662.
83. Pablos-Méndez, A.; Knirsch, C. A.; Barr, R. G.; Lerner, B. H.; Frieden, T. R. Nonadherence in tuberculosis treatment: predictors and consequences in New York City. *Am. J. Med.* **1997**, 102, 2, 164–170.
84. Kaona, F. A.; Tuba, M.; Siziya, S.; Sikaona, L. An assessment of factors contributing to treatment adherence and knowledge of TB transmission among patients on TB treatment. *BMC Public Health* **2004**, 4, 68.
85. Dheda, K.; Gumbo, T.; Gandhi, N. R.; Murray, M.; Theron, G.; Udwadia, Z.; Migliori, G. B.; Warren, R. Global control of tuberculosis: from extensively drug-resistant to untreatable tuberculosis. *Lancet Respir. Med.* **2014**; 2, 321–338.
86. World Health Organization. Global tuberculosis report **2014**. http://www.who.int/tb/publications/global_report/en/ (accessed on April 7, 2015).
87. Colditz, G. A.; Brewer, T. F.; Berkey, C. S.; Wilson, M. E.; Burdick, E.; Fineberg, H. V.; Mosteller, F. Efficacy of BCG vaccine in the prevention of tuberculosis. Meta-analysis of the published literature. *JAMA* **1994**, 271, 9, 698–702.
88. Zheng, W.; Thorne, N.; McKew, J. C. Phenotypic screens as a renewed approach for drug discovery. *Drug Discov. Today* **2013**, 18, 21/22, 1067–1073.
89. Swinney, D. C. Phenotypic vs. target-based drug discovery for first-in-class medicines. *Clin. Pharmacol. Ther.* **2013**, 93, 4, 299–301.
90. Swinney, D. C.; Anthony, J. How were new medicines discovered? *Nat. Rev. Drug Discov.* **2011**, 10, 507–519.
91. Chen, X. P.; Du, G. H. Target validation: a door to drug discovery. *Drug Discov. Ther.* **2007**, 1, 23–29.
92. Overington, J. P.; Al-Lazikani, B.; Hopkins, A. L. How many drug targets are there? *Nat. Rev. Drug Discov.* **2006**, 5, 12, 993–996.
93. Lundstrom, K. An overview on GPCRs and drug discovery: Structure-based drug design and structural biology on GPCRs. *Methods Mol. Biol.* **2009**, 552, 51–66.
94. Lindsay, M. A. Target discovery. *Nat. Rev. Drug Dis.* **2003**, 2, 10, 831–838.

95. Hughes, J. P.; Rees, S.; Kalindjian, S. B.; Philpott, K. L. Principles of early drug discovery. *Br. J. Pharmacol.* **2011**, 162, 1239–1249.
96. Summons, R. E.; Jahnke, L. L.; Hope, J. M.; Logan, G. A. 2-Methylhopanoids as biomarkers for cyanobacterial oxygenic photosynthesis. *Nature* **1999**, 400, 554–557.
97. Brocks, J. J.; Logan, G. A.; Buick, R.; Summons, R. E. Archean molecular fossils and the early rise of eukaryotes. *Science* **1999**, 285, 5430, 1033–1036.
98. Lange, B. M.; Rujan, T.; Martin, W.; Croteau, R. Isoprenoid biosynthesis: the evolution of two ancient and distinct pathways across genomes. *Proc. Natl. Acad. Sci. USA* **2000**, 97, 13172–13177.
99. Sacchettini, J. C.; Poulter, C. D. Creating isoprenoid diversity. *Science* **1997**, 277, 5333, 1788–1789.
100. Holstein, S. A.; Hohl, R. J. Isoprenoids: Remarkable diversity of form and function. *Lipids* **2004**, 39, 4, 293–309.
101. Ruzicka, L. The isoprene rule and the biogenesis of terpenic compounds. *Experientia* **1953**, 9, 10, 357–367.
102. Ruzicka, L. The isoprene rule and the biogenesis of terpenic compounds. 1953. *Experientia* **1994**, 50, 4, 395–405.
103. Amdur, B. H.; Rilling, H.; Bloch, K. The enzymatic conversion of mevalonic acid to squalene. *J. Am. Chem. Soc.* **1957**, 79, 10, 2646–2647.
104. Katsuki, H.; Bloch, K. Studies on the biosynthesis of ergosterol in yeast: Formation of methylated intermediates. *J. Biol. Chem.* **1967**, 242, 2, 222–227.
105. Lynen, F. Biosynthetic pathways from acetate to natural products. *Pure Appl. Chem.* **1967**, 14, 1, 137–167.
106. Banthorpe, D. V.; Charlwood, B. V.; Francis, M. J. O. Biosynthesis of monoterpenes. *Chem. Rev.* **1972**, 72, 2, 115–155.
107. Alberts, A. W.; Chen, J.; Kuron, G. *et al.* Mevinolin: A highly potent competitive inhibitor of hydroxymethylglutaryl-coenzyme A reductase and a cholesterol-lowering agent. *Proc. Natl. Acad. Sci. U S A.* **1980**, 77, 7, 3957–3961.
108. Bach, T. J.; Lichtenthaler, H. K. Inhibition by mevinolin of plant growth, sterol formation and pigment accumulation. *Physiol. Plant.* **1983**, 59, 1, 50–60.

-
109. Treharne, K. J.; Mercer, E. I.; Goodwin, T. W. Incorporation of [¹⁴C]carbon dioxide and [2-¹⁴C]mevalonic acid into terpenoids of higher plants during chloroplast development. *Biochem. J.* **1966**, 99, 239–245.
110. Zhou, D.; White, R. H. Early steps of isoprenoid biosynthesis in *Escherichia coli*. *Biochem. J.* **1991**, 273, 627–634.
111. Rohmer, M.; Knani, M.; Simonin, P.; Sutter, B.; Sahm, H. Isoprenoid biosynthesis in bacteria: a novel pathway for the early steps leading to isopentenyl diphosphate. *Biochem. J.* **1993**, 295, 2, 517–524.
112. Eisenreich, W.; Schwarz, M.; Cartayrade, A.; Arigoni, D.; Zenk, M. H.; Bacher, A. The deoxyxylulose phosphate pathway of terpenoid biosynthesis in plants and microorganisms. *Chem. Biol.* **1998**, 5, 9, R221–R233.
113. Lois L. M.; Campos N, Putra, S. R.; Danielsen, K.; Rohmer, M. Boronat, A. Cloning and characterization of a gene from *Escherichia coli* encoding a transketolase-like enzyme that catalyzes the synthesis of D-1-deoxyxylulose 5-phosphate, a common precursor for isoprenoid, thiamin, and pyridoxol biosynthesis. *Proc. Natl. Acad. Sci. U S A.* **1998**, 95, 5, 2105–2110.
114. Takahashi, S.; Kuzuyama, T.; Watanabe, H.; Seto, H. A 1-deoxy-D-xylulose 5 - phosphate reductoisomerase catalyzing the formation of 2-C-methyl-D-erythritol 4 phosphate in an alternative nonmevalonate pathway for terpenoid biosynthesis. *Proc. Natl. Acad. Sci. U S A.* **1998**, 95, 17, 9879–9884.
115. Rohdich, F.; Wungsintaweekul, J.; Fellermeier, M.; Sagner, S.; Herz, S.; Kis, K.; Eisenreich, W.; Bacher, A.; Zenk, M. H. Cytidine 5'-triphosphate-dependent biosynthesis of isoprenoids: YgbP protein of *Escherichia coli* catalyzes the formation of 4-diphosphocytidyl 2-C-methylerythritol. *Proc. Natl. Acad. Sci. U S A.* **1999**, 96, 21, 11758–11763.
116. Luttgen, H.; Rohdich, F.; Herz, S.; Wungsintaweekul, J.; Hecht, S.; Schuhr, C. A.; Fellermeier, M.; Sagner, S.; Zenk, M. H.; Bacher, A.; Eisenreich, W. Biosynthesis of terpenoids: YchB protein of *Escherichia coli* phosphorylates the 2-hydroxy group of 4 diphosphocytidyl-2C-methyl-D-erythritol. *Proc. Natl. Acad. Sci. U S A.* **2000**, 97, 3, 1062–1067.
117. Herz, S.; Wungsintaweekul, J.; Schuhr, C. A.; Hecht, S.; Luttgen, H.; Sagner, S.; Fellermeier, M.; Eisenreich, W.; Zenk, M. H.; Bacher, A.; Rohdich, F. Biosynthesis of

terpenoids: YgbB protein converts 4-diphosphocytidyl-2C-methyl-D-erythritol 2-phosphate to 2C-methyl-D-erythritol 2,4-cyclodiphosphate. *Natl. Acad. Sci. U S A.* **2000**, 97, 6, 2486–2490.

118. Hecht, S.; Eisenreich, W.; Adam, P.; Amslinger, S.; Kis, K.; Bacher, A.; Arigoni, D.; Rohdich, F. Studies on the nonmevalonate pathway to terpenes: The role of the GcpE (IspG) protein. *Proc. Natl. Acad. Sci. U S A* **2001**, 98, 26, 14837–14842.

119. Rohdich, F.; Hecht, S.; Gartner, K.; Adam, P.; Krieger, C.; Amslinger, S.; Arigoni, D.; Bacher, A.; Eisenreich, W. Studies on the nonmevalonate terpene biosynthetic pathway: Metabolic role of IspH (LytB) protein. *Proc. Natl. Acad. Sci. U S A.* **2002**, 99, 3, 1158–1163.

120. Putra, S. R.; Disch, A.; Bravo, J. M.; Rohmer, M. Distribution of mevalonate and glyceraldehyde-3-phosphate/pyruvate routes for isoprenoid biosynthesis in some Gram-negative bacteria and mycobacteria. *FEMS Microbiol. Lett.* **1998**, 164, 1, 169–175.

121. Testa, C. A.; Brown, M. J. The methylerythritol phosphate pathway and its significance as a novel drug target. *Curr. Pharm. Biotechnol.* **2003**, 4, 4, 248–259.

122. Rohmer, M.; Grosdemange-Billiard, C.; Seemann, M.; Tritsch, D. Isoprenoid biosynthesis as a novel target for antibacterial and antiparasitic drugs. *Curr. Opin. Investig. Drugs* **2004**, 5, 2, 154–162.

123. Wilding, E. I.; Brown, J. R.; Bryant, A. P.; Chalker, A. F.; Holmes, D. J.; Ingraham, K. A.; Iordanescu, S.; So, C. Y.; Rosenberg, M.; Gwynn, M. N. Identification, evolution, and essentiality of the mevalonate pathway for isopentenyl diphosphate biosynthesis in Gram-positive Cocci. *J. Bacteriol.* **2000**, 182, 15, 4319–4327.

124. Jomaa, H.; Wiesner, J.; Sanderbrand, S.; Altincicek, B.; Weidemeyer, C.; Hintz, M.; Turbachova, I.; Eberl, M.; Zeidler, J.; Lichtenthaler, H. K.; Soldati, D.; Beck, E. Inhibitors of the non-mevalonate pathway of isoprenoid biosynthesis as antimalarial drugs. *Science* **1999**, 285, 5433, 1573–1576.

125. Shanmugasundram, A.; Gonzalez-Galarza, F. F.; Wastling, J. M.; Vasieva, O.; Jones, A. R. Library of Apicomplexan Metabolic Pathways: a manually curated database for metabolic pathways of apicomplexan parasites. *Nucleic Acids Res.* **2012**, 1–8.

126. Rohmer, M. The discovery of a mevalonate-independent pathway for isoprenoid biosynthesis in bacteria, algae and higher plants. *Nat. Prod. Rep.* **1999**, 16, 565–574.

-
127. Seto, H.; Watanabe, H.; Furihata, K. Simultaneous operation of the mevalonate and non-mevalonate pathways in the biosynthesis of isopentenyl diphosphate in *Streptomyces aeriovifer*. *Tetrahedron Lett.* **1996**, 37, 44, 7979–1982.
128. Boucher, Y.; Doolittle, W. F. The role of lateral gene transfer in the evolution of isoprenoid biosynthesis pathways. *Mol. Microbiol.* **2000**, 37, 4, 703–716.
129. Odom, A. R. Five questions about non-mevalonate isoprenoid biosynthesis. *PLoS Pathog.* **2011**, 7, 12, e1002323.
130. Van der Meer, J. Y.; Hirsch, A. K. H. The isoprenoid-precursor dependence of *Plasmodium* spp. *Nat. Prod. Rep.* **2012**, 29, 721–728.
131. Heuston, S.; Begley, M.; Gahan, C. G. M; Hill, C. Isoprenoid biosynthesis in bacterial pathogens. *Microbiology* **2012**, 158, 1389–1401.
132. Hirsch, A. K. H.; Diederich, F. The non-mevalonate pathway to isoprenoid biosynthesis: A potential source of new drug targets. *Chimia* **2008**, 62, 4, 226–230.
133. Hale, I.; O'Neill, P. M.; Berry, N. G.; Odom, A.; Sharma, R. The MEP pathway and the development of inhibitors as potential anti-infective agents. *MedChemComm* **2012**, 3, 418–433.
134. Hunter, W. N. The non-mevalonate pathway of isoprenoid precursor biosynthesis. *J. Biol. Chem.* **2007**, 282, 21573–21577.
135. Masini, T.; Kroezen, B. S.; Hirsch, A. K. H. Druggability of the enzymes of the non mevalonate-pathway. *Drug Discov. Today* **2013**, 18, 23/24, 1256–1262.
136. Jackson, E. R.; Dowd, C. S. Inhibition of 1-deoxy-D-xylulose-5-phosphate reductoisomerase (Dxr): a review of the synthesis and biological evaluation of recent inhibitors. *Curr. Top. Med. Chem.* **2012**, 12, 706–728.
137. Ricagno, S.; Grolle, S.; Bringer-Meyer, S.; Sahm, H.; Lindqvist, Y.; Schneider, G. Crystal structure of 1-deoxy-D-xylulose-5-phosphate reductoisomerase from *Zymomonas mobilis* at 1.9-Å resolution. *Biochim. Biophys. Acta-Proteins Proteomics* **2004**, 1698, 1, 37–44.
138. Mac Sweeney, A.; Lange, R.; Fernandes, R. P. M.; Schulz, H.; Dale, G. E.; Douangamath, A.; Proteau, P. J.; Oefner, C. The crystal structure of *E. coli* 1-deoxy-D-xylulose-5-phosphate reductoisomerase in a ternary complex with the antimalarial compound fosmidomycin and NADPH reveals a tight-binding closed enzyme conformation. *J. Mol. Biol.* **2005**, 345, 1, 115–127.

139. Umeda, T.; Tanaka, N.; Kusakabe, Y.; Nakanishi, M.; Kitade, Y.; Nakamura, K. T. Molecular basis of fosmidomycin's action on the human malaria parasite *Plasmodium falciparum*. *Sci. Rep.* **2011**, 1, Article 9.
140. Giessmann, D.; Heidler, P.; Haemers, T.; Van Calenbergh, S.; Reichenberg, A.; Jomaa, H.; Weidemeyer, C.; Sanderbrand, S.; Wiesner, J.; Link, A. Towards new antimalarial drugs: synthesis of non-hydrolyzable phosphate mimics as feed for a predictive QSAR study on 1-deoxy-D-xylulose-5-phosphate reductoisomerase inhibitors. *Chem. Biodivers.* **2008**, 5, 643–656.
141. Hoeffler, J. F.; Tritsch, D.; Grosdemange-Billiard, C.; Rohmer, M. Isoprenoid biosynthesis via the methylerythritol phosphate pathway. Mechanistic investigations of the 1-deoxy-D-xylulose 5-phosphate reductoisomerase. *Eur. J. Biochem.* **2002**, 269, 18, 4446–4457.
142. Lauw, S.; Illarionova, V.; Bacher, A.; Rohdich, F.; Eisenreich, W. Biosynthesis of isoprenoids: studies on the mechanism of 2C-methyl-D-erythritol-4-phosphate synthase. *FEBS J.* **2008**, 275, 16, 4060–4073.
143. Wong, A.; Munos, J. W.; Devasthali, V.; Johnson, K. A.; Liu, H. W. Study of 1-deoxy-D-xylulose-5-phosphate reductoisomerase: Synthesis and evaluation of fluorinated substrate analogues. *Org. Lett.* **2004**, 6, 20, 3625–3628.
144. Li, H.; Tian, J.; Sun, W.; Qin, W.; Gao, W. Y. Mechanistic insights into 1-deoxy-D-xylulose 5-phosphate reductoisomerase, a key enzyme of the MEP terpenoid biosynthetic pathway. *FEBS J.* **2013**, 280, 5896–5905.
145. Murkin, A. S.; Manning, K. A.; Kholodar, S. A. Mechanism and inhibition of 1-deoxy-D-xylulose-5-phosphate reductoisomerase. *Bioorg. Chem.* **2014**, 57, 171–185.
146. Wong, U.; Cox, R. J. The chemical mechanism of D-1-deoxyxylulose-5-phosphate reductoisomerase from *Escherichia coli*. *Angew. Chem. Int. Ed.* **2007**, 46, 26, 4926–4929.
147. Munos, J. W.; Pu, X.; Mansoorabadi, S. O.; Kim, H. J.; Liu, H. W. A secondary kinetic isotope effect study of the 1-deoxy-D-xylulose-5-phosphate reductoisomerase catalyzed reaction: evidence for a retroaldol-aldol rearrangement. *J. Am. Chem. Soc.* **2009**, 131, 6, 2048–2049.

148. Proteau, P. J.; Woo, Y. H.; Williamson, R. T.; Phaosiri, C. Stereochemistry of the reduction step mediated by recombinant 1-deoxy-D-xylulose 5-phosphate isomeroeductase. *Org. Lett.* **1999**, 1, 6, 921–923.
149. Arigoni, D.; Giner, J. S.; Sagner, S.; Wungsintaweekul, J.; Zenk, M. H.; Kis, K.; Bacher, A.; Eisenreich, W. Stereochemical course of the reduction step in the formation of 2 C-methylerythritol from the terpene precursor 1-deoxyxylulose in higher plants. *Chem. Commun.* **1999**, 1127–1128.
150. Sangari, F. J.; Perez-Gil, J.; Carretero-Paulet, L.; Garcia-Lobo, J. M.; Rodriguez Concepcion, M. A new family of enzymes catalyzing the first committed step of the methylerythritol 4-phosphate (MEP) pathway for isoprenoid biosynthesis in bacteria. *Proc. Natl. Acad. Sci. U S A.* **2010**, 107, 32, 14081–14086.
151. Moreno, E. Retrospective and prospective perspectives on zoonotic brucellosis. *Front. Microbiol.* **2014**, 5, Article 213.
152. Okuhara, M.; Kuroda, Y.; Goto, T.; Okamoto, M.; Terano, H.; Kohsaka, M.; Aoki, H.; Imanaka, H. Studies on new phosphonic acid antibiotics. I. FR-900098, isolation and characterization. *J. of Antibiot.* **1980**, 33, 1, 13–17.
153. Okuhara, M.; Kuroda, Y.; Goto, T.; Okamoto, M.; Terano, H.; Kohsaka, M.; Aoki, H.; Imanaka, H. Studies on new phosphonic acid antibiotics. III. Isolation and characterization of FR-31564, FR-32863 and FR-33289. *J. Antibiot.* **1980**, 33, 1, 24–28.a
154. Iguchi, E.; Okuhara, M.; Kohsaka, M.; Aoki, H.; Imanaka, H. Studies on new phosphonic acid antibiotics. II. Taxonomic studies on producing organisms of the phosphonic acid and related compounds. *J. Antibiot.* **1980**, 33, 19–23.
155. Neu, H. C.; Kamimura, T. *In vitro* and *in vivo* antibacterial activity of FR-31564, a phosphonic acid antimicrobial agent. *Antimicrob. Agents Chemother.* **1981**, 19, 6, 1013–1023.
156. Kuemmerle, H. P.; Murakawa, T.; Soneoka, K.; Konishi, T. Fosmidomycin: a new phosphonic acid antibiotic. Part I: Phase I tolerance studies. *Int. J. Clin. Pharmacol. Ther. Toxicol.* **1985**, 23, 10, 515–520.
157. Kuemmerle, H. P.; Murakawa, T.; Sakamoto, H.; Sato, N.; Konishi, T.; De Santis, F. Fosmidomycin, a new phosphonic acid antibiotic. Part II: 1. Human pharmacokinetics. 2.

Preliminary early phase IIa clinical studies. *Int. J. Clin. Pharmacol. Ther. Toxicol.* **1985**, 23, 10, 521–528.

158. Kuemmerle, H. P.; Murakawa, T. De Santis, F. Pharmacokinetic evaluation of fosmidomycin, a new phosphonic acid antibiotic. *Chemioterapia.* **1987**, 6, 2, 113–119.

159. Kuzuyama, T.; Shimizu, T.; Takahashi, S.; Seto, H. Fosmidomycin, a specific inhibitor of 1-deoxy-D-xylulose 5-phosphate reductoisomerase in the nonmevalonate pathway for terpenoid biosynthesis. *Tetrahedron Lett.* **1998**, 39, 43, 7913–7916.

160. Grolle, S.; Bringer-Meyer, S.; Sahm, H. Isolation of the *dxr* gene of *Zymomonas mobilis* and characterization of the 1-deoxy-D-xylulose 5-phosphate reductoisomerase. *FEMS Microbiol. Lett.* **2000**, 191, 131–137.

161. Dhiman, R. K.; Schaeffer, M. L.; Bailey, A. M.; Testa, C. A.; Scherman, H.; Crick, D. C. 1-Deoxy-D-xylulose 5-phosphate reductoisomerase (IspC) from *Mycobacterium tuberculosis*: towards understanding mycobacterial resistance to fosmidomycin. *J. Bacteriol.* **2005**, 187, 24, 8395–8402.

162. Mincheva, Z.; Courtois, M.; Andreu, F.; Rideau, M.; Viaud-Massuard, M. C. Fosmidomycin analogues as inhibitors of monoterpenoid indole alkaloid production in *Catharanthus roseus* cells. *Phytochemistry* **2005**, 66, 15, 1797–1803.

163. Henriksson, L. M.; Unge, T.; Carlsson, J.; Aqvist, J.; Mowbray, S. L.; Jones, T. A. Structures of *Mycobacterium tuberculosis* 1-deoxy-D-xylulose-5-phosphate reductoisomerase provide new insights into catalysis. *J. Biol. Chem.* **2007**, 282, 27, 19905–19916.

164. Zhang, B.; Watts, K. M.; Hodge, D.; Kemp, L. M.; Hunstad, D. A.; Hicks, L. M.; Odom, A. R. A second target of the antimalarial and antibacterial agent fosmidomycin revealed by cellular metabolic profiling. *Biochemistry* **2011**, 50, 17, 3570–3577.

165. Missinou, M. A.; Borrmann, S.; Schindler, A.; Issifou, S.; Adegnika, A. A.; Matsiegui, P. B.; Binder, R.; Lell, B.; Wiesner, J.; Baranek, T.; Jomaa, H.; Kremsner, P. G. Fosmidomycin for malaria. *Lancet.* **2002**, 360, 9349, 1941–1942.

166. Lell, B.; Ruangweerayut, R.; Wiesner, J.; Missinou, M. A.; Schindler, A.; Baranek, T.; Hintz, M.; Hutchinson, D.; Jomaa, H.; Kremsner, P. G. Fosmidomycin, a novel chemotherapeutic agent for malaria. *Antimicrob. Agents Chemother.* **2003**, 47, 2, 735–738.

-
167. Wiesner, J.; Henschker, D.; Hutchinson, D. B.; Beck, E.; Jomaa, H. *In vitro* and *in vivo* synergy of fosmidomycin, a novel antimalarial drug, with clindamycin. *Antimicrob. Agents Chemother.* **2002**, 46, 9, 2889–2894.
168. Borrmann, S.; Adegnika, A. A.; Matsiegui, P. B.; Issifou, S.; Schindler, A.; Mawili Mboumba, D. P.; Baranek, T.; Wiesner, J.; Jomaa, H.; Kremsner, P. G. Fosmidomycin-clindamycin for *Plasmodium falciparum* infections in African children. *J. Infect. Dis.* **2004**, 189, 5, 901–908.
169. Borrmann, S.; Adegnika, A. A.; Moussavou, F. *et al.* Short-course regimens of artesunate-fosmidomycin in treatment of uncomplicated *Plasmodium falciparum* malaria. *Antimicrob. Agents Chemother.* **2005**, 49, 9, 3749–3754.
170. Borrmann, S.; Lundgren, I.; Oyakhirome, S. *et al.* Fosmidomycin plus clindamycin for treatment of pediatric patients aged 1 to 14 years with *Plasmodium falciparum* malaria. *Antimicrob. Agents Chemother.* **2006**, 50, 8, 2713–2718.
171. Lanaspá, M.; Moraleda, C.; Machevo, S. *et al.* Inadequate efficacy of a new formulation of fosmidomycin-clindamycin combination in Mozambican children less than three years old with uncomplicated *Plasmodium falciparum* malaria. *Antimicrob. Agents Chemother.* **2012**, 56, 6, 2923–2928.
172. International Clinical Trials Registry Platform. World Health Organization. Evaluation of fosmidomycin and piperazine in the treatment of acute falciparum malaria (FOSPIP) <http://apps.who.int/trialsearch/Trial2.aspx?TrialID=NCT02198807>. (Last accessed May 13, **2015**).
173. Steinbacher, S.; Kaiser, J.; Eisenreich, W.; Huber, R.; Bacher, A.; Rohdich, F. Structural basis of fosmidomycin action revealed by the complex with 2-C-methyl-D-erythritol 4-phosphate synthase (IspC) - Implications for the catalytic mechanism and anti-malaria drug development. *J. Biol. Chem.* **2003**, 278, 20, 18401–18407.
174. Bjorkelid, C.; Bergfors, T.; Unge, T.; Mowbray, S. L.; Jones, T. A. Structural studies on *Mycobacterium tuberculosis* Dxr in complex with the antibiotic FR-900098. *Acta Crystallogr. D. Biol. Crystallogr.* **2012**, 68, 134–143.
175. Yin, X.; Proteau, P. J. Characterization of native and histidine-tagged deoxyxylulose 5-phosphate reductoisomerase from the cyanobacterium *Synechocystis* sp. PCC6803. *Biochim. Biophys. Acta.* **2003**, 1652, 1, 75–81.

176. Rohdich, F.; Lauw, S.; Kaiser, J.; Feicht, R.; Köhler, P.; Bacher, A.; Eisenreich, W. Isoprenoid biosynthesis in plants – 2C-methyl-D-erythritol-4-phosphate synthase (IspC protein) of *Arabidopsis thaliana*. *FEBS J.* **2006**, *273*, 19, 4446–4458.
177. Koppisch, A. T.; Fox, D. T.; Blagg, B. S.; Poulter, C. D. *E. coli* MEP synthase: steady-state kinetic analysis and substrate binding. *Biochemistry* **2002**, *41*, 1, 236–243.
178. Woo, Y.; Fernandes, R. P. M.; Proteau, P. J. Evaluation of fosmidomycin analogs as inhibitors of the *Synechocystis* sp. PCC6803 1-deoxy-D-xylulose 5-phosphate reductoisomerase. *Bioorg. Med. Chem.* **2006**, *14*, 2375–2385.
179. Merklé, L.; de Andrés-Gomez, A.; Dick, B.; Cox, R. J.; Godfrey, C. R. A. A fragment based approach to understanding inhibition of 1-deoxy-D-xylulose-5-phosphate reductoisomerase. *Chembiochem.* **2005**, *6*, 10, 1866–1874.
180. Argyrou, A.; Blanchard, J. S. Kinetic and chemical mechanism of *Mycobacterium tuberculosis* 1-deoxy-D-xylulose-5-phosphate isomeroreductase. *Biochemistry* **2004**, *43*, 4375–4384.
181. Murakawa, T.; Sakamoto, H.; Fukada, S.; Konishi, T.; Nishida, M. Pharmacokinetics of fosmidomycin, a new phosphonic acid antibiotic. *Antimicrob. Agents Chemother.* **1982**, *21*, 2, 224–230.
182. Na-Bangchang, K.; Ruengweerayut, R.; Karbwang, J.; Chauemung, A.; Hutchinson, D. Pharmacokinetics and pharmacodynamics of fosmidomycin monotherapy and combination therapy with clindamycin in the treatment of multidrug resistant falciparum malaria. *Malar. J.* **2007**, *6*, 1, 70.
183. Brown, A. C.; Parish, T. Dxr is essential in *Mycobacterium tuberculosis* and fosmidomycin resistance is due to a lack of uptake. *BMC Microbiol.* **2008**, *8*, Article 78.
184. Abdallah, A. M.; Gey Van Pittius, N. C.; Champion, P. A.; Cox, J.; Luirink, J.; Vandenbroucke-Grauls, C. M.; Appelmelk, B. J.; Bitter W. Type VII secretion--mycobacteria show the way. *Nat. Rev. Microbiol.* **2007**, *5*, 11, 883–891.
185. Kojo, H.; Shigi, Y.; Nishida, M. FR-31564, a new phosphonic acid antibiotic: Bacterial resistance and membrane permeability. *J. Antibiot.* **1980**, *33*, 1, 44–48.
186. Sakamoto, Y.; Furukawa, S.; Ogihara, H.; Yamasaki, M. Fosmidomycin resistance in adenylate cyclase deficient (*cya*) mutants of *Escherichia coli*. *Biosci. Biotechnol. Biochem.* **2003**, *67*, 9, 2030–2033.

187. Nair, S. C.; Brooks, C. F.; Goodman, C. D.; Sturm, A.; McFadden, G. I.; Sundriyal, S.; Anglin, J. L.; Song, Y.; Moreno, S. N.; Striepen, B. Apicoplast isoprenoid precursor synthesis and the molecular basis of fosmidomycin resistance in *Toxoplasma gondii*. *J. Exp. Med.* **2011**, *208*, 7, 1547–1559.
188. Baumeister, S.; Wiesner, J.; Reichenberg, A.; Hintz, M.; Bietz, S.; Harb, O. S.; Roos, D. S.; Kordes, M.; Friesen, J.; Matuschewski, K.; Lingelbach, K.; Jomaa, H.; Seeber, F., Fosmidomycin uptake into *Plasmodium* and *Babesia*-infected erythrocytes is facilitated by parasite-induced new permeability pathways. *Plos One* **2011**, *6*, 5, e19334.
189. Miller, M. J. Synthesis and therapeutic potential of hydroxamic acid based siderophores and analogues. *Chem. Rev.* **1989**, *89*, 7, 1563–1579.
190. O'Brien, E. C.; Farkas, E.; Gil, M. J.; Fitzgerald, D.; Castineras, A.; Nolan, K. B. Metal complexes of salicylhydroxamic acid (H₂Sha), anthranilic hydroxamic acid and benzohydroxamic acid. Crystal and molecular structure of [Cu(phen)₂(Cl)]Cl X H₂Sha, a model for a peroxidase-inhibitor complex. *J. Inorg. Biochem.* **2000**, *79* (1-4), 47–51.
191. Lou, B.; Yang, K. Molecular diversity of hydroxamic acids: Part II. Potential therapeutic applications. *Mini Rev. Med. Chem.* **2003**, *6*, 609–620.
192. Sanderson, L.; Taylor, G. W.; Aboagye, E. O.; Alao, J. P.; Latigo, J. R.; Coombes, R. C.; Vigushin, D. M. Plasma pharmacokinetics and metabolism of the histone deacetylase inhibitor trichostatin A after intraperitoneal administration to mice. *Drug Metab. Dispos.* **2004**, *32*, 10, 1132–1138.
193. Cobb, R. E.; Bae, B.; Li, Z.; DeSieno, M. A.; Nair, S. K. Zhao, H. Structure-guided design and biosynthesis of a novel FR-900098 analogue as a potent *Plasmodium falciparum* 1-deoxy-D-xylulose-5-phosphate reductoisomerase (Dxr) inhibitor. *Chem. Commun.* **2015**, *51*, 2526–2528.
194. Deng, L.; Endo, K.; Kato, M.; Cheng, G.; Yajima, S.; Song, Y. Structures of 1-deoxy-D-xylulose-5-phosphate reductoisomerase/lipophilic phosphonate complexes. *ACS Med. Chem. Lett.* **2011**, *2*, 2, 165–170.
195. Kuntz, L.; Tritsch, D.; Grosdemange-Billiard, C.; Hemmerlin, A.; Willem, A.; Bacht, T.; Rohmer, M. Isoprenoid biosynthesis as a target for antibacterial and antiparasitic drugs: Phosphonohydroxamic acids as inhibitors of deoxyxylulose phosphate reducto-isomerase. *Biochem. J.* **2005**, *386*, 127–135.

196. Zinglé, C.; Kuntz, L.; Tritsch, D.; Grosdemange-Billiard, C.; Rohmer, M. Isoprenoid biosynthesis via the methylerythritol phosphate pathway: structural variations around phosphonate anchor and spacer of fosmidomycin, a potent inhibitor of deoxyxylulose phosphate reductoisomerase. *J. Org. Chem.* **2010**, 75, 10, 3203–3207.
197. Silber, K.; Heidler, P.; Kurz, T.; Klebe, G. AFMoC enhances predictivity of 3D QSAR: A case study with DOXP-reductoisomerase. *J. Med. Chem.* **2005**, 48, 3547–3563.
198. Ortmann, R.; Wiesner, J.; Silber, K.; Klebe, G.; Jomaa, H.; Schlitzer, M. Novel deoxyxylulosephosphate-reductoisomerase inhibitors: fosmidomycin derivatives with spacious acyl residues. *Arch. Pharm. Chem. Life Sci.* **2007**, 340, 483–490.
199. Goble, J. L.; Adendorff, M. R.; de Beer, T. A. P.; Stephens, L. L.; Blatch, G. L. The malarial drug target *Plasmodium falciparum* 1-deoxy-D-xylulose-5-phosphate reductoisomerase (PfDxr): development of a 3-D model for identification of novel, structural and functional features and for inhibitor screening. *Protein Pept. Lett.* **2010**, 17, 1, 109–120.
200. Behrendt, C. T.; Kunfermann, A.; Illarionova, V.; Matheussen, A.; Grawert, T.; Groll, M.; Rohdich, F.; Bacher, A.; Eisenreich, W.; Fischer, M.; Maes, L.; Kurz, T. Synthesis and antiparasmodial activity of highly active reverse analogues of the antimalarial drug candidate fosmidomycin. *ChemMedChem* **2010**, 5, 10, 1673–1676.
201. Behrendt, C. T.; Kunfermann, A.; Illarionova, V.; Matheussen, A.; Pein, M. K.; Gräwert, T.; Kaiser, J.; Bacher, A.; Eisenreich, W.; Illarionov, B.; Fischer, M.; Maes, L.; Groll, M.; Kurz, T. Reverse fosmidomycin derivatives against the antimalarial drug target IspC (Dxr). *J. Med. Chem.* **2011**, 54, 6796–6802.
202. San Jose, G.; Jackson, E. R.; Uh, E.; Johnny, C.; Haymond, A.; Lundberg, L.; Pinkham, C.; Kehn-Hall, K.; Boshoff, H. I.; Couch, R. D.; Dowd C. S. Design of potential bisubstrate inhibitors against *Mycobacterium tuberculosis* (Mtb) 1-deoxy-D-xylulose 5-phosphate reductoisomerase (Dxr)-evidence of a novel binding mode. *Med. Chem. Commun.* **2013**, 4, 1099–1104.
203. Haemers, T.; Wiesner, J.; Busson, R.; Jomaa, H.; van Calenbergh, S. Synthesis of α -aryl-substituted and conformationally restricted fosmidomycin analogues as promising antimalarials. *Eur. J. Org. Chem.* **2006**, 17, 3856–3863.
204. Zinglé, C.; Kuntz, L.; Tritsch, D.; Grosdemange-Billiard, C.; Rohmer, M. Modifications around the hydroxamic acid chelating group of fosmidomycin, an inhibitor of the

- metalloenzyme 1-deoxyxylulose 5-phosphate reductoisomerase (Dxr). *Bioorg. Med. Chem. Lett.* **2012**, 22, 6563–6567.
205. Bock, C. W.; Kaufman Katz, A.; Markham, G. D.; Glusker, J. P. J. Manganese as a replacement for magnesium and zinc: Functional comparison of the divalent ions. *J. Am. Chem. Soc.* **1999**, 121, 32, 7360–7372.
206. Deng, L.; Sundriyal, S.; Rubio, V.; Shi, Z. Z.; Song, Y. Coordination chemistry based approach to lipophilic inhibitors of 1-deoxy-D-xylulose-5-phosphate reductoisomerase. *J. Med. Chem.* **2009**, 52, 21, 6539–6542.
207. Andaloussi, M.; Lindh, M.; Bjorkelid, C.; Suresh, S.; Wieckowska, A.; Iyer, H.; Karlén, A.; Larhed, M. Substitution of the phosphonic acid and hydroxamic acid functionalities of the Dxr inhibitor FR900098: An attempt to improve the activity against *Mycobacterium tuberculosis*. *Bioorg. Med. Chem. Lett.* **2011**, 21, 5403–5407.
208. Williams, S. L.; de Oliveira, C. A. F.; Vazquez, H.; McCammon, J. A. From Zn to Mn: The Study of novel manganese-binding groups in the search for new drugs against tuberculosis. *Chem. Biol. Drug Des.* **2011**, 77, 117–123.
209. Bodill, T.; Conibear, A. C.; Blatch, G. L.; Lobb, K. A.; Kaye, P. T. Synthesis and evaluation of phosphonated *N*-heteroarylcarboxamides as DOXP-reductoisomerase (Dxr) inhibitors. *Bioorg. Med. Chem.* **2011**, 19, 1321–1327.
210. Amin, E.; Saboury, A. A.; Mansuri-Torshizi, H.; Moosavi-Movahedi, A. A. Potent inhibitory effects of benzyl and *p*-xylidine-bis dithiocarbamate sodium salts on activities of mushroom tyrosinase. *J. Enzyme Inhib. Med. Chem.* **2010**, 25, 2, 272–281.
211. Montel, S.; Midrier, C.; Volle, J. N.; Braun, R.; Haaf, K.; Willms, L.; Pirat, J. L.; Virieux, D. Functionalized phosphanyl-Phosphonic acids as unusual complexing units as analogues of fosmidomycin. *Eur. J. Org. Chem.* **2012**, 17, 3237–3248.
212. Konzuch, S.; Umeda, T.; Held, J. *et al.* Binding modes of reverse fosmidomycin analogs toward the antimalarial target IspC. *J. Med. Chem.* **2014**, 57, 21, 8827–8838.
213. Hemmi, K.; Takeno, H.; Hashimoto, M.; Kamiya, T. Studies on phosphonic acid antibiotics. IV. Synthesis and antibacterial activity of analogs of 3-(*N*-acetyl-*N*-hydroxyamino)-propylphosphonic acid (FR-900098). *Chem. Pharm. Bull.* **1982**, 30, 1, 111–118.

214. Jackson, E. R.; San Jose, G.; Brothers, R. C.; Edelstein, E. K.; Sheldon, Z.; Haymond, A.; Johnny, C.; Boshoff, H. I.; Couch, R. D.; Dowd, C. S. The effect of chain length and unsaturation on Mtb Dxr inhibition and antitubercular killing activity of FR9000098 analogs. *Bioorg. Med. Chem. Lett.* **2014**, 24, 2, 649–653.
215. Perruchon, J.; Ortmann, R.; Altenkamper, M.; Silber, K.; Wiesner, J.; Jomaa, H.; Klebe, G.; Schlitzer, M. Studies addressing the importance of charge in the binding of fosmidomycin-like molecules to deoxyxylulosephosphate reductoisomerase. *ChemMedChem*, **2008**, 3, 8, 1232–1241.
216. Katayama, N.; Tsubotani, S.; Nozaki, Y.; Harada, S.; Ono, H. Fosfadecin and fosfocytocin, new nucleotide antibiotics produced by bacteria. *J. Antibiot.* **1990**, 43, 3, 238–246.
217. Haemers, T.; Wiesner, J.; Van Poecke, S.; Goeman, J.; Henschker, D.; Beck, E.; Jomaa, H.; Van Calenbergh, S. Synthesis of α -substituted fosmidomycin analogues as highly potent *Plasmodium falciparum* growth inhibitors. *Bioorg. Med. Chem. Lett.* **2006**, 16, 1888–1891.
218. Devreux, V.; Wiesner, J.; Jomaa, H.; Rozenski, J.; Van der Eycken, J.; Van Calenbergh, S. Divergent strategy for the synthesis of α -aryl-substituted fosmidomycin analogues. *J. Org. Chem.* **2007**, 72, 3783–3789.
219. Andaloussi, M.; Henriksson, L. M.; Wieckowska, A.; Lindh, M.; Bjorkelid, C.; Larsson, A. M.; Suresh, S.; Iyer, H.; Srinivasa, B. R.; Bergfors, T.; Unge, T.; Mowbray, S. L.; Larhed, M.; Jones, T. A.; Karlén, A. Design, synthesis, and X-ray crystallographic studies of alpha-aryl substituted fosmidomycin analogues as inhibitors of Mycobacterium tuberculosis 1-deoxy-D xylulose 5-phosphate reductoisomerase. *J. Med. Chem.* **2011**, 54, 4964–4976.
220. Nordqvist, A.; Bjorkelid, C.; Andaloussi, M.; Jansson, A. M.; Mowbray, S. L.; Karlén, A.; Larhed, M. Synthesis of functionalized cinnamaldehyde derivatives by an oxidative heck reaction and their use as starting materials for preparation of mycobacterium tuberculosis 1 deoxy-D-xylulose-5-phosphate reductoisomerase inhibitors. *J. Org. Chem.* **2011**, 76, 8986–8998.
221. Deng, L.; Diao, J.; Chen, P.; Pujari, V.; Yao, Y.; Cheng, G.; Crick, D. C.; Prasad, B. V.; Song, Y. Inhibition of 1-deoxy-D-xylulose-5-phosphate reductoisomerase by lipophilic phosphonates: SAR, QSAR, and crystallographic studies. *J. Med. Chem.* **2011**, 54, 13, 4721–4734.

222. Xue, J.; Diao, J.; Cai, G.; Deng, L.; Zheng, B.; Yao, Y.; Song, Y. Antimalarial and structural studies of pyridine-containing inhibitors of 1-deoxyxylulose-5-phosphate reductoisomerase. *ACS Med. Chem. Lett.* **2013**, 4, 278–282.
223. Jansson, A. M.; Wieckowska, A.; Bjorkelid, C.; Yahiaoui, S.; Sooriyaarachchi, S.; Lindh, M.; Bergfors, T.; Dharavath, S.; Desroses, M.; Suresh, S.; Andaloussi, M.; Nikhil, R.; Sreevalli, S.; Srinivasa, B. R.; Larhed, M.; Jones, T. A.; Karlén, A.; Mowbray, S. L. Dxr inhibition by potent mono- and disubstituted fosmidomycin analogues. *J. Med. Chem.* **2013**, 56, 15, 6190–6199.
224. Kunfermann, A.; Lienau, C.; Illarionov, B.; Held, J.; Gräwert, T.; Behrendt, C. T.; Werner, P.; Hähn, S.; Eisenreich, W.; Riederer, U.; Mordmüller, B.; Bacher, A.; Fischer, M.; Groll, M.; Kurz, T. IspC as target for anti-infective drug discovery: synthesis, enantiomeric separation, and structural biology of fosmidomycin thia isosters. *J. Med. Chem.* **2013**, 56, 8151–8162.
225. Nieschalk, J.; Batsanov, A. S.; O'Hagan, D.; Howard, J. A. K. Synthesis of monofluoro- and difluoro-methylenephosphonate analogues of sn-glycerol-3-phosphate as substrates for glycerol-3-phosphate dehydrogenase and the X-ray structure of the fluoromethylenephosphonate moiety. *Tetrahedron* **1996**, 52, 1, 165–176.
226. Verbrugghen, T.; Cos, P.; Maes, L.; Van Calenbergh, S. Synthesis and evaluation of α -halogenated analogues of 3-(acetylhydroxyamino)propylphosphonic acid (FR9000098) as antimalarials. *J. Med. Chem.* **2010**, 53, 14, 5342–5346.
227. Kurz, T.; Schluter, K.; Kaula, U.; Bergmann, B.; Walter, R. D.; Geffken, D. Synthesis and antimalarial activity of chain substituted pivaloyloxymethyl ester analogues of fosmidomycin and FR900098. *Bioorg. Med. Chem.* **2006**, 14, 5121–5135.
228. Schluter, K.; Walter, R. D.; Bergmann, B.; Kurz, T. Arylmethyl substituted derivatives of fosmidomycin: Synthesis and antimalarial activity. *Eur. J. Med. Chem.* **2006**, 41, 12, 1385–1397.
229. Devreux, V.; Wiesner, J.; Goeman, J. L.; Van der Eycken, J.; Jomaa, H.; Van Calenbergh, S. Synthesis and biological evaluation of cyclopropyl analogues of fosmidomycin as potent *Plasmodium falciparum* growth inhibitors. *J. Med. Chem.* **2006**, 49, 2656–2660.
230. Kurz, T.; Schluter, K.; Pein, M.; Behrendt, C.; Bergmann, B.; Walter, R. D. Conformationally restrained aromatic analogues of fosmidomycin and FR900098. *Arch. Pharm. Chem.* **2007**, 340, 339–344.

231. Gadakh, B.; Pouyez, J.; Wouters, J.; Venkatesham, A.; Cos, P.; Van Aerschot, A. *N*-Acylated sulfonamide congeners of fosmidomycin lack any inhibitory activity against Dxr. *Bioorg. Med. Chem. Lett.* **2015**, 25, 7, 1577–1579.
232. Reichenberg, A.; Wiesner, J.; Weidemeyer, C.; Dreiseidler, E.; Sanderbrand, S.; Altincicek, B.; Beck, E.; Schlitzerc, M.; Jomaa, H. Diaryl ester prodrugs of FR900098 with improved *in vivo* antimalarial activity. *Bioorg. Med. Chem. Lett.* **2001**, 11, 833–835.
233. Ortmann, R.; Wiesner, J.; Reichenberg, A.; Henschker, D.; Beck, E.; Jomaa, H.; Schlitzer, M. Acyloxyalkyl ester Prodrugs of FR900098 with improved *in vivo* anti-malarial activity. *Bioorg. Med. Chem. Lett.* **2003**, 13, 13, 2163–2166.
234. Ortmann, R.; Wiesner, J.; Reichenberg, A.; Henschker, D.; Beck, E.; Jomaa, H.; Schlitzer, M. Alkoxy-carbonyloxyethyl ester prodrugs of FR900098 with improved *in vivo* antimalarial activity. *Arch. Pharm. Chem. Life Sci.* **2005**, 338, 7, 305–314.
235. Kurz, T.; Behrendt, C.; Pein, M.; Kaula, U.; Bergmann, B.; Walter, R. D. γ -Substituted bis(pivaloyloxymethyl)ester analogues of fosmidomycin and FR900098. *Arch. Pharm. Chem. Life Sci.* **2007**, 340, 12, 661–666.
236. Uh, E.; Jackson, E. R.; San Jose, G.; Maddox, M.; Lee, R. E.; Boshoff, H. I.; Dowd, C.S. Antibacterial and antitubercular activity of fosmidomycin, FR900098, and their lipophilic analogs. *Bioorg. Med. Chem. Lett.* **2011**, 21, 23, 6973–6976.
237. Krise, J. P.; Stella, V. J. Prodrugs of phosphates, phosphonates, and phosphinates. *Adv. Drug Delivery Rev.* **1996**, 19, 2, 287–310.
238. Brücher, K.; Gräwert, T.; Konzuch, S.; Held, J.; Lienau, C. Behrendt, C.; Illarionov, B.; Maes, L.; Bacher, A.; Wittlin, S.; Mordmüller, B.; Fischer, M.; Kurz, T. Prodrugs of reverse fosmidomycin analogues. *J. Med. Chem.* **2015**, 58, 2025–2035.

Chapter II

SCOPE AND STRATEGIES

II. SCOPE AND STRATEGIES

With pressure mounting worldwide on both the economic and social fronts, the need for new improved therapeutics for rolling back the incidence of malaria and tuberculosis deaths remains urgent. Unfortunately, fosmidomycin does not fit fully into the current reversal plan because of its unfavorable pharmacokinetic properties. However, it serves as a valuable starting point for further optimization towards new drugs, given its good clinical record as an antimalarial and indeed, its potential to kill other Dxr-dependent pathogens like Mtb. The overall scope of this PhD work is to synthesize new Dxr inhibitors that combine good potency with improved druglike properties and to evaluate their potential as antimalarial and/or antitubercular agents. This endeavor will also expand knowledge on the SAR of fosmidomycin analogues as Dxr inhibitors. Towards this end, different strategies will be employed according to the following specific objectives:

- **Chapter III:** The high polarity and hydrolysis-associated toxicity of fosmidomycin's metal chelating retrohydroxamate group, are a setback to its use as a drug. Since SAR data indicate that despite its efficient metal binding potential, this group is not indispensable, the focus of this chapter will be to investigate the possibility of replacing the retrohydroxamate of fosmidomycin with alternative bidentate ligands. Amide derivatives (**3.1**, Figure II.1) will be prepared and evaluated. These analogues are expected to show higher stability *in vivo* and an overall enhanced lipophilic character, anticipated to improve cellular uptake.
- **Chapter V:** Hitherto, substitutions at the α -position of fosmidomycin have been widely explored, leading to analogues with promising activities. However, manipulation of the β -position has received much less attention. The acetyl congener of fosmidomycin (FR900098) and compound **1.6** have been shown to exhibit comparable inhibitory activity against EcDxr. Therefore, we aim at assessing the effect of introducing a methyl group or a (substituted) phenyl ring (**5.1**) in the β -position of **1.6** on Dxr inhibition. Compounds **5.2** will also be synthesized, first to investigate the optimal linker length between the propyl backbone of **1.6** and an unsubstituted phenyl ring. The most favorable linker will then be combined with

decorated phenyl rings, in an effort to sort out the influence of lipophilicity, electronic and steric properties on Dxr binding.

- **Chapter VI:** Electron withdrawing aryl and halogen substituents in the α -position of fosmidomycin have a role in increasing the acidity of the phosphonic acid group, thereby leading to a stronger interaction with the phosphate binding site of Dxr. Such effect could possibly be achieved by incorporating a nitrogen atom into the α -position of the three-carbon chain of **1.6**. The lower electronegativity of nitrogen compared to oxygen may lead to a better stability of the phosphoramides **6.1** compared to the phosphate in fosfoxacin, a potent but unstable Dxr inhibitor. Additionally, we plan to investigate the possibility to derivatize the α -nitrogen atom for the construction of a small library of new fosmidomycin analogues.
- **Chapter VII:** Masking the polar phosphonate with lipophilic ester prodrug groups has proven successful in improving diffusion across biological membranes thereby increasing the activity against intact pathogen cells and the *in vivo* or oral activity. In an effort to reduce the toxicity associated with the hydrolysis of such ester groups, we envision a new concept of masking one of the phosphonic acid OH groups as an integral part of a cyclic phosphonate prodrug, to yield analogues like **7.7**. Different prodrug moieties can then be used to mask the 'other' phosphonate OH function. We anticipate that *in vivo* hydrolysis would liberate the α -*ortho*-hydroxyphenyl-substituted phosphonic acid from parent compound inside the cell.

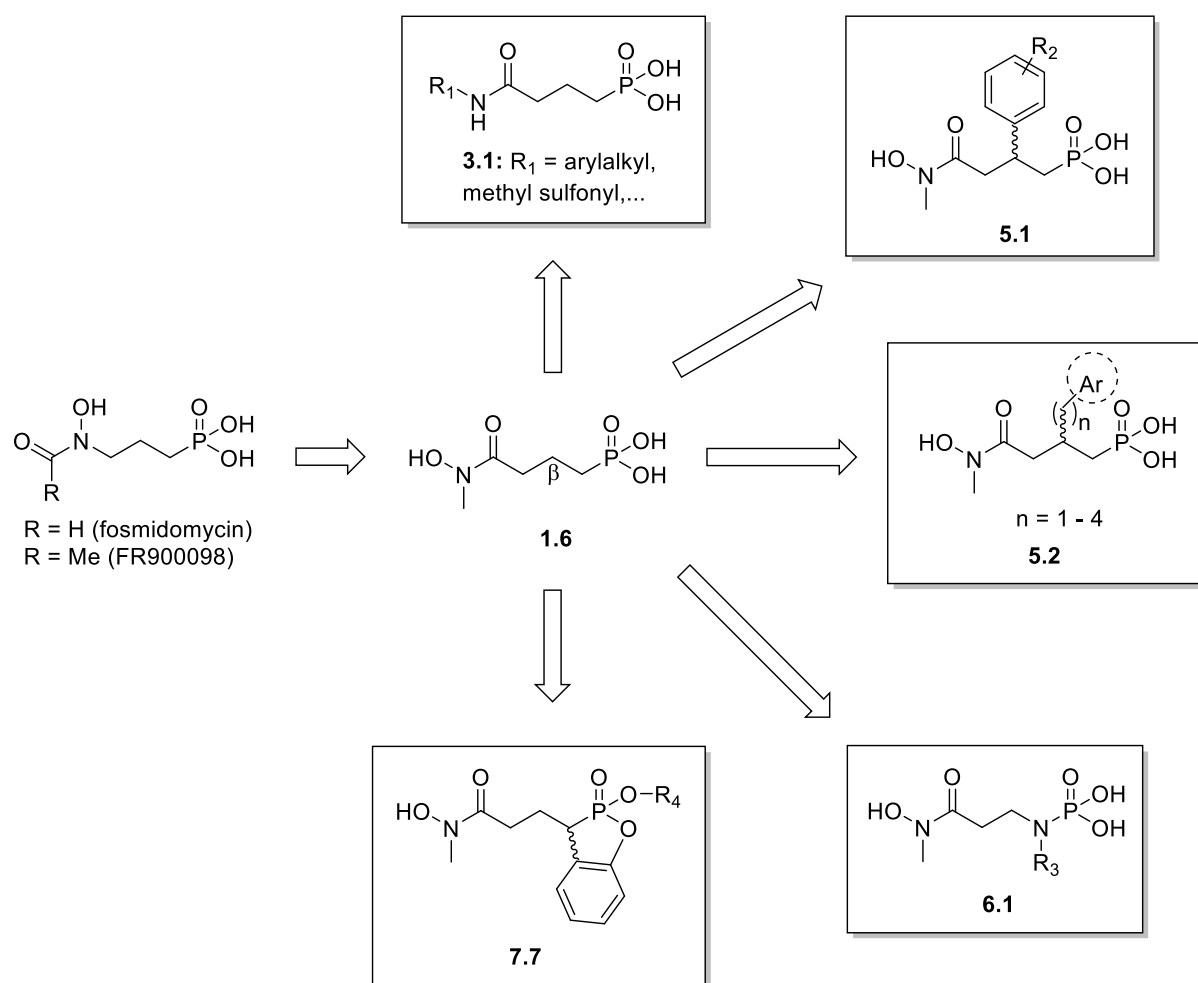


Figure II.1: Planned modifications of fosmidomycin.

List of Collaborators

Where applicable throughout this thesis, the following studies were conducted in collaboration with the following partners:

- 1) ***In vitro P. falciparum* growth inhibition.** *In vitro P. falciparum* growth inhibition assay was performed by the Laboratory for Microbiology, Parasitology and Hygiene (Prof. L. Maes and P. Cos), Faculty of Pharmaceutical, Biomedical and Veterinary Sciences, University of Antwerp. Universiteitsplein 1, B-2610 Antwerp, Belgium.
- 2) ***E. coli* Dxr inhibition.** The *E. coli* Dxr assay was performed by the Unit of Theoretical and Structural Physico-chemistry (Prof. J. Wouters), Department of Chemistry, University of Namur, Rue de Bruxelles 61, Namur B-5000, Belgium.
- 3) ***M. tuberculosis* Dxr inhibition.** The *M. tuberculosis* Dxr inhibition assay was performed by the Department of Chemistry and Biochemistry (Prof. R. Couch), George Mason University, Manassas, Virginia 20110, The United States of America.
- 4) ***P. falciparum* Dxr inhibition and crystallography.** The PfDxr assay and crystallography was performed by the Department of Cell and Molecular Biology, Science for Life Laboratory (Prof. S. Mowbray), Biomedical Center, Uppsala University, Box 596, SE-751 24 Uppsala, Sweden.
- 5) **Antimicrobial susceptibility testing.** The *M. smegmatis* assay was performed by the Laboratory of Pharmaceutical Microbiology (Prof. T. Coenye), Faculty of Pharmaceutical Sciences, Ghent University, Ottergemsesteenweg 460, B-9000 Ghent, Belgium.
- 6) **Molecular modeling.** Modeling of compound **5.2c** into MtbDxr was conducted by Dr. A. Alex, Evenor Consulting Ltd., Eastry, CT13 0JW, United Kingdom.

Chapter III

HYDROXAMATE-MODIFIED

ANALOGUES OF

FOSMIDOMYCIN

III. HYDROXAMATE-MODIFIED ANALOGUES OF FOSMIDOMYCIN

III.A. Introduction

The chelating ability of hydroxamates often makes them potent metalloenzyme inhibitors. Despite this strength, most hydroxamic acids suffer from poor oral bioavailability and low selectivity in metal binding; chelating other metals (e.g., Zn^{2+} , Cu^{2+} , etc.) besides Mn^{2+} and Mg^{2+} and Co^{2+} , which are relevant for Dxr catalysis.^{1,2} In addition, hydroxamic acids may be rapidly degraded *in vivo* by hydrolysis, glucuronidation and sulfation and may suffer from poor pharmacokinetic and toxicological profiles.³ As noted already in the general introduction, attempts to circumvent these hydroxamate-associated limitations in fosmidomycin analogues by replacing this moiety with alternative metal ion chelators have yielded mixed results. Mostly, such modifications have resulted in compounds that elicit poor biological activity profiles although a handful of analogues in this category still raise the prospects of overcoming this barrier.

Early in this project, we aimed to more systematically investigate the possibilities of replacing the hydroxamate group of fosmidomycin with effective alternative bidentate ligands. San Jose *et al.* reported a more efficient coordination of the metal cation by amide- versus *O*-linked substituents on the hydroxamate of fosmidomycin and also highlighted the contribution of an aromatic group to improved lipophilicity of analogues.⁴ Therefore, as a first step, we prepared and evaluated amide derivatives represented by the general structure **3.1** (Figure III.1).

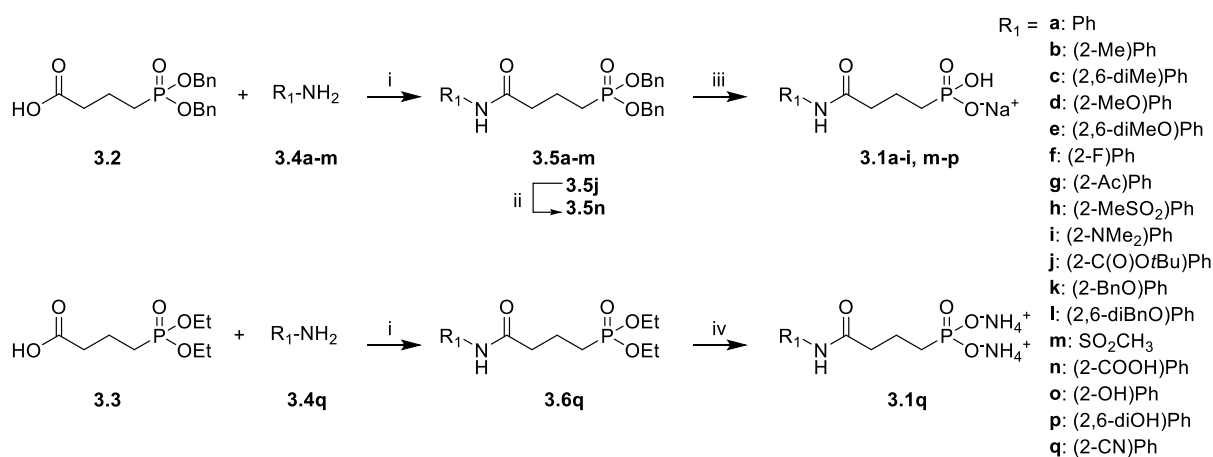


Figure III.1: Planned amide derivatives of fosmidomycin.

We envisaged a contribution to chelation by *ortho*-substituents on the amide-linked aromatic ring. Compounds with an N-H moiety between carbonyl and sulfonyl groups are very acidic ($pK_a \sim 2$). At physiological pH, the presence of a negative charge at this position would be expected to improve the interaction with the active-site metal ion.⁵ Therefore, we included one analogue with a methyl sulfonyl group in *ortho* position of the phenyl ring (compound **3.1h**, Figure III.2), as well as a (non-aromatic) sulfonamide (compound **3.1m**). In order to ascertain the influence of electronic factors on chelation, aromatic substituents with various electronic properties were selected.

III.B. Synthesis

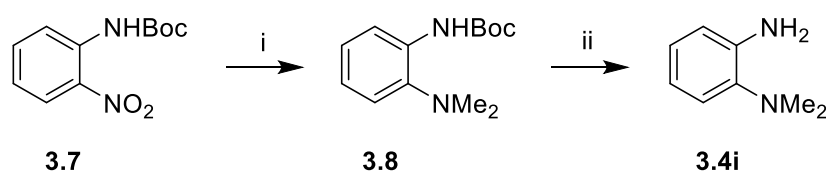
The synthesis of the amide derivatives **3.1a–i**, **m–q** is outlined in Scheme III.1. Carboxylic acid **3.2** was readily prepared starting from commercially available ethyl 4-bromo-butyrates and dibenzyl phosphite as previously described by Kuntz *et al.*⁶



Scheme III.1 Reagents and conditions: (i) oxalyl chloride, DMF, CH₂Cl₂, 45 °C, 2–3 h, 40%–75%; (ii) TFA/CH₂Cl₂ (for **3.5j**); (iii) H₂, Pd/C, MeOH, NaOHaq., 25 °C, 10–15 min, quant.; (iv) TMSBr, CH₂Cl₂, H₂O, NH₄OHaq., quant.

Anticipation that the cyano substituent on aniline **3.4q** would be susceptible to hydrogenation later in the synthesis necessitated the use of the diethyl protected phosphonate **3.3**, obtained from saponification of commercially available triethyl 4-phosphonobutyrate, for reaction with this aniline. With the exception of anilines **3.4i** and **3.4l**, all other anilines used were commercially available. Synthesis of **3.4i** (Scheme III.2) started from 2-nitro-aniline which was easily converted to the NH-Boc protected form as described by McNeil and Kelly.⁷ Subsequent *N,N*-dimethylation, followed by Boc removal

afforded the aniline. Compound **3.4i** was prepared from 2,6-dihydroxyaniline according to a literature procedure.⁸



Scheme III.2 Reagents and conditions: (i) formaldehyde, HCOOH, H₂, Pd/C, MeOH, 90%; (ii) acetyl chloride, MeOH.

Anilines are often poor nucleophiles, thus carboxylic acids **3.2** and **3.3** were first converted to their respective acid chlorides by treatment with oxalyl chloride before subsequent nucleophilic substitution of **3.4a–m**, **3.4q** to generate a small library of the protected amides **3.5a–m**, and **3.6q** in moderate yields. The ¹H-NMR spectrum of **3.5c** displays two peaks at 2.17 ppm and 2.21 ppm for the 2,6-dimethyl protons corresponding to the *E* and *Z* amide rotamers in a 5/1 ratio. Hydrolysis of the tertiary butyl ester group of **3.5j** with TFA (20% in dichloromethane) further converted this intermediate to **3.5n**. Using benzyl protection for both the phosphonate and the aryl substituent (**3.5k** and **3.5l**) allowed a mild single deprotection by catalytic hydrogenolysis in the presence of palladium over activated charcoal at room temperature to access targets **3.1a–i**, **m–p**. TMSBr mediated deprotection of **3.6q** and basic workup yielded **3.1q** as the bisammonium salt.

III.C. Biological evaluation

The ability of the final compounds to inhibit the *E. coli* Dxr and *M. tuberculosis* Dxr was investigated using a spectrophotometric assay monitoring the substrate dependent oxidation of NADPH, essentially as described by Jawaid *et al.*^{9,10} As shown in Figure III.2, at a concentration of 100 μM, all compounds failed to significantly inhibit the *E. coli* or Mtb Dxr. Likewise all compounds were found essentially inactive against *P. falciparum* K1 in human erythrocytes (IC₅₀ > 64 μM). Similar to fosmidomycin, we expected that the phosphonate group of these analogs would be accommodated in the phosphate binding pocket of Dxr. With the three-carbon spacer unaltered, the introduced modification of the hydroxamate group is determining the lack of Dxr inhibitory activity. Monodentate ligands include virtually all anions and simple Lewis bases.

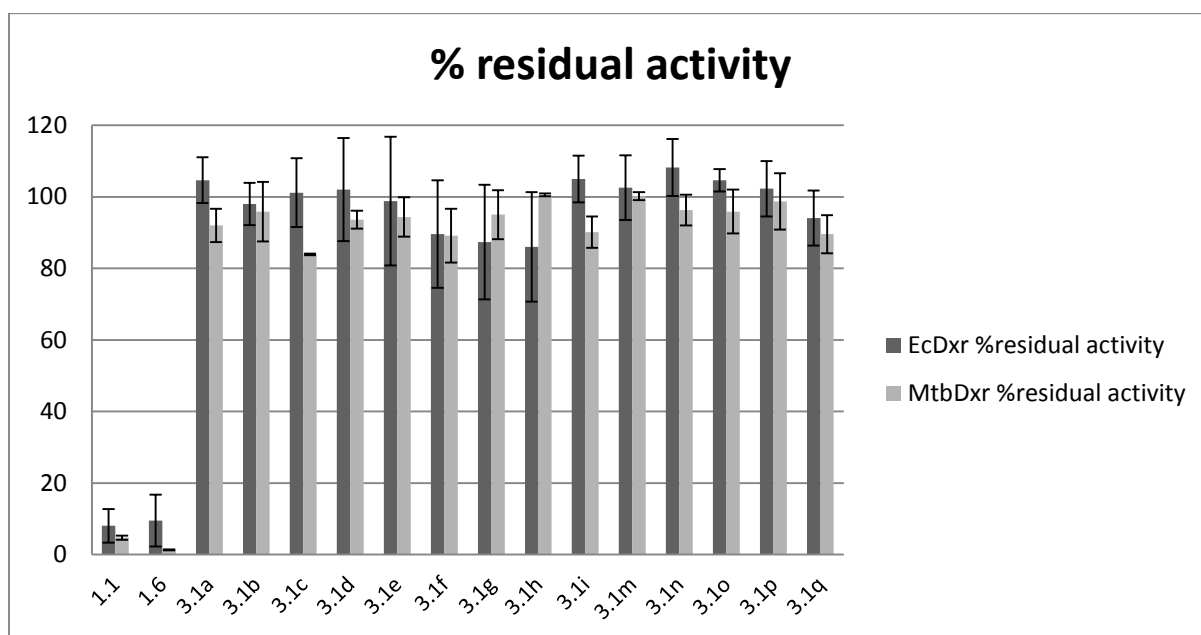


Figure III.2: Relative activity of **3.1a–i, m–q** on purified *E. coli* (dark grey) and Mtb Dxr (light-grey).

While anticipating that the bivalent metal cation would be more readily bound by electron rich substituents on the aromatic ring, we expected that the analogues with 2,6-disubstituted aromatic rings would elicit better enzyme inhibition than their monosubstituted counterparts, since possible rotation of the amide bond would still assure a favorable conformation (*cis*) with respect to the carbonyl oxygen. Even though the hard metal ion character of Mg^{2+} favors the formation of stable complexes with dioxygen based hard ligands, *O*-linked substituents on the ring did not improve the inhibitory ability of these analogues. Carboxylate is a known chelating group¹¹ but in the assay conditions, the group was possibly protonated thereby reducing the chelating potency of the carboxylate oxygen of **3.1n** with the Mg^{2+} ion. Obviously, the presence of an aromatic ring improved the lipophilicity of these analogues. However, limited flexibility around the amide bond seems detrimental for inhibitory activity. Maybe, the introduction of methylene groups between the N-H and the (substituted) phenyl ring could increase the likelihood of adopting of a better conformation for occupation of ‘alternative’ binding pockets or a better fitting of the compound into the active site.

In the course of our work, Bodill *et al.* reported similar modifications of the retrohydroxamate moiety of fosmidomycin.¹² Out of a series of phosphonated *N*-

(hetero)arylcarboxamide analogues with one, two, three or four methylene groups linking the phosphonate to the carboxamide group, they found that increasing the number of methylene groups in the spacer (particularly to three or four methylene groups) decreases the Dxr inhibitory activity dramatically. The authors noted that while receptor cavity size constraints is an important determinant of binding, allosteric and reverse orientation ligand binding modes cannot be excluded.

III.D. Conclusions

In conclusion, amide derivatives of fosmidomycin were synthesized from simple starting materials. These analogues were inactive against *E. coli* Dxr, *Mtb* Dxr and *P. falciparum* K1 possibly due their inability to adopt a favorable conformation necessary for the Dxr active site metal chelation. Replacing the hydroxamate group of fosmidomycin with an alternative and efficient bidentate metal binding group in Dxr inhibitors, remains a daunting challenge as previously noted.¹³

III.E. Experimental details

General Methods and Materials.

¹H-, ¹³C-, ¹⁹F- and ³¹P-NMR spectra were recorded in CDCl₃, or D₂O on a Mercury 300 spectrometer (Varian, Palo Alto, CA, USA). Chemical shifts are given in parts per million (ppm) (δ relative to TMS for ¹H and ¹³C. In ³¹P NMR, signals are referenced to the CDCl₃ or D₂O lock resonance frequency according to IUPAC referencing, with H₃PO₄ set to 0.00 ppm. High resolution mass spectroscopy spectra for all compounds were also recorded on a LCT Premier XE orthogonal time-of flight spectrometer with API-ES source (Waters, Alliance 2695XE-LCT Premier XETM, Zellik, Belgium). Preparative HPLC purifications were carried out using a Laprep preparative HPLC system equipped with an Xbridge Prep C18 column (19 mm \times 250 mm, 5 μ m) using a water/acetonitrile/formic acid gradient solvent system. All synthesized compounds were \geq 95% pure as verified by LCMS. All solvents and chemicals were used as purchased unless otherwise stated.

Dxr inhibition assay. The *E. coli* Dxr assay was performed by the Unit of Theoretical and Structural Physico-chemistry, Department of Chemistry, University of Namur, Belgium

(FUNDP). The *M. tuberculosis* Dxr inhibition assay was performed by the Department of Chemistry and Biochemistry, George Mason University, Manassas, The United States of America. Inhibition of Dxr activity was measured in a spectrophotometric assay by monitoring the oxidation of NADPH to NADP⁺, using the absorption of NADPH at 340 nm. The EcDxr and MtbDxr assays were performed at 37 °C with 100 nM and 890 μM enzyme, respectively. With either enzyme, assays contained a saturating concentration of NADPH and a DOXP concentration fixed at the K_M. The slope of inhibited reaction was compared to the slope of uninhibited reaction to calculate the residual activity.

***In vitro P. falciparum* growth inhibition assay.** Performed by the Laboratory for Microbiology, Parasitology and Hygiene, Faculty of Pharmaceutical, Biomedical and Veterinary Sciences, University of Antwerp. The chloroquine-resistant *P. falciparum* K1-strain was cultured in human erythrocytes (O+) at 37 °C under a low oxygen atmosphere (3% O₂, 4% CO₂, and 93% N₂) in RPMI-1640, supplemented with 10% human serum. Assays were performed in 96-well microtiter plates, each well containing 10 μL of the watery compound dilutions together with 200 μL of the malaria parasite inoculum i.e. infected human red blood cells (1% parasitaemia, 2% haematocrit). Parasite multiplication was measured by the Malstat method:¹⁴ After 72 h incubation, test plates were frozen and stored at -20 °C. Following thawing, 20 μL of each well was transferred into another plate together with 100 μL Malstat reagent and 20 μL of a 1/1 mixture of phenazine ethosulfate (0.1 mg/mL) and nitro blue tetrazolium grade III (2 mg/mL). Change in color was measured spectrophotometrically at 655 nm. Each MIC₅₀ determination was performed in triplicate.

General Procedure for the Synthesis of Protected Amides 3.5a–p, 3.6q

To a 0.5 M solution of the acid **3.2/3.3** in dichloromethane under nitrogen atmosphere, was added oxalyl chloride (2 eq.) and a few drops of DMF at room temperature. After effervescence subsided, the mixture was heated to reflux at 45 °C for 2 h. It was then cooled to room temperature, concentrated *in vacuo*, co-evaporated three times with toluene and then re-dissolved in dichloromethane. The aniline (2 eq.) was then added at 0 °C, followed by DIPEA (3 eq.) and the mixture stirred overnight at room temperature. The reaction was quenched by addition of NaHCO₃ and the aqueous layer was extracted three times with dichloromethane. The combined organic layer was washed once with brine, dried over

Na₂SO₄ and concentrated in vacuo. Purification by silica gel chromatography using a toluene/acetone or dichloromethane/methanol solvent system gave access to the pure protected amides (30%–75% yields).

Dibenzyl 3-(phenylcarbamoyl)propylphosphonate (3.5a). ¹H NMR (300 MHz, CDCl₃) δ_H ppm 1.55–2.09 (m, 4H, P-CH₂-CH₂), 2.47 (t, *J* = 6.82 Hz, 2H, CH₂-CONHPh), 4.89–5.11 (m, 4H, CH₂-Ph), 6.99–7.55 (m, 15H, Ar-H), 8.27 (br. s, 1H, NH). ¹³C-NMR (75 MHz, CDCl₃) δ_C ppm 18.93 (d, ²*J*_{P-C} = 6.32 Hz, C2), 24.42 (d, ¹*J*_{P-C} = 139.32 Hz, C1), 36.82 (d, ³*J*_{P-C} = 8.85 Hz), 67.39 (d, ²*J*_{P-C} = 6.63 Hz, PhCH₂, C3), 119.77 (Ar-C), 119.87 (Ar-C), 124.23 (Ar-C), 128.22 (Ar-C), 128.80 (Ar-C), 136.12 (³*J*_{P-C} = 5.53 Hz, C_{ipso}-PhCH₂), 136.31, (Ar-C) 138.39 (Ar-C), 170.71 (C=O). ³¹P-NMR (121.5 MHz, CDCl₃): δ_P ppm = 34.00. HRMS (ESI): calculated for C₂₄H₂₇NO₄P [(M+H)⁺], 424.1672; found 424.1698.

Dibenzyl 3-(o-tolylcarbamoyl)propylphosphonate (3.5b). ¹H NMR (300 MHz, CDCl₃) δ_H ppm 1.70–2.12 (m, 4H, P-CH₂-CH₂), 2.24 (s, Ph-CH₃), 2.51 (t, *J* = 6.74 Hz, 2H, CH₂-CONHPh), 4.87–5.12 (m, 4H, CH₂-Ph), 7.00–7.23 (m, 3H), 7.28–7.38 (m, 10H, Ar-H), 7.55 (br. s, 1H, NH), 7.78 (d, *J* = 7.91 Hz, 1H, Ar-H). ¹³C-NMR (75 MHz, CDCl₃) δ_C ppm 18.18 (PhCH₃), 19.16 (d, ²*J*_{P-C} = 6.32 Hz, C2), 24.75 (d, ¹*J*_{P-C} = 140.21 Hz, C1), 36.87 (d, ³*J*_{P-C} = 9.34 Hz, C3), 67.52 (²*J*_{P-C} = 6.54 Hz, PhCH₂), 123.35 (Ar-C), 125.32 (Ar-C), 126.85 (Ar-C), 128.18 (Ar-C), 128.74 (Ar-C), 128.86 (Ar-C), 130.70 (Ar-C), 136.00 (Ar-C), 136.43 (d, ³*J*_{P-C} = 5.93 Hz, C_{ipso}-PhCH₂), 170.70 (C=O). ³¹P-NMR (121.5 MHz, CDCl₃): δ_P ppm = 33.77. HRMS (ESI): calculated for C₂₅H₂₉NO₄P [(M+H)⁺], 438.1829; found 438.1831.

Dibenzyl 3-(2,6-dimethylphenylcarbamoyl)propylphosphonate (3.5c). ¹H NMR (300 MHz, CDCl₃) δ_H ppm 1.69–2.12 (m, 4H, P-CH₂-CH₂), 2.17 (5/6 of 6H, s, Ph-CH₃), 2.17 (1/6 of 6H, s, Ph-CH₃), 2.49 (t, *J* = 7.16 Hz, 2H, CH₂-CONHPh), 4.86–5.14 (m, 4H, CH₂-Ph), 7.02–7.14 (m, 3H, Ar-H), 7.29–7.38 (m, 10H, Ar-H). ¹³C-NMR (75 MHz, CDCl₃) δ_C ppm 18.79 (Ph-CH₃), 19.22 (d, ²*J*_{P-C} = 5.21 Hz, C2), 25.20 (d, ¹*J*_{P-C} = 140.50 Hz, C1), 36.24 (d, ³*J*_{P-C} = 10.92 Hz, C3), 67.49 (d, ²*J*_{P-C} = 6.69 Hz, PhCH₂), 127.47 (Ar-C), 128.28 (Ar-C), 128.38 (Ar-C), 128.74 (Ar-C), 128.87 (Ar-C), 134.14 (Ar-C), 135.53 (Ar-C), 136.48 (d, ³*J*_{P-C} = 5.85 Hz, C_{ipso}-PhCH₂), 170.57 (C=O). ³¹P-NMR (121.5 MHz, CDCl₃): δ_P ppm = 33.63. HRMS (ESI): calculated for C₂₆H₃₁NO₄P [(M+H)⁺], 452.1985; found 452.1990.

Dibenzyl 3-(2-methoxyphenylcarbamoyl)propylphosphonate (3.5d). ^1H NMR (300 MHz, CDCl_3) δ_{H} ppm 1.74-2.12 (m, 4H, P- $\text{CH}_2\text{-CH}_2$), 2.47 (t, $J = 7.04$ Hz, 2H, $\text{CH}_2\text{-CONHPh}$), 3.83 (s, 3H, NHPh-O-CH_3), 4.91-5.10 (m, 4H, $\text{CH}_2\text{-Ph}$), 6.86 (dd, $J = 1.17$ Hz, 7.91 Hz, 1H, Ar-H), 6.94 (td, $J = 1.46$ Hz, 7.61 Hz, 1H, Ar-H), 7.03 (td, $J = 1.76$ Hz, 7.62 Hz), 7.26-7.40 (m, 10H, Ar-H), 7.82 (br. s, 1H, NH), 8.33 (dd, $J = 1.17$ Hz, 7.91 Hz, 1H, Ar-H). ^{13}C -NMR (75 MHz, CDCl_3) δ_{C} ppm 18.61 (d, $^2J_{\text{P-C}} = 4.98$ Hz, C2), 25.09 (d, $^1J_{\text{P-C}} = 140.42$ Hz, C1), 37.48 (d, $^3J_{\text{P-C}} = 13.27$ Hz, C3), 55.67 (Ph-O- CH_3) 67.23 ($^2J_{\text{P-C}} = 6.64$ Hz, Ph CH_2), 109.97 (Ar-C), 119.98 (Ar-C), 121.08 (Ar-C), 123.76 (Ar-C), 127.61 (Ar-C), 127.99 (Ar-C), 128.46 (Ar-C), 128.65 (Ar-C), 136.41 (d, $^3J_{\text{P-C}} = 6.08$ Hz, $\text{C}_{\text{ipso-PhCH}_2}$), 147.889 (Ar-C), 170.03 (CO). ^{31}P -NMR (121.5 MHz, CDCl_3): δ_{P} ppm = 33.52. HRMS (ESI): calculated for $\text{C}_{25}\text{H}_{29}\text{NO}_5\text{P}$ [(M+H) $^+$], 454.1778; found 454.1791.

Dibenzyl 3-(2,6-dimethoxyphenylcarbamoyl)propylphosphonate (3.5e). ^1H NMR (300 MHz, CDCl_3) δ_{H} ppm 1.85-2.11 (m, 4H, P- $\text{CH}_2\text{-CH}_2$), 2.33-2.59 (m, 2H, $\text{CH}_2\text{-CONHPh}$), 3.75 (br. s, 6H, OCH_3) 4.86-5.12 (m, 4H, $\text{CH}_2\text{-Ph}$), 6.55 (d, $J = 8.51$ Hz, 2H, Ar-H), 7.17 (t, $J = 8.52$ Hz, 1H, Ar-H) 7.27-7.36 (m, 10H, Ar-H). ^{13}C -NMR (75 MHz, CDCl_3) δ_{C} ppm 18.12 (Ph- CH_3), 22.26 (d, $^2J_{\text{P-C}} = 5.35$ Hz, C2), 25.28 (d, $^1J_{\text{P-C}} = 139.10$ Hz, C1), 36.21 (d, $^3J_{\text{P-C}} = 9.83$ Hz, C3), 67.38 (d, $^2J_{\text{P-C}} = 6.58$ Hz, Ph CH_2), 127.39 (Ar-C), 128.20 (Ar-C), 128.32 (Ar-C), 128.45 (Ar-C), 128.92 (Ar-C), 129.13 (Ar-C), 135.51 (Ar-C), 136.97 (d, $^3J_{\text{P-C}} = 6.08$ Hz, $\text{C}_{\text{ipso-PhCH}_2}$), 165.22 (CO). ^{31}P -NMR (121.5 MHz, CDCl_3): δ_{P} ppm = 33.07. HRMS (ESI): calculated for $\text{C}_{26}\text{H}_{31}\text{NO}_6\text{P}$ [(M+H) $^+$], 484.1884 ; found 484.0402.

Dibenzyl 3-(2-fluorophenylcarbamoyl)propylphosphonate (3.5f). ^1H NMR (300 MHz, CDCl_3) δ_{H} ppm 1.76-2.01 (m, 4H, P- $\text{CH}_2\text{-CH}_2$), 2.50 (t, $J = 7.06$ Hz, 2H, $\text{CH}_2\text{-CONHPh}$), 4.88-5.15 (m, 4H, $\text{CH}_2\text{-Ph}$), 6.96-7.16 (m, 3H, Ar-H), 7.28-7.39 (m, 10H, Ar-H), 7.84 (br. s, 1H, NH), 8.25 (t, $J = 8.18$ Hz, 1H, Ar-H). ^{13}C -NMR (75 MHz, CDCl_3) δ_{C} ppm 18.64 (d, $^2J_{\text{P-C}} = 5.24$ Hz, C2), 24.71 (d, $^1J_{\text{P-C}} = 140.37$ Hz, C1), 36.85 (d, $^3J_{\text{P-C}} = 10.64$ Hz, C3), 67.29 (d, $^2J_{\text{P-C}} = 6.59$ Hz, Ph CH_2), 114.86 (d, $^2J_{\text{F-C}} = 19.38$ Hz, F-Ph), 122.02 (Ar-C), 124.36 (d, $^2J_{\text{F-C}} = 7.58$ Hz, F-Ph), 124.49 (d, $^3J_{\text{F-C}} = 3.79$ Hz, F-Ph), 128.00 (Ar-C), 128.49 (Ar-C), 128.62 (Ar-C), 136.26 (d, $^3J_{\text{P-C}} = 5.71$ Hz, $\text{C}_{\text{ipso-PhCH}_2}$), 152.42 (d, $^1J_{\text{F-C}} = 243.71$ Hz, F-Ph), 170.43 (CO). ^{31}P -NMR (121.5 MHz, CDCl_3): δ_{P} ppm = 33.60. HRMS (ESI): calculated for $\text{C}_{24}\text{H}_{26}\text{FNO}_4\text{P}$ [(M+H) $^+$], 442.1578; found 442.1586.

Dibenzyl 3-(2-acetylphenylcarbamoyl)propylphosphonate (3.5g). ^1H NMR (300 MHz, CDCl_3) δ_{H} ppm 1.80-2.12 (m, 4H, P- $\text{CH}_2\text{-CH}_2$), 2.49 (t, $J = 7.11$ Hz, 2H, $\text{CH}_2\text{-CONHPh}$), 2.65 (s, 3H,

OCCH₃), 4.93-5.11 (m, 4H, CH₂-Ph), 7.11 (dd, 1H, *J* = 1.17 Hz, 8.23 Hz, Ar-H), 7.29-7.38 (m, 10H, Ar-H), 7.54 (dd, *J* = 1.68 Hz, 8.52 Hz, 1H, Ar-H), 7.88 (dd, *J* = 1.50 Hz, 7.86 Hz, 1H, Ar-H), 8.72 (dd, *J* = 1.10 Hz, 8.52, 1H Ar-H), 11.70 (br. s, 1H, NH). ¹³C-NMR (75 MHz, CDCl₃) δ_C ppm 18.59 (d, ²*J*_{P-C} = 4.42 Hz, C2), 25.45 (d, ¹*J*_{P-C} = 140.98 Hz, C1), 28.69 (PhCOCH₃), 38.45 (d, ³*J*_{P-C} = 16.03 Hz, C3), 67.25 (d, ²*J*_{P-C} = 6.63 Hz, PhCH₂), 120.82 (Ar-C), 121.90 (Ar-C), 122.45 (Ar-C), 128.01 (Ar-C), 128.45 (Ar-C), 128.70 (Ar-C), 131.79 (Ar-C), 135.30 (Ar-C), 136.45 (d, ³*J*_{P-C} = 6.08 Hz, C_{ipso}-PhCH₂), 141.07 (Ar-C), 174.24 (C=O), 202.91 (PhCOCH₃). ³¹P-NMR (121.5 MHz, CDCl₃): δ_P ppm = 33.43. HRMS (ESI): calculated for C₂₆H₂₉NO₅P [(M+H)⁺], 466.1778; found 466.1779.

Dibenzyl 3-(2-(methylsulfonyl)phenylcarbamoyl)propylphosphonate (3.5h). ¹H NMR (300 MHz, CDCl₃) δ_H ppm 1.74-2.12 (m, 4H, P-CH₂-CH₂), 2.50 (t, *J* = 7.10 Hz, 2H, CH₂-CONHPh), 2.99 (br. s, 3H, SO₂-CH₃), 4.92-5.11 (m, 4H, CH₂-Ph), 7.21-7.29 (m, 2H, Ar-H), 7.30-7.37 (m, 10H, Ar-H), 7.62 (td, *J* = 1.62 Hz, 7.07 Hz, 1H, Ar-H), 7.90 (dd, *J* = 1.62 Hz, 7.98 Hz), 8.45 (dd, *J* = 1.27 Hz, 8.01 Hz, 1H, Ar-H). ¹³C-NMR (75 MHz, CDCl₃) δ_C ppm 18.56 (d, ²*J*_{P-C} = 5.07 Hz, C2), 25.42 (d, ¹*J*_{P-C} = 141.36 Hz, C1), 37.92 (d, ³*J*_{P-C} = 14.76 Hz, C3), 44.41 (-PhSO₂CH₃), 67.47 (d, ²*J*_{P-C} = 6.82 Hz, PhCH₂), 123.06 (Ar-C), 124.40 (Ar-C), 127.28 (Ar-C), 128.21 (Ar-C), 128.68 (Ar-C), 128.85 (Ar-C), 129.54 (Ar-C), 135.54 (Ar-C), 136.53 (d, ³*J*_{P-C} = 5.81 Hz, C_{ipso}-PhCH₂), 137.11 (Ar-C), 170.66 (C=O). ³¹P-NMR (121.5 MHz, CDCl₃): δ_P ppm = 33.10. HRMS (ESI): calculated for C₂₅H₂₉NO₆PS [(M+H)⁺], 502.1448; found 502.1470.

Dibenzyl 3-(2-(dimethylamino)phenylcarbamoyl)propylphosphonate (3.5i). ¹H NMR (300 MHz, CDCl₃) δ_H ppm 1.75-2.12 (m, 4H, P-CH₂-CH₂), 2.49 (t, *J* = 7.07 Hz, 2H, CH₂-CONHPh), 2.60 (br. s, 6H, N-(CH₃)₂), 4.92-5.10 (m, 4H, CH₂-Ph), 7.00-7.18 (m, 3H, Ar-H), 7.27-7.38 (m, 10H, Ar-H), 8.33 (d, 1H, *J* = 7.78, Ar-H), 8.43 (br. s, 1H, NH). ¹³C-NMR (75 MHz, CDCl₃) δ_C ppm 18.80 (d, ²*J*_{P-C} = 4.81 Hz, C2), 25.51 (d, ¹*J*_{P-C} = 140.87 Hz, C1), 37.89 (d, ³*J*_{P-C} = 14.19 Hz, C3), 45.00 (N-CH₃), 67.41 (d, ²*J*_{P-C} = 6.60 Hz, PhCH₂), 119.72 (Ar-C), 120.12 (Ar-C), 123.92 (Ar-C), 125.26 (Ar-C), 128.15 (Ar-C), 128.63 (Ar-C), 128.82 (Ar-C), 133.53 (Ar-C), 136.58 (d, ³*J*_{P-C} = 6.02 Hz, C_{ipso}-PhCH₂), 142.87 (Ar-C), 170.16 (C=O). ³¹P-NMR (121.5 MHz, CDCl₃): δ_P ppm = 33.53. HRMS (ESI): calculated for C₂₆H₃₂N₂O₄P [(M+H)⁺], 467.2094; found 467.2330.

Dibenzyl 3-(2-(tert-butoxycarbonyl)phenylcarbamoyl)propylphosphonate (3.5j). ¹H NMR (300 MHz, CDCl₃) δ_H ppm 1.59 (br. s, 9H, O-tBu), 1.77-2.13 (m, 4H, P-CH₂-CH₂), 2.50 (t, *J* = 7.21 Hz,

2H, $\text{CH}_2\text{-CONHPh}$), 4.93-5.11 (m, 4H, $\text{CH}_2\text{-Ph}$), 7.05 (td, $J = 1.10$ Hz, 7.38, 1H, Ar-H), 7.25-7.38 (m, 10H, Ar-H), 7.49 (td, $J = 1.75$ Hz, 7.38 Hz, 1H, Ar-H), 7.97 (dd, $J = 1.75$ Hz, 8.32 Hz 1H, Ar-H), 8.67 (dd, $J = 1.06$ Hz, 8.51 Hz 1H, Ar-H), 11.20 (br. s, 1H, NH). $^{13}\text{C-NMR}$ (75 MHz, CDCl_3) δ_{C} ppm 18.66 (d, $^2J_{\text{P-C}} = 4.94$ Hz, C2), 25.54 (d, $^1J_{\text{P-C}} = 140.62$ Hz, C1), 28.41 (PhCOOCCH_3), 38.55 (d, $^3J_{\text{P-C}} = 15.82$ Hz, C3), 67.38 (d, $^2J_{\text{P-C}} = 6.35$ Hz, PhCH_2), 82.66 (Ar-C), 116.62 (Ar-C), 120.47 (Ar-C), 122.48 (Ar-C), 128.15 (Ar-C), 128.57 (Ar-C), 128.79 (Ar-C), 131.24 (Ar-C), 134.31 (Ar-C), 136.63 (d, $^3J_{\text{P-C}} = 5.92$ Hz, $\text{C}_{\text{ipso-PhCH}_2}$), 141.71 (Ar-C), 167.91 (COOtBu), 170.96 (CO). $^{31}\text{P-NMR}$ (121.5 MHz, CDCl_3): δ_{P} ppm = 33.41.

Dibenzyl 3-(2-(benzyloxy)phenylcarbamoyl)propylphosphonate (3.5k). $^1\text{H NMR}$ (300 MHz, CDCl_3) δ_{H} ppm 1.74-2.10 (m, 4H, P- $\text{CH}_2\text{-CH}_2$), 2.40 (t, $J = 7.21$ Hz, 2H, $\text{CH}_2\text{-CONHPh}$), 4.86-5.16 (m, 4H, $\text{CH}_2\text{-Ph}$), 5.10 (br. s, 2H, NH-Ph-O- $\text{CH}_2\text{-Ph}$), 6.88-7.05 (m, 3H, Ar-H), 7.24-7.43 (m, 15H, Ar-H), 7.79 (br. s, 1H, NH), 8.35 (td, $J = 2.47$ Hz, 7.84 Hz, 1H, Ar-H). $^{13}\text{C-NMR}$ (75 MHz, CDCl_3) δ_{C} ppm 19.25 (d, $^2J_{\text{P-C}} = 4.98$ Hz, C2), 25.66 (d, $^1J_{\text{P-C}} = 140.43$ Hz, C1), 38.00 (d, $^3J_{\text{P-C}} = 14.37$ Hz, C), 67.54 ($^2J_{\text{P-C}} = 6.6.63$ Hz, PhCH_2), 71.50 (NH-Ph-O- $\text{CH}_2\text{-Ph}$), 112.35 (Ar-C), 120.72 (Ar-C), 122.04 (Ar-C), 124.28 (Ar-C), 128.09(Ar-C), 128.49(Ar-C), 128.90 (Ar-C), 128.95 (Ar-C), 129.14 (Ar-C), 129.35 (Ar-C), 136.91 (d, $^3J_{\text{P-C}} = 6.09$ Hz, $\text{C}_{\text{ipso-PhCH}_2}$), 136.97 (Ar-C), 147.66 (Ar-C), 170.49 (CO). $^{31}\text{P-NMR}$ (121.5 MHz, CDCl_3): δ_{P} ppm = 33.55. HRMS (ESI): calculated for $\text{C}_{31}\text{H}_{33}\text{NO}_5\text{P}$ [(M+H) $^+$], 530.2091; found 530.2122.

Dibenzyl 3-(2,6-bis(benzyloxy)phenylcarbamoyl)propylphosphonate (3.5l). $^1\text{H NMR}$ (300 MHz, CDCl_3) δ_{H} ppm 1.69-1.98 (m, 4H, P- $\text{CH}_2\text{-CH}_2$), 2.38 (app. s, 2H, $\text{CH}_2\text{-CONHPh}$), 5.82-5.01 (m, 4H, P-O- $\text{CH}_2\text{-Ph}$), 5.06 (s, 4H, N-Ph-O- $\text{CH}_2\text{-Ph}$), 6.62 (d, $J = 8.57$ Hz, 2H, Ar-H), 7.12 (t, $J = 8.39$ Hz, 1H, Ar-H), 7.21-7.45 (m, 20 H, Ar-H). $^{13}\text{C-NMR}$ (75 MHz, CDCl_3) δ_{C} ppm 18.19 (C2), 24.49 (d, $^1J_{\text{P-C}} = 138.22$ Hz, C1), 36.07 (C3), 67.02 (d, $^2J_{\text{P-C}} = 6.59$ Hz, PhCH_2OP), 70.71 (NH-PhO CH_2Ph), 106.08 (Ar-C), 115.21 (Ar-C), 127.33 (Ar-C), 127.89 (Ar-C), 128.31 (Ar-C), 128.53 (Ar-C), 136.39, (d, $^3J_{\text{P-C}} = 5.53$ Hz, $\text{C}_{\text{ipso-PhCH}_2}$), 138.81 (Ar-C), 154.92 (CO). $^{31}\text{P-NMR}$ (121.5 MHz, CDCl_3): δ_{P} ppm = 34.16.

Dibenzyl (4-(methylsulfonamido)-4-oxobutyl)phosphonate (3.5m). $^1\text{H NMR}$ (300 MHz, CDCl_3) δ_{H} ppm 1.75-2.04 (m, 4H, P- $\text{CH}_2\text{-CH}_2$), 2.47 (t, $J = 7.03$ Hz, 2H, $\text{CH}_2\text{-CONHPh}$), 3.21 (s, 3H, SO_2NHCH_3), 4.89-5.11 (m, 4H, $\text{CH}_2\text{-Ph}$), 7.28-7.40 (m, 10H, Ar-H), 10.63 (br.s, 1H, NH). $^{13}\text{C-NMR}$ (75 MHz, CDCl_3) δ_{C} ppm 17.79 (d, $^2J_{\text{P-C}} = 5.93$ Hz, C2), 24.46 (d, $^1J_{\text{P-C}} = 140.57$ Hz, C1),

35.84 (d, $^3J_{P-C} = 10.02$ Hz, C3), 41.61 (SO₂NHCH₃), 67.93 (d, $^2J_{P-C} = 6.47$ Hz, PhCH₂), 128.14 (Ar-C), 128.88 (Ar-C), 128.93 (Ar-C), 136.18 (d, $^3J_{P-C} = 5.81$ Hz, C_{ipso}-PhCH₂), 172.17 (CO). ^{31}P -NMR (121.5 MHz, CDCl₃): δ_P ppm = 33.41. HRMS (ESI): calculated for C₁₉H₂₅NO₆PS [(M+H)⁺], 426.1140; found 426.1162.

2-(4-(Bis(benzyloxy)phosphoryl)butanamido)benzoic acid (3.5n). Compound **3.5j** (0.416 g) was dissolved in a dichloromethane/TFA mixture (5/1, 8 mL) at 0 °C. After stirring for an hour, TLC analysis showed a completed reaction. Toluene (15 mL) was then added to the reaction mixture before concentration *in vacuo*. Column chromatography (97.5% CH₂Cl₂/2% MeOH/0.5% CH₃COOH) yielded 272 mg of **3.5n** as an oil (73% yield). 1H NMR (300 MHz, CDCl₃) δ_H ppm 1.94-2.17 (m, 4H, P-CH₂-CH₂), 2.52 (t, $J = 6.26$ Hz, 2H, CH₂-CONHPh), 4.87-5.14 (m, 4H, CH₂-Ph), 7.06 (td, $J = 1.08$ Hz, 8.10 Hz, 1H, Ar-H), 7.27-7.35 (m, 10H, Ar-H), 7.51 (td, $J = 1.08$ Hz, 8.28 Hz, 1H, Ar-H), 8.10 (dd, $J = 1.68$ Hz, 8.10 Hz, 1H, Ar-H), 8.66 (td, $J = 1.00$ Hz, 8.39 Hz, 1H, Ar-H), 11.44 (br.s 1H, NH). ^{13}C -NMR (75 MHz, CDCl₃) δ_C ppm 18.25 (d, $^2J_{P-C} = 5.04$ Hz, C2), 25.22 (d, $^1J_{P-C} = 140.04$ Hz, C1), 38.52 (d, $^3J_{P-C} = 17.22$ Hz, C3), 67.96 (d, $^2J_{P-C} = 6.52$ Hz, PhCH₂), 115.55 (Ar-C), 120.23 (Ar-C), 122.72 (Ar-C), 128.21 (Ar-C), 128.77 (Ar-C), 128.86 (Ar-C), 131.81 (Ar-C), 134.71 (Ar-C), 136.14 (d, $^3J_{P-C} = 5.92$ Hz, C_{ipso}-PhCH₂), 141.89 (Ar-C), 170.90 (CO), 170.98 (CO). ^{31}P -NMR (121.5 MHz, CDCl₃): δ_P ppm = 26.02.

Diethyl 3-(2-cyanophenylcarbamoyl)propylphosphonate (3.6q). 1H NMR (300 MHz, CDCl₃) δ_H ppm 1.34 (t, $J = 7.11$ Hz, 6H, P-O-CH₂CH₃), 1.79-2.17 (m, 4H, P-CH₂-CH₂), 2.64 (t, $J = 7.11$ Hz, 2H, CH₂-CONHPh), 4.01-4.23 (m, 4H, -O-CH₂-CH₃), 7.19 (dd, $J = 1.05$ Hz, 7.64 Hz, 1H, Ar-H), 7.51-7.66 (m, 2H, Ar-H), 8.14 (br. s, 1H, NH), 8.28 (dd, $J = 1.10$ Hz, 8.96 Hz, 1H Ar-H). ^{13}C -NMR (75 MHz, CDCl₃) δ_C ppm 16.49 (d, $^3J_{P-C} = 6.32$ Hz, P-O-CH₂-CH₃), 18.58 (d, $^2J_{P-C} = 6.32$ Hz, C2), 24.43 (d, $^1J_{P-C} = 141.21$ Hz, C1), 37.02 (d, $^3J_{P-C} = 12.19$ Hz, C3), 61.75 (d, $^2J_{P-C} = 6.06$ Hz, P-O-CH₂-CH₃), 102.97 (Ar-C), 116.46 (CN), 122.10 (Ar-C), 124.39 (Ar-C), 132.46 (Ar-C), 134.04 (Ar-C), 140.37 (Ar-C), 170.86 (CO). ^{31}P -NMR (121.5 MHz, CDCl₃): δ_P ppm = 32.14. HRMS (ESI): calculated for C₂₅H₂₂N₂O₄P [(M+H)⁺], 325.1317; found 325.1317.

General procedure for hydrogenolysis towards targets 3.1a-i, m-p

The amide (100 - 150 mg) was dissolved in MeOH (10 mL) and Pd/C (10%) was added under inert atmosphere. The resulting mixture was then stirred under hydrogen atmosphere for 10 minutes and the progress monitored by mass spectrometry. At completion, the reaction

mixture was filtered and neutralized with 1 eq. of a NaOH. The mixture was concentrated *in vacuo*, re-dissolved in a mixture of water and *t*-butanol, frozen and lyophilized to afford the desired targets compounds **3.1a-i, m-p** as a white powder in quantitative yield.

Sodium hydrogen3-(phenylcarbamoyl)propylphosphonate (3.1a). ^1H NMR (300 MHz, D_2O) δ_{H} ppm 1.40-1.56 (m, 2H, $-\text{CH}_2-$), 1.78-1.93 (m, 2H, $\text{P}-\text{CH}_2-$), 2.46 (t, $J = 7.47$ Hz, 2H, CH_2 -CONHPh), 7.24 (dt, $J = 5.78, 2.82$ Hz, 1H, Ar-H), 7.34-7.46 (m, 4 H, Ar-H). ^{13}C -NMR (75 MHz, D_2O) δ_{C} ppm 21.13 (d, $^2J_{\text{P-C}} = 3.71$ Hz, C2), 28.55 (d, $^1J_{\text{P-C}} = 131.25$ Hz, C1), 38.10 (d, $^3J_{\text{P-C}} = 16.61$ Hz, C3), 122.45 (Ar-C), 125.79 (Ar-C), 129.33 (Ar-C), 136.92 (Ar-C), 176.00 (C=O). ^{31}P -NMR (121.5 MHz, D_2O): δ_{P} ppm = 22.06. HRMS (ESI): calculated for $\text{C}_{10}\text{H}_{13}\text{NO}_4\text{P}$ [(M-H) $^-$], 242.0588; found 242.0061.

Sodium hydrogen3-(o-tolylcarbamoyl)propylphosphonate (3.1b). ^1H NMR (300 MHz, D_2O) δ_{H} ppm 1.47-1.62 (m, 2H, $-\text{CH}_2-$), 1.70-1.90 (m, 2H, $\text{P}-\text{CH}_2-$), 2.10 (s, Ph- CH_3), 2.40 (t, $J = 7.44$ Hz, 2H, CH_2 -CONHPh), 7.18-7.35 (m, 4H, Ar-H), 8.42 (br. s, 1H, NH). ^{13}C -NMR (75 MHz, D_2O) δ_{C} ppm 17.14 (Ph- CH_3), 21.06 (d, $^2J_{\text{P-C}} = 3.65$ Hz, C2), 28.42 (d, $^1J_{\text{P-C}} = 131.87$ Hz, C1), 37.68 (d, $^3J_{\text{P-C}} = 16.61$ Hz, C3), 126.76 (Ar-C), 127.21 (Ar-C), 127.81 (Ar-C), 130.89 (Ar-C), 134.56 (Ar-C), 137.97 (Ar-C), 176.47 (C=O). ^{31}P -NMR (121.5 MHz, D_2O): δ_{P} ppm = 23.60. HRMS (ESI): calculated for $\text{C}_{11}\text{H}_{15}\text{NO}_4\text{P}$ [(M-H) $^-$], 256.0744; found 256.0322.

Sodium hydrogen3-(2,6-dimethylphenylcarbamoyl)propylphosphonate (3.1c). ^1H NMR (300 MHz, D_2O) δ_{H} ppm 1.47-1.65 (m, 2H, $-\text{CH}_2-$), 1.80-2.20 (m, 2H, $\text{P}-\text{CH}_2-$), 2.17 (s, 6H, Ph- CH_3), 2.54 (t, $J = 7.47$ Hz, 2H, CH_2 -CONHPh), 7.07-7.25 (m, 3H, Ar-H). ^{13}C -NMR (75 MHz, D_2O) δ_{C} ppm 17.44 (Ph- CH_3), 21.11 (d, $^2J_{\text{P-C}} = 3.44$ Hz, C2), 28.68 (d, $^1J_{\text{P-C}} = 131.75$ Hz, C1), 37.24 (d, $^3J_{\text{P-C}} = 17.28$ Hz, C3), 128.21 (Ar-C), 133.48 (Ar-C), 136.31 (Ar-C), 176.37 (C=O). ^{31}P -NMR (121.5 MHz, D_2O): δ_{P} ppm = 22.47. HRMS (ESI): calculated for $\text{C}_{12}\text{H}_{17}\text{NO}_4\text{P}$ [(M-H) $^-$], 270.0901; found 270.0319.

Sodium hydrogen3-(2-methoxyphenylcarbamoyl)propylphosphonate (3.1d). ^1H NMR (300 MHz, D_2O) δ_{H} ppm 1.37-1.52 (m, 2H, $-\text{CH}_2-$), 1.77-1.92 (m, 2H, $\text{P}-\text{CH}_2-$), 2.47 (t, $J = 7.52$ Hz, 2H, CH_2 -CONHPh), 3.83 (s, 3H, Ph-O- CH_3), 7.00 (td, $J = 7.65$ Hz, 1.33 Hz, 1H, Ar-H), 7.09 (dd, $J = 8.31$ Hz, 1.24 Hz, 1H, Ar-H), 7.20-7.32 (m, 1H, Ar-H), 7.52 (dd, $J = 7.87$ Hz, 1.68 Hz, 1H, Ar-H). ^{13}C -NMR (75 MHz, D_2O) δ_{C} ppm 21.40 (d, $^2J_{\text{P-C}} = 3.36$ Hz, C2), 28.94 (d, $^1J_{\text{P-C}} = 130.12$ Hz, C1), 38.04 (d, $^3J_{\text{P-C}} = 16.84$ Hz, C3), 56.01 (Ph-O- CH_3), 112.30 (Ar-C), 121.07 (Ar-C), 125.20

(Ar-C), 125.53 (Ar-C), 127.65 (Ar-C), 152.22 (Ar-C), 176.45 (C=O). ³¹P-NMR (121.5 MHz, D₂O): δ_P ppm = 21.28. HRMS (ESI): calculated for C₁₁H₁₅NO₅P [(M-H)⁻], 272.0693; found 272.0129.

Sodium hydrogen3-(2,6-dimethoxyphenylcarbamoyl)propylphosphonate (3.1e). ¹H NMR (300 MHz, D₂O) δ_H ppm 1.42-1.57 (m, 2H, -CH₂-), 1.69-1.88 (m, 2H, P-CH₂-), 2.40 (t, *J* = 7.39 Hz, 2H, CH₂-CONHPh), 3.71 (s, 6H, Ph-O-CH₃), 6.66 (d, *J* = 8.47 Hz, 2H, Ar-H), 7.33 (t, *J* = 8.47 Hz, 1H, Ar-H). ¹³C-NMR (75 MHz, D₂O) δ_C ppm 20.82 (d, ²*J*_{P-C} = 3.64 Hz, C2), 28.05 (d, ¹*J*_{P-C} = 132.26 Hz, C1), 37.12 (d, ³*J*_{P-C} = 17.22 Hz, C3), 56.34 (PhOCH₃), 105.38 (Ar-C), 113.06 (Ar-C), 129.44 (Ar-C), 155.33 (Ar-C), 176.72 (C=O). ³¹P-NMR (121.5 MHz, D₂O): δ_P ppm = 24.34. HRMS (ESI): calculated for C₁₂H₁₇NO₆P [(M+H)⁺], 302.0799; found 302.0074.

Sodium hydrogen3-(2-fluorophenylcarbamoyl)propylphosphonate (3.1f). ¹H NMR (300 MHz, D₂O) δ_H ppm 1.44-1.61 (m, 2H, -CH₂-), 1.80-1.94 (m, 2H, P-CH₂-), 2.51 (t, *J* = 7.32 Hz, 2H, CH₂-CONHPh), 7.13-7.33 (m, 3H, Ar-H), 7.53 (td, *J* = 1.74 Hz, 7.63 Hz, 1H, Ar-H). ¹³C-NMR (75 MHz, D₂O) δ_C ppm 20.89 (d, ²*J*_{P-C} = 3.54 Hz, C2), 28.30 (d, ¹*J*_{P-C} = 131.37 Hz, C1), 37.50 (d, ³*J*_{P-C} = 17.13 Hz, C3), 116.05 (d, *J*_{F-C} = 19.91 Hz, Ar-C), 124.03 (d, *J*_{F-C} = 3.36 Hz, Ar-C), 124.71 (d, *J*_{F-C} = 12.74 Hz, Ar-C), 126.62 (Ar-C), 128.08 (d, *J*_{F-C} = 7.95 Hz, Ar-C), 157.44 (Ar-C), 176.42 (C=O). ³¹P-NMR (121.5 MHz, D₂O): δ_P ppm = 22.63. HRMS (ESI): calculated for C₁₀H₁₂FNO₄P [(M-H)⁻], 260.0494; found 260.0001.

Sodium hydrogen3-(2-acetylphenylcarbamoyl)propylphosphonate (3.1g). ¹H NMR (300 MHz, D₂O) δ_H ppm 1.24 (s, 3H, PhCOCH₃), 1.40-1.58 (m, 2H, -CH₂-), 1.84-1.99 (m, 2H, P-CH₂-), 2.51 (t, *J* = 7.13 Hz, 2H, CH₂-CONHPh), 7.20-7.43 (m, 4H, Ar-H), ¹³C-NMR (75 MHz, D₂O) δ_C ppm 21.43 (d, ²*J*_{P-C} = 3.87 Hz, C2), 29.10 (d, ¹*J*_{P-C} = 129.92 Hz, C1), 29.71 (PhCOCH₃), 37.69 (d, ³*J*_{P-C} = 16.58 Hz, C3), 126.83 (Ar-C), 127.98 (Ar-C), 128.23 (Ar-C), 129.40 (Ar-C), 133.94 (Ar-C), 141.189 (Ar-C), 177.12 (-C=O-), 177.20 (-C(=O)CH₃). ³¹P-NMR (121.5 MHz, D₂O): δ_P ppm = 22.19. HRMS (ESI): calculated for C₁₂H₁₅NO₅P [(M-H)⁻], 284.0693; found 284.0693.

Sodium hydrogen3-(2-(methylsulfonyl)phenylcarbamoyl)propylphosphonate (3.1h). ¹H NMR (300 MHz, D₂O) δ_H ppm 1.40-1.58 (m, 2H, -CH₂-), 1.81-1.98 (m, 2H, P-CH₂-), 2.57 (t, *J* = 7.66 Hz, 2H, CH₂-CONHPh), 3.23 (s, 3H, -Ph-SO₂CH₃), 7.57 (td, *J* = 1.36 Hz, 7.73 Hz, 1H, Ar-H), 7.65 (dd, *J* = 1.36 Hz, 8.13 Hz, 1H, Ar-H), 7.79 (td, *J* = 1.49 Hz, 7.73 Hz, 1H, Ar-H), 8.01 (dd, *J* = 8.00 Hz, 1.53 Hz, 1H, Ar-H). ¹³C-NMR (75 MHz, D₂O) δ_C ppm 20.97 (d, ²*J*_{P-C} = 3.37 Hz, C2), 28.89 (d, ¹*J*_{P-C} = 130.92 Hz, C1), 37.91 (d, ³*J*_{P-C} = 17.13 Hz, C3), 43.14 (-Ph-SO₂CH₃), 128.31 (Ar-C),

129.60 (Ar-C), 129.83 (Ar-C), 133.81 (Ar-C), 134.67 (Ar-C), 135.82 (Ar-C), 177.16 (C=O). ^{31}P -NMR (121.5 MHz, D_2O): δ_{P} ppm = 22.51. HRMS (ESI): calculated for $\text{C}_{11}\text{H}_{15}\text{NO}_6\text{PS}$ [(M-H) $^-$], 320.0363; found 319.9703.

Sodium hydrogen3-(2-(dimethylamino)phenylcarbamoyl)propylphosphonate (3.1i). ^1H NMR (300 MHz, D_2O) δ_{H} ppm 1.37-1.56 (m, 2H, -CH $_2$ -), 1.79-1.96 (m, 2H, P-CH $_2$ -), 2.51 (t, J = 7.52 Hz, 2H, CH $_2$ -CONHPh), 2.62 (s, 6H, Ph-N-CH $_3$), 7.07-7.15 (m, 1H, Ar-H), 7.22-7.29 (m, 2H, Ar-H), 7.45 (app. d, J = 7.65 Hz, 1H, Ar-H). ^{13}C -NMR (75 MHz, D_2O) δ_{C} ppm 21.31 (d, $^2J_{\text{P-C}}$ = 3.69 Hz, C2), 29.11 (d, $^1J_{\text{P-C}}$ = 130.27 Hz, C1), 38.17 (d, $^3J_{\text{P-C}}$ = 16.91 Hz, C3), 43.71 (Ph-N-CH $_3$), 120.11 (Ar-C), 123.95 (Ar-C), 126.90 (Ar-C), 127.79 (Ar-C), 129.99 (Ar-C), 147.99 (Ar-C), 176.57 (C=O). ^{31}P -NMR (121.5 MHz, D_2O): δ_{P} ppm = 24.24. HRMS (ESI): calculated for $\text{C}_{12}\text{H}_{18}\text{N}_2\text{O}_4\text{P}$ [(M-H) $^-$], 285.1010; found 285.0459.

Sodium hydrogen (4-(methylsulfonamido)-4-oxobutyl)phosphonate (3.1m). ^1H NMR (300 MHz, D_2O) δ_{H} ppm 1.55-1.69 (m, 2H, -CH $_2$ -), 1.78-1.92 (m, 2H, P-CH $_2$ -), 2.40 (t, J = 7.27 Hz, 2H, CH $_2$ -CONHPh), 2.39 (s, 3H, -N-SO $_2$ CH $_3$). ^{13}C -NMR (75 MHz, D_2O) δ_{C} ppm 19.78 (d, $^2J_{\text{P-C}}$ = 3.87 Hz, C2), 27.41 (d, $^1J_{\text{P-C}}$ = 133.24 Hz, C1), 38.62 (d, $^3J_{\text{P-C}}$ = 17.14 Hz, C3), 40.10 (-N-SO $_2$ CH $_3$), 180.33 (C=O). ^{31}P -NMR (121.5 MHz, D_2O): δ_{P} ppm = 25.22. HRMS (ESI): calculated for $\text{C}_5\text{H}_{11}\text{NO}_6\text{PS}$ [(M-H) $^-$], 244.0050; found 244.0611.

Sodium hydrogen3-(2-carboxyphenylcarbamoyl)propylphosphonate (3.1n). ^1H NMR (300 MHz, D_2O) δ_{H} ppm 1.55-1.70 (m, 2H, -CH $_2$ -), 1.81-1.98 (m, 2H, P-CH $_2$ -), 2.51 (t, J = 7.31 Hz, 2H, CH $_2$ -CONHPh), 7.22 (td, J = 1.03 Hz, 7.64 Hz, 1H, Ar-H), 7.50 (td, J = 1.65 Hz, 7.64 Hz, 1H, Ar-H), 7.85 (dd, J = 7.83, 1.60 Hz, 1H, Ar-H), 8.01 (app. d, 1H, Ar-H). ^{13}C -NMR (75 MHz, D_2O) δ_{C} ppm 19.97 (d, $^2J_{\text{P-C}}$ = 3.95 Hz, C2), 27.37 (d, $^1J_{\text{P-C}}$ = 133.39 Hz, C1), 38.45 (d, $^3J_{\text{P-C}}$ = 17.66 Hz, C3), 121.99 (Ar-C), 124.67 (Ar-C), 125.10 (Ar-C), 130.71 (Ar-C), 132.22 (Ar-C), 137.17 (Ar-C), 173.83 (CO, PhCOOH), 174.88 (CO, -CH $_2$ -CO-NH-). ^{31}P -NMR (121.5 MHz, D_2O): δ_{P} ppm = 24.98. HRMS (ESI): calculated for $\text{C}_{11}\text{H}_{13}\text{NO}_6\text{P}$ [(M-H) $^-$], 286.0486; found 286.0268.

Sodium hydrogen3-(2-hydroxyphenylcarbamoyl)propylphosphonate (3.1o). ^1H NMR (300 MHz, D_2O) δ_{H} ppm 1.46-1.61 (m, 2H, -CH $_2$ -), 1.79-1.96 (m, 2H, P-CH $_2$ -), 2.51 (t, J = 7.44 Hz, 2H, CH $_2$ -CONHPh), 6.88-7.03 (m, 2H, Ar-H), 7.18 (td, J = 1.79 Hz, 7.45 Hz, 1H, Ar-H), 7.35 (dd, J = 7.83 Hz, 1.60 Hz, 1H, Ar-H). ^{13}C -NMR (75 MHz, D_2O) δ_{C} ppm 20.85 (d, $^2J_{\text{P-C}}$ = 3.84 Hz, C2), 28.25 (d, $^1J_{\text{P-C}}$ = 131.65 Hz, C1), 37.47 (d, $^3J_{\text{P-C}}$ = 17.18 Hz, C3), 116.89 (Ar-C), 120.73 (Ar-C),

124.10 (Ar-C), 126.37 (Ar-C), 128.15 (Ar-C), 149.83 (Ar-C), 176.39 (C=O). ^{31}P -NMR (121.5 MHz, D_2O): δ_{P} ppm = 22.85. HRMS (ESI): calculated for $\text{C}_{10}\text{H}_{13}\text{NO}_5\text{P}$ [(M+H) $^+$], 258.0537; found 258.0058.

Sodium hydrogen3-(2,6-dihydroxyphenylcarbamoyl)propylphosphonate (3.1p). ^1H NMR (300 MHz, D_2O) δ_{H} ppm 1.48-1.66 (m, 2H, -CH $_2$ -), 1.78-1.99 (m, 2H, P-CH $_2$ -), 2.54 (t, J = 7.43 Hz, 2H, CH $_2$ -CONHPh), 6.52 (d, J = 8.33 Hz, 2H, Ar-H), 7.07 (t, J = 8.22 Hz, 1H, Ar-H). ^{13}C -NMR (75 MHz, D_2O) δ_{C} ppm 20.63 (d, $^2J_{\text{P-C}}$ = 3.95 Hz, C2), 28.12 (d, $^1J_{\text{P-C}}$ = 131.80 Hz, C1), 37.02 (d, $^3J_{\text{P-C}}$ = 16.52 Hz, C3), 108.25 (Ar-C), 111.93 (Ar-C), 129.19 (Ar-C), 152.84 (Ar-C), 177.01 (C=O). ^{31}P -NMR (121.5 MHz, D_2O): δ_{P} ppm = 22.22. HRMS (ESI): calculated for $\text{C}_{10}\text{H}_{13}\text{NO}_6\text{P}$ [(M-H) $^-$], 274.0486; found 273.9962.

Bisammomium3-(2-cyanophenylcarbamoyl)propylphosphonate (3.1q). Intermediate **3.6q** (150 mg, 0.334 mmol) was dissolved in dry dichloromethane under inert atmosphere and cooled to 0 °C. TMSBr (0.5 mL, 3.3 mmol) was added dropwise while stirring. The icebath was removed after 10 minutes and the reaction stirred at room temperature for 24 hours. ^{31}P confirmed that the starting phosphonate was completely deprotected (shift from δ = 32–25 ppm). The volatiles were removed *in vacuo*, the crude material was dissolved in 5% aqueous ammonia and washed with diethyl ether. Lyophilization of the ammonia solution yielded the product as a brown solid in quantitative yield. ^1H NMR (300 MHz, D_2O) δ_{H} ppm 1.50-1.65 (m, 2H, -CH $_2$ -), 1.85-2.20 (m, 2H, P-CH $_2$ -), 2.68 (t, J = 7.58 Hz, 2H, CH $_2$ -CONHPh), 7.45 (td, J = 0.99 Hz, 7.96 Hz, 1H, Ar-H), 7.60 (d, J = 8.05 Hz, 1H, Ar-H), 7.77 (td, J = 1.51 Hz, 7.20 Hz, 1H, Ar-H), 8.08 (dd, J = 1.33 Hz, 7.96 Hz, 1H, Ar-H). ^{13}C -NMR (75 MHz, D_2O) δ_{C} ppm 21.55 (d, $^2J_{\text{P-C}}$ = 3.87 Hz, C2), 27.80 (d, $^1J_{\text{P-C}}$ = 136.00 Hz, C1), 35.65 (d, $^3J_{\text{P-C}}$ = 16.59 Hz, C3), 121.59 (Ph-C \equiv N), 126.40 (Ar-C), 126.65 (Ar-C), 127.45 (Ar-C), 134.95 (Ar-C), 149.45 (Ar-C), 157.68 (Ar-C), 162.45 (C=O). ^{31}P -NMR (121.5 MHz, D_2O): δ_{P} ppm = 25.00. HRMS (ESI): calculated for $\text{C}_{11}\text{H}_{13}\text{N}_2\text{O}_4\text{P}$ [(M-H) $^-$], 267.0540; found 267.0823.

o-(Dimethylamino)aniline (**3.4i**). To a solution of **3.7** (0.5 g; 2 mmol) in MeOH (100 mL) was added formalin (14 mL), Pd/C 10% (160 mg) and formic acid (1 mL). The resulting mixture was allowed to stir under a hydrogen atmosphere for 3 h, after which, the mixture was filtered over a celite path and the filtrate concentrated to about 25 mL. The mixture was then basified by adding NaHCO_3 and the water layer was extracted three times with EtOAc (3

× 50 mL). The combined organic phase was washed once with brine and dried over Na₂SO₄. Column chromatography (Hexane/EtOAc 95:5) yielded **3.8** (0.450 g, 90%) as a colorless oil. Subsequent treatment of **3.8** with 30% TFA in dichloromethane at 0°C afforded **3.4i** which was used for the next step without further purification.

Tert-butyl 2-(dimethylamino)phenylcarbamate (3.8). ¹H NMR (300 MHz, CDCl₃) δ_H ppm 1.54 (br. s, 9H, *tert*-Bu), 2.62 (s, 6H, N-CH₃), 6.96 (td, *J* = 1.16 Hz, 7.57 Hz, 1H, Ar-H), 7.05-7.16 (m, 2H, Ar-H), 7.70 (br. s, 1H, NH), 8.07 (d, *J* = 8.17). ¹³C-NMR (75 MHz, CDCl₃) δ_C ppm 28.93 (CH₃ of *tert*-Bu), 44.83 (N-CH₃), 80.27 (C_q of *tert*-Bu), 117.97 (Ar-C), 120.16 (Ar-C), 122.51 (Ar-C), 125.22 (Ar-C), 134.13 (Ar-C), 142.35 (Ar-C), 153.29 (C=O). HRMS (ESI): calculated for C₁₃H₂₁N₂O₂ [(M+H)⁺], 237.1598; found 237.1602.

REFERENCES

1. Lou, B.; Yang, K. Molecular diversity of hydroxamic acids. Part II. Potential therapeutic applications. *Mini Rev. Med. Chem.* **2003**, 3, 6, 609–20.
2. O'Brien, E. C.; Farkas, E.; Gil, M. J.; Fitzgerald, D.; Castineras, A.; Nolan, K. B. Metal complexes of salicylhydroxamic acid (H₂Sha), anthranilic hydroxamic acid and benzohydroxamic acid. Crystal and molecular structure of [Cu(phen)₂(Cl)]ClPH₂Sha, a model for a peroxidase inhibitor complex. *J. Inorg. Biochem.* **2000**, 79, 47–51.
3. Sanderson, L.; Taylor, G. W.; Aboagye, E. O.; Alao, J. P.; Latigo, J. R.; Coombes, R. C.; Vigushin, D. M. Plasma pharmacokinetics and metabolism of the histone deacetylase inhibitor trichostatin a after intraperitoneal administration to mice. *Drug Metab. Dispos.* **2004**, 32, 1132–1138.
4. San Jose, G.; Jackson, E. R.; Uh, E.; Johny, C.; Haymond, A.; Lundberg, L.; Pinkham, C.; Kehn-Hall, K.; Boshoff, H. I.; Couch, R. D.; *et al.* Design of potential bisubstrate inhibitors against *Mycobacterium tuberculosis* (Mtb) 1-deoxy-D-xylulose 5-phosphate reductoisomerase (Dxr)-evidence of a novel binding mode. *Med. Chem. Commun.* **2013**, 4, 1099–1104.
5. Gavalda, S.; Braga, R.; Dax, C.; Vigroux, A.; Blonski, C. N-Sulfonyl hydroxamate derivatives as inhibitors of class II fructose-1,6-diphosphate aldolase. *Bioorg. Med. Chem. Lett.* **2005**, 15, 5375–5377.
6. Kuntz, L.; Tritsch, D.; Grosdemange-Billiard, C.; Hemmerlin, A.; Willem, A.; Bacht, T.; Rohmer, M. Isoprenoid biosynthesis as a target for antibacterial and antiparasitic drugs: Phosphonohydroxamic acids as inhibitors of deoxyxylulose phosphate reducto-isomerase. *Biochem. J.* **2005**, 386, 127–135.
7. McNeil, D. W.; Kelly, T. A. A simple method for the protection of aryl amines as their *t*-butylcarbamoyl (Boc) derivatives. *Tetrahedron Lett.* **1994**, 35, 9003–9006.
8. Sumandeep, K. G.; Hao, X.; Kirchoff, P. D.; Cierpicki, T.; Turbiak, A. J.; Wan, B.; Zhang, N.; Peng, K. W.; Franzblau, S. G.; Garcia, G. A.; *et al.* Structure-based design of novel benzoxazinorifamycins with potent binding affinity to wild-type and rifampin-resistant mutant *Mycobacterium tuberculosis* RNA polymerases. *J. Med. Chem.* **2012**, 55, 3814–3826.

9. Jawaid, S.; Seidle, H.; Zhou, W.; Abdirahman, H.; Abadeer, M.; Hix, J. H.; van Hoek, M. L.; Couch, R. D. Kinetic characterization and phosphoregulation of the *Francisella tularensis* 1-deoxy-D-xylulose 5-phosphate reductoisomerase (MEP Synthase). *PLoS One* **2009**, *4*, e8288.
10. Haymond, A.; Johny, C.; Dowdy, T.; Schweibenz, B.; Villarroel, K.; Young, R.; Mantooth, C. J.; Patel, T.; Bases, J.; San Jose, G.; Jackson, E. R.; Dowd, C. S.; Couch, R. D. Kinetic characterization and allosteric inhibition of the *Yersinia pestis* 1-deoxy-D-xylulose 5 phosphate reductoisomerase (MEP synthase). *PLoS One* **2014**, e106243.
11. Larsen, T. M.; Wedekind, J. E.; Rayment, I.; Reed, G. H. A Carboxylate oxygen of the substrate bridges the magnesium ions at the active Site of enolase: Structure of the yeast enzyme complexed with the equilibrium mixture of 2-phosphoglycerate and phosphoenolpyruvate at 1.8 Å Resolution. *Biochemistry* **1996**, *35*, 4351–4358.
12. Bodill, T.; Conibear, A. C.; Mutorwa, M. K. M.; Goble, J. L.; Blatch, G. L.; Lobb, K. A.; Klein, R.; Kaye, P. T. Exploring DOXP-reductoisomerase binding limits using phosphonated *N*-aryl and *N*-heteroarylcarboxamides as DXR inhibitors. *Bioorg. Med. Chem.* **2013**, *21*, 4332–4341.
13. Zinglé, C.; Kuntz, L.; Tritsch, D.; Grosdemange, C. B.; Rohmer, M. Modifications around the hydroxamic acid chelating group of fosmidomycin, an inhibitor of the metalloenzyme 1-deoxyxylulose 5-phosphate reductoisomerase (DXR). *Bioorg. Med. Chem. Lett.* **2012**, *22*, 6563–6567.
14. Cos, P.; Vlietinck, A. J.; Vanden Berghe, D.; Maes, L. Anti-infective potential of natural products: How to develop a stronger *in vitro* proof-of-concept. *J. Ethnopharmacol.* **2006**, *106*, 290–302.

Chapter IV

GENERAL CONSIDERATIONS ON PHOSPHONATE CHEMISTRY

IV. GENERAL CONSIDERATIONS ON PHOSPHONATE CHEMISTRY

Phosphonates represent a large group of chemical compounds with a wide range of applications in pharmaceuticals and as intermediates in synthetic chemistry. An important challenge in preparing phosphonate compounds is the introduction of the phosphonic acid group and the subsequent removal of the phosphonate protecting groups. Several synthetic methodologies exist for the construction of C-P bonds including the Michaelis-Arbusov reaction, the Michael addition, the Michaelis-Becker reaction, the Horner-Wadsworth-Emmons reaction and some coupling reactions. Within the context of this PhD study, the C-P bond formation principles and the phosphonate deprotection strategies used are briefly discussed below.

IV.A. Formation of the C-P bond in phosphonates

IV.A.1. The Michaelis-Arbusov reaction

One of the most useful approaches for forming a C-P bond, the Michaelis-Arbusov reaction is a double substitution nucleophilic bi-molecular (S_N2) process between an alkyl halide (bromide or iodide) and a trialkylphosphite (Figure IV.1), promoted by heat. The transformation is initiated by an S_N2 reaction of the nucleophilic trialkylphosphite with the alkyl halide to give a phosphonium intermediate and a halide anion. A second S_N2 reaction of the displaced halide anion with the phosphonium intermediate affords the phosphonate ester along with an alkyl halide.

Despite its popularity, a couple of drawbacks limit the universal application of this strategy to access phosphonates. For instance, both aryl and vinyl phosphonates (the corresponding halides of which react weakly with phosphites) and α -hydroxyl/ α -amino phosphonates (whose corresponding halides are unstable) are not affordable via this strategy. In the case of phosphite reaction with α -haloketones, the products are vinyl phosphates (the Perkow reaction) instead of alkyl phosphonates. Concerns over a further restriction on the scope of

suitable substrates for the Michaelis-Arbusov reaction by the required high temperatures, have led to the development of room-temperature variants of this reaction.^{1,2}

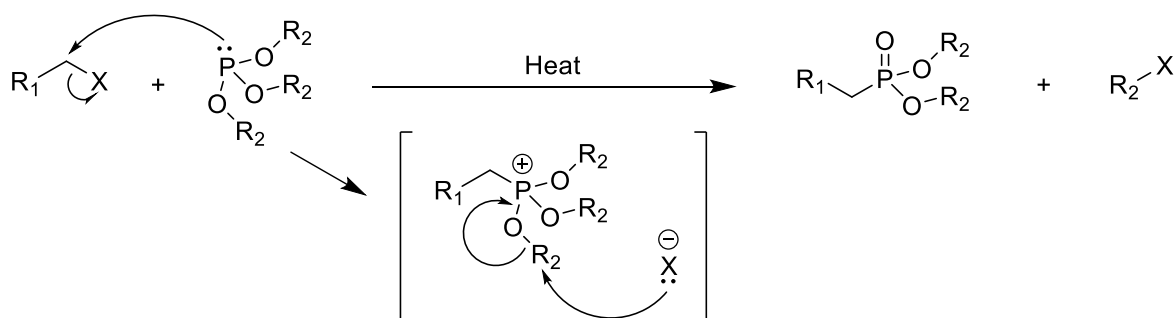


Figure IV.1: Mechanism of the Michaelis-Arbusov reaction.

IV.A.2. Phosphonylation by Michael addition

The Michael addition, refers to the 1,4-addition of a stabilized or 'soft' nucleophile (also known as Michael donor, which can be carbon or heteroatom based) to an alkene or alkyne that is in conjugation with an activating group such as a carbonyl (Michael acceptor). Michael addition of a di- or tri-alkylphosphite or a dialkyl methylphosphonate anion to such α,β -unsaturated compounds (Figure IV.2, path **a**, **b** and **c** respectively) results in the corresponding dialkyl phosphonic esters. The existence of two tautomeric forms of H-phosphonates (**a**) is an important feature, since the presence of a lone electron pair on the phosphorus atom of the phosphite tautomer allows these compounds to react readily as nucleophilic species.³ The use of trialkylphosphites as nucleophiles (**b**) implies a different mechanistic pathway involving the addition of an external nucleophilic agent (e.g. phenol), which participates in a Michaelis-Arbusov type rearrangement after the conjugate addition step, to deliver the phosphonate moiety.⁴ A strong base is required for nucleophile generation from dialkyl methylphosphonates (**c**). The nucleophiles attack at the vinylogous position of the electron-deficient system to yield a stabilized carbanion intermediate, which is then trapped with an electrophile (a proton in the simplest case) to furnish the 1,4-addition product.

If a large excess of the conjugated compound is used, it is possible to get a double-Michael (dialkylated) product, while the use of 'hard' nucleophiles will lead to a 1,2-attack on the carbonyl.

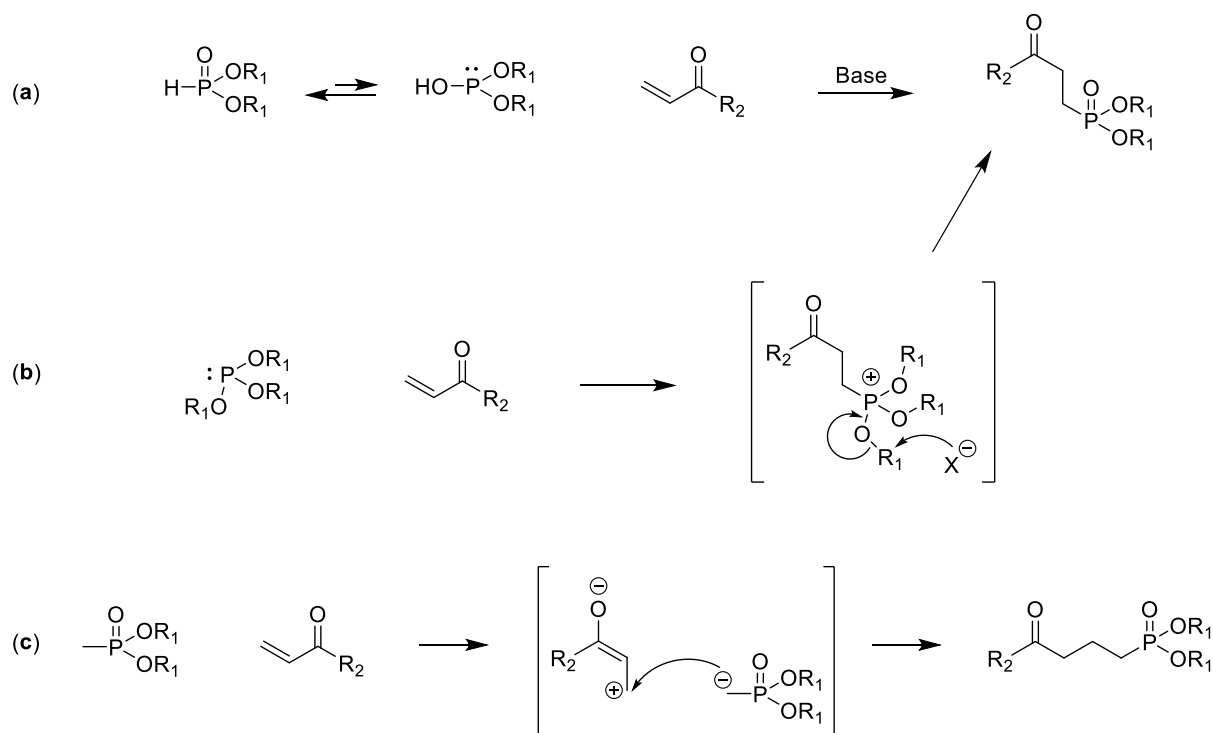


Figure IV.2: Michael addition of various phosphorus-based nucleophiles to an electron deficient carbonyl compound.

IV.B. Phosphonate deprotection strategies

The methyl, ethyl or isopropyl esters of pentavalent organophosphorus compounds can be cleaved by refluxing in concentrated hydrochloric acid (HCl) or hydrobromic (HBr) acid (Figure IV.3).

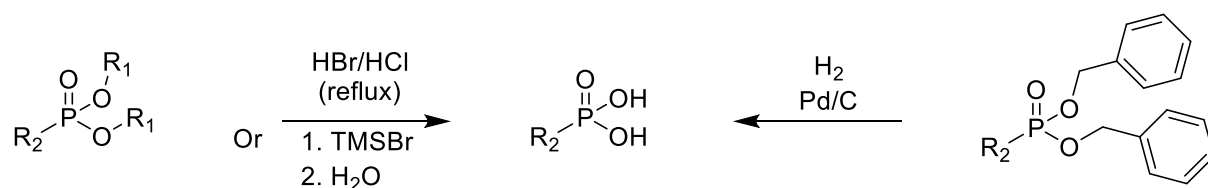


Figure IV.3: Phosphonate deprotection options.

Since these harsh conditions may be incompatible with other functionalities, bromotrimethylsilane (TMSBr) has been widely used as a mild but efficient alternative.⁵ Treatment with the latter leads to the formation of trimethylsilyl esters of phosphonic acid, which are easily cleaved to afford the acid by the action of protic solvents. The deprotection

(Figure IV.4) starts with an attack on the silicon atom in TMSBr by the P=O oxygen of the phosphonate, expelling bromide anion from TMSBr and leading to the formation of a phosphonium-like intermediate. Next, P=O is recreated from one of the alkoxy groups upon attack of the bromide anion on the carbon closest to a bridging oxygen, leading to the formation of alkyl bromide. The sequence is repeated for cleavage of the remaining phosphonate ester to yield bis(trimethylsilyl) phosphonate. The latter is then hydrolyzed by water to deliver the free phosphonic acid.

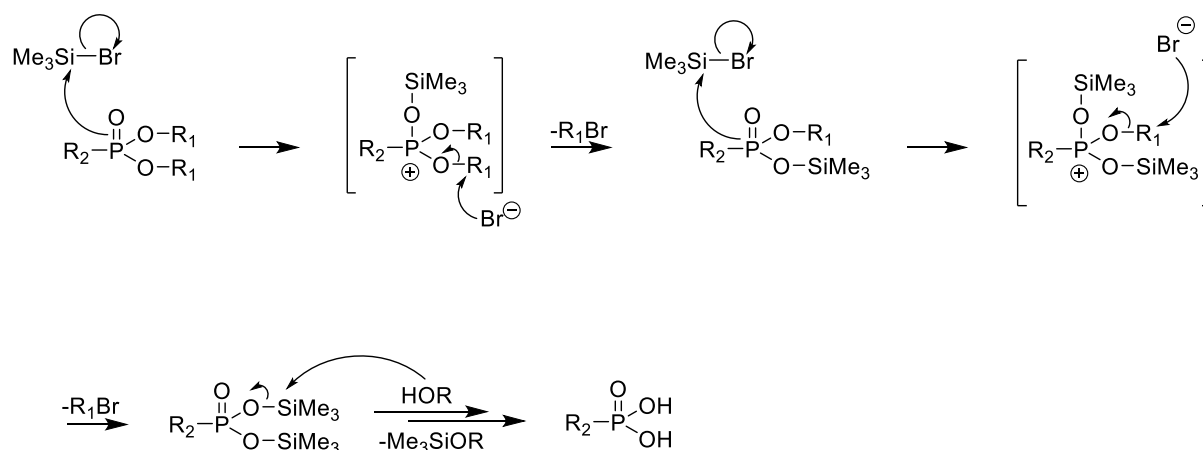


Figure IV.4: Mechanism of phosphonate deprotection by TMSBr.

Alternatively, catalytic hydrogenation is used to deprotect dibenzyl-protected phosphonates.

REFERENCES

1. Kedrowski, S. M. A. and Dougherty, D. A. A room-temperature alternative to the Arbuzov reaction: the reductive deoxygenation of acyl phosphonates. *Org. Lett.* **2010**, 12, 18, 3990–3993.
2. Rajeshwaran, G. G.; Nandakumar, M.; Sureshbabu, R.; Mohanakrishnan, A. K. Lewis acid-mediated Michaelis-Arbuzov reaction at room temperature: A facile preparation of arylmethyl/heteroarylmethyl phosphonates. *Org. Lett.* **2011**, 13, 6, 1270–1273.
3. Rulev, A. Y. Recent advances in Michael addition of H-phosphonates. *RSC Adv.* **2014**, 4, 26002–26012.
4. Hwan Kim, S.; Hee Kim, S.; Jin Kim, H.; Nyoung Kim, J. An efficient conjugate addition of dialkyl phosphite to electron-deficient olefins: The use of a nucleophilic organocatalyst to form a strong base. *Bull. Korean Chem. Soc.* **2013**, 34, 3, 989–992.
5. Blazewska, K. M. McKenna reaction-which oxygen attacks bromotrimethylsilane? *J. Org. Chem.* **2014**, 79, 408–412.

Chapter V

BETA-SUBSTITUTED

ANALOGUES OF

FOSMIDOMYCIN

V. BETA-SUBSTITUTED ANALOGUES OF FOSMIDOMYCIN

V.A. Introduction

A survey of the most successful modifications on the fosmidomycin/FR900098 scaffold clarifies that the propyl spacer linking the phosphonate and the hydroxamate group is the most amenable of the three structural segments. The knowledge that both cellular access and binding to Dxr may be improved by electron-withdrawing α -(aryl) substituents, reinforces the view that new alterations on this carbon chain may be a step in the right direction. Although substitution of the α -position of fosmidomycin has been widely explored, manipulation of the β -position has received much less attention.

V.B. β -(Alkyl)aryl analogues

After Timothy Haemers of our research group found that the β -oxa derivative of FR900098 (**5.3**, Figure V.1) was almost equipotent to this lead,¹ Brucher *et al.* demonstrated that β -oxa modifications combined with α -aryl substituents may afford potent PfDxr inhibitors (e.g., **5.4a**), with promising *in vitro* antiplasmodial activity.² The Kurz group showed that replacement of the β -methylene group with a sulfur atom in **5.4b** resulted in lower IC₅₀ values for *E. coli* and MtbDxr compared with the oxa ligand **5.4a**.³ Furthermore, they demonstrated that the PfDxr inhibitory activity of the *S*-(+)-enantiomers was clearly superior to that of the *R*-(-) diastomers (e.g., *S*-(+)-**5.4c** IC₅₀ = 9.4 nM, *R*-(-)-**5.4c** IC₅₀ = 12 μ M), in agreement with results from crystallographic studies on the Dxr binding of **1.38e** (section I.E.2.2.) and related analogues carried out by Andaloussi *et al.*⁴ and Jansson *et al.*⁵

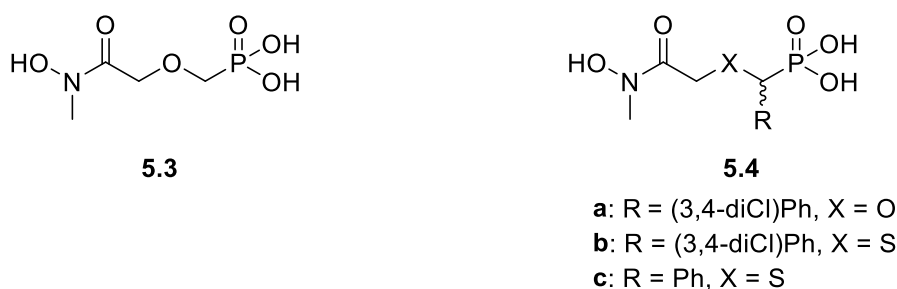
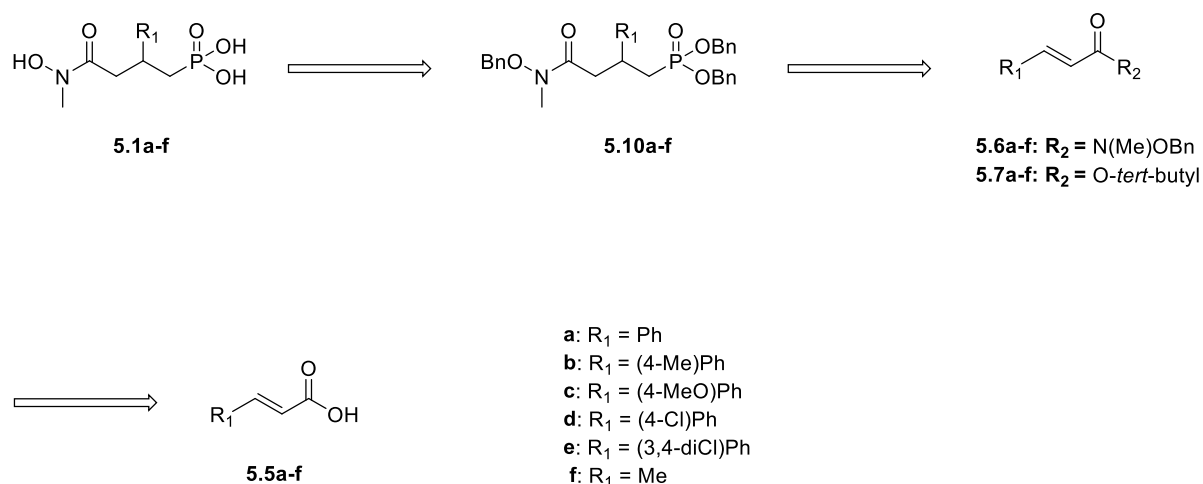
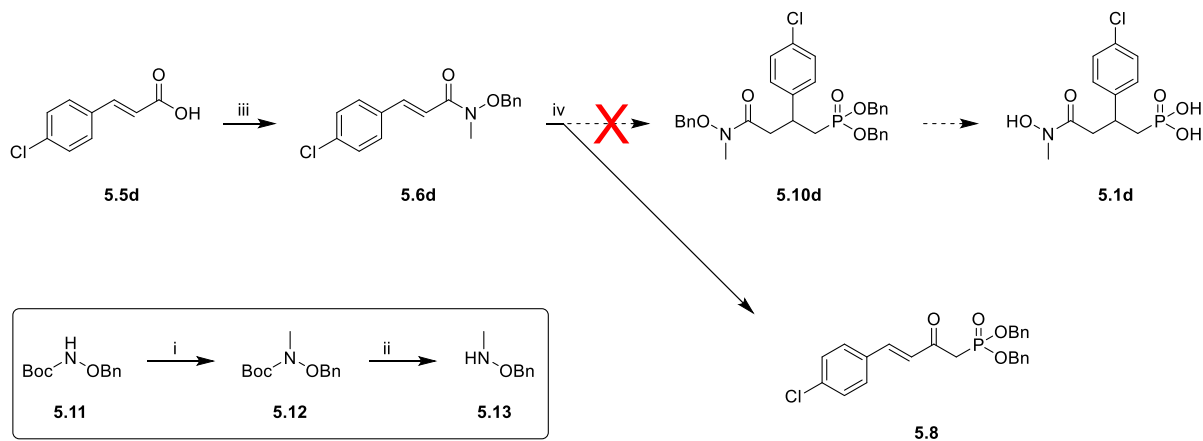


Figure V.1: Structures of reported β -modified analogues of FR900098.



Scheme V.1: Retrosynthesis of the strategy towards **5.1a–f**.

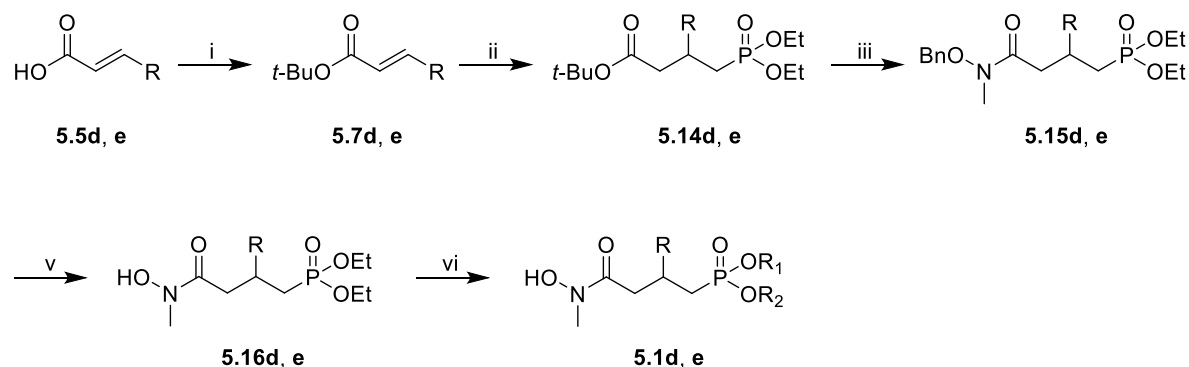
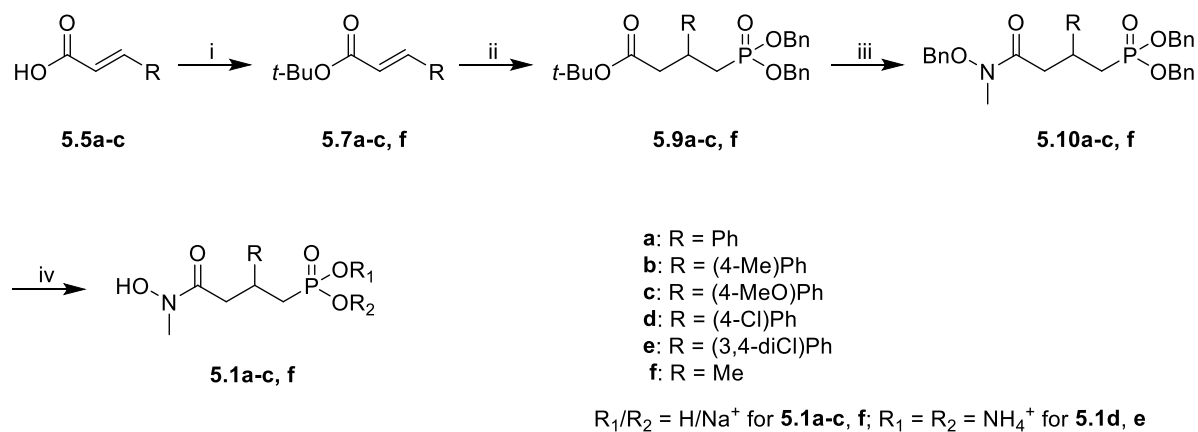
Since phosphonate addition to the respective cinnamic hydroxamates would afford the shortest synthetic route, this option was considered first. As outlined in Scheme V.2, during the first attempt starting from commercially available 4-chlorocinnamic acid (**5.5d**), the Michael addition step proved unsuccessful as only the undesired 1,2-addition product (**5.8**) was observed.



Scheme V.2 Reagents and conditions: (i) MeI, NaH, DMF, rt, overnight, 93%; (ii) TFA, CH_2Cl_2 , 45 min; (iii)(a) $(\text{COCl})_2$, DMF, CH_2Cl_2 , 0 °C, 5 h; (b) **5.13**, Et_3N , CH_2Cl_2 , rt, 16 h, 72%; (iv) $\text{CH}_3\text{P}(\text{O})(\text{OBn})_2$, $n\text{-BuLi}$, THF, -78 °C, 1.5 h, 33%.

This unfavorable outcome forced us to the alternative synthetic strategy, using the *tert*-butyl ester of the respective cinnamic acids as a surrogate Michael acceptor for the preparation of compounds **5.1a–f** (Scheme V.3). The commercially available cinnamic acids **5.5a–e** were esterified by treatment with di-*tert*-butyl dicarbonate in *tert*-butanol.¹¹

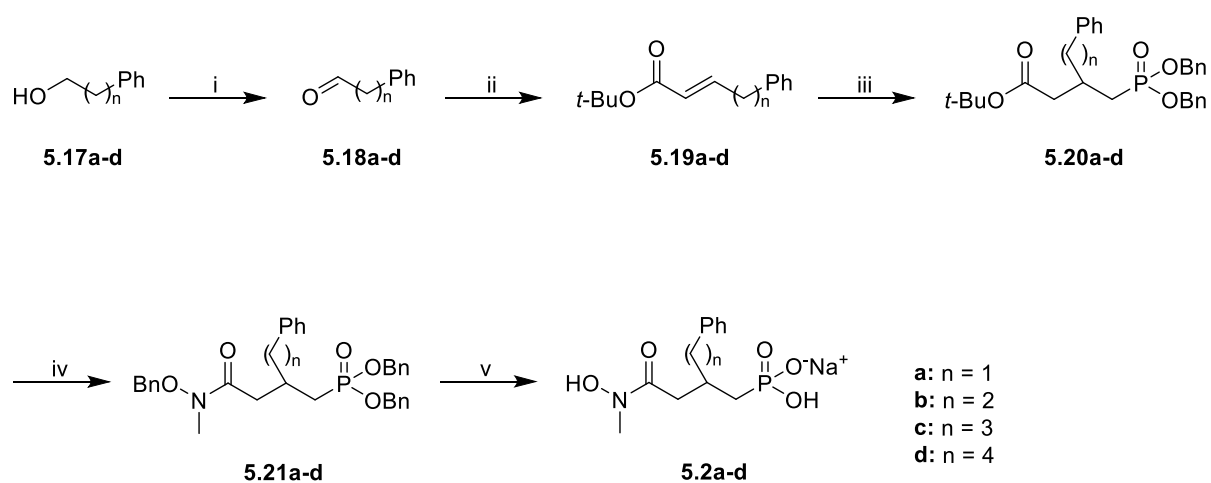
The resulting *tert*-butyl cinnamates **5.7a–c** and the purchased *tert*-butyl crotonate **5.7f** served as Michael acceptors in a reaction with dibenzyl methylphosphonate to furnish predominantly the desired 1,4-addition adducts **5.9a–c,f** as described by Yamaguchi and co-workers.¹² Previously encountered complications during catalytic hydrogenation of related compounds bearing a chlorinated phenyl ring led to the use of diethyl methylphosphonate as a Michael donor for addition to **5.7d** and **5.7e** to yield **5.14d** and **5.14e**, respectively.



Scheme V.3 Reagents and conditions: (i) Boc_2O , DMAP, *tert*-BuOH, rt, overnight, (68%–92%); (ii) $(BnO)_2OPMe$ (for **5.9a–c, f**; 72% (**5.9a**), 73% (**5.9b**), 69% (**5.9c**), $(EtO)_2OPMe$ (for **5.14d** and **5.14e**), *n*-BuLi, THF, $-78\text{ }^\circ\text{C}$, 2.5 h, **5.14d** (71%), **5.14e** (73%); (iii) (a) TFA, CH_2Cl_2 , 45 min, $0\text{ }^\circ\text{C}$ to rt; (b) $MeNH(OBn)$, EDC, DMAP, CH_2Cl_2 , rt, overnight, 51% (**5.10a**), 56% (**5.10b**), 47% (**5.10c**), 62% (**5.10f**), 46% (**5.15d**), 49% (**5.15e**); (iv) H_2 , Pd/C, MeOH, NaOH(aq), $25\text{ }^\circ\text{C}$, 10–15 min, quant.; (v) BCl_3 , CH_2Cl_2 , $-78\text{ }^\circ\text{C}$, 1 h, 79% (**5.16d**), 74% (**5.16e**); (vi) (a) TMSBr, BSTFA, CH_2Cl_2 , $0\text{ }^\circ\text{C}$ to rt, 22 h; (b) H_2O , NH_4OH (aq), quant.

Hydrolysis of the *tert*-butyl ester group of **5.9a–c,f** and **5.14d,e** with 20% TFA in CH₂Cl₂ and subsequent EDC-mediated coupling of the resulting carboxylic acids with *O*-benzyl-*N*-methyl hydroxylamine yielded the protected *N*-methyl-hydroxamates **5.10a–c,f** and **5.15d,e**. Compounds **5.10a–c** and **5.10f** were deprotected by catalytic hydrogenolysis to access target phosphonates **5.1a–c** and **7f**. The hydroxamate group of **5.15d** and **5.15e** was unmasked with BCl₃. Bromotrimethyl silane mediated deprotection of phosphonate esters **5.16d** and **5.16e** and basic workup yielded **5.1d–e** as bisammonium salts.

The synthesis of target compounds **5.2a–d** is outlined in Scheme V.4. The preparation of the appropriate Michael acceptors **5.19a–d** commenced with a Dess–Martin oxidation of commercially available alcohols **5.17a–d** to afford aldehydes **5.18a–d**, which were swiftly transformed to the corresponding *tert*-butyl esters **5.19a–d** via Wittig olefination. Michael addition of dibenzyl methylphosphonate to **5.19a–d** predominantly afforded 1,4-addition adducts **5.20a–d** due to steric hindrance of the *tert*-butyl group. Compounds **5.20a–d** were converted to the desired phosphonates **5.2a–d** as before.



Scheme V.4 Reagents and conditions: (i) Dess-Martin periodinane, CH₂Cl₂; (ii) Ph₃P=CHCOO*tert*-Bu, toluene, 120 °C, overnight, 80% (**5.19a**), 84% (**5.19b**), 79% (**5.19c**), 87% (**5.19d**); (iii) (BnO)₂OPMe, *n*-BuLi, THF, –78 °C, 2.5 h, 66% (**5.20a**), 63% (**5.20b**), 71% (**5.20c**), 68% (**5.20d**); (iv) (a) TFA, CH₂Cl₂, 45 min, 0 °C to rt,; (b) MeNH(OBn), EDC, DMAP, CH₂Cl₂, rt, 43% (**5.21a**), 60% (**5.21b**), 68% (**5.21c**), 74% (**5.21d**); (v) H₂, Pd/C, MeOH, NaOH(aq), 25 °C, 10–15 min, quant.

³⁵P NMR spectra of **5.1a–f** and **5.2a** indicate that these appear as rotameric mixtures, a known^{13,14} phenomenon that was further validated by variable temperature ³¹P NMR studies.

V.B.2. Biological evaluation

Final compounds were tested for inhibition of recombinant enzymes using a spectrophotometric assay monitoring the substrate-dependent oxidation of NADPH associated with the Dxr-catalyzed reaction (see section III.D.).

Initially, Dxr inhibition was studied at a compound concentration of 100 μM (Figure V.3). At this point, differences among the enzymes and compounds were already evident. As anticipated, the known hydroxamate **1.6**¹⁰ was highly effective at inhibiting MtbDxr. A lipophilic prodrug of this compound has recently been shown to effectively inhibit *M. smegmatis* growth in Kirby–Bauer disk diffusion assays.¹⁵ In contrast, compounds **5.1a–e** had only modest activity on MtbDxr and EcDxr. Interestingly, compound **5.1f**, characterized by the presence of a β-methyl substituent rather than the bulkier aromatic group, retained good inhibitory activity. Other noteworthy trends were the fact that **5.2a–d** were more potent on EcDxr than the **5.1**-series compounds and that PfDxr was more effectively inhibited than the other two enzymes. IC₅₀ values of the most promising compounds are reported in Table V.1. Again, differences between the various enzymes were apparent. PfDxr was most easily inhibited (followed by EcDxr), and for this enzyme, the **5.2**-series compounds were more potent than **5.1a–c**. For the homologue series **5.2a–d**, the activity against EcDxr was most dependent on the linker length, although all enzymes were sensitive to this parameter to some degree. In general, a three-carbon linker appeared to be best for EcDxr and MtbDxr, but both three- and four-carbon linkers showed very good activity on PfDxr.

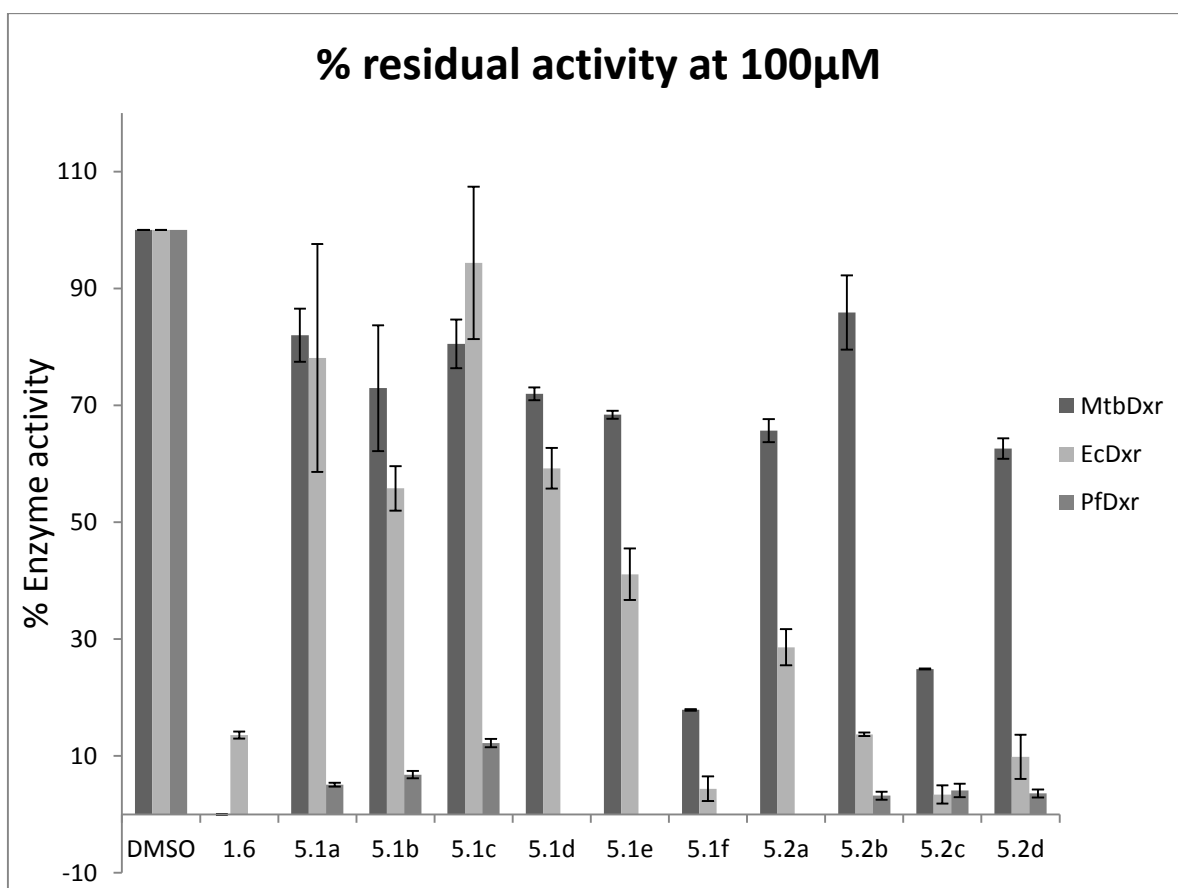


Figure V.3: Residual Dxr activity upon treatment with 100 μM of the indicated compounds.

The enzyme assays for EcDxr and MtbDxr were performed at 37 $^{\circ}\text{C}$ with a saturating concentration of NADPH (150 μM), a DOXP concentration fixed at its K_M (47 μM for MtbDxr and 100 μM for EcDxr), and 100 μM of the indicated inhibitor. For MtbDxr, the results were identical whether the enzyme was pre-incubated with the inhibitor for 10 min prior to the addition of NADPH or the enzyme was pre-incubated with NADPH prior to the addition of the inhibitor. For EcDxr, the enzyme was pre-incubated with the inhibitor and the cofactor for 5 min at 37 $^{\circ}\text{C}$. Enzyme activity was initiated by adding the substrate DOXP. Details specific to the assay for PfDxr are outlined in the experimental details below. Enzyme activity was spectrophotometrically monitored immediately following the addition of DOXP at 340 nm. Residual enzyme activity is relative to an assay performed with vehicle alone (DMSO).

All assays were performed in duplicate for MtbDxr and in triplicate for EcDxr, and bars indicate standard deviation.

Table V.1: IC₅₀ (± sd) Values for recombinant Dxr from *E. coli*, *M. tuberculosis*, and *P. falciparum*.

Compound	IC ₅₀ (μM)		
	EcDxr	MtbDxr	PfDxr
fosmidomycin (1.1)	0.030 ± 0.008	0.438 ± 0.09	0.036 ± 0.006
1.6	0.159 ± 0.018	1.15 ± 0.21	nd
5.1a	nd	nd	3.3 ± 0.17
5.1b	nd	nd	9.3 ± 0.75
5.1c	nd	nd	18.8 ± 4.2
5.1f	0.205 ± 0.052	7.13 ± 1.2	nd
5.2a	nd	nd	nd
5.2b	31.39 ± 21.61	nd	1.36 ± 0.02
5.2c	0.843 ± 0.163	10.35 ± 1.3	0.117 ± 0.012
5.2d	6.67 ± 1.48	273.2 ± 54.6	0.069 ± 0.005

nd = not determined

Table V.2 summarizes the antibacterial/antiparasitic activity of these compounds. Of the compounds evaluated against *E. coli*, only **1.6** showed moderate activity (MIC₅₀ 15.6–31.25 μM, generally comparable to those of fosmidomycin and FR900098). The most promising MtbDxr inhibitors, **1.6** and **5.2c**, were also tested against intact *M. smegmatis* cells. *M. smegmatis* was used as a model for Mtb due to its nonpathogenicity and shorter doubling time.¹⁶ However, as for the other compounds tested (Table V.2), they showed no activity (MIC₅₀ > 250 μM). Overall, the lack of correlation between activity against purified enzymes and activity against whole bacteria suggests a lack of uptake or active efflux of these molecules.

All analogues were also evaluated *in vitro* for schizontocidal activity against the *P. falciparum* K1 strain. This activity correlated surprisingly well with the PfDxr inhibitory activity summarized in Table V.1. Compounds **5.1a–e** were not active against blood stage *P. falciparum*. Compound **1.6**, the congener of **1.2** with a hydroxamate group, showed potent antiplasmodial activity (IC₅₀ < 0.26 μM). Introduction of a β-methyl group (**5.1f**) was well tolerated (IC₅₀ = 0.74 μM). The activity trend in the homologue series **5.2b–d** was similar to

that observed for PfDxr enzyme inhibition and indicates that a linker of three or four carbons is optimal in this case.

Table V.2: MIC₅₀ Values against *in vitro* growth of *E. coli* and *M. smegmatis* and IC₅₀ values against the *P. falciparum*-K1 Strain.

Compound	MIC ₅₀ (μM)					<i>P. falciparum</i> -K1 IC ₅₀ (μM)
	<i>E. coli</i>			<i>M. smegmatis</i>		
	ATCC 8739	ATCC 25922	K-12	ATCC 607	ATCC 700084	
fosmidomycin (1.1)	0.98	250	7.8	>250	>250	1.73 ± 0.89 ¹⁷
FR900098 (1.2)	7.8	62.5	15.6	>250	>250	0.42 ± 0.17 ¹⁷
1.6	31.25	15.6	31.25	>250	>250	0.26 ± 0.02
5.1a	>250	>250	>250	>250	>250	>64
5.1b	>250	>250	>250	>250	>250	>64
5.1c	>250	>250	>250	>250	>250	>64
5.1d	>250	>250	>250	>250	>250	>64
5.1e	>250	>250	>250	>250	>250	>64
5.1f	nd	nd	nd	nd	nd	0.74 ± 0.13
5.2a	nd	nd	nd	nd	nd	≥56.8 ± 10.1
5.2b	>250	>250	>250	>250	>250	35.4 ± 8.7
5.2c	>250	>250	>250	>250	>250	0.43 ± 0.09
5.2d	>250	>250	>250	>250	>250	<0.25 ± 0.00

nd = not determined

Comparison of the *P. falciparum*-K1 growth inhibition assay with the enzyme activity results suggests that there is an improved interaction with the *Plasmodium* enzyme with longer linker lengths, but there could also be a positive influence on cell permeability.

V.B.3. X-ray structures of PfDxr in complex with four inhibitors

The structures of PfDxr in complex with four of the new β-substituted inhibitors (**5.1a**, **5.1b**, **5.2c**, and **5.2d**) have been solved at resolutions of 1.9, 2.1, 1.6, and 1.9 Å, respectively. Although the compounds were synthesized as racemic mixtures, the high resolution of the study (Figures V.4, V.5 and V.6) allowed us to identify the favored enantiomer for each

ligand. Tests of both enantiomers in the refinement strongly suggested that all compounds were bound primarily as the *R*-enantiomer, although chemical rules of priority mean that the actual arrangement of the β -substituent at the chiral carbon is different for **5.1a** and **5.1b** compared with **5.2c** and **5.2d**.

The protein in the complexes with **5.1a** and **5.1b** is for the most part identical, with an rms distance of only 0.2 Å when the subunits are compared. The largest difference is at Pro294 of the active-site flap, where the C α position differs by approximately 1 Å in the two structures; there is well-ordered electron density for all residues in the respective flaps. This movement is directly linked to the addition of the methyl group in **5.1b** and correlates well with the observation that IC₅₀ increases as larger groups are added at this position. Interactions with the hydroxamate and phosphonate are essentially the same.

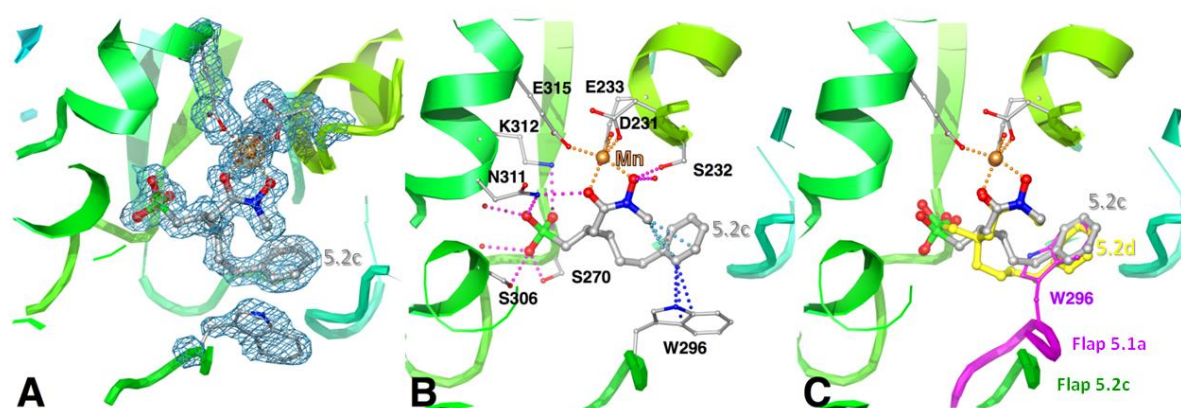


Figure V.4: Active site of PfDxr bound to **5.2c** and **5.2d**. The background cartoon was created with a red-to-blue rainbow coloring for one chain. Water molecules are shown as small red spheres, and the Mn²⁺ ion is gold. (A) Electron density for the inhibitor **5.2c** and selected nearby residues is contoured at the rms value of the σ -weighted ($2m|F_o| - D|F_c|$) electron density map¹⁸ ($0.33 \text{ e}/\text{\AA}^3$) in light blue, as well as at $2.5 \text{ e}/\text{\AA}^3$ (gold) to show the higher electron density near the metal ion. (B) Magenta colored dots show hydrogen-bond interactions between **5.2c** and protein or solvent, while gold ones show metal coordination; blue and cyan dots indicate close contacts ($<3.7 \text{ \AA}$) between the phenyl group of **5.2c** and the indole ring of Trp296 from the flap or within the inhibitor, respectively. (C) The structures of bound **5.2c** and **5.2d** are superimposed. The flap in the complex with **5.1a** is shown in magenta for comparison.

The methyl group of the hydroxamic acid in each case makes close interactions with the indole ring of Trp296 (Figure V.5C). Both of these protein structures are quite similar to the complexes with fosmidomycin and FR900098, with the caveat that His293, Met298, and Ile302 must adjust somewhat to accommodate the new β -substituent.

More substantial differences are observed for the complexes with **5.2c** and **5.2d**. As can be seen in Figure V.5C, the β -substituents are placed in a very different way in the two series of compounds. Again, most of the protein is very similar, but the active-site flaps are pushed further away as the β -substituent of **5.2c** and **5.2d** displaces Trp296. In the **5.2c** complex, density is weak between 293 and 295 of both chains. Only the flap of the A molecule of the **5.2d** complex has continuous density at the rms of the map; in the B-site, there is a break between residues 292 and 296.

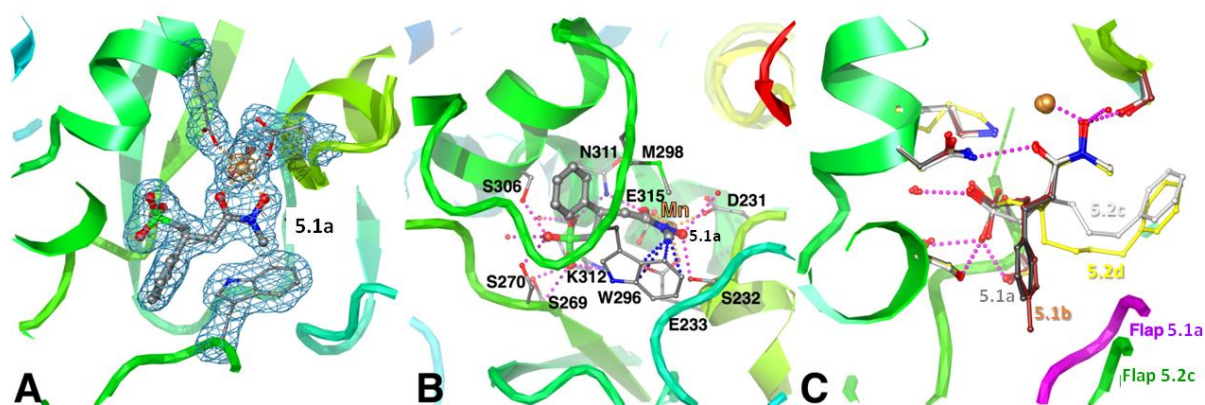


Figure V.5: Active site of PfDxr bound to **5.1a** and **5.1b**. The cartoon is presented as described for Figure V.4. (A) Electron density for **5.1a** and selected nearby residues is contoured at the rms of the map ($0.28 \text{ e}/\text{\AA}^3$) in light blue, as well as at $2.5 \text{ e}/\text{\AA}^3$ (gold) to show the higher electron density near the metal ion. (B) Magenta-colored dots show hydrogen-bond interactions between **5.1a** and protein or solvent, while gold ones show metal coordination; blue dots indicate close contacts ($<3.7 \text{ \AA}$) between the methyl group of **5.1a** and the indole ring of Trp296 from the flap. (C) The structures of bound **5.1a**, **5.1b**, **5.2c**, and **5.2d** are superimposed. The flap in the complex with **5.1a** is shown in magenta for comparison with that of **5.2c**. Dots indicate the hydrogen bond interactions of **5.2c** with the enzyme and solvent.

In each complex, the methylene linker of the inhibitor is found in a depression described in numerous Ca-aryl complexes, wedged between three ordered and one often disordered loop (containing PfDxr residues 272, 338, 358, and 296, respectively).

As shown in Figures V.4C and V.5C, the flexibility of the linker means it can take on a boomerang shape that allows the phenyl group of each inhibitor to interact with its methyl group (Figure V.4B). The phenyl ring occupies the place normally assumed by the indole ring of the conserved tryptophan of the flap (Figure V.4C), resulting in acyl-group-toring interactions similar to those seen in the **5.1a** and **5.1b** complexes (Figure V.5B and Figure V.6), as well as **1.2** ternary complexes.¹⁹ In three of the four active sites where we are able to observe Trp296, the face of the indole ring stacks on the edge of the phenyl ring of the inhibitor (Figure V.4B).

These favorable interactions are achieved in the **5.2c** complex with the same ligand backbone conformation normally observed in antibiotic/NADPH ternary complexes. In the **5.2d** complex, fitting in the extra methylene group while conserving the position of the phenyl group requires a rearrangement of the fosmidomycin backbone (Figures V.4C and V.5C).

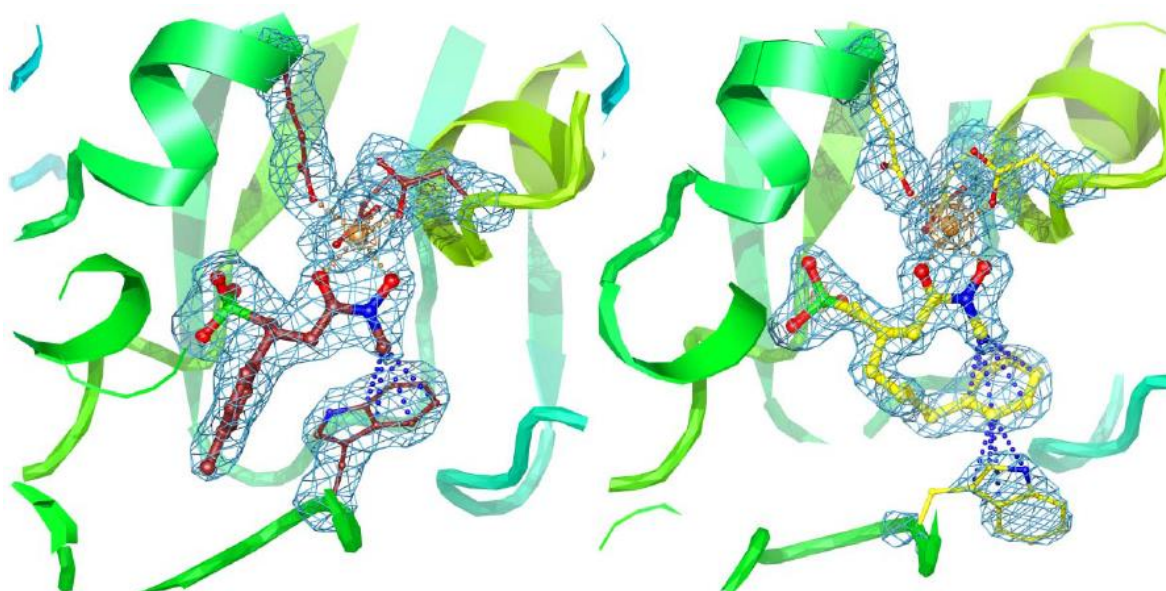


Figure V.6: Electron density and aromatic interactions for compounds **5.1b** and **5.2d**.

While the position of the hydroxamate remains unchanged, there are small but significant changes in the orientation of the phosphonate. These changes do not cause a ripple of

differences in protein side chains involved in phosphonate binding, but instead there is a rearrangement of which phosphonate oxygen interacts with which hydrogen-bond donor. Figure V.5C shows a superposition of the hydrogen bond donors that interact with **5.1a**, **5.1b**, **5.2c**, or **5.2d**. Clearly, they are structurally highly conserved, while the phosphonate groups are not so tightly clustered. The analysis shows that only one phosphonate oxygen has the full set of three interacting groups in all complexes, a second oxygen has two interacting groups, and the third has either two or three interacting groups. The rearrangement of the fosmidomycin backbone in **5.2c** would produce a close contact with the usual conformation seen for Lys312, and so a small conformational change is needed to relieve this clash while maintaining an interaction with the phosphonate (Figure V.5C). The side chain of His293 does not contribute to phosphonate binding in any of the complexes, in contrast to observations in antibiotic/NADPH ternary complexes.

In all active sites, in all complexes, the hydroxamic acid group adopts a synperiplanar conformation ($O=C-N-O$ angle is 0°), in which both oxygen atoms coordinate to the manganese, as does a single carboxyl oxygen atom from each of the highly conserved acidic residues, Asp231, Asp233, and Glu315. The differences from the usual set of interactions observed in the antibiotic/NADPH ternary complexes are merely a consequence of the hydroxamate group in the new structures. Figures V.4C and V.5B show that the hydrogen bonding interactions are conserved, and the *N*-formyl oxygen now accepts a hydrogen bond from Asn311-ND2, while the *N*-hydroxyl oxygen interacts with Ser232-OG and a conserved water molecule.

V.B.4. Molecular modeling on MtbDxr

At present, it is not clear why such large differences are observed for the inhibition of the different enzymes. Modeling experiments were therefore performed in an attempt to gain insights into how the new inhibitors might interact with MtbDxr. Specifically, we were interested in understanding how the phenylpropyl substituent of **5.2c** might be interacting with the Trp-containing loop of Dxr. In the X-ray structure of MtbDxr in complex with **1.2** (PDB code 4A03),¹⁹ a loop containing Trp203 closes over the bound ligand, while this loop is disordered in the reported X-ray structures of Dxr cocomplexes with α -phenyl-substituted analogues, which are all less potent inhibitors of the enzyme.

When comparing the predicted binding of **5.1f** and the aromatic analogues **5.2a–d** to the measured binding of fosmidomycin, one makes an interesting observation with respect to Ser213. In the cocrystal structure with fosmidomycin bound, Ser213 is hydrogen bonded to the phosphonate of the ligand. This same orientation is predicted when **5.1f** is bound. For the aromatic analogues, however, Ser213 is reoriented and points instead toward His200. It appears that the hydrogen bonding between Ser213 and the phosphonate is disrupted upon binding of the aromatic analogues. His203 appears to bind to Ser213 in order to compensate for the loss of interaction with the phosphonate. This might explain the loss of activity of aromatic analogues **5.2a–d** relative to fosmidomycin.

The modeled structure of **5.2c** (white carbons) compared with the X-ray structure of the protein with fosmidomycin bound (green carbons) is shown in Figure V.7. In the minimized structure of **5.2c**, the aromatic ring occupies almost exactly the same position as the phenyl portion of Trp203 in the complex with fosmidomycin. Since the aromatic ring of Trp203 occupies what is presumably a stable position in the folded protein, it could be assumed that this position would also be favorable for a ligand to occupy when the loop needs to be displaced for steric reasons. This could be described as an aromatic “hotspot”. Therefore, it could be that this results in favorable van der Waals and lipophilic interactions of the phenyl ring in this position, which accounts for the better activity of **5.2c** compared with the shorter **5.2b**, which may not reach the hotspot, and **5.2d**, where the carbon chain is too long for the phenyl to occupy the same position. In addition, Trp203 in the loop of the minimized structure with **5.2c** makes an edge-to-face interaction with the phenyl ring of the ligand, potentially stabilizing the loop and ligand in this position.

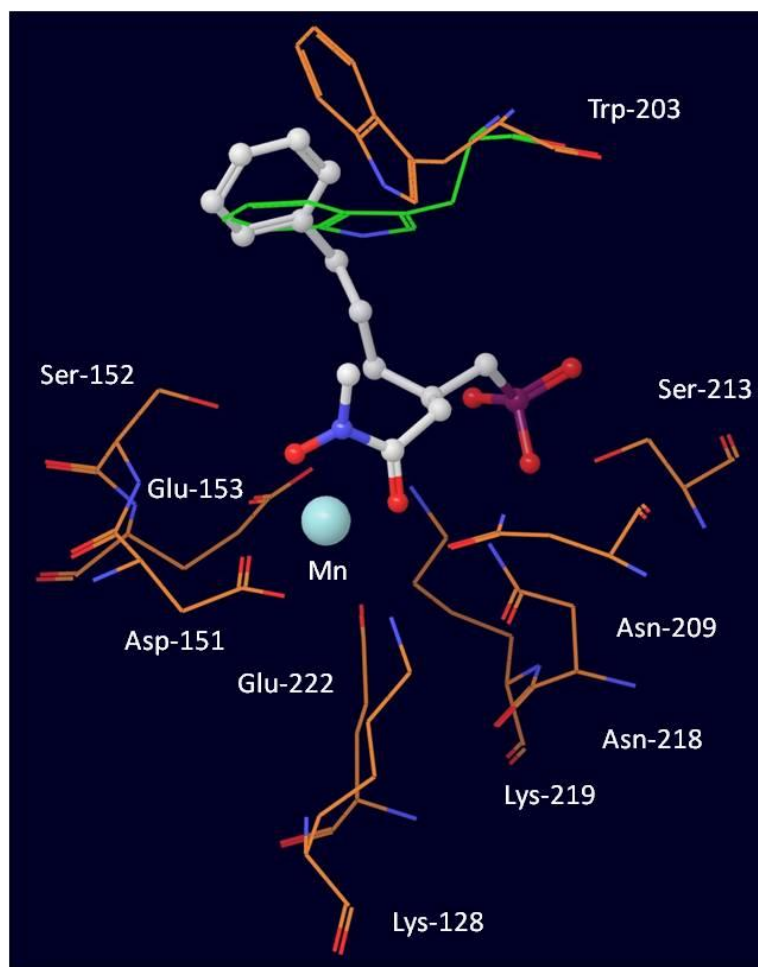


Figure V.7: Optimized geometry of **5.2c** in the minimized protein structure PDB entry 4A03 (MtbDxr). Only relevant residues close to the ligand are shown for clarity and labeled according to their residue numbers in the 4A03 structure. The position of Trp203 in 4A03 is shown with green carbon atoms. The carbon atoms of the optimized protein residues are shown in orange, while the ligand carbon atoms are shown in white. The position of the Trp203 indole ring overlaps with the position of the phenyl ring in **5.2c**. In the optimized structure, Trp203 forms a T-stacking interaction with the phenyl ring of **5.2c**.

V.B.5. Conclusions

In this thesis, the first systematic study on β -substituted analogues of fosmidomycin was conducted. A series of analogues with different aromatic moieties connected directly to the β -carbon (**5.1a–e**) failed to inhibit EcDxr and MtbDxr and proved moderately active against PfDxr. None of these compounds was capable of inhibiting the growth of *E. coli*, *M. smegmatis*, or *P. falciparum* strain K-1. Exploration of alkyl linkers of different lengths

between the β -carbon and a phenyl ring resulted in establishment of a three-carbon linker (**5.2c**) as optimal for *E. coli* and *M. tuberculosis* Dxr inhibition and a four-carbon linker (**5.2d**) for inhibition of *P. falciparum* Dxr. While compounds **5.2a–d** also lacked activity against *E. coli* and *M. smegmatis*, **5.2c** and **5.2d** showed submicromolar schizontocidal activity against the *P. falciparum* K1 strain, where essentially the same SAR was observed as for PfDxr inhibition. Interestingly, the activity of **5.2c** and **5.2d** surpassed that of **5.1f**, indicating a favorable contribution of the phenylpropyl and phenylbutyl substituents to antiplasmodial growth inhibition.

Crystallographic studies on four of the compounds most active on PfDxr (**5.1a**, **5.1b**, **5.2c**, and **5.2d**) show two different, novel modes of binding to the enzyme. The compounds showing the best enzyme inhibition and best *in vitro* activity against the parasite mimic the favorable interactions between the indole ring of the conserved tryptophan in the flap with the fosmidomycin backbone that have been seen in a number of antibiotic-bound ternary complexes. However, this mimicry is achieved by intramolecular interactions within each inhibitor (**5.2c**, **5.2d**), such that the phenyl ring common to this series spatially overlaps the usual position of the indole ring. Rearrangement of the flap results in favorable interactions between the phenyl ring of the inhibitors and the tryptophan. The improved activity of **5.2d** compared with **5.2c** is likely a consequence of this set of interactions.

V.B.6. Experimental details

General Methods and Materials. See section III.E.

All synthesized compounds were $\geq 95\%$ pure as verified by LCMS. NMR analysis showed a rotameric mixture for some of the prepared compounds. At high temperature (80 °C), the phosphorus signals of the two rotameric forms of a representative compound (**5.1b**) merged into a single peak.

***P. falciparum* Dxr inhibition assay and crystallography.** The PfDxr assay and crystallography was performed by the Department of Cell and Molecular Biology, Science for Life Laboratory, Uppsala University, Sweden. The activity of PfDxr was evaluated at room temperature at an enzyme concentration of 0.5 μM . The K_m for DXP was determined to be 100 μM , and that for NADPH was 120 μM ; k_{cat} was 0.5 s^{-1} . Each IC_{50} experiment contained 15.5 μL of reaction buffer mix (50 mM Na-HEPES pH 7.5, 1.5 mM MnCl_2 , 100 mM NaCl), 5 μL PfDxr (in 100 mM NaCl, 0.01% Brij-35 and 50 mM Na-HEPES pH 7.5), 2.5 μL NADPH (in dH_2O , final concentration 150 μM), 2 μL of dH_2O or inhibitor solution and 25 μL of DXP (in dH_2O , final concentration 150 μM). The reported IC_{50} values were based on triplicates. Co-crystallization experiments produced complexes with four ligands (**5.1a**, **5.1b**, **5.2c** and **5.2d**).

Modeling of compound 5.2c into MtbDxr. The Evenor Consulting Ltd., United Kingdom conducted modeling studies on **5.2c** with MtbDxr. All available X-ray structures of MtbDxr with manganese (PDB codes 2y1c and 2y1e), **1.38e** (PDB code 2y1d), **1.38e**-NADPH (PDB codes 2y1f and 4a03) and **1.37e** (PDB code 2y1g) were superimposed. Ligand structures were superimposed on the fosmidomycin scaffold and geometries were fully optimized using the OPLS2005 force field in Macromodel 9.9 (Schrodinger Inc.).²⁰ Protein residues within 10 Å from the inhibitor were treated as fully flexible, only the Mn^{2+} ion was kept fixed. Explicit hydrogen atoms were added to the protein using Macromodel. Geometry optimizations of ligand-protein complexes were performed for fosmidomycin, **1.6**, **5.1a**, **5.1f** and **5.2a–d**. All water molecules from the 4a03 X-ray structure within 10 Å around the ligands were kept and were also optimized.

Antimicrobial susceptibility testing. The *M. smegmatis* assay was performed by the Laboratory of Pharmaceutical Microbiology, Ghent University, Belgium. The minimal

inhibitory concentration that reduces growth of *M. smegmatis* cultures to maximum 50% of the untreated control (MIC₅₀) was determined according to the European Committee on Antimicrobial Susceptibility Testing (EUCAST) standard broth microdilution protocol.²¹ Each MIC₅₀ determination was performed in triplicate.

General Procedure I: Synthesis of *tert*-butyl cinnamates 5.7a–e

To a 0.1 M solution of the appropriate cinnamic acid (40–45 mmol, 1 equiv) in *tert*-butanol at 35 °C, was added di-*tert*-butyl dicarbonate (2.0 equiv) and 4-dimethylaminopyridine (0.3 equiv). The mixture was heated to 35 °C overnight and then poured into water and extracted three times with dichloromethane. The organic fractions were pooled, washed once with brine and dried over Na₂SO₄. Filtration, *in vacuo* concentration and subsequent silica gel column chromatography gave the respective *tert*-butyl cinnamates. Characterization was in agreement with reported data.^{22,23}

General Procedure II: Dess-Martin oxidation and concomitant Wittig olefination

A 0.05 M solution of the starting material in CH₂Cl₂ and a nitrogen atmosphere was cooled to 0 °C. Solid Dess-Martin periodinane (2.0 equiv) was added and the temperature was allowed to rise to RT. Upon completion of the reaction (TLC monitoring; typically 3 hours), the mixture was washed with a mixture (5:1 v/v) of NaHCO₃ (sat. aq.) and Na₂S₂O₃ (aq. 2.0 M). The formed water layer was then extracted three times with diethyl ether. The organic fractions were combined, washed with HCl (0.1 M, once), brine (once) and dried over anhydrous Na₂SO₄ before *in vacuo* concentration. The resulting crude aldehyde was dissolved in toluene under a nitrogen atmosphere and 3.0 equiv of *tert*-butyl (triphenylphosphoranylidene)acetate was added. The mixture was refluxed at 120 °C overnight. It was allowed to cool to RT and concentrated *in vacuo*. The crude mixture was adsorbed onto celite and purified by silica gel chromatography.

General procedure III: Michael addition of methylphosphonatediesters to α,β -unsaturated *tert*-butyl esters.

To a 1.0 M solution of dibenzylmethyl- or diethylmethyl-phosphonate (2.0 equiv) in THF was added *n*-BuLi (1.6 M solution in hexanes, 2.0 equiv) at -78 °C under a N₂ atmosphere. After 30 minutes, a 0.5 M solution of the α,β -unsaturated ester (1.0 equiv) in THF was added

dropwise. When the reaction was complete (typically 3 hours), the reaction was quenched with sat. aq. NH_4Cl and transferred to a separatory funnel. The aqueous solution was extracted three times with EtOAc. The organic fractions were combined, washed once with brine, dried (Na_2SO_4), filtered and concentrated. Column chromatography of the residue yielded the Michael adduct.

General procedure IV: Acidic cleavage of the *tert*-butyl ester and protected hydroxamate formation.

A 0.1 M solution of the *tert*-butyl ester (1.0 equiv) in $\text{CH}_2\text{Cl}_2/\text{TFA}$ (80:20) at 0 °C, was stirred for 2 hours, after which an excess of toluene was added to the reaction mixture and concentrated *in vacuo*. The crude acid was redissolved in CH_2Cl_2 (0.1 M), followed by addition of EDC (1.2 equiv), DMAP (1.2 equiv) and DiPEA (2.0 equiv). *O*-Benzyl-*N*-methylhydroxylamine TFA salt (1.2 equiv) was added as a 0.2 M solution in CH_2Cl_2 , and the ensemble was allowed to stir overnight at room temperature. The mixture was quenched with sat. aq. NaHCO_3 , extracted three times with CH_2Cl_2 , washed with brine and dried over Na_2SO_4 . Column chromatography produced the protected hydroxamic acids.

General procedure V: Catalytic hydrogenolysis of benzyl protective groups.

The benzyl protected compound was dissolved in MeOH (10 mg/mL) under a nitrogen atmosphere and a catalytic amount of Pd/C (10 %) was added. The resulting mixture was then stirred under a hydrogen atmosphere for 10 minutes. Upon completion of the reaction (confirmed by MS), the mixture was filtered and neutralized with 1.0 equiv of NaOH (aq. 1.0M). It was then concentrated *in vacuo*, re-dissolved in a mixture of water and *tert*-butanol (1:1 v/v, 1.0 mL/10 mg starting material), frozen and lyophilized affording the desired phosphonic acid monosodium salts in quantitative yield.

General procedure VI: Boron trichloride mediated selective debenzylation of the hydroxamate.

A 0.1 M solution of the benzylated hydroxamate in dichloromethane was cooled to -75 °C. BCl_3 (1 M solution in CH_2Cl_2 , 3.0 equiv) was added dropwise and the mixture allowed to stir at this temperature for 45 minutes. Next, the reaction mixture was poured into aqueous NaHCO_3 , and extracted 4 times with CH_2Cl_2 . The organic fractions were combined, washed

with brine, dried (Na₂SO₄), filtered and concentrated *in vacuo*. The residue was purified by silica gel column chromatography to obtain the free hydroxamate.

General procedure VII: Trimethylbromosilane mediated deprotection of diethyl phosphonates.

To a 0.1 M solution of starting material in dichloromethane, was added BSTFA (4.0 equiv). The mixture was allowed to stir at room temperature for 15 minutes before an ice bath was installed, and TMSBr (10.0 equiv) was added. The ice bath was removed after 10 minutes, and the reaction allowed to stir until phosphorus NMR confirmed complete deprotection. All volatiles were removed *in vacuo* and the resultant oil was re-dissolved in acetonitrile. Concentrated ammonia was added, and the mixture was allowed to stir at room temperature for 20 minutes. Evaporation of volatiles and subsequent lyophilization from a mixture of *tert*-butanol and water afforded the compound in quantitative yield.

Dibenzyl 2-phenyl-3-(tert-butoxycarbonyl)propylphosphonate (5.9a). Prepared from compound **5.7a** (715 mg, 3.50 mmol) according to general procedure III. Colorless oil; purification 1.5:1 Hex/EtOAc v/v; yield 72%. ¹H NMR (300 MHz, CDCl₃) δ_H ppm 1.25 (br s, 9H, *t*-Bu), 2.17 (dd, *J* = 3.5 Hz, 18.6 Hz, 1H, P-CH₂-), 2.19 (dd, *J* = 2.8 Hz, 18.6 Hz, 1H, P-CH₂-), 2.52 (ddd, *J* = 1.3 Hz, *J* = 9.3 Hz, 15.2 Hz, 1H, -CH₂-CO), 2.78 (dd, *J* = 6.2 Hz, 15.2 Hz, 1H, -CH₂-CO), 3.44-3.62 (m, 1H, -CH-), 4.66-4.87 (m, 4H, -CH₂Ph), 7.17-7.36 (m, 15H, Ar-H). ¹³C-NMR (75 MHz, CDCl₃) δ_C ppm 27.8, 32.8 (d, ¹*J*_{C-P} = 139.2 Hz), 36.9 (d, ²*J*_{C-P} = 3.1 Hz), 43.1 (d, ³*J*_{C-P} = 12.9 Hz), 66.8 (d, ²*J*_{C-P} = 6.5 Hz), 67.1 (d, ²*J*_{C-P} = 6.4 Hz), 80.5, 126.9, 127.5, 127.8, 127.9, 128.3, 128.4, 136.2 (d, ³*J*_{C-P} = 6.2 Hz), 136.3 (d, ³*J*_{C-P} = 6.1 Hz), 142.9 (d, ³*J*_{C-P} = 8.9 Hz), 170.5. ³¹P-NMR (121.5 MHz, CDCl₃): δ_P ppm = 32.9. HRMS (ESI): calculated for C₂₈H₃₄O₅P [(M+H)⁺], 481.2138; found 481.2148.

Dibenzyl 2-(p-methylphenyl)-3-(tert-butoxycarbonyl)propylphosphonate (5.9b). Prepared from compound **5.7b** (680 mg, 3.11 mmol) according to general procedure III. Colorless oil; purification 2:1 Hex/EtOAc v/v; yield 73%. ¹H NMR (300 MHz, CDCl₃) δ_H ppm 1.27 (br s, 9H, *t*-Bu), 2.11-2.23 (m, 2H, P-CH₂-), 2.28 (s, 3H, -Ph-CH₃), 2.50 (ddd, *J* = 1.5 Hz, 9.2 Hz, 15.2 Hz, 1H, -CH₂-CO), 2.75 (dd, *J* = 6.4 Hz, 15.2 Hz, 1H, -CH₂-CO), 3.40-3.57 (m, 1H, -CH-), 4.68-4.88 (m, 4H, -CH₂-Ph), 7.01-7.11 (m, 4H, Ar-H), 7.18-7.36 (m, 10H, Ar-H). ¹³C-NMR (75 MHz, CDCl₃) δ_C ppm 21.0, 27.9, 32.8 (d, ¹*J*_{C-P} = 139.6 Hz), 36.5 (d, ²*J*_{C-P} = 3.2 Hz), 43.3 (d, ³*J*_{C-P} = 12.8 Hz), 66.8

(d, $^2J_{C-P} = 6.4$ Hz), 67.0 (d, $^2J_{C-P} = 6.6$ Hz), 80.4, 127.3, 127.8, 127.8, 128.2, 128.5, 129.1, 136.3 (d, $^2J_{C-P} = 6.1$ Hz), 136.4 (d, $^2J_{C-P} = 6.0$ Hz), 139.9 (d, $^3J_{C-P} = 8.8$ Hz), 170.7. $^{31}\text{P-NMR}$ (121.5 MHz, CDCl_3): δ_{P} ppm = 31.4. HRMS (ESI): calculated for $\text{C}_{29}\text{H}_{36}\text{O}_5\text{P}$ [(M+H) $^+$], 495.2295; found 495.2315.

Dibenzyl 2-(p-methoxyphenyl)-3-(tert-butoxycarbonyl)propylphosphonate (5.9c). Prepared from compound **5.7c** (700 mg, 2.99 mmol) according to general procedure III. White crystal; purification 1:1 Hex/EtOAc v/v; yield 69%. $^1\text{H NMR}$ (300 MHz, CDCl_3) δ_{H} ppm 1.27 (br s, 9H, *t*-Bu), 2.04-2.27 (m, 2H, P-CH₂-), 2.48 (ddd, $J = 1.4$ Hz, 9.3 Hz, 15.2 Hz, 1H, -CH₂-CO), 2.73 (dd, $J = 6.3$ Hz, 15.2 Hz, 1H, -CH₂-CO), 3.40-3.57 (m, 1H, -CH-), 3.74 (s, 3H, -Ph-O-CH₃), 4.68-4.91 (m, 4H, -CH₂Ph), 6.78 (d, $J = 8.5$ Hz, 2H, Ar-H), 7.11 (d, $J = 8.5$ Hz, 2H, Ar-H), 7.18-7.37 (m, 10H, Ar-H). $^{13}\text{C-NMR}$ (75 MHz, CDCl_3) δ_{C} ppm 27.8, 32.9 (d, $^1J_{C-P} = 137.7$ Hz), 36.2 (d, $^2J_{C-P} = 3.5$ Hz), 43.4 (d, $^3J_{C-P} = 12.2$ Hz), 55.1, 66.8 (d, $^2J_{C-P} = 5.8$ Hz), 67.0 (d, $^2J_{C-P} = 5.8$ Hz), 80.4, 113.7, 127.8, 127.8, 128.2, 128.4, 134.9 (d, $^3J_{C-P} = 8.5$ Hz), 136.2 (d, $^3J_{C-P} = 5.9$ Hz), 136.3 (d, $^3J_{C-P} = 5.3$ Hz), 158.4, 170.5. $^{31}\text{P-NMR}$ (121.5 MHz, CDCl_3): δ_{P} ppm = 30.25 HRMS (ESI): calculated for $\text{C}_{29}\text{H}_{36}\text{O}_6\text{P}$ [(M+H) $^+$], 511.2244; found 511.2260.

Dibenzyl 2-methyl-3-(tert-butoxycarbonyl)propylphosphonate (5.9f). Prepared from compound *tert*-butylcrotonate (890 mg, 6.26 mmol) according to general procedure III. Colorless oil; purification 1.5:1 Hex/EtOAc v/v; yield 62%. $^1\text{H NMR}$ (300 MHz, CDCl_3) δ_{H} ppm 1.08 (d, $J = 6.5$ Hz, 3H, -CH(CH₃)-), 1.42 (br s, 9H, *t*-Bu), 1.61-1.79 (m, 2H, P-CH₂-), 1.83-2.00 (m, 1H, -CH₂-CO), 2.06-2.20 (m, 1H, -CH-), 2.28-2.47 (m, 2H, -CH₂-CO), 4.90-5.10 (m, 4H, -CH₂-Ph), 7.27-7.41 (m, 10H, Ar-H). $^{13}\text{C-NMR}$ (75 MHz, CDCl_3) δ_{C} ppm 21.7 ($^3J_{C-P} = 8.6$ Hz), 25.1 ($^2J_{C-P} = 5.2$ Hz), 27.8, 32.4 ($^1J_{C-P} = 139.5$ Hz), 39.7 ($^3J_{C-P} = 12.0$ Hz), 67.01 ($^2J_{C-P} = 6.5$ Hz), 67.03 ($^2J_{C-P} = 6.5$ Hz), 76.2, 127.9, 127.9, 129.2, 134.5, 136.17 ($^3J_{C-P} = 5.9$ Hz), 173.3. $^{31}\text{P-NMR}$ (121.5 MHz, CDCl_3): δ_{P} ppm = 32.87. HRMS (ESI): calculated for $\text{C}_{23}\text{H}_{32}\text{O}_5\text{P}$ [(M+H) $^+$], 419.1982; found 419.1904.

Dibenzyl 3-(N-(benzyloxy)-N-methylcarbamoyl)-2-phenylpropylphosphonate (5.10a). Prepared from compound **5.9a** (1.0 g, 2.08 mmol) according to general procedure IV. Colorless oil; purification 97:3 $\text{CH}_2\text{Cl}_2/\text{MeOH}$ v/v; yield 51%. $^1\text{H NMR}$ (300 MHz, CDCl_3) δ_{H} ppm 2.04-2.39 (m, 2H, P-CH₂-), 2.69-2.90 (m, 2H, -CH₂-CON-), 3.07 (s, 3H, N-CH₃), 3.56-3.75 (m, 1H, -CH(Ph)-), 4.63 (s, 2H, NOCH₂Ph) 4.67-4.91 (m, 4H, POCH₂Ph), 7.13-7.41 (m, 20H, Ar-

H). ^{13}C -NMR (75 MHz, CDCl_3) δ_{C} ppm 32.2 (d, $^1J_{\text{C-P}} = 137.6$ Hz), 36.1 (d, $^2J_{\text{C-P}} = 3.4$ Hz), 39.8 (d, $^3J_{\text{C-P}} = 12.6$ Hz), 66.8 (d, $^2J_{\text{C-P}} = 6.4$ Hz), 67.1 (d, $^2J_{\text{C-P}} = 6.4$ Hz), 76.1, 126.8, 127.5, 127.8, 127.9, 128.1, 128.2, 128.5, 128.7, 128.9, 129.2, 134.5, 136.3, (d, $^3J_{\text{C-P}} = 6.6$ Hz), 136.4 (d, $^3J_{\text{C-P}} = 6.4$ Hz), 143.6 (d, $^3J_{\text{C-P}} = 8.4$ Hz), 172.9. ^{31}P -NMR (121.5 MHz, CDCl_3): δ_{P} ppm = 33.16. HRMS (ESI): calculated for $\text{C}_{32}\text{H}_{35}\text{NO}_5\text{P}$ [(M+H) $^+$], 544.2247; found 544.2318.

Dibenzyl 3-(N-(benzyloxy)-N-methylcarbamoyl)-2-p-tolylpropylphosphonate (5.10b).

Prepared from compound **5.9b** (980 mg, 1.98 mmol) according to general procedure IV. Colorless oil; purification 97:3 $\text{CH}_2\text{Cl}_2/\text{MeOH}$ v/v; yield 56%. ^1H NMR (300 MHz, CDCl_3) δ_{H} ppm 2.04-2.37 (m, 5H, P- CH_2 -, Ph- CH_3), 2.69-2.90 (m, 2H, $-\text{CH}_2\text{CO}$), 3.08 (s, 3H, N- CH_3), 3.54-3.71 (m, 1H, $-\text{CH}-$), 4.64 (s, 2H, $-\text{NOCH}_2\text{Ph}$), 4.70-4.89 (m, 4H, POCH_2Ph), 7.05 (m, 4H, Ar-H), 7.15-7.40 (m, 15H, Ar-H). ^{13}C -NMR (75 MHz, CDCl_3) δ_{C} ppm 20.9, 32.2 (d, $^1J_{\text{C-P}} = 139.6$ Hz), 35.5, 39.7 (d, $^3J_{\text{C-P}} = 11.8$ Hz), 66.6 (d, $^2J_{\text{C-P}} = 5.7$ Hz), 66.8 (d, $^3J_{\text{C-P}} = 6.4$ Hz), 66.4, 127.2, 127.6, 127.7, 128.0, 128.3, 128.5, 128.7, 130.0, 129.1, 134.4, 136.0, 136.2 (d, $^3J_{\text{C-P}} = 6.9$ Hz), 136.3 (d, $^3J_{\text{C-P}} = 6.3$ Hz), 140.4 (d, $^3J_{\text{C-P}} = 8.3$ Hz), 172.7. ^{31}P -NMR (121.5 MHz, CDCl_3): δ_{P} ppm = 31.67. HRMS (ESI): calculated for $\text{C}_{33}\text{H}_{37}\text{NO}_5\text{P}$ [(M+H) $^+$], 558.2404; found 558.2408.

Dibenzyl 3-(N-(benzyloxy)-N-methylcarbamoyl)-2-(4-methoxyphenyl)propylphosphonate (5.10c).

Prepared from compound **5.9c** (850 mg, 1.67 mmol) according to general procedure IV. Colorless oil; purification gradient 0–5% MeOH in CH_2Cl_2 ; yield 47%. ^1H NMR (300 MHz, CDCl_3) δ_{H} ppm 2.01-2.37 (m, 2H, P- CH_2 -), 2.66-2.88 (m, 2H, $-\text{CH}_2\text{-CO}$), 3.07 (s, 3H, N- CH_3), 3.53-3.70 (m, 1H, $-\text{CH}-$), 3.72 (s, 3H, Ph-O- CH_3), 4.64 (s, 2H, NOCH_2Ph), 4.70-4.90 (m, 4H, $-\text{CH}_2\text{-Ph}$), 6.76 (d, $J = 8.8$ Hz, 2H, Ar-H), 7.08 (d, $J = 8.8$ Hz, 2H, Ar-H), 7.14-7.39 (m, 15H, Ar-H). ^{13}C -NMR (75 MHz, CDCl_3) δ_{C} ppm 32.3 ($^1J_{\text{C-P}} = 138.72$ Hz), 35.2 ($^3J_{\text{C-P}} = 3.99$ Hz), 39.9 ($^3J_{\text{C-P}} = 13.1$ Hz), 55.0, 66.6 ($^2J_{\text{C-P}} = 7.1$ Hz), 66.8 ($^2J_{\text{C-P}} = 7.0$ Hz), 75.9, 113.7, 127.6, 127.8, 128.1, 128.1, 128.3, 128.3, 128.6, 128.8, 129.1, 134.4, 135.5 ($^3J_{\text{C-P}} = 9.0$ Hz), 136.2 ($^3J_{\text{C-P}} = 7.1$ Hz), 136.33 ($^3J_{\text{C-P}} = 7.1$ Hz), 158.2. ^{31}P -NMR (121.5 MHz, CDCl_3): δ_{P} ppm = 30.59. HRMS (ESI): calculated for $\text{C}_{33}\text{H}_{37}\text{NO}_6\text{P}$ [(M+H) $^+$], 574.2353; found 574.2306.

Dibenzyl 3-(N-(benzyloxy)-N-methylcarbamoyl)-2-methylpropylphosphonate (5.10f).

Prepared from compound **5.9f** (1.0 g, 2.39 mmol) according to general procedure IV. Colorless oil; purification gradient 0–5% MeOH in CH_2Cl_2 ; yield 62%. ^1H NMR (300 MHz, CDCl_3) δ_{H} ppm 1.06 (d, $J = 6.5$ Hz, 3H, $-\text{CH}(\text{CH}_3)\text{-CH}_2$ -), 1.61-1.73 (m, 1H, P- CH_2 -), 1.88-2.05 (m,

1H, P-CH₂-), 2.26-2.60 (m, 3H, -CH(CH₃)-, -CH₂-CO), 3.15 (s, 1H, N-CH₃), 4.75 (s, NOCH₂Ph), 4.89-5.09 (m, 4H, -CH₂-Ph), 7.27-7.42 (m, 15H, Ar-H). ¹³C-NMR (75 MHz, CDCl₃) δ_C ppm 21.4 (³J_{C-P} = 8.6 Hz), 25.2 (²J_{C-P} = 5.2 Hz), 32.3 (¹J_{C-P} = 138.5 Hz), 39.7 (³J_{C-P} = 12.9 Hz), 67.0 (²J_{C-P} = 6.5 Hz), 67.0 (²J_{C-P} = 6.5 Hz), 76.2, 127.9, 127.9, 128.3, 128.5, 128.7, 128.9, 129.3, 134.5, 136.5 (³J_{C-P} = 6.1 Hz), 173.7. ³¹P-NMR (121.5 MHz, CDCl₃): δ_P ppm = 33.16. HRMS (ESI): calculated for C₂₇H₃₃NO₅P [(M+H)⁺], 482.2091; found 482.2086.

Diethyl 2-(p-chlorophenyl)-3-(tert-butoxycarbonyl)propylphosphonate (5.14d). Prepared from compound **5.7d** (784 mg, 3.28 mmol) according to general procedure III. Pale yellow oil; purification 1.5:1 Hex/Me₂CO v/v; yield 71%. ¹H NMR (300 MHz, CDCl₃) δ_H ppm 1.17-1.34 (m, 6H, P-CH₂CH₃), 1.29 (br, 9H, *t*-Bu), 1.96-2.22 (m, 2H, -CH₂-), 2.52 (dd, *J* = 9.5 Hz, 15.8 Hz, 1H, -CH₂-CO), 2.80 (dd, *J* = 6.3 Hz, 15.8 Hz, 1H, -CH₂-CO), 3.40-3.58 (m, 1H, -CH-), 3.86-4.05 (m, 4H, P-CH₂CH₃), 7.18 (d, *J* = 8.4 Hz, 2H, Ar-H), 7.27 (d, *J* = 8.4 Hz, 2H, Ar-H). ¹³C-NMR (75 MHz, CDCl₃) δ_C ppm 16.1 (d, ³J_{C-P} = 16.1 Hz), 16.1 (d, ³J_{C-P} = 6.3 Hz), 27.7, 32.2 (d, ¹J_{C-P} = 140.8 Hz), 36.3 (d, ²J_{C-P} = 3.5 Hz), 42.8 (d, ³J_{C-P} = 12.7 Hz), 61.2 (d, ²J_{C-P} = 6.9 Hz), 61.4 (d, ²J_{C-P} = 6.9 Hz), 80.5, 128.3, 128.8, 132.3, 141.5 (d, ³J_{C-P} = 9.6 Hz), 170.2. ³¹P-NMR (121.5 MHz, CDCl₃): δ_P ppm 28.47. HRMS (ESI): calculated for C₁₈H₂₉ClO₅P [(M+H)⁺], 391.1436; found 391.1610.

Diethyl 2-(3,4-dichlorophenyl)-3-(tert-butoxycarbonyl)propylphosphonate (5.14e). Prepared from compound **5.7e** (656 mg, 2.40 mmol) according to general procedure III. Pale yellow oil; purification 1:1 Hex/Me₂CO v/v; yield 73%. ¹H NMR (300 MHz, CDCl₃) δ_H ppm 1.22 (t, *J* = 7.1 Hz, 3H, -OCH₂CH₃), 1.23 (t, *J* = 7.2 Hz, 3H, -OCH₂CH₃), 1.32 (br, 9H, *t*-Bu), 1.95-2.21 (m, 2H, P-CH₂-), 2.52 (ddd, *J* = 1.2 Hz, 9.3 Hz, 15.8 Hz, 1H, -CH₂-CO), 2.80 (dd, *J* = 6.1 Hz, 15.8 Hz, 1H, -CH₂-CO), 3.40-3.55 (m, 1H, -CH-), 3.88-4.07 (m, 4H, OCH₂CH₃), 7.10 (dd, *J* = 2.1 Hz, 8.4 Hz, 1H, Ar-H), 7.34 (d, *J* = 2.1 Hz, 1H, Ar-H), 7.37 (d, *J* = 8.4 Hz, 1H, Ar-H). ¹³C-NMR (75 MHz, CDCl₃) δ_C ppm 16.2 (d, ³J_{C-P} = 2.9 Hz), 16.3 (d, ³J_{C-P} = 2.4 Hz), 27.9, 32.1 (d, ¹J_{C-P} = 140.7 Hz), 36.3 (d, ²J_{C-P} = 3.9 Hz), 42.7 (d, ³J_{C-P} = 12.1 Hz), 61.5 (d, ²J_{C-P} = 7.8 Hz), 61.6 (d, ²J_{C-P} = 7.3 Hz), 80.9, 126.9, 129.6, 130.2, 130.6, 132.2, 143.4 (d, ³J_{C-P} = 9.0 Hz), 170.1. ³¹P-NMR (121.5 MHz, CDCl₃): δ_P ppm = 27.96. HRMS (ESI): calculated for C₁₈H₂₈Cl₂O₅P [(M+H)⁺], 425.1046; found 425.1029.

Diethyl 3-(N-(benzyloxy)-N-methylcarbamoyl)-2-(4-chlorophenyl)propylphosphonate (5.15d). Prepared from compound **5.14d** (870 mg, 2.23 mmol) according to general procedure IV.

Colorless oil; purification 97:3 CH₂Cl₂/MeOH v/v; yield 46%. ¹H NMR (300 MHz, CDCl₃) δ_H ppm 1.16 (app. t, *J* = 7.1 Hz, 3H, P-CH₂CH₃), 1.21 (app. t, *J* = 7.1 Hz, 3H, P-CH₂CH₃), 1.91-2.26 (m, 2H, P-CH₂-), 2.67-2.89 (m, 2H, -CH₂-CO-), 3.10 (s, 3H, N-CH₃), 3.50-3.66 (m, 1H, -CH-), 3.86-4.03 (m, 4H, POCH₂Ph), 4.72 (app. d., *J* = 3.3 Hz, 2H, NOCH₂Ph), 7.02-7.15 (m, 2H, Ar-H), 7.21-7.27 (m, 2H Ar-H), 7.30-7.42 (m, 5H, Ar-H). ¹³C-NMR (75 MHz, CDCl₃) δ_C ppm 16.11-6.39 (m), 31.88 (d, ¹*J*_{C-P} = 140.2 Hz), 35.50 (d, ²*J*_{C-P} = 3.2 Hz), 39.60 (d, ³*J*_{C-P} = 12.5 Hz), 61.33 (d, ²*J*_{C-P} = 6.4 Hz), 61.55 (d, ²*J*_{C-P} = 6.6 Hz), 76.2, 128.4, 128.7, 128.9, 129.0, 129.3, 132.3, 134.4, 140.4, 142.3 (d, ³*J*_{C-P} = 8.3 Hz), 167.1. ³¹P-NMR (121.5 MHz, CDCl₃): δ_P ppm 29.87. HRMS (ESI): calculated for C₂₂H₃₀ClNO₅P [(M+H)⁺], 454.1545; found 454.0736.

Diethyl 3-(N-(benzyloxy)-N-methylcarbamoyl)-2-(3,4-dichlorophenyl)propylphosphonate (5.15e). Prepared from compound **5.14e** (700 mg, 1.65 mmol) according to general procedure IV. Colorless oil; purification 95:5 CH₂Cl₂/MeOH v/v; yield 49%. ¹H NMR (300 MHz, CDCl₃) δ_H ppm 1.18 (app. t, *J* = 7.1 Hz, 3H, P-CH₂CH₃), 1.22 (app. t, *J* = 7.2 Hz, 3H, P-CH₂CH₃), 1.86-2.24 (m, 2H, P-CH₂-), 2.61-2.85 (m, 2H, -CH₂-CO-), 3.12 (s, 3H, N-CH₃), 3.44-3.62 (m, 1H, -CH-), 3.82-4.05 (m, 4H, POCH₂CH₃), 4.75 (s, 2H, NOCH₂Ph), 7.02 (dd, *J* = 2.2 Hz, 8.34 Hz, 1H, Ar-H), 7.23-7.44 (m, 7H, Ar-H). ¹³C-NMR (75 MHz, CDCl₃) δ_C ppm 16.2 (d, ³*J*_{C-P} = 6.8 Hz), 16.3 (d, ³*J*_{C-P} = 6.6 Hz), 31.7 (d, ¹*J*_{C-P} = 140.4 Hz), 33.4, 35.3 (d, ²*J*_{C-P} = 3.3 Hz), 39.3 (d, ³*J*_{C-P} = 13.1 Hz), 61.4 (d, ²*J*_{C-P} = 6.7 Hz), 61.6 (d, ²*J*_{C-P} = 6.6 Hz), 76.1, 127.1, 128.7, 129.0, 129.3, 129.5, 130.2, 130.4, 132.1, 134.3, 144.1 (d, ³*J*_{C-P} = 7.9 Hz), 172.3. ³¹P-NMR (121.5 MHz, CDCl₃): δ_P ppm 28.22. HRMS (ESI): calculated for C₂₂H₂₉Cl₂NO₅P [(M+H)⁺], 488.1155; found 488.1144.

Diethyl 3-(N-hydroxy-N-methylcarbamoyl)-2-(4-chlorophenyl)propylphosphonate (5.16d). Prepared from compound **5.15d** (400 mg, 0.88 mmol) according to general procedure VI. Colorless oil; purification gradient 0–10% MeOH in CH₂Cl₂, 1% triethylamine; yield 79%. ¹H NMR (300 MHz, CDCl₃) δ_H ppm 1.18 (app. t, *J* = 7.1 Hz, 3H, P-CH₂CH₃), 1.26 (app. t, *J* = 7.0 Hz, 3H, P-CH₂CH₃), 1.90-2.37 (m, 2H, P-CH₂-), 2.66-2.80 (m, 1H of -CH₂-CO-), 3.11-3.29 (m, 3H, N-CH₃, 1H of -CH₂-CO-), 3.51-3.74 (m, 1H, -CH-), 3.82-3.05 (m, 4H, POCH₂Ph), 7.15-7.33 (m, 4H, Ar-H), 9.46 (s, 1H, N-OH). ¹³C-NMR (75 MHz, CDCl₃) δ_C ppm 16.0-16.5 (m), 31.5 (d, ¹*J*_{C-P} = 139.2 Hz), 33.2, 35.8 (d, ³*J*_{C-P} = 8.7 Hz), 37.7 (d, ²*J*_{C-P} = 7.0 Hz), 61.9 (d, ²*J*_{C-P} = 7.2 Hz), 62.2 (d, ²*J*_{C-P} = 6.5 Hz), 128.6, 128.7, 132.5, 142.7 (d, ³*J*_{C-P} = 11.1 Hz), 171.7. ³¹P-NMR (121.5 MHz, CDCl₃): rotamers at δ_P ppm 29.46, 30.85. HRMS (ESI): calculated for C₁₅H₂₄ClNO₅P [(M+H)⁺], 364.1075; found 364.0480.

Diethyl 3-(N-hydroxy-N-methylcarbamoyl)-2-(3,4-dichlorophenyl)propylphosphonate (5.16e). Prepared from compound **5.15e** (350 mg, 0.72 mmol) according to general procedure VI. Colorless oil; purification gradient 0–10% MeOH in CH₂Cl₂, 1% triethylamine; yield 74%. ¹H NMR (300 MHz, CDCl₃) δ_H ppm 1.21 (app. t, *J* = 7.2 Hz, 3H, P-CH₂CH₃), 1.27 (app. t, *J* = 7.1 Hz, 3H, P-CH₂CH₃), 2.00–2.27 (m, 2H, P-CH₂-), 2.74 (dd, *J* = 6.5 Hz, 15.17 Hz, 1H, -CH₂CO), 3.19 (dd, *J* = 8.1 Hz, 15.2 Hz, 1H, -CH₂CO), 3.22 (s, 3H, N-CH₃), 3.52–3.72 (m, 1H, -CH-), 3.87–4.07 (m, 4H, -POCH₂CH₃), 7.14 (d, *J* = 8.1 Hz, 1H, Ar-H), 7.32–7.45 (m, 2H, Ar-H), 9.44 (s, 1H, N-OH). ¹³C-NMR (75 MHz, CDCl₃) δ_C ppm 16.2 (d, ³*J*_{C-P} = 6.7 Hz), 16.3 (d, ³*J*_{C-P} = 6.4 Hz), 31.3 (d, ¹*J*_{C-P} = 141.7 Hz), 35.6 (d, ²*J*_{C-P} = 3.3 Hz), 35.9, 37.6 (d, ³*J*_{C-P} = 7.5 Hz), 62.0 (d, ²*J*_{C-P} = 6.9 Hz), 62.3 (d, ²*J*_{C-P} = 7.8 Hz), 126.9, 129.3, 130.4, 132.4, 130.7, 144.5 (d, ³*J*_{C-P} = 12.2 Hz), 171.4. ³¹P-NMR (121.5 MHz, CDCl₃): rotamers at δ_P ppm 29.01, 30.45. HRMS (ESI): calculated for C₁₅H₂₃Cl₂NO₅P [(M+H)⁺], 398.0685; found 398.0705.

(E)-tert-butyl 4-phenylbut-2-enoate (5.19a). Prepared from compound **5.17a** (1.0 g, 8.19 mmol) according to general procedure II. Yellow oil; purification 97:3 Hex/Et₂O v/v; yield 80% over two steps. ¹H NMR (300 MHz, CDCl₃) δ_H ppm 1.46 (br, 9H, *t*-Bu), 3.46 (dd, *J* = 1.6 Hz, 6.7 Hz, 2H -CH₂-), 5.73 (dt, *J* = 1.7 Hz, 15.6 Hz, 1H, -CH=CH-CO-), 6.99 (dt, *J* = 6.7 Hz, 15.5 Hz, 1H, -CH=CH-CO-), 7.14–7.34 (m, 5H, Ar-H). ¹³C-NMR (75 MHz, CDCl₃) δ_C ppm 28.1, 38.1, 80.2, 124.1, 126.5, 128.6, 128.8, 137.9, 145.9, 165.8.

(E)-tert-butyl 5-phenylpent-2-enoate (5.19b). Prepared from compound **5.17b** (1.0 g, 7.34 mmol) according to general procedure II. Colorless oil; purification 97:3 Hex/Et₂O v/v; yield 84% over two steps. ¹H NMR (300 MHz, CDCl₃) δ_H ppm 1.48 (br, 9H, *t*-Bu), 2.43–2.54 (m, 2H, -CH₂C=CH-), 2.78 (t, *J* = 7.4 Hz, 2H, Ph-CH₂-), 5.78 (dt, *J* = 1.8 Hz, 15.5 Hz, 1H, -CH=CH-CO-), 6.90 (dt, *J* = 6.7 Hz, 15.5 Hz, 1H, -CH=CH-CO-), 7.13–7.43 (m, 5H, Ar-H). ¹³C-NMR (75 MHz, CDCl₃) δ_C ppm 28.2, 33.8, 34.5, 80.1, 123.4, 126.1, 128.3, 128.5, 141.1, 147.0, 166.0.

(E)-tert-butyl 6-phenylhex-2-enoate (5.19c). Prepared from compound **5.17c** (1.5 g, 9.99 mmol) according to general procedure II. Colorless oil; purification 98:2 Hex/Et₂O v/v; yield 79% over two steps. ¹H NMR (300 MHz, CDCl₃) δ_H ppm 1.48 (br, 9H, *t*-Bu), 1.78 (app. quin, 2H, -CH₂-), 2.15–2.25 (m, 2H, -CH₂CH=CH-), 2.64 (t, *J* = 7.6 Hz, 2H, Ph-CH₂-), 5.75 (dt, *J* = 1.6 Hz, 15.6 Hz, 1H, CH=CH-CO-), 6.87 (dt, *J* = 6.8 Hz, 15.6 Hz, 1H, -CH=CH-CO-), 7.13–7.33 (m, 5H, Ar-H). ¹³C-NMR (75 MHz, CDCl₃) δ_C ppm 28.2, 29.8, 31.5, 35.3, 80.1, 123.3, 125.9, 128.4,

128.4, 141.8, 147.5, 166.1. HRMS (ESI): calculated for $C_{16}H_{23}O_2$ [(M+H)⁺], 247.1693; found 247.1630.

(E)-*tert*-butyl 7-phenylhept-2-enoate (**5.19d**). Prepared from compound **5.17d** (1.0 g, 6.09 mmol) according to general procedure II. Colorless oil; purification 98:2 Hex/Et₂O v/v; yield 87% over two steps. ¹H NMR (300 MHz, CDCl₃) δ_H ppm 1.44-1.55 (m, 9H, *t*-Bu, 2H, -CH₂-), 1.58-1.71 (m, 2H, -CH₂-), 2.14-2.24 (m, 2H, -CH₂-), 2.61 (t, *J* = 7.5 Hz, 2H, Ph-CH₂-), 5.7 (dt, *J* = 1.6 Hz, 15.6 Hz, 1H, -CH=CH-CO-), 6.84 (dt, *J* = 6.9 Hz, 15.6 Hz, 1H, -CH=CH-CO-), 7.13-7.32 (m, 5H, Ar-H). ¹³C-NMR (75 MHz, CDCl₃) δ_C ppm 27.7, 28.2, 30.9, 31.9, 35.7, 80.0, 123.1, 125.7, 123.3, 128.4, 142.3, 147.7, 166.1. HRMS (ESI): calculated for $C_{17}H_{25}O_2$ [(M+H)⁺], 261.1849; found 261.1865.

Dibenzyl 2-((tert-butoxycarbonyl)methyl)-3-phenylpropylphosphonate (**5.20a**). Prepared from compound **5.19a** (1.2 g, 5.50 mmol) according to general procedure III. Colorless oil; purification 5:1 Hex/Me₂CO v/v; yield 66%. ¹H NMR (300 MHz, CDCl₃) δ_H ppm 1.41 (br, 9H, *t*-Bu), 1.624-2.03 (m, 2H, P-CH₂-), 2.32-2.40 (m, 2H, -CH₂-CO), 2.38-2.56 (m, 3H, -CH(CH₂-Ph)-), 4.81-5.18 (m, 4H, O-CH₂-Ph), 7.01-7.41 (m, 15H, Ar-H). ¹³C-NMR (75 MHz, CDCl₃) δ_C ppm 28.0, 29.4 (d, ¹*J*_{C-P} = 138.9 Hz), 30.5 (d, ²*J*_{C-P} = 4.5 Hz), 32.2, 37.1 (d, ³*J*_{C-P} = 11.1 Hz), 41.2 (d, ³*J*_{C-P} = 9.1 Hz), 67.12 (d, ²*J*_{C-P} = 6.1 Hz), 67.13 (d, ²*J*_{C-P} = 6.50 Hz), 80.40, 127.30, 127.32, 127.9, 128.4, 139.81 (d, ³*J*_{C-P} = 6.06 Hz), 139.84 (d, ³*J*_{C-P} = 6.1 Hz), 141.1, 173.3. ³¹P-NMR (121.5 MHz, CDCl₃): δ_P ppm = 33.0. HRMS (ESI): calculated for $C_{29}H_{36}O_5P$ [(M+H)⁺], 495.2295; found 495.2321.

Dibenzyl 2-((tert-butoxycarbonyl)methyl)-4-phenylbutylphosphonate (**5.20b**). Prepared from compound **5.19b** (1.0 g, 4.30 mmol) according to general procedure III. Colorless oil; purification 5:1 Hex/Me₂CO v/v; yield 63%. ¹H NMR (300 MHz, CDCl₃) δ_H ppm 1.41 (br, 9H, *t*-Bu), 1.62-2.00 (m, 4H, -CH₂-), 2.22-2.39 (m, 2H, -CH₂-), 2.43-2.52 (m, 1H, -CH-), 2.56 (t, *J* = 8.4 Hz, 2H, -CH₂-), 4.89-5.09 (m, 4H, -CH₂-Ph), 7.07-7.26 (m, 5H, Ar-H), 7.30-7.37 (m, 10H, Ar-H). ¹³C-NMR (75 MHz, CDCl₃) δ_C ppm 28.1, 29.8 (d, ¹*J*_{C-P} = 138.8 Hz), 30.1 (d, ²*J*_{C-P} = 4.7 Hz), 32.7, 36.33 (d, ³*J*_{C-P} = 10.1 Hz), 40.1 (d, ³*J*_{C-P} = 9.4 Hz), 67.0 (d, ²*J*_{C-P} = 6.4 Hz), 67.1 (d, ²*J*_{C-P} = 6.5 Hz), 80.4, 125.7, 127.9, 128.3, 128.5, 136.3 (d, ³*J*_{C-P} = 6.1 Hz), 136.4 (d, ³*J*_{C-P} = 6.1 Hz), 141.7, 171.5. ³¹P-NMR (121.5 MHz, CDCl₃): δ_P ppm = 33.04. HRMS (ESI): calculated for $C_{30}H_{38}O_5P$ [(M+H)⁺], 509.2451; found 509.2466.

Dibenzyl 2-((tert-butoxycarbonyl)methyl)-5-phenylpentylphosphonate (5.20c). Prepared from compound **5.19c** (1.35 g, 5.48 mmol) according to general procedure III. Colorless oil; purification 6:1 Hex/Me₂CO v/v; yield 71%. ¹H NMR (300 MHz, CDCl₃) δ_H ppm 1.41 (br, 9H, *t*-Bu), 1.42-1.63 (m, 4H, -CH₂-), 1.72-2.03 (m, 2H, -CH₂-), 2.16-2.56 (m, 4H, -CH₂-, 1H, -CH-), 4.86-5.09 (m, 4H, -CH₂-Ph), 7.03-7.47 (m, 15H, Ar-H). ¹³C-NMR (75 MHz, CDCl₃) δ_C ppm 28.0, 28.3, 29.8 (d, ¹J_{C-P} = 139.4 Hz), 30.3 (d, ²J_{C-P} = 4.1 Hz), 34.2 (d, ³J_{C-P} = 10.4 Hz), 35.8, 40.2 (d, ³J_{C-P} = 9.6 Hz), 66.9 (d, ²J_{C-P} = 6.2 Hz), 67.1 (d, ²J_{C-P} = 6.3 Hz), 80.3, 125.6, 127.9, 128.2, 128.3, 128.49, 129.4, 136.4 (d, ³J_{C-P} = 6.1 Hz), 136.4 (d, ³J_{C-P} = 6.1 Hz), 142.2, 171.6. ³¹P-NMR (121.5 MHz, CDCl₃): δ_P ppm 33.16. HRMS (ESI): calculated for C₃₁H₄₀O₅P [(M+H)⁺], 523.2608; found 523.2411.

Dibenzyl 2-((tert-butoxycarbonyl)methyl)-6-phenylhexylphosphonate (5.20d). Prepared from compound **5.19d** (1.0 g, 3.84 mmol) according to general procedure III. Colorless oil; purification 6:1 Hex/Me₂CO v/v; yield 68%. ¹H NMR (300 MHz, CDCl₃) δ_H ppm 1.20-1.35 (m, 2H, -CH₂-), 1.41 (br, 9H, *t*-Bu), 1.43-1.61 (m, 4H, -CH₂-), 1.77-1.92 (m, 2H, -CH₂-), 2.16-2.32 (m, 3H, -CH₂-, -CH-), 2.55 (t, *J* = 7.6 Hz, 2H, -CH₂-), 4.90-5.08 (m, 4H, -CH₂-Ph), 7.10-7.37 (m, 15H, Ar-H). ¹³C-NMR (75 MHz, CDCl₃) δ_C ppm 26.0, 28.1, 29.9 (d, ¹J_{C-P} = 138.4 Hz), 30.3 (d, ²J_{C-P} = 3.9 Hz), 31.3, 34.4 (d, ³J_{C-P} = 10.2 Hz), 35.7, 40.2 (d, ³J_{C-P} = 9.7 Hz), 67.0 (d, ²J_{C-P} = 6.6 Hz), 67.1 (d, ²J_{C-P} = 6.7.1 Hz), 80.3, 125.6, 127.9, 128.2, 128.3, 128.3, 128.5, 136.4 (d, ³J_{C-P} = 6.3 Hz), 136.4 (d, ³J_{C-P} = 6.3 Hz), 142.5, 171.7. ³¹P-NMR (121.5 MHz, CDCl₃): δ_P ppm = 33.32. HRMS (ESI): calculated for C₃₂H₄₂O₅P [(M+H)⁺], 537.2764; found 537.2784.

Dibenzyl 2-((N-(benzyloxy)-N-methylcarbamoyl)methyl)-3-phenylpropylphosphonate (5.21a). Prepared from compound **5.20a** (1.0 g, 2.02 mmol) according to general procedure IV. Colorless oil; purification gradient 0–5% MeOH in CH₂Cl₂; yield 43%. ¹H NMR (300 MHz, CDCl₃) δ_H ppm 1.77-2.07 (m, 2H, P-CH₂-), 2.40-2.83 (m, 5H, -CH₂-CO-, -CH-CH₂-Ph), 3.11 (s, 3H, N-CH₃), 4.63 (s, 2H, NOCH₂Ph), 4.86-5.05 (m, 4H, POCH₂Ph), 7.07-7.42 (m, 20H, Ar-H). ¹³C-NMR (75 MHz, CDCl₃) δ_C ppm 29.0 (d, ¹J_{C-P} = 138.7 Hz), 31.6 (d, ²J_{C-P} = 3.1 Hz), 35.9 (d, ³J_{C-P} = 9.6 Hz), 40.9 (d, ³J_{C-P} = 11.4 Hz), 67.2 (d, ²J_{C-P} = 6.6 Hz), 67.3 (d, ²J_{C-P} = 6.7 Hz), 76.1, 126.2, 127.9, 127.9, 128.3, 128.3, 128.5, 128.6, 128.8, 129.2, 129.4, 134.5, 136.6 (d, ³J_{C-P} = 6.8 Hz), 136.7 (d, ³J_{C-P} = 6.4 Hz), 139.6, 165.7. ³¹P-NMR (121.5 MHz, CDCl₃): δ_P ppm 33.28. HRMS (ESI): calculated for C₃₃H₃₇NO₅P [(M+H)⁺], 558.2404; found 558.2431.

Dibenzyl 2-((N-(benzyloxy)-N-methylcarbamoyl)methyl)-4-phenylbutylphosphonate (5.21b). Prepared from compound **5.20b** (1.0 g, 1.97 mmol) according to general procedure IV. Colorless oil; purification gradient 0–5% MeOH in CH₂Cl₂; yield 60%. ¹H NMR (300 MHz, CDCl₃) δ_H ppm 1.64–2.09 (m, 4H, -CH₂-), 2.31–2.58 (m, 3H, -CH₂-, 1H, -CH-), 2.65 (dd, *J* = 7.1 Hz, *J* = 16.5 Hz, 1H, -CH₂-), 3.14 (s, 3H, N-CH₃), 4.73 (br. s, 2H, NOCH₂Ph), 4.87–5.08 (m, 4H, -CH₂-Ph), 7.04–7.26 (m, 5H, Ar-H), 7.27–7.39 (m, 15H, Ar-H). ¹³C-NMR (75 MHz, CDCl₃) δ_C ppm 29.6 (d, ²*J*_{C-P} = 4.0 Hz), 29.6 (d, ¹*J*_{P-C} = 138.2 Hz), 32.9, 33.5, 36.5 (³*J*_{C-P} = 9.6 Hz), 36.6 (³*J*_{C-P} = 6.7 Hz), 67.0 (²*J*_{C-P} = 6.5 Hz), 76.1, 125.7, 127.9, 127.9, 128.3, 128.3, 128.5, 128.6, 128.9, 129.3, 134.6, 136.4 (³*J*_{C-P} = 6.3 Hz), 173.7. ³¹P-NMR (121.5 MHz, CDCl₃): δ_P ppm = 32.26. HRMS (ESI): calculated for C₃₄H₃₉NO₅P [(M+H)⁺], 572.2560; found 572.2585.

Dibenzyl 2-((N-(benzyloxy)-N-methylcarbamoyl)methyl)-5-phenylpentylphosphonate (5.21c). Prepared from compound **5.20c** (1.5 g, 2.87 mmol) according to general procedure IV. Colorless oil; purification gradient 0–5% MeOH in CH₂Cl₂; yield 68%. ¹H NMR (300 MHz, CDCl₃) δ_H ppm 1.36–1.63 (m, 4H, -CH₂-), 1.72–2.03 (m, 2H, -CH₂-), 2.26–2.66 (m, 5H, -CH₂-, -CH-), 3.12 (s, 3H, N-CH₃), 4.72 (s, 2H, NOCH₂Ph), 4.82–5.06 (m, 4H, POCH₂Ph), 7.03–7.43 (m, 20H, Ar-H). ¹³C-NMR (75 MHz, CDCl₃) δ_C ppm 28.2, 28.6, 29.7 (d, ²*J*_{C-P} = 3.2 Hz), 29.7 (d, ¹*J*_{C-P} = 138.6 Hz), 34.6 (d, ³*J*_{C-P} = 9.3 Hz), 35.8, 36.7 (d, ³*J*_{C-P} = 8.3 Hz), 66.8–67.2 (m), 76.1, 125.7, 127.9, 128.2, 128.3, 128.4, 128.51, 128.53, 128.7, 128.9, 129.3, 136.5 (d, ³*J*_{C-P} = 7.0 Hz), 142.4, 172.1. ³¹P-NMR (121.5 MHz, CDCl₃): δ_P ppm 33.40. HRMS (ESI): calculated for C₃₅H₄₁NO₅P [(M+H)⁺], 586.2717; found 586.2709.

Dibenzyl 2-((N-(benzyloxy)-N-methylcarbamoyl)methyl)-6-phenylhexylphosphonate (5.21d). Prepared from compound **5.20d** (1.28 g, 2.39 mmol) according to general procedure IV. Colorless oil; purification gradient 0–15% MeOH in CH₂Cl₂; yield 74%. ¹H NMR (300 MHz, CDCl₃) δ_H ppm 1.12–1.31 (m, 2H, -CH₂-), 1.34–1.56 (m, 4H, -CH₂-), 1.71–2.02 (m, 2H, -CH₂-), 2.22–2.63 (m, 4H, -CH₂-, 1H, -CH-), 3.11 (s, 3H, N-CH₃), 4.69 (s, 2H, -NOCH₂Ph), 4.88–5.06 (m, 4H, POCH₂Ph), 7.07–7.42 (m, 20H, Ar-H). ¹³C-NMR (75 MHz, CDCl₃) δ_C ppm 25.9, 27.9, 29.4 (d, ²*J*_{C-P} = 3.9 Hz), 29.5 (d, ¹*J*_{C-P} = 137.7 Hz), 31.1, 34.4 (d, ³*J*_{C-P} = 9.4 Hz), 35.5, 36.5 (d, ³*J*_{C-P} = 9.4 Hz), 66.6–66.8 (m), 75.8, 125.4, 127.7, 128.0, 128.1, 128.2, 128.3, 128.4, 128.6, 129.1, 134.4, 136.2–136.3 (m), 142.3, 173.6. ³¹P-NMR (121.5 MHz, CDCl₃): δ_P ppm = 32.52. HRMS (ESI): calculated for C₃₆H₄₃NO₅P [(M+H)⁺], 600.2873; found 600.2814.

Sodium hydrogen3-(N-hydroxy-N-methylcarbamoyl)-2-phenylpropylphosphonate (5.1a). Prepared from compound **5.10a** (150 mg, 0.28 mmol) according to general procedure V. White powder. ^1H NMR (300 MHz, D_2O) δ_{H} ppm 1.69-1.96 (m, 2H, P- CH_2 -), 2.89-3.14 (m, 5H, - CH_2 -, N- CH_3), 3.23-3.50 (m, 1H, - CH -) 7.16-7.41 (m, 5H, Ar-H). ^{13}C -NMR (75 MHz, D_2O) δ_{C} ppm 29.4, 36.1 (d, $^1J_{\text{C-P}} = 127.7$ Hz), 38.1 (d, $^2J_{\text{C-P}} = 2.8$ Hz), 38.5 (d, $^3J_{\text{C-P}} = 5.3$ Hz), 126.3, 127.3, 128.4, 146.1 (d, $^3J_{\text{C-P}} = 12.1$ Hz), 174.0. ^{31}P -NMR (121.5 MHz, D_2O): rotamers at δ_{P} ppm 19.64, 19.87. HRMS (ESI): calculated for $\text{C}_{11}\text{H}_{15}\text{NO}_5\text{P}$ [(M-H) $^-$], 272.0693; found 272.0622.

Sodium hydrogen3-(N-hydroxy-N-methylcarbamoyl)-2-p-tolylpropylphosphonate (5.1b). Prepared from compound **5.10b** (150 mg, 0.27 mmol) according to general procedure V. White powder. ^1H NMR (300 MHz, D_2O) δ_{H} ppm 1.73-1.97 (m, 2H, P- CH_2 -), 2.26 (s, 3H, Ph- CH_3), 2.86-3.09 (m, 5H, - CH_2 -CO, N- CH_3), 3.20-3.46 (m, 1H, - CH -), 7.10-7.25 (m, 4H, Ar-H). ^{13}C -NMR (75 MHz, D_2O) δ_{C} ppm 20.2, 35.9, 36.1 (d, $^1J_{\text{C-P}} = 130.5$ Hz), 37.7 (d, $^2J_{\text{C-P}} = 2.8$ Hz), 38.9 (d, $^3J_{\text{C-P}} = 6.7$ Hz), 127.5, 129.2, 136.5, 142.8 (d, $^3J_{\text{C-P}} = 13.1$ Hz), 174.4. ^{31}P -NMR (121.5 MHz, D_2O): rotamers at δ_{P} ppm 24.34, 24.65. HRMS (ESI): calculated for $\text{C}_{12}\text{H}_{17}\text{NO}_5\text{P}$ [(M-H) $^-$], 286.0849; found 286.0816.

Sodium hydrogen3-(N-hydroxy-N-methylcarbamoyl)-2-(4-methoxyphenyl)propylphosphonate (5.1c). Prepared from compound **5.10c** (200 mg, 0.35 mmol) according to general procedure V. White powder. ^1H NMR (300 MHz, D_2O) δ_{H} ppm 1.55-1.81 (m, 2H, P- CH_2 -), 2.72-2.98 (m, 5H, - CH_2 -CO, N- CH_3), 3.11-3.37 (m, 1H, - CH -), 3.71 (s, 3H, Ph-O- CH_3), 6.84 (d, $J = 7.4$ Hz, 2H, Ar-H), 7.18 (d, $J = 7.4$ Hz, 2H, Ar-H). ^{13}C -NMR (75 MHz, D_2O) δ_{C} ppm 36.8, 37.1 (d, $^1J_{\text{C-P}} = 132.9$ Hz), 40.3 (d, $^3J_{\text{C-P}} = 8.3$ Hz), 45.6 (d, $^2J_{\text{C-P}} = 5.8$ Hz), 55.4, 113.6, 128.6, 139.5 (d, $^3J_{\text{C-P}} = 11.7$ Hz), 156.7, 167.8. ^{31}P -NMR (121.5 MHz, D_2O): δ_{P} ppm = 20.79, 20.83. HRMS (ESI): calculated for $\text{C}_{12}\text{H}_{17}\text{NO}_6\text{P}$ [(M-H) $^-$], 302.0799; found 302.0926.

3-(N-hydroxy-N-methylcarbamoyl)-2-(p-chlorophenyl)propylphosphonic acid, bisammonium salt (5.1d). Prepared from compound **5.16d** (200 mg, 0.55 mmol) according to general procedure VII. Brown powder. ^1H NMR (300 MHz, D_2O) δ_{H} ppm 1.87-2.09 (m, 2H, P- CH_2 -), 2.81-2.97 (m, 2H, - CH_2 -CO-), 3.04 (s, 5/6 of N- CH_3), 3.11 (s, 1/6 of N- CH_3), 3.24-3.51 (m, 1H, - CH -), 7.20-7.38 (m, 4H, Ar-H). ^{13}C -NMR (75 MHz, D_2O) δ_{C} ppm 34.8 (d, $^1J_{\text{C-P}} = 131.6$ Hz), 35.6, 37.0 (d, $^2J_{\text{C-P}} = 2.5$ Hz), 39.4 (d, $^3J_{\text{C-P}} = 10.8$ Hz), 128.3, 128.8, 131.5, 142.7 (d, $^3J_{\text{C-P}} = 9.5$ Hz),

173.6. ^{31}P -NMR (121.5 MHz, D_2O): rotamers at δ_{P} ppm 23.25, 23.52. HRMS (ESI): calculated for $\text{C}_{11}\text{H}_{14}\text{ClNO}_5\text{P}$ [(M-H) $^-$], 306.0304; found 306.0306.

3-(N-hydroxy-N-methylcarbamoyl)-2-(3,4-dichlorophenyl)propylphosphonic acid, bisammonium salt (5.1e). Prepared from compound **5.16e** (150 mg, 0.38 mmol) according to general procedure VII. Brown powder. ^1H NMR (300 MHz, D_2O) δ_{H} ppm 1.84-2.08 (m, 2H, P- CH_2^-), 2.57-3.02 (m, 2H, $-\text{CH}_2-\text{CO}$), 3.06 (s, 5/6 of N- CH_3), 3.16 (s, 1/6 of N- CH_3), 3.24-3.50 (m, 1H, $-\text{CH}-$), 7.18 (dd, $J = 2.18$ Hz, 8.50 Hz, 1H, Ar-H), 7.40-7.50 (m, 2H, Ar-H). ^{13}C -NMR (75 MHz, D_2O) δ_{C} ppm 34.8 (d, $^1J_{\text{C-P}} = 131.5$ Hz), 35.9, 37.2 (d, $^2J_{\text{C-P}} = 2.7$ Hz), 39.5 (d, $^3J_{\text{C-P}} = 11.3$ Hz), 127.51, 129.53, 129.8, 130.4, 131.6, 144.9 (d, $^3J_{\text{C-P}} = 9.4$ Hz), 173.6. ^{31}P -NMR (121.5 MHz, D_2O): rotamers at δ_{P} ppm 22.47, 22.72. HRMS (ESI): calculated for $\text{C}_{11}\text{H}_{13}\text{Cl}_2\text{NO}_5\text{P}$ [(M-H) $^-$], 339.9914; found 340.0130.

Sodium hydrogen 3-(N-hydroxy-N-methylcarbamoyl)-2-methylpropylphosphonate (5.1f). Prepared from compound **5.10f** (125 mg, 0.26 mmol) according to general procedure V. Colorless oil. ^1H NMR (300 MHz, D_2O) δ_{H} ppm 1.01 (d, $J = 8.40$ Hz, 3H, $-\text{CH}(\text{CH}_3)-$), 1.41-1.72 (m, 2H, P- CH_2^-), 2.06-2.34 (m, 1H, $-\text{CH}-$), 2.36-2.49 (m, 1H, $-\text{CH}_2-\text{CO}$), 2.59 (dd, $J = 6.3$ Hz, 14.02 Hz), 3.20 (s, 5/6 of N- CH_3), 3.38 (s, 1/6 of N- CH_3). ^{13}C -NMR (75 MHz, D_2O) δ_{C} ppm 20.6 (d, $^3J_{\text{C-P}} = 8.0$ Hz), 28.6 (d, $^2J_{\text{C-P}} = 3.4$ Hz), 35.0 (d, $^3J_{\text{C-P}} = 132.1$ Hz), 36.1, 40.2 (d, $^3J_{\text{C-P}} = 13.3$ Hz), 175.2. ^{31}P -NMR (121.5 MHz, D_2O): rotamers at δ_{P} ppm 25.03, 25.42. HRMS (ESI): calculated for $\text{C}_6\text{H}_{13}\text{NO}_5\text{P}$ [(M-H) $^-$], 210.0537; found 210.1632.

Sodium hydrogen 2-((N-hydroxy-N-methylcarbamoyl)methyl)-3-phenylpropylphosphonate (5.2a). Prepared from compound **5.21a** (200 mg, 0.36 mmol) according to general procedure V. White powder. ^1H NMR (300 MHz, D_2O) δ_{H} ppm 1.46-1.79 (m, 2H, P- CH_2^-), 2.34-2.66 (m, 4H, $-\text{CH}_2^-$), 2.80-2.9 (m, 1H, $-\text{CH}-$), 3.08 (s, 5/6 of N- CH_3), 3.18 (s, 1/6 of N- CH_3), 7.13-7.39 (m, 5H, Ar-H). ^{13}C -NMR (75 MHz, D_2O) δ_{C} ppm 32.2 (d, $^1J_{\text{C-P}} = 132.3$ Hz), 32.7 (d, $^2J_{\text{C-P}} = 3.8$ Hz), 35.8, 36.6, 41.0 (d, $^3J_{\text{C-P}} = 9.2$ Hz), 126.2, 128.4, 129.4, 140.4, 174.6. ^{31}P -NMR (121.5 MHz, D_2O): rotamers at δ_{P} ppm 24.68, 25.01. HRMS (ESI): calculated for $\text{C}_{12}\text{H}_{17}\text{NO}_5\text{P}$ [(M-H) $^-$], 286.0850; found 286.0821.

Sodium hydrogen 2-((N-hydroxy-N-methylcarbamoyl)methyl)-4-phenylbutylphosphonate (5.2b). White powder. Prepared from compound **5.21b** (130 mg, 0.23 mmol) according to general procedure V. ^1H NMR (300 MHz, D_2O) δ_{H} ppm 1.34-1.84 (m, 4H, $-\text{CH}_2^-$), 2.08-2.27 (m,

1H, -CH-), 2.54-2.77 (m, 4H, -CH₂-), 3.20 (s, 5/6 of N-CH₃), 3.35 (s, 1/6 of N-CH₃), 7.17-7.40 (m, 5H, Ar-H). ¹³C-NMR (75 MHz, D₂O) δ_C ppm 32.0 (d, ¹J_{C-P} = 3.7 Hz), 32.5, 33.0 (d, ¹J_{C-P} = 129.9 Hz), 36.1, 36.3 (d, ³J_{C-P} = 6.4 Hz), 37.7 (d, ³J_{C-P} = 10.6 Hz), 126.0, 128.7, 128.8, 143.5, 175.0. ³¹P-NMR (121.5 MHz, D₂O): δ_P ppm 22.47. HRMS (ESI): calculated for C₁₃H₁₉NO₅P [(M-H)⁻], 300.1006; found 300.1204.

Sodium hydrogen 2-((N-hydroxy-N-methylcarbamoyl)methyl)-5-phenylpentylphosphonate (5.2c). Prepared from compound **5.21c** (175 mg, 0.30 mmol) according to general procedure V. White powder. ¹H NMR (300 MHz, D₂O) δ_H ppm 1.28-1.70 (m, 6H, -CH₂-), 2.05-2.26 (m, 1H, -CH-), 2.50-2.72 (m, 4H, P-CH₂-, CH₂-CON-), 3.18 (s, 5/6 of N-CH₃), 3.35 (s, 1/6 of N-CH₃), 7.18-7.36 (m, 5H, Ar-H). ¹³C-NMR (75 MHz, D₂O) δ_C ppm 28.2, 31.8 (d, ²J_{C-P} = 3.6 Hz), 33.0 (d, ¹J_{C-P} = 130.1 Hz), 35.0 (d, ³J_{C-P} = 10.3 Hz), 35.3, 36.1, 36.6 (d, ³J_{C-P} = 6.2 Hz), 126.0, 128.7, 128.8, 143.7, 175.2. ³¹P-NMR (121.5 MHz, D₂O): δ_P ppm = 23.18. HRMS (ESI): calculated for C₁₄H₂₁NO₅P [(M-H)⁻], 314.1163; found 314.1101.

Sodium hydrogen 2-((N-hydroxy-N-methylcarbamoyl)methyl)-6-phenylhexylphosphonate (5.2d). Prepared from compound **5.21d** (175 mg, 0.29 mmol) according to general procedure V. White powder. ¹H NMR (300 MHz, D₂O) δ_H ppm 1.20-1.66 (m, 8H, -CH₂-), 2.11 (m, 1H, -CH-), 2.46-2.68 (m, 4H, -CH₂-), 3.18 (s, 5/6 of N-CH₃), 3.34 (s, 1/6 of N-CH₃), 7.15-7.38 (m, 5H, Ar-H). ¹³C-NMR (75 MHz, D₂O) δ_C ppm 25.6, 31.2, 31.9 (d, ²J_{C-P} = 3.8 Hz), 33.1 (d, ¹J_{C-P} = 130.2 Hz), 35.1, 35.3 (d, ³J_{C-P} = 10.0 Hz), 36.1, 36.6 (d, ³J_{C-P} = 7.0 Hz), 125.9, 128.7, 128.8, 143.7, 175.3. ³¹P-NMR (121.5 MHz, D₂O): δ_P ppm = 23.20. HRMS (ESI): calculated for C₁₅H₂₃NO₅P [(M-H)⁻], 328.1319; found 328.1340.

V.C. β -Arylpropyl- analogues of fosmidomycin

As has been described above, Dxr isozymes contain a strictly conserved tryptophan residue within a flexible loop that undergoes an induced-fit conformational change upon fosmidomycin binding, closing over and interacting with the bound inhibitor. This flexible loop is considered essential for Dxr's catalytic activity.^{24,25,26,27,28} Murkin and coworkers demonstrated a change in the rate-limiting step of the *M. tuberculosis* Dxr catalyzed reaction upon alteration of Trp203 in the flexible loop, thereby establishing a functional link between this amino acid and chemical barrier crossing.²⁹ Inhibition and binding studies with fosmidomycin further reinforced the importance of the flexible loop and the conserved Trp in particular, for ligand association. Structural evaluation of a series of Dxr-bound compounds like **5.22** and **5.23** (Figure V.8) showed that the indole group of Trp211 in EcDxr is considerably displaced in order to accommodate the inhibitors' pyridine/quinoline rings, which form π - π stacking or charge-transfer interactions with the indole of that Trp residue.³⁰

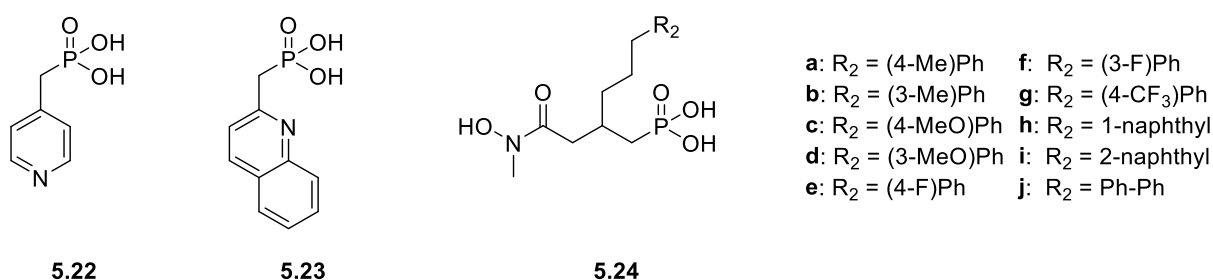


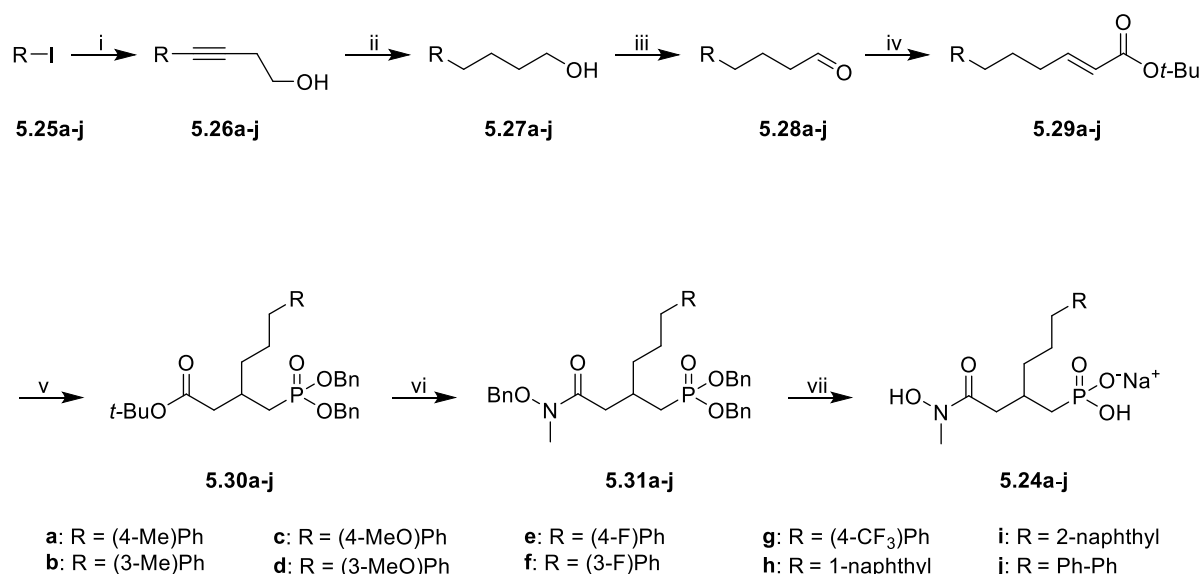
Figure V.8: Relevant Dxr inhibitors (**5.22** and **5.23**) and target β -substituted (**5.24a–j**) fosmidomycin analogues.

The findings reported in Section V.B make clear that direct introduction of aromatic rings at the β -carbon (**5.1a–e**) affords moderate PfDxr inhibitors and a 3-carbon linker between the reverse fosmidomycin propyl backbone and a phenyl ring (**5.2c**) seems optimal for *E. coli* and *M. tuberculosis* Dxr inhibition, while both a phenylpropyl (**5.2c**) and a phenylbutyl (**5.2d**) substituent affords potent PfDxr inhibition. This observation is rationalized by crystallographic studies of PfDxr in complex with **5.2c** and **5.2d**, which show that the phenyl rings of both compounds spatially overlap and occupy the 'usual' position of the indole ring of the conserved Trp296 residue in ternary complexes of active site metal-containing^{19,24,26} and metal-free structures.²⁵ This allows an intra-molecular interaction between the phenyl

ring and methyl group of the hydroxamic acid that is equivalent to the *inter*-molecular interactions observed in ternary complexes with FR900098.^{19,26} Rearrangement of the loop results in favorable interactions between these phenyl rings and the tryptophan residue. Importantly, both analogues showed submicromolar schizontocidal activity against the *P. falciparum* K1 strain, where essentially the same SAR was observed as for PfDxr inhibition. We therefore embarked on a follow-up study aimed at exploring the influence of lipophilicity, electronic and steric properties of the phenylpropyl side chain of **5.2c**. While anticipating that analogues **5.24a–j** would retain the capacity to occupy the aromatic 'hotspot', we envisioned reinforced interactions between their phenyl substituents and the loop residues.

V.C.1. Synthesis

The synthesis of **5.24a–j** (Scheme V.5) was achieved starting from commercially available aryl iodides **5.25a–j**. Sonogashira coupling with but-3-yn-1-ol afforded the corresponding alkynols **5.26a–j**, which were readily converted to **5.27a–j** upon catalytic hydrogenation.



Scheme V.5 Reagents and conditions: i) but-3-yn-1-ol, PdCl₂(PPh₃), CuI, Et₃N, 117 °C; ii) H₂, Pd/C, MeOH; iii) Dess-Martin periodinane, CH₂Cl₂; iv) Ph₃P=CHCOOt_{er}-Bu, toluene, 120 °C, 59% (**5.29a**), 51% (**5.29b**), 64% (**5.29c**), 65% (**5.29d**), 53% (**5.29e**), 49% (**5.29f**), 60% (**5.29g**), 67% (**5.29h**), 67% (**5.29i**), 61% (**5.29j**); v) (BnO)₂OPMe, n-BuLi, THF, -78 °C, 54% (**5.30a**), 45% (**5.30b**), 53% (**5.30c**), 47% (**5.30d**), 43% (**5.30e**), 47% (**5.30f**), 62% (**5.30g**), 55% (**5.30h**), 49% (**5.30i**), 71% (**5.30j**); vi) (a) TFA, CH₂Cl₂, 45 min, 0 °C to rt; (b) MeN(OBn)H, EDC, DMAP,

CH₂Cl₂, 18 h rt, 71% (**5.31a**), 72% (**5.31b**), 57% (**5.31c**), 51% (**5.31d**), 71% (**5.31e**), 69% (**5.31f**), 55% (**5.31g**), 44% (**5.31h**), 78% (**5.31i**), 68% (**5.31j**); vii) H₂, Pd/C, MeOH, NaOHaq., 25 °C, 10-15 min, quant.

Dess-Martin oxidation to the corresponding aldehydes **5.28a–j** and subsequent Wittig olefination afforded the α,β -unsaturated esters **5.29a–j**, which served as electrophiles in a Michael reaction with dibenzyl methylphosphonate to yield the respective 1,4-addition adducts **5.30a–j**. Hydrolysis of the *tert*-butyl ester and EDC-mediated coupling with *O*-benzyl-*N*-methyl-hydroxylamine gave **5.31a–j**. Finally, removal of all benzyl protecting groups by catalytic hydrogenolysis afforded the desired analogues **5.24a–j**.

V.C.2. Biological evaluation

The title compounds were tested for their capacity to inhibit recombinant EcDxr and PfDxr (Table V.3) using a spectrophotometric assay monitoring the substrate-dependent oxidation of NADPH associated with the Dxr-catalyzed reaction as described in section III.D.

Fosmidomycin and FR900098 remain superior in inhibition of EcDxr, PfDxr and Pf-K1 growth, when compared to **5.2c** and its phenyl ring derivatives **5.24a–5.24j**. Surprisingly, none of the changes introduced in **5.24a–5.24j** relative to **5.24c**, improve the inhibition of EcDxr. The assortment of substituents that induce variable electronic and steric effects was expected to yield some outliers in the inhibition of this enzyme. *Meta* substitution seems to be favorable for PfDxr inhibition as the *meta*-methyl- (**5.24b**) and the *meta*-fluoro (**5.24f**) analogues both surpass **5.2c** in inhibition of this enzyme. This is not an absolute pattern, however, as **5.24d** does not perform better than **5.24c**. Steric bulk is clearly relevant as both the 1-naphthyl- (**5.24h**) and the 2-naphthyl- (**5.24i**) analogues perform poorly in the enzyme assays while **5.24h**, **5.24i** and **5.24j** all rank amongst the poorest in inhibiting Pf-K1 growth. Note that the above (section V.B.3.) crystallography studies showed that upon binding, the rearrangement of the fosmidomycin backbone in **5.2c** would produce a close contact with the usual conformation seen for Lys312, and so a small conformational change is needed to relieve this clash while maintaining an interaction with the phosphonate. Even if their 'extra' aromatic moieties confer improved lipophilicity and therefore better cellular access, steric constraints at the Dxr active site probably obstruct tight binding of **5.24h**, **5.24i** and **5.24j**.

Table V.3: *In vitro* inhibition of recombinant Dxrs from *E. coli* and *P. falciparum* and MIC₅₀ values against *in vitro* growth of the *P. falciparum* K1 strain.

Compound	IC ₅₀ (μM)		<i>P. falciparum</i> K1
	EcDxr	PfDxr	IC ₅₀ (μM)
fosmidomycin (1.1)	0.03	0.036 ± 0.006	1.7 ± 0.89 ¹⁷
FR900098 (1.2)	0.03	0.018 ³¹	0.42 ± 0.17 ¹⁷
5.2c	0.84	0.117 ± 0.012	2.67 ± 0.43
5.24a	1.04	0.56 ± 0.007	1.37 ± 1.23
5.24b	10.40	0.05 ± 0.007	19.97 ± 15.98
5.24c	1.18	0.12 ± 0.006	3.84 ± 2.50
5.24d	0.97	0.15 ± 0.006	7.83 ± 3.65
5.24e	10.53	3.2 ± 0.115	51.42 ± 21.79
5.24f	2.00	0.07 ± 0.001	5.72 ± 4.38
5.24g	7.33	0.27 ± 0.01	45.72 ± 21.28
5.24h	13.91	0.28 ± 0.015	49.34 ± 18.90
5.24i	4.07	0.87 ± 0.03	46.63 ± 15.40
5.24j	nd	1.6 ± 0.25	64 ± 0.0

nd = not determined

Generally, the changes introduced in **5.24a–5.24j** relative to **5.24c** did not improve the MIC₅₀ values against *in vitro* growth of *P. falciparum* K1 strain. It is puzzling to see that **5.24b** does not elicit a MIC₅₀ value consistent with its PfDxr inhibition, rather effecting lower inhibition compared to its isomer (**5.24a**), which shows only modest PfDxr inhibition. Remarkably, methyl-substitution of the aromatic ring at the meta-position (**5.24b**) increases PfDxr inhibition, while it unfavorably influences EcDxr inhibition. A similar trend is observed for the meta-fluoro analogue **5.24f**.

V.C.3. X-ray structures of PfDxr in complex with seven inhibitors

The structures of PfDxr in complex with seven of the new β-substituted inhibitors (**5.24a–d**, **5.24f**, **5.24g**, and **5.24h**) have been solved. All seven of the new β-substituted complexes were found to take on the same general structure seen in the **5.2c** complex (section V.B.3.), but can be grouped into two sets depending on whether they represent *meta*- or *para*-

substitutions to the phenyl ring. The structures for 3 *meta*- (**5.24b**, **5.24d**, **5.24f**) and 3 *para*- (**5.24a**, **5.24c**, **5.24g**) substitutions, as well as **5.24h** (which was included as a member of the *meta*-class) are shown in Figure V.9. The members of the *meta*-class form a tight cluster of eight independent structures (including both subunits of the dimers), where the phenyl rings of the new compounds closely overlap that observed in the **5.2c** complex (Figure V.9B). Interactions of the phosphonate and hydroxamic acid groups in all complexes are essentially identical to that of the **5.2c** complex, as is the overall conformation of the fosmidomycin backbone. All members adopt the same pose, where the substituent is directed towards the indole ring of Trp296 in the **5.2c** complex; none points in the other direction, towards His341. However, all inhibitors have an effect on the positioning of the indole ring, and on the quality of the electron density of the flap. Unsurprisingly, the introduction of a naphthalene ring in **5.24h** causes a large change in the conformation of Trp293, which is needed to prevent clashes with the indole (Figure V.9B); the flap in this structure is well defined. Although there are no close contacts to the indole ring, only a few atoms of one edge of the naphthalene ring are solvent-exposed.

The slightly smaller methoxyphenyl substituent in **5.24d** also causes a movement of the tryptophan residue, to prevent close contacts between the indole ring and the methyl group. The flap is rather well defined in both chains, as is the density for the indole group, but the change in conformation results in a loss of the close contacts to the indole seen in the **5.2c** complex. The methoxyphenyl group is approximately planar, and so occupies the same place as the corresponding portion of the naphthalene ring of **5.24h** (Figure V.9B). The oxygen of the methoxy group does not form any hydrogen bonding interactions with the protein, and is shielded from the solvent by residues near 360. The introduction of the methyl and fluorine substituents in **5.24b** and **5.24f**, respectively, would result in close contacts to one edge of the indole, if the conformation seen in the **5.2c** complex were maintained (three contacts are predicted, of 2.5 Å and ~3.1 Å, in **5.24b** and **5.24f**, respectively). Instead, the flap moves, and the electron density in a three-residue region of the flap at and prior to Trp296 becomes poorly defined; the indole ring is moderately clear in only one of the four active sites (that of the 6f A-chain). Both **5.24b** and **5.24f** show better IC_{50s} than **5.2c**, however, while the other three *meta*-substitutes have slightly higher values (Table V.3).

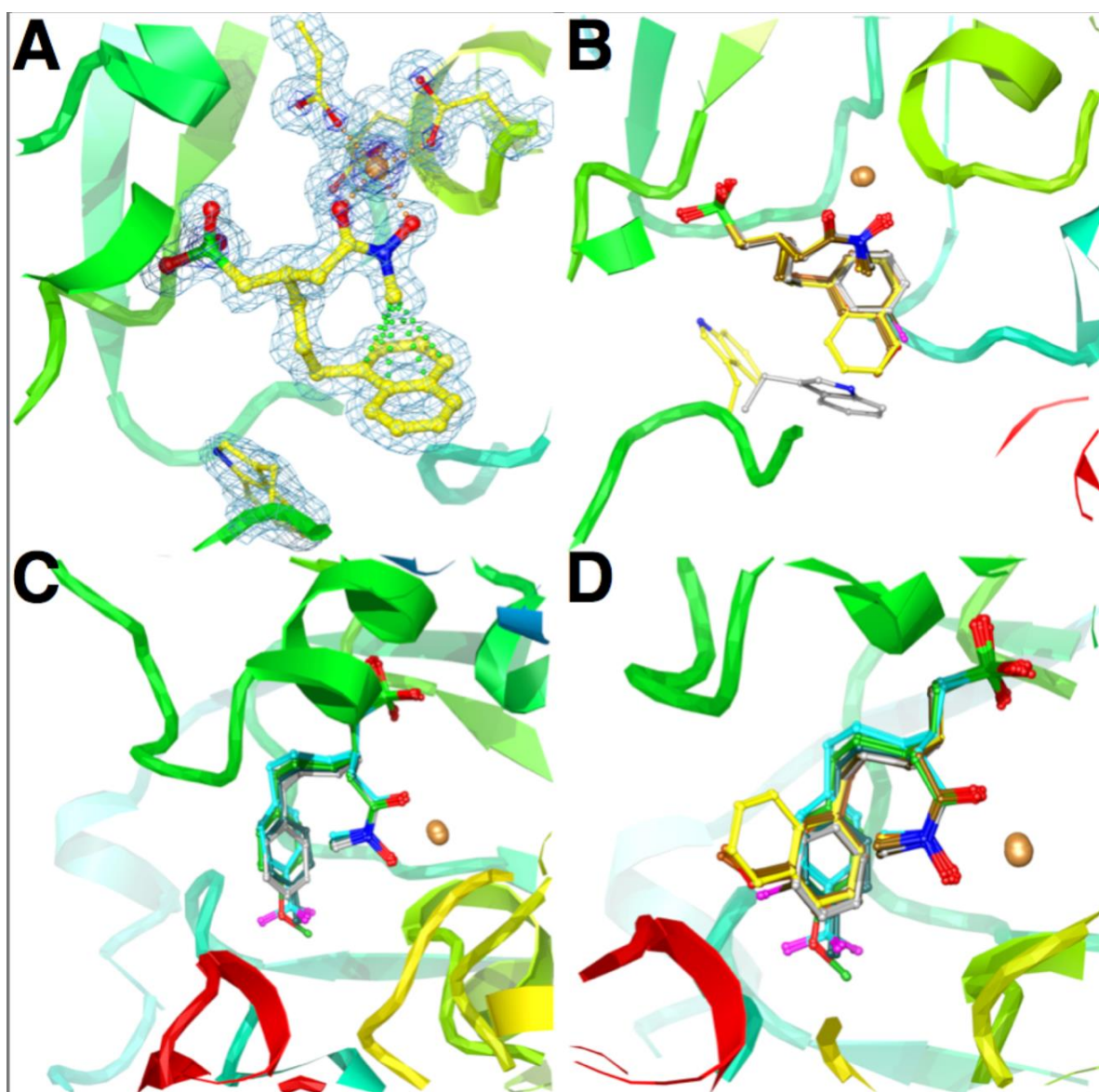


Figure V.9: X-ray structures of Dxr inhibitors. (A) Electron density for the inhibitor **5.24h** and selected nearby atoms, contoured at the rms value of the σ -weighted ($2m|F_o| - D|F_c|$) electron-density map¹⁸ ($0.39 \text{ e}/\text{\AA}^3$) in light blue, as well as at $2.5 \text{ e}/\text{\AA}^3$ (gold) to show the higher electron density near the metal ion. (B) Superimposed structures of the *meta*-class compounds, **5.24b** (light brown), **5.24d** (orange), **5.24f** (dark brown) and **5.24h** (yellow), on **5.2c** (dark gray). The well-defined flap residue, Trp296, of **5.24h** and **5.2c** is seen to undergo a conformational change. (C) Superimposed structures of the *para*-class compounds, **5.24a** (dark green), **5.24c** (light green) and **5.24g** (cyan), on **5.2d** (dark grey). Fluorine atoms are shown in magenta. (D) All the structures superimposed, using the same coloring scheme defined in panels B and C.

The lack of well-defined interactions between the best inhibitors and the indole ring of Trp296 suggests that the interactions with the indole that are observed in the **5.2c** complex are not the most important determinants of the observed IC₅₀s. We attribute this pattern to subtle changes in the intra-molecular interactions of the phenyl ring of each inhibitor with the methyl group of the hydroxamic acid. It is striking that the longer the substituent, the higher the IC₅₀ observed. We suggest that the most energetically favorable phenyl/methyl interaction, which presumably dominates in solution, depends on the size of the substituent. This conformation becomes harder to attain in the enzyme complexes, because it occurs in the context of other enzyme-inhibitor interactions.

The members of the *para*-group (**5.24a**, **5.24c**, **5.24g**) form a cluster of six independent structures (Figure V.9B). The interactions at the phosphonate and hydroxamic acid groups are essentially identical in all complexes, as is the conformation of the fosmidomycin backbone. While their phenyl rings are closely co-planar with that of the **5.2c** complex, the separate rings are not so tightly clustered and each is shifted to some degree within the binding site. The smallest shift is associated with the smallest substitution: ~0.5 Å for **5.24a**, ~0.7 Å for **5.24c** and ~1.0 Å for **5.24g**. This effect is achieved by small differences in the torsion angles of the bonds between the ring and the phosphonate group, which give the effect of splaying the methylene linker, while sliding the ring in the plane of the phenyl ring seen in **5.2c** (Figure V.9C). The important intra-ligand ring-methyl group interactions are, therefore, maintained in all complexes (Figure V.9D).

Again, the electron density in each complex is poorly defined in regions of the flap; the indole ring of Trp296 well defined in only three active sites. In these three complexes, Trp296 is similar to the **5.2c** complex, and the indole ring helps to shield the edge of the phenyl ring of the inhibitor. Two of the fluorine atoms in the **5.24g** substitution interact with a water molecule that is structurally highly conserved (although slightly displaced in the **5.24a** complex), while the oxygen atom in the methoxy-substituent of **5.24c** accepts a hydrogen bond from the main-chain amino nitrogen of residue 359. Overall, the *para*-substituted ligands are poorer inhibitors than their *meta*-equivalents (placing **5.24i** in the *para*-group, as the *para*-equivalent of **5.24h**). This is probably due to the translation of the relevant phenyl group from its energetically-preferred position in the **5.2c** complex, although

this is compensated for in part by interactions of **5.24g** and **5.24c** with structurally-conserved polar atoms

V.C.4. Conclusions

The introduction of substituents on the phenyl ring of **5.2c** that will reinforce interactions of analogues with the aromatic 'hot spot' that is clearly influential in the binding of **5.2c** shows to not be a trivial task. It tends out that the supposed interactions with the conserved tryptophan residue in this area do not account majorly for the outcome of the binding, and hence even when the interactions do happen, the fate of Dxr inhibition still lies in other factors (such as the active site stretching and the implications on the H-bonding interactions with the inhibitor), which should be systematically investigated. X-rays studies corroborate the adverse steric effects caused by the 1-naphthyl group in **5.24h**. All the prepared compounds **5.24a-j** failed to elicit similar potency as fosmidomycin or FR900098 as EcDxr, PfDxr and *P. falciparum* K1 strain growth inhibitors. Given that some analogues performed better than **5.2c** in inhibiting PfDxr (the 3-fluoro phenyl and the 3-methylphenyl), there remains a wealth of knowledge to be understood on details of active site interactions beyond the well described aromatic hotspot.

V.C.5. Experimental details

General Methods and Materials. See sections III.E. and V.B.6.

General Procedure I: Sonogashira coupling towards aralkynols 5.26a–j

To a solution of the aryl iodide (5.25a–j) in degassed triethylamine, was added $\text{PdCl}_2(\text{PPh}_3)_2$, CuI and but-3-yn-1-ol. The reaction mixture was refluxed at 117 °C for 3 h after which, it was cooled and concentrated *in vacuo*. Column chromatography using a Hex/EtOAc solvent system afforded compounds 5.26a–j.

General Procedure II: Triple bond reduction

To a solution of the alkyne 5.26a–j in MeOH, was added 10 % of Pd/C under a nitrogen atmosphere. Molecular hydrogen (H_2) was bubbled through the mixture for 30 minutes followed by filtration through a Whatman filter paper path. *In vacuo* concentration yielded compounds 5.27a–j which were used for the next step without further purification.

General Procedure III: Dess-Martin oxidation and concomitant Wittig olefination

A solution of the starting material (5.27a–j) in CH_2Cl_2 and a nitrogen atmosphere was cooled to 0 °C. Dess-Martin periodinane (2.0 equiv) was added and the mixture allowed to attain RT. After stirring for 3 h, TLC analysis showed a completed reaction. The reaction mixture was washed once with a 5:1 mixture of NaHCO_3 (sat. aq.) and $\text{Na}_2\text{S}_2\text{O}_3$ (aq. 2.0 M), and the water layer extracted three times with diethyl ether. The combined organic layer was washed successively with a 0.1 M solution of HCl and brine, dried over anhydrous Na_2SO_4 and concentrated *in vacuo* to obtain the corresponding aldehyde (5.28a–j) which was used without further purification. The aldehyde was dissolved in toluene under nitrogen atmosphere and *tert*-butyl (triphenylphosphoranylidene)acetate (3 equiv) was added. An overnight reflux at 120°C, was followed by cooling and *in vacuo* concentration. Sorption of the crude on celite and silica gel chromatography gave access to the *tert*-butyl esters 5.29a–j.

General procedure IV: Michael addition of methylphosphonatediesters to α,β -unsaturated *tert*-butyl esters.

To a solution of dibenzylmethyl phosphonate (2 eq.) in THF and under a nitrogen atmosphere was added *n*-BuLi (2 eq.) at -78 °C. After 30 minutes, a solution of the ester was added to the reaction mixture dropwise. Three hours later, the reaction showed to be complete by TLC and was quenched with NH₄Cl (sat. aq.). The water layer was extracted three times with EtOAc. Organic fractions were pooled, washed once with brine and dried over anhydrous Na₂SO₄. Column chromatography (EtOAc/Hex system) afforded the adducts **5.30a–j**.

General procedure V: Acidic cleavage of the *tert*-butyl ester and protected hydroxamate formation

A 0.1 M solution of the starting material (**5.30a–j**) in CH₂Cl₂/TFA (80:20), at 0 °C, was stirred for two hours, after which an excess of toluene was added to the reaction mixture and concentrated *in vacuo*. The crude acid was redissolved in CH₂Cl₂ (0.1 M), followed by addition of EDC (1.2 equiv), DMAP (1.2 equiv) and triethylamine (2.0 equiv). *O*-Benzyl-*N*-methylhydroxylamine TFA salt (1.2 equiv) was added as a 0.2 M solution in CH₂Cl₂, and the mixture stirred overnight at RT. The reaction was subsequently quenched with sat. aq. NaHCO₃, extracted three times with CH₂Cl₂, washed with brine and dried over Na₂SO₄. Column chromatography (CH₂Cl₂/MeOH system) produced the protected hydroxamic acids **5.31a–j**.

General procedure VI: Catalytic hydrogenolysis of benzyl protective groups

The benzyl protected compound **5.31a–j** (100-130 mg) was dissolved in MeOH (10 ml) under inert atmosphere and 10 % of Pd/C was added. The resulting mixture was then stirred under hydrogen atmosphere while monitoring the progress by mass spectroscopy. At completion (about 10 minutes), the reaction mixture was filtered and neutralized with NaOH (1 equiv). The reaction mixture was then concentrated *in vacuo*, re-dissolved in a 1:1 (v/v) mixture of water and *tert*-butanol, frozen and lyophilized to afford the desired targets compounds **5.24a–j** as monosodium phosphonic acid salts in quantitative yield.

Tert-butyl (E)-6-(p-tolyl)hex-2-enoate (5.29a). Prepared according to general procedure III. Purification 1:1 toluene/hexane v/v; yield 59%. ^1H NMR (300 MHz, CDCl_3) δ_{H} ppm 1.47 (br. s, 9H, *t*-Bu), 1.75 (app. quint. $J = 8.0$ Hz, 2H, $-\text{CH}_2-$), 2.12-2.23 (m, 2H, $-\text{CH}_2-$), 2.30 (s, 3H, Ph-CH_3), 2.58 (t, $J = 7.5$ Hz, 2H, $-\text{CH}_2-$), 5.74 (dt, $J = 1.5$ Hz, 15.6 Hz, 1H, $-\text{CH}=\underline{\text{CH}}\text{CO}$), 6.87 (dt $J = 7.1$ Hz, 15.6 Hz, 1H, $-\text{CH}=\text{CHCO}$), 7.00-7.16 (m, 4H, Ar-H). ^{13}C -NMR (75 MHz, CDCl_3) δ_{C} ppm 20.9, 28.1, 29.7, 31.4, 34.7, 79.9, 123.2, 128.2, 128.9, 135.2, 138.6, 147.5, 170.0. HRMS (ESI): calculated for $\text{C}_{17}\text{H}_{25}\text{O}_2$ [(M+H) $^+$], 261.1849; found 261.1856.

Tert-butyl (E)-6-(m-tolyl)hex-2-enoate (5.29b). Prepared according to general procedure III. Purification 1:1 toluene/hexane v/v; yield 51%. ^1H NMR (300 MHz, CDCl_3) δ_{H} ppm 1.44 (br. s, 9H, *t*-Bu), 1.76 (app. quint. $J = 7.7$ Hz, 2H, $-\text{CH}_2-$), 2.14-2.24 (m, 2H, $-\text{CH}_2-$), 2.32 (s, 3H, Ph-CH_3), 2.59 (t, $J = 7.7$ Hz, 2H, $-\text{CH}_2-$), 5.75 (dt, $J = 1.6$ Hz, 15.6 Hz, 1H, $-\text{CH}=\underline{\text{CH}}\text{CO}$), 6.87 (dt $J = 6.9$ Hz, 15.5 Hz, 1H, $-\text{CH}=\text{CHCO}$), 6.93-7.02 (m, 3H Ar-H), 7.12-7.20 (m, 1H, Ar-H). ^{13}C -NMR (75 MHz, CDCl_3) δ_{C} ppm 21.3, 28.1, 29.7, 31.5, 35.2, 80.0, 123.3, 125.4, 126.6, 128.2, 129.2, 137.8, 141.7, 147.5, 166.0. HRMS (ESI): calculated for $\text{C}_{17}\text{H}_{25}\text{O}_2$ [(M+H) $^+$], 261.1849; found 261.1852.

Tert-butyl (E)-6-(4-methoxyphenyl)hex-2-enoate (5.29c). Prepared according to general procedure III. Purification 1:1 toluene/hexane v/v; yield 64%. ^1H NMR (300 MHz, CDCl_3) δ_{H} ppm 1.47 (br. s, 9H, *t*-Bu), 1.73 (app. quint. $J = 7.7$ Hz, 2H, $-\text{CH}_2-$), 2.12-2.23 (m, 2H, $-\text{CH}_2-$), 2.32 (s, 3H, Ph-CH_3), 2.57 (t, $J = 7.4$ Hz, 2H, $-\text{CH}_2-$), 3.76 (s, 3H, PhOCH_3), 5.74 (dt, $J = 1.7$ Hz, 15.7 Hz, 1H, $-\text{CH}=\underline{\text{CH}}\text{CO}$), 6.82 (dt $J = 6.4$ Hz, 15.7 Hz, 1H, $-\text{CH}=\text{CHCO}$), 7.26-7.42 (m, 4H, Ar-H). ^{13}C -NMR (75 MHz, CDCl_3) δ_{C} ppm 28.1, 29.8, 31.3, 34.2, 55.1, 78.3, 113.7, 123.2, 129.2, 133.7, 147.5, 157.7, 166.0. HRMS (ESI): calculated for $\text{C}_{17}\text{H}_{25}\text{O}_3$ [(M+H) $^+$], 277.1798; found 277.1790.

Tert-butyl (E)-6-(3-methoxyphenyl)hex-2-enoate (5.29d). Prepared according to general procedure III. Purification 1:1 toluene/hexane v/v; yield 65%. ^1H NMR (300 MHz, CDCl_3) δ_{H} ppm 1.46 (br. s, 9H, *t*-Bu), 1.76 (app. quint. $J = 7.6$ Hz, 2H, $-\text{CH}_2-$), 2.16-2.24 (m, 2H, $-\text{CH}_2-$), 2.57 (t, $J = 7.6$ Hz, 2H, $-\text{CH}_2-$), 3.72 (s, 3H, PhOCH_3), 5.73 (dt, $J = 1.6$ Hz, 15.7 Hz, 1H, $-\text{CH}=\underline{\text{CH}}\text{CO}$), 6.87 (dt $J = 6.9$ Hz, 15.7 Hz, 1H, $-\text{CH}=\text{CHCO}$), 6.92-7.04 (m, 3H Ar-H), 7.12-7.21 (m, 1H, Ar-H). ^{13}C -NMR (75 MHz, CDCl_3) δ_{C} ppm 27.9, 28.1, 29.4, 31.5, 35.8, 80.0, 123.3, 125.4,

126.6, 128.2, 129.2, 137.8, 141.7, 146.8, 165.4. HRMS (ESI): calculated for C₁₇H₂₅O₃ [(M+H)⁺], 277.1798; found 277.1799.

Tert-butyl (E)-6-(4-fluorophenyl)hex-2-enoate (5.29e): Prepared according to general procedure III. Purification 1:1 toluene/hexane v/v; yield 53%. ¹H NMR (300 MHz, CDCl₃) δ_H ppm 1.47 (br. s, 9H, *t*-Bu), 1.66-1.82 (app. quint, *J* = 7.6 Hz, 2H, -CH₂-), 2.19 (m, 2H, -CH₂-), 2.60 (t, *J* = 7.4 Hz, 2H, -CH₂-), 5.75 (dt, *J* = 1.7 Hz, 15.80 Hz, 1H, -CH=CHCO), 6.80-7.00 (m, 3H, -CH=CHCO, Ar-H), 7.06-7.15 (m, 2H, Ar-H). ¹³C-NMR (75 MHz, CDCl₃) δ_C ppm 28.1, 29.8, 31.3, 34.4, 80.0, 115.0 (d, ²*J*_{C-F} = 20.9 Hz), 123.4, 129.7 (d, ³*J*_{C-F} = 8.8 Hz), 137.3 (d, ⁴*J*_{C-F} = 3.6 Hz), 147.2, 161.3 (d, ¹*J*_{C-F} = 242.9 Hz), 166.0. HRMS (ESI): calculated for C₁₆H₂₂FO₂ [(M+H)⁺], 265.1598; found 265.1597.

Tert-butyl (E)-6-(3-fluorophenyl)hex-2-enoate (5.29f): Prepared according to general procedure III. Purification 1:1 toluene/hexane v/v; yield 49%. ¹H NMR (300 MHz, CDCl₃) δ_H ppm 1.48 (br. s, 9H, *t*-Bu), 1.78 (app. quint. *J* = 8.0 Hz, 2H, -CH₂-), 2.15-2.25 (m, 2H, -CH₂-), 2.63 (t, *J* = 7.7 Hz, 2H, -CH₂-), 5.75 (dt, *J* = 1.7 Hz, 15.6 Hz, 1H, -CH=CHCO), 6.79-6.97 (m, 4H, -CH=CHCO, Ar-H), 7.18-7.27 (m, 1H, Ar-H). ¹³C-NMR (75 MHz, CDCl₃) δ_C ppm 28.1, 29.4, 31.3, 34.9 (d, ⁴*J*_{C-F} = 1.8 Hz), 80.1, 112.7, 115.2 (d, ²*J*_{C-F} = 21.1 Hz), 123.5, 124.0 (d, ⁴*J*_{C-F} = 2.8 Hz), 129.7 (d, ³*J*_{C-F} = 8.2 Hz), 144.3 (d, ³*J*_{C-F} = 7.1 Hz), 147.1, 162.8 (d, ²*J*_{C-F} = 245.5 Hz), 166.0. HRMS (ESI): calculated for C₁₆H₂₂FO₂ [(M+H)⁺], 265.1598; found 265.1599.

Tert-butyl (E)-6-(4-(trifluoromethyl)phenyl)hex-2-enoate (5.29g). Prepared according to general procedure III. Purification 1:1 toluene/hexane v/v; yield 60%. ¹H NMR (300 MHz, CDCl₃) δ_H ppm 1.48 (br. s, 9H, *t*-Bu), 1.80 (app. quint. *J* = 7.5 Hz, 2H, -CH₂-), 2.21 (m, 2H, -CH₂-), 2.69 (t, *J* = 7.8 Hz, -CH₂-), 5.76 (dt, *J* = 1.8 Hz, 15.6 Hz, 1H, -CH=CHCO), 6.86 (dt, *J* = 6.8 Hz, 15.6 Hz, 1H, -CH=CHCO), 7.28 (d, *J* = 9.0 Hz, 2H, Ar-H), 7.54 (d, *J* = 8.5 Hz, 2H, Ar-H). ¹³C-NMR (75 MHz, CDCl₃) δ_C ppm 28.1, 29.4, 31.3, 35.0, 80.1, 123.6, 124.3 (quart., ¹*J*_{C-F} = 271.9 Hz), 125.3 (quart., ³*J*_{C-F} = 7.2 Hz), 128.3 (quart., ²*J*_{C-F} = 32.5 Hz), 128.7, 145.9, 146.9, 165.9. HRMS (ESI): calculated for C₁₇H₂₂F₃O₂ [(M+H)⁺], 315.1566; found 315.1570.

Tert-butyl (E)-6-(naphthalen-1-yl)hex-2-enoate (5.29h). Prepared according to general procedure III. Purification 1:1 toluene/hexane v/v; yield 67%. ¹H NMR (300 MHz, CDCl₃) δ_H ppm 1.47 (br. s, 9H, *t*-Bu), 1.90 (app. quint. *J* = 7.6 Hz, 2H, -CH₂-), 2.21-2.31 (m, 2H, -CH₂-), 3.08 (t, *J* = 7.6 Hz, -CH₂-), 5.78 (dt, *J* = 1.5 Hz, 15.6 Hz, 1H, -CH=CHCO), 6.91 (dt, *J* = 6.9 Hz,

15.6 Hz, 1H, -CH=CHCO), 7.26-7.53 (m, 4H, Ar-H), 7.70 (d, $J = 8.4$ Hz, 1H, Ar-H), 7.80-8.00 (m, 2H, Ar-H). $^{13}\text{C-NMR}$ (75 MHz, CDCl_3) δ_{C} ppm 28.1, 28.9, 31.8, 32.4, 80.0, 123.4, 123.6, 125.4, 125.5, 125.7, 126.0, 126.7, 128.7, 131.7, 133.9, 137.8, 147.3, 166.0. HRMS (ESI): calculated for $\text{C}_{20}\text{H}_{25}\text{O}_2$ [(M+H) $^+$], 297.1849, found 297.1854.

Tert-butyl (E)-6-(naphthalen-2-yl)hex-2-enoate (5.29i). Prepared according to general procedure III. Purification 1:1 toluene/hexane v/v; yield 67%. $^1\text{H NMR}$ (300 MHz, CDCl_3) δ_{H} ppm 1.48 (br. s, 9H, *t*-Bu), 1.84 (app. quint. $J = 8.1$ Hz, 2H, -CH $_2$ -), 2.21 (m, 2H, -CH $_2$ -), 2.77 (t, $J = 7.7$ Hz, -CH $_2$ -), 5.76 (dt, $J = 1.6$ Hz, 15.2 Hz, 1H, -CH=CHCO), 6.89 (dt, $J = 7.3$ Hz, 15.8 Hz, 1H, -CH=CHCO), 7.29 (dd, $J = 1.8$ Hz, 8.4 Hz, 1H, Ar-H), 7.36-7.47 (m, 2H, Ar-H), 7.58 (s, 1H, Ar-H), 7.71-7.81 (m, 2H, Ar-H). $^{13}\text{C-NMR}$ (75 MHz, CDCl_3) δ_{C} ppm 28.1, 29.5, 31.4, 35.3, 80.0, 123.3, 125.1, 125.8, 126.4, 127.1, 127.3, 127.5, 127.9, 132.0, 133.5, 139.2, 147.4, 166.0. HRMS (ESI): calculated for $\text{C}_{20}\text{H}_{25}\text{O}_2$ [(M+H) $^+$], 297.1849; found 297.1852.

Tert-butyl (E)-6-([1,1'-biphenyl]-4-yl)hex-2-enoate (5.29j). Prepared according to general procedure III. Purification 1:1 toluene/hexane v/v; yield 61%. $^1\text{H NMR}$ (300 MHz, CDCl_3) δ_{H} ppm 1.48 (br. s, 9H, *t*-Bu), 1.84 (app. quint. $J = 7.5$ Hz, 2H, -CH $_2$ -), 2.21-2.35 (m, 2H, -CH $_2$ -), 2.65 (t, $J = 7.8$ Hz, -CH $_2$ -), 5.75 (dt, $J = 1.7$ Hz, 15.7 Hz, 1H, -CH=CHCO), 6.90 (dt, $J = 6.8$ Hz, 15.7 Hz, 1H, -CH=CHCO), 7.22 (d, $J = 8.5$ Hz, 2H, Ar-H), 7.27-7.67 (m, 7H, Ar-H). $^{13}\text{C-NMR}$ (75 MHz, CDCl_3) δ_{C} ppm 28.1, 29.6, 31.4, 34.8, 80.0, 123.4, 126.9, 127.0, 127.1, 128.7, 128.8, 138.8, 140.8, 141.0, 147.4, 166.0. HRMS (ESI): calculated for $\text{C}_{22}\text{H}_{27}\text{O}_2$ [(M+H) $^+$], 323.2006, mass not found.

*Tert-butyl 3-((bis(benzyloxy)phosphoryl)methyl)-6-(*p*-tolyl)hexanoate (5.30a)*. Prepared according to general procedure IV. Purification 2:1 hexane/ethyl acetate v/v; yield 54%. $^1\text{H NMR}$ (300 MHz, CDCl_3) δ_{H} ppm 1.38 (br. s, 9H, *t*-Bu), 1.42-1.62 (m, 4H, -CH $_2$ -), 1.76-1.95 (m, 2H, -CH $_2$ -), 2.19-2.32 (m, 5H, Ph-CH $_3$, -CH $_2$ -), 2.35-2.54 (m, 3H, -CH $_2$ -, -CH-), 4.87-5.08 (m, 4H, -CH $_2$ -Ph), 6.97-7.08 (m, 4H, Ar-H), 7.28-7.35 (m, 10H, Ar-H). $^{13}\text{C-NMR}$ (75 MHz, CDCl_3) δ_{C} ppm 21.2, 28.3, 28.7, 30.1 (d, $^1J_{\text{C-P}} = 138.6$ Hz), 30.6 (d, $^2J_{\text{C-P}} = 4.1$ Hz), 31.1, 34.5 (d, $^3J_{\text{C-P}} = 10.1$ Hz), 35.6, 40.5 (d, $^3J_{\text{C-P}} = 9.3$ Hz), 66.9 (d, $^2J_{\text{C-P}} = 6.6$ Hz), 67.0 (d, $^2J_{\text{C-P}} = 6.6$ Hz), 80.2, 127.9, 127.9, 128.2, 128.3, 128.5, 128.9, 135.0, 136.4 (d, $^3J_{\text{C-P}} = 6.2$ Hz), 136.4 (d, $^3J_{\text{C-P}} = 6.0$ Hz), 139.1, 171.6. $^{31}\text{P-NMR}$ (121.5 MHz, CDCl_3): δ_{P} ppm = 33.29. HRMS (ESI): calculated for $\text{C}_{32}\text{H}_{42}\text{O}_5\text{P}$ [(M+H) $^+$], 537.2764; found 537.2778.

Tert-butyl 3-((bis(benzyloxy)phosphoryl)methyl)-6-(m-tolyl)hexanoate (5.30b). Prepared according to general procedure IV. Purification 2:1 hexane/ethyl acetate v/v; yield 45%. ^1H NMR (300 MHz, CDCl_3) δ_{H} ppm 1.39 (br. s, 9H, *t*-Bu), 1.42-1.63 (m, 4H, $-\text{CH}_2-$), 1.78-1.98 (m, 2H, $-\text{CH}_2-$), 2.17-2.34 (m, 5H, $\text{Ph}-\underline{\text{CH}}_3$, $-\text{CH}_2-$), 2.35-2.54 (m, 3H, $-\text{CH}-$, $-\text{CH}_2-$), 4.88-5.08 (m, 4H, $-\text{CH}_2-\text{Ph}$), 6.88-7.00 (m, 3H, Ar-H), 7.14 (t, $J = 7.7$ Hz, 1H, Ar-H), 7.28-7.37 (m, 10H, Ar-H). ^{13}C -NMR (75 MHz, CDCl_3) δ_{C} ppm 21.6, 28.3, 28.6, 30.1 (d, $^1J_{\text{C-P}} = 138.6$ Hz), 30.6 (d, $^2J_{\text{C-P}} = 3.9$ Hz), 34.6 (d, $^3J_{\text{C-P}} = 10.3$ Hz), 36.1, 40.5 (d, $^3J_{\text{C-P}} = 10.3$ Hz), 67.3 (d, $^2J_{\text{C-P}} = 6.2$ Hz), 80.6, 125.6, 126.7, 128.2, 128.4, 128.6, 128.8, 128.4, 136.7 (d, $^3J_{\text{C-P}} = 7.1$ Hz), 138.0, 142.5, 171.9. ^{31}P -NMR (121.5 MHz, CDCl_3): δ_{P} ppm = 33.29. HRMS (ESI): calculated for $\text{C}_{32}\text{H}_{42}\text{O}_5\text{P}$ [(M+H) $^+$], 537.2764; found 537.2786.

Tert-butyl 3-((bis(benzyloxy)phosphoryl)methyl)-6-(4-methoxyphenyl)hexanoate (5.30c). Prepared according to general procedure IV. Purification 2:1 hexane/ethyl acetate v/v; yield 53%. ^1H NMR (300 MHz, CDCl_3) δ_{H} ppm 1.39 (br. s, 9H, *t*-Bu), 1.43-1.97 (m, 6H, $-\text{CH}_2-$), 2.17-2.52 (m, 5H, $-\text{CH}_2-$, $-\text{CH}-$), 3.77 (s, 3H, PhOCH_3), 4.88-5.10 (m, 4H, $-\text{CH}_2-\text{Ph}$), 6.79 (d, $J = 9.1$ Hz, 2H, Ar-H), 7.02 (d, $J = 9.1$ Hz, 2H, Ar-H), 7.26-7.44 (m, 10H, Ar-H). ^{13}C -NMR (75 MHz, CDCl_3) δ_{C} ppm 28.0, 28.5, 29.8 (d, $^1J_{\text{C-P}} = 138.5$ Hz), 30.3 (d, $^2J_{\text{C-P}} = 3.9$ Hz), 34.2 (d, $^3J_{\text{C-P}} = 10.7$ Hz), 34.9, 40.2 (d, $^3J_{\text{C-P}} = 9.9$ Hz), 55.2, 67.0 (d, $^2J_{\text{C-P}} = 6.1$ Hz), 67.0 (d, $^2J_{\text{C-P}} = 6.7$ Hz), 80.3, 113.7, 127.9, 128.3, 128.5, 129.2, 134.3, 136.4 (d, $^3J_{\text{C-P}} = 5.3$ Hz), 136.4 (d, $^3J_{\text{C-P}} = 5.9$ Hz), 157.7, 171.6. ^{31}P -NMR (121.5 MHz, CDCl_3): 32.18. HRMS (ESI): calculated for $\text{C}_{32}\text{H}_{42}\text{O}_6\text{P}$ [(M+H) $^+$], 553.2714; found 553.2717.

Tert-butyl 3-((bis(benzyloxy)phosphoryl)methyl)-6-(3-methoxyphenyl)hexanoate (5.30d). Prepared according to general procedure IV. Purification 2:1 hexane/ethyl acetate v/v; yield 47%. ^1H NMR (300 MHz, CDCl_3) δ_{H} ppm 1.39 (br. s, 9H, *t*-Bu), 1.42-1.63 (m, 4H, $-\text{CH}_2-$), 1.76-1.93 (m, 2H, $-\text{CH}_2-$), 2.19-2.54 (m, 5H, $-\text{CH}_2-$, $-\text{CH}-$), 3.76 (s, 3H, PhOCH_3), 4.87-5.08 (m, 4H, $-\text{CH}_2-\text{Ph}$), 6.65-6.74 (m, 3H, Ar-H), 7.16 (t, $J = 8.1$ Hz, 1H, Ar-H), 7.28-7.36 (m, 10H, Ar-H). ^{13}C -NMR (75 MHz, CDCl_3) δ_{C} ppm 28.3, 28.5, 30.2 (d, $^1J_{\text{C-P}} = 139.8$ Hz), 30.6 (d, $^2J_{\text{C-P}} = 4.1$ Hz), 34.5 (d, $^3J_{\text{C-P}} = 11.0$ Hz), 36.1, 40.4 (d, $^3J_{\text{C-P}} = 9.4$ Hz), 55.3, 67.2 (d, $^2J_{\text{C-P}} = 4.1$ Hz), 67.3 (d, $^2J_{\text{C-P}} = 4.3$ Hz), 80.6, 111.2, 114.4, 121.0, 128.2, 128.6, 128.8, 129.5, 136.6 (d, $^3J_{\text{C-P}} = 1.5$ Hz), 136.7 (d, $^3J_{\text{C-P}} = 6.0$ Hz), 136.7 (d, $^3J_{\text{C-P}} = 6.0$ Hz), 144.1, 159.8, 171.9. ^{31}P -NMR (121.5 MHz, CDCl_3): δ_{P} ppm = 33.24. HRMS (ESI): calculated for $\text{C}_{32}\text{H}_{42}\text{O}_6\text{P}$ [(M+H) $^+$], 553.2714; found 553.2717.

Tert-butyl 3-((bis(benzyloxy)phosphoryl)methyl)-6-(4-fluorophenyl)hexanoate (5.30e).

Prepared according to general procedure IV. Purification 2:1 hexane/ethyl acetate v/v; yield 43%. ^1H NMR (300 MHz, CDCl_3) δ_{H} ppm 1.38 (br. s, 9H, *t*-Bu), 1.42-1.61 (m, 4H, $-\text{CH}_2-$), 1.76-1.96 (m, 2H, $-\text{CH}_2-$), 2.16-2.34 (m, 2H, $-\text{CH}_2-$), 2.18-2.52 (m, 3H, $-\text{CH}_2-$, $-\text{CH}-$), 4.89-5.08 (m, 4H, $-\text{CH}_2-\text{Ph}$), 6.78-6.96 (m, 2H, Ar-H), 7.03 (m, 2H, Ar-H), 7.28-7.37 (m, 10H, Ar-H). ^{13}C -NMR (75 MHz, CDCl_3) δ_{C} ppm 28.0, 28.4, 29.9 (d, $^1J_{\text{C-P}} = 138.9$ Hz), 30.3 (d, $^2J_{\text{C-P}} = 3.9$ Hz), 34.1 (d, $^3J_{\text{C-P}} = 10.2$ Hz), 34.9, 40.2, (d, $^3J_{\text{C-P}} = 10.2$ Hz), 67.0 (m), 80.3, 114.9 (d, $^2J_{\text{C-F}} = 20.4$ Hz), 127.9, 128.3, 128.5, 129.6 (d, $^3J_{\text{C-F}} = 7.7$ Hz), 136.4 (d, $^3J_{\text{C-P}} = 6.3$ Hz), 137.8 (d, $^4J_{\text{C-F}} = 3.3$ Hz), 161.1 (d, $^1J_{\text{C-F}} = 243.0$ Hz), 171.6. ^{31}P -NMR (121.5 MHz, CDCl_3): δ_{P} ppm = 33.00. HRMS (ESI): calculated for $\text{C}_{31}\text{H}_{39}\text{FO}_5\text{P}$ [(M+H) $^+$], 541.2514; found 541.2519.

Tert-butyl 3-((bis(benzyloxy)phosphoryl)methyl)-6-(3-fluorophenyl)hexanoate (5.30f).

Prepared according to general procedure IV. Purification 2:1 hexane/ethyl acetate v/v; yield 47%. ^1H NMR (300 MHz, CDCl_3) δ_{H} ppm 1.33-1.40 (br. s, 9H, *t*-Bu), 1.41-1.61 (m, 4H, $-\text{CH}_2-$), 1.72-1.97 (m, 2H, $-\text{CH}_2-$), 2.18-2.33 (2H, m, $-\text{CH}_2-$), 2.36-2.55 (m, 3H, $-\text{CH}_2-$, $-\text{CH}-$), 4.89-5.08 (m, 4H, $-\text{CH}_2-\text{Ph}$), 6.76-6.90 (m, 3H, Ar-H), 7.19 (td, 1H, $J = 6.08$ Hz, 13.96 Hz, Ar-H), 7.29-7.39 (m, 10H, Ar-H). ^{13}C -NMR (75 MHz, CDCl_3) δ_{C} ppm 28.2, 28.3, 30.2 (d, $^1J_{\text{C-P}} = 139.9$ Hz), 30.5 (d, $^2J_{\text{C-P}} = 4.9$ Hz), 34.4 (d, $^3J_{\text{C-P}} = 10.8$ Hz), 35.7, 40.5 (d, $^3J_{\text{C-P}} = 9.8$ Hz), 66.9 (d, $^2J_{\text{C-P}} = 6.6$ Hz), 67.0 (d, $^2J_{\text{C-P}} = 6.4$ Hz), 80.6, 112.8 (d, $^2J_{\text{C-F}} = 21.0$ Hz), 115.4 (d, $^2J_{\text{C-F}} = 20.7$ Hz), 124.2 (d, $^4J_{\text{C-F}} = 3.1$ Hz), 128.2, 128.6, 128.8, 129.9 (d, $^3J_{\text{C-F}} = 8.3$ Hz), 136.3 (d, $^3J_{\text{C-P}} = 6.3$ Hz), 136.4 (d, $^3J_{\text{C-P}} = 6.4$ Hz), 145.1 (d, $^3J_{\text{C-F}} = 7.3$ Hz), 162.8 (d, $^1J_{\text{C-F}} = 246.5$ Hz), 171.8. ^{31}P -NMR (121.5 MHz, CDCl_3): δ_{P} ppm = 33.16. HRMS (ESI): calculated for $\text{C}_{31}\text{H}_{39}\text{FO}_5\text{P}$ [(M+H) $^+$], 541.2514; found 541.2515.

Tert-butyl 3-((bis(benzyloxy)phosphoryl)methyl)-6-(4-(trifluoromethyl)phenyl)hexanoate (5.30g).

Prepared according to general procedure IV. Purification 2:1 hexane/ethyl acetate v/v; yield 62%. ^1H NMR (300 MHz, CDCl_3) δ_{H} ppm 1.37 (br. s, 9H, *t*-Bu), 1.41-1.64 (m, 4H, $-\text{CH}_2-$), 1.72-1.96 (m, 2H, $-\text{CH}_2-$), 2.18-2.61 (m, 5H, $-\text{CH}_2-$, $-\text{CH}-$), 4.90-5.09 (m, 4H, $-\text{CH}_2-\text{Ph}$), 7.19 (d, $J = 8.0$ Hz, 2H, Ar-H), 7.28-7.36 (m, 10H, Ar-H), 7.49 (d, $J = 8.0$ Hz, 2H, Ar-H). ^{13}C -NMR (75 MHz, CDCl_3) δ_{C} ppm 28.3, 28.4, 30.2 (d, $^1J_{\text{C-P}} = 138.2$ Hz), 30.6 (d, $^2J_{\text{C-P}} = 5.4$ Hz), 34.4 (d, $^3J_{\text{C-P}} = 10.8$ Hz), 35.9, 40.6 (d, $^3J_{\text{C-P}} = 9.2$ Hz), 67.4 (d, $^2J_{\text{C-P}} = 6.7$ Hz), 67.5 (d, $^2J_{\text{C-P}} = 6.6$ Hz), 80.8, 124.6 (quart., $^1J_{\text{C-F}} = 271.5$ Hz), 125.5 (quart., $^3J_{\text{C-F}} = 3.8$ Hz), 128.3, 128.5 (quart., $^2J_{\text{C-F}} = 27.1$ Hz), 128.7, 128.9, 129.0, 136.7 (d, $^3J_{\text{C-P}} = 6.0$ Hz), 146.7, 171.9. ^{31}P -NMR (121.5 MHz, CDCl_3): δ_{P} ppm = 31.86. HRMS (ESI): calculated for $\text{C}_{32}\text{H}_{39}\text{F}_3\text{O}_5\text{P}$ [(M+H) $^+$], 591.2482; found 591.2487.

Tert-butyl 3-((bis(benzyloxy)phosphoryl)methyl)-6-(naphthalen-1-yl)hexanoate (5.30h).

Prepared according to general procedure IV. Purification 2:1 hexane/ethyl acetate v/v; yield 55%. ¹H NMR (300 MHz, CDCl₃) δ_H ppm 1.37 (br. s, 9H, *t*-Bu), 1.45-1.75 (m, 4H, -CH₂-), 1.77-1.94 (m, 2H, -CH₂-), 2.20-2.49 (m, 3H, -CH₂-, -CH-), 2.98 (t, *J* = 7.1 Hz, 2H, -CH₂-), 4.86-5.09 (m, 4H, -CH₂-Ph), 7.21-7.39 (m, 12H, Ar-H), 7.41-7.51 (m, 2H, Ar-H), 7.68 (d, *J* = 8.4 Hz, 1H, Ar-H), 7.80-7.86 (m, 1H, Ar-H), 7.93-7.99 (m, 1H, Ar-H). ¹³C-NMR (75 MHz, CDCl₃) δ_C ppm 27.8, 28.2, 30.1 (d, ¹*J*_{C-P} = 138.8 Hz), 30.5 (d, ²*J*_{C-P} = 4.5 Hz), 33.1, 34.8 (d, ³*J*_{C-P} = 10.9 Hz), 40.3 (d, ³*J*_{C-P} = 10.0 Hz), 66.9 (d, ²*J*_{C-P} = 6.7 Hz), 7.2 (d, ²*J*_{C-P} = 6.4 Hz), 80.5, 123.9, 125.5, 125.6, 125.84, 126.0, 126.7, 128.1, 128.5, 128.7, 128.9, 131.9, 134.0, 135.3 (d, ³*J*_{C-P} = 6.4 Hz), 135.7 (d, ³*J*_{C-P} = 6.1 Hz), 138.5, 171.7. ³¹P-NMR (121.5 MHz, CDCl₃): δ_P ppm = 33.23. HRMS (ESI): calculated for C₃₅H₄₂O₅P [(M+H)⁺], 573.2764; found 573.2761.

Tert-butyl 3-((bis(benzyloxy)phosphoryl)methyl)-6-(naphthalen-2-yl)hexanoate (5.30i).

Prepared according to general procedure IV. Purification 2:1 hexane/ethyl acetate v/v; yield 49%. ¹H NMR (300 MHz, CDCl₃) δ_H ppm 1.39 (br. s, 9H, *t*-Bu), 1.44-1.96 (m, 6H, -CH₂-), 2.21-2.53 (m, 3H, -CH₂-, -CH-), 2.71 (t, *J* = 7.2 Hz, 2H, -CH₂-), 4.91-5.10 (m, 4H, -CH₂-Ph), 7.25-7.49 (m, 13H, Ar-H), 7.56 (s, 1H, Ar-H), 7.73-7.83 (m, 3H, Ar-H). ¹³C-NMR (75 MHz, CDCl₃) δ_C ppm 28.0, 28.1, 29.9 (d, ¹*J*_{C-P} = 139.1 Hz), 30.3 (d, ²*J*_{C-P} = 4.5 Hz), 34.2 (d, ³*J*_{C-P} = 10.5 Hz), 35.9, 40.2 (d, ³*J*_{C-P} = 9.8 Hz), 66.9 (d, ²*J*_{C-P} = 5.8 Hz), 67.00 (d, ²*J*_{C-P} = 6.9 Hz), 80.3, 125.0, 125.8, 126.3, 127.2, 127.3, 127.5, 127.8, 127.9, 128.3, 128.5, 131.9, 133.5, 136.4 (d, ²*J*_{C-P} = 6.2 Hz), 139.7, 171.6. ³¹P-NMR (121.5 MHz, CDCl₃): δ_P ppm = 32.13. HRMS (ESI): calculated for C₃₅H₄₂O₅P [(M+H)⁺], 573.2764; found 573.2772.

Tert-butyl 6-([1,1'-biphenyl]-4-yl)-3-((bis(benzyloxy)phosphoryl)methyl)hexanoate (5.30j).

Prepared according to general procedure IV. Purification 2:1 hexane/ethyl acetate v/v; yield 71%. ¹H NMR (300 MHz, CDCl₃) δ_H ppm 1.38 (br. s, 9H, *t*-Bu), 1.42-1.99 (m, 6H, -CH₂-), 2.20-2.63 (m, 5H, -CH₂-, -CH-), 4.88-5.09 (m, 4H, -CH₂-Ph), 7.17 (d, *J* = 8.2 Hz, 2H, Ar-H), 7.25-7.60 (m, 17H, Ar-H). ¹³C-NMR (75 MHz, CDCl₃) δ_C ppm 28.0, 28.2, 29.9 (d, ¹*J*_{C-P} = 138.5 Hz), 30.3 (d, ²*J*_{C-P} = 3.9 Hz), 34.2 (d, ³*J*_{C-P} = 10.9 Hz), 35.4, 40.2 (d, ³*J*_{C-P} = 9.3 Hz), 67.0 (d, ²*J*_{C-P} = 6.6 Hz), 67.1 (d, ²*J*_{C-P} = 6.4 Hz), 80.3, 126.9, 127.0, 127.9, 128.0, 128.3, 128.5, 128.6, 128.7, 136.3 (d, ³*J*_{C-P} = 6.1 Hz), 136.4 (d, ³*J*_{C-P} = 6.1 Hz), 138.6, 141.0, 141.3, 171.6. ³¹P-NMR (121.5 MHz, CDCl₃): δ_P ppm = 31.83. HRMS (ESI): calculated for C₃₇H₄₄O₅P [(M+H)⁺], 599.2921; found 599.2928.

Dibenzyl (2-(2-((benzyloxy)(methyl)amino)-2-oxoethyl)-5-(p-tolyl)pentyl)phosphonate (5.31a). Prepared according to general procedure V. Purification 3:1 hexane/acetone v/v; yield 71%. ^1H NMR (300 MHz, CDCl_3) δ_{H} ppm 1.34-1.58 (m, 4H, $-\text{CH}_2-$), 1.72-2.05 (m, 3H, $-\text{CH}_2-$, $-\text{CH}-$), 2.30 (s, 3H, $\text{Ph}-\text{CH}_3$), 2.37-2.65 (m, 4H, $-\text{CH}_2-$), 3.13 (s, 3H, $\text{N}-\text{CH}_3$), 4.72 (s, 2H, NOCH_2Ph), 4.86-5.06 (m, 4H, $-\text{POCH}_2\text{Ph}$), 6.98 (d, $J = 8.1$ Hz, 2H, Ar-H), 7.05 (d, $J = 8.1$ Hz, 2H, Ar-H), 7.28-7.36 (m, 15H, Ar-H). ^{13}C -NMR (75 MHz, CDCl_3) δ_{C} ppm 19.2, 21.0, 28.7, 29.6 (d, $^1J_{\text{C-P}} = 139.3$ Hz), 29.6 (d, $^2J_{\text{C-P}} = 5.1$ Hz), 33.5, 34.6 (d, $^3J_{\text{C-P}} = 10.2$ Hz), 35.4, 36.6 (d, $^3J_{\text{C-P}} = 9.2$ Hz), 67.1 (d, $^2J_{\text{C-P}} = 6.3$ Hz), 67.5 (d, $^2J_{\text{C-P}} = 6.1$ Hz), 76.1, 127.9, 127.9, 128.2, 128.3, 128.5, 128.6, 128.9, 128.9, 129.3, 134.5, 135.0, 136.5(m), 139.3, 173.8. ^{31}P -NMR (121.5 MHz, CDCl_3): δ_{P} ppm = 33.55. HRMS (ESI): calculated for $\text{C}_{36}\text{H}_{43}\text{NO}_5\text{P}$ [(M+H) $^+$], 600.2873; found 600.2903.

Dibenzyl (2-(2-((benzyloxy)(methyl)amino)-2-oxoethyl)-5-(m-tolyl)pentyl)phosphonate (5.31b). Prepared according to general procedure V. Purification 98:2 dichloromethane/methanol v/v; yield 72%. ^1H NMR (300 MHz, CDCl_3) δ_{H} ppm 1.37-1.59 (m, 4H, $-\text{CH}_2-$), 1.74-2.04 (m, 2H, $-\text{CH}_2-$), 2.30 (s, 3H, $\text{Ph}-\text{CH}_3$), 2.37-2.65 (m, 5H, $-\text{CH}_2-$, $-\text{CH}-$), 3.12 (s, 3H, $\text{N}-\text{CH}_3$), 4.72 (s, 2H, NOCH_2Ph), 4.89-5.05 (m, 4H, $-\text{POCH}_2\text{Ph}$), 6.86-7.00 (m, 3H, Ar-H), 7.13 (t, $J = 7.4$ Hz, 1H, Ar-H), 7.27-7.36 (m, 15H, Ar-H). ^{13}C -NMR (75 MHz, CDCl_3) δ_{C} ppm 21.3, 28.5, 28.6, 28.6 (d, $^3J_{\text{C-P}} = 8.8$ Hz), 29.5 (d, $^1J_{\text{C-P}} = 138.8$ Hz), 29.6 (d, $^2J_{\text{C-P}} = 4.9$ Hz), 34.6 (d, $^3J_{\text{C-P}} = 10.8$ Hz), 35.7, 66.9 (m), 76.0, 125.3, 126.3, 127.8, 128.1, 128.2, 128.5, 128.6, 128.8, 129.1, 129.2, 136.4 (m), 137.6, 142.3, 171.9. ^{31}P -NMR (121.5 MHz, CDCl_3): δ_{P} ppm = 33.54. HRMS (ESI): calculated for $\text{C}_{36}\text{H}_{43}\text{NO}_5\text{P}$ [(M+H) $^+$], 600.2873; found 600.2883.

Dibenzyl (2-(2-((benzyloxy)(methyl)amino)-2-oxoethyl)-5-(4-methoxyphenyl)pentyl)phosphonate (5.31c). Prepared according to general procedure V. Purification 3:1 hexane/acetone v/v; yield 57%. ^1H NMR (300 MHz, CDCl_3) δ_{H} ppm 1.34-1.59 (m, 4H, $-\text{CH}_2-$), 1.73-2.04 (m, 2H, $-\text{CH}_2-$), 2.26-2.65 (m, 5H, $-\text{CH}_2-$, $-\text{CH}-$), 3.13 (s, 3H, $\text{N}-\text{CH}_3$), 3.75 (s, 3H, PhOCH_3), 4.72 (s, 2H, $-\text{NOCH}_2\text{Ph}$), 4.88-5.07 (m, 4H, $-\text{POCH}_2\text{Ph}$), 6.78 (d, $J = 9.6$ Hz, 2H, Ar-H), 7.00 (d, $J = 9.6$ Hz, 2H, Ar-H), 7.27-7.39 (m, 15H, Ar-H). ^{13}C -NMR (75 MHz, CDCl_3) δ_{C} ppm 29.1, 29.9 (d, $^2J_{\text{C-P}} = 4.3$ Hz), 30.0, 30.1 (d, $^1J_{\text{C-P}} = 136.9$ Hz), 34.8 (d, $^3J_{\text{C-P}} = 9.8$ Hz), 35.1, 36.9 (d, $^3J_{\text{C-P}} = 9.2$ Hz), 55.5, 67.2 (d, $^2J_{\text{C-P}} = 6.7$ Hz), 67.3 (d, $^2J_{\text{C-P}} = 6.1$ Hz), 76.3, 113.9, 128.2, 128.5, 128.8, 128.9, 129.1, 129.5, 129.6, 134.7, 134.8 (d, $^3J_{\text{C-P}} = 5.5$ Hz), 136.7, 157.9, 173.5. ^{31}P -NMR (121.5 MHz, CDCl_3): δ_{P} ppm = 32.35. HRMS (ESI): calculated for $\text{C}_{36}\text{H}_{43}\text{NO}_6\text{P}$ [(M+H) $^+$], 616.2823; found 616.2830.

Dibenzyl (2-(2-((benzyloxy)(methyl)amino)-2-oxoethyl)-5-(3-methoxyphenyl)pentyl)phosphonate (5.31d). Prepared according to general procedure V. Purification 5:1 dichloromethane/ethyl acetate v/v; yield 51%. ^1H NMR (300 MHz, CDCl_3) δ_{H} ppm 1.35-1.61 (m, 4H, $-\text{CH}_2-$), 1.72-2.07 (m, 2H, $-\text{CH}_2-$), 2.27-2.67 (m, 5H, $-\text{CH}_2-$, $-\text{CH}-$), 3.12 (s, 3H, $\text{N}-\text{CH}_3$), 3.75 (s, 3H, PhOCH_3), 4.72 (s, 2H, $-\text{NOCH}_2\text{Ph}$), 4.87-5.07 (m, 4H, $-\text{POCH}_2\text{Ph}$), 6.64-6.74 (m, 3H, Ar-H), 7.16 (t, $J = 7.9$ Hz, 1H, Ar-H), 7.26-7.37 (m, 15H, Ar-H). ^{13}C -NMR (75 MHz, CDCl_3) δ_{C} ppm 28.4, 29.5 (d, $^2J_{\text{C-P}} = 4.5$ Hz), 29.6 (d, $^1J_{\text{C-P}} = 138.4$ Hz), 29.7, 34.5 (d, $^3J_{\text{C-P}} = 10.3$ Hz), 35.8, 36.6 (d, $^3J_{\text{C-P}} = 9.0$ Hz), 55.0, 66.8 (d, $^2J_{\text{C-P}} = 6.7$ Hz), 66.9 (d, $^2J_{\text{C-P}} = 6.6$ Hz), 76.0, 110.9, 114.0, 120.7, 127.8, 128.2, 128.4, 128.6, 128.8, 129.1, 129.2, 134.5, 136.4 (d, $^3J_{\text{C-P}} = 6.1$ Hz), 136.4 (d, $^3J_{\text{C-P}} = 6.1$ Hz), 144.0, 159.5, 173.7. ^{31}P -NMR (121.5 MHz, CDCl_3): δ_{P} ppm = 32.31. HRMS (ESI): calculated for $\text{C}_{36}\text{H}_{43}\text{NO}_6\text{P}$ [(M+H) $^+$], 616.2823; found 616.2831.

Dibenzyl (2-(2-((benzyloxy)(methyl)amino)-2-oxoethyl)-5-(4-fluorophenyl)pentyl)phosphonate (5.31e). Prepared according to general procedure V. Purification 3:1 hexane/acetone v/v; yield 71%. ^1H NMR (300 MHz, CDCl_3) δ_{H} ppm 1.36-1.56 (m, 4H, $-\text{CH}_2-$), 1.71-2.02 (m, 2H, $-\text{CH}_2-$), 2.23-2.50 (m, 5H, $-\text{CH}_2-$, $-\text{CH}-$), 3.13 (s, 3H, $\text{N}-\text{CH}_3$), 4.73 (s, 2H, $-\text{NOCH}_2\text{Ph}$), 4.87-5.09 (m, 4H, $-\text{POCH}_2\text{Ph}$), 6.85-7.06 (m, 4H, Ar-H), 7.27-7.39 (m, 15H, Ar-H). ^{13}C -NMR (75 MHz, CDCl_3) δ_{C} ppm 28.6, 29.6 (d, $^2J_{\text{C-P}} = 4.3$ Hz), 29.7 (d, $^3J_{\text{C-P}} = 10.0$ Hz), 34.4 (d, $^3J_{\text{C-P}} = 10.0$ Hz), 34.9, 36.7 (d, $^3J_{\text{C-P}} = 10.0$ Hz), 37.0, 66.9 (d, $^2J_{\text{C-P}} = 6.6$ Hz), 67.0 (d, $^2J_{\text{C-P}} = 6.3$ Hz), 76.1, 114.9 (d, $^2J_{\text{C-F}} = 21.8$ Hz), 127.8 (d, $^3J_{\text{C-F}} = 9.8$ Hz), 127.9, 128.3, 128.6, 128.9, 129.2, 129.5, 134.5, 136.4 (d, $^3J_{\text{C-P}} = 6.7$ Hz), 137.9 (d, $^4J_{\text{C-F}} = 4.2$ Hz), 161.2 (d, $^1J_{\text{C-F}} = 242.42$ Hz), 173.4. ^{31}P -NMR (121.5 MHz, CDCl_3): δ_{P} ppm = 32.11. HRMS (ESI): calculated for $\text{C}_{35}\text{H}_{40}\text{FNO}_5\text{P}$ [(M+H) $^+$], 604.2623; found 604.2657.

Dibenzyl (2-(2-((benzyloxy)(methyl)amino)-2-oxoethyl)-5-(3-fluorophenyl)pentyl)phosphonate (5.31f). Prepared according to general procedure V. Purification 3:1 hexane/acetone v/v; yield 69%. ^1H NMR (300 MHz, CDCl_3) δ_{H} ppm 1.32-1.58 (m, 4H, $-\text{CH}_2-$), 1.69-2.03 (m, 2H, $-\text{CH}_2-$), 2.25-2.53 (m, 5H, $-\text{CH}_2-$, $-\text{CH}-$), 3.13 (s, 3H, $\text{N}-\text{CH}_3$), 4.73 (s, 2H, $-\text{NOCH}_2\text{Ph}$), 4.86-5.09 (m, 4H, $-\text{POCH}_2\text{Ph}$), 6.73-7.92 (m, 3H, Ar-H), 7.14-7.38 (m, 16H, Ar-H). ^{13}C -NMR (75 MHz, CDCl_3) δ_{C} ppm 28.2, 29.6 (d, $^2J_{\text{C-P}} = 4.1$ Hz), 29.7 (d, $^1J_{\text{C-P}} = 137.6$ Hz), 31.6, 34.4 (d, $^3J_{\text{C-P}} = 9.83$ Hz), 35.5, 36.7 (d, $^3J_{\text{C-P}} = 9.1$ Hz), 66.9 (d, $^2J_{\text{C-P}} = 6.7$ Hz), 67.0 (d, $^2J_{\text{C-P}} = 6.0$ Hz), 76.1, 112.5 (d, $^2J_{\text{C-F}} = 22.0$ Hz), 115.1 (d, $^2J_{\text{C-F}} = 22.0$ Hz), 124.0 (d, $^4J_{\text{C-F}} = 3.1$ Hz), 127.9, 128.3, 128.5, 128.6, 128.9, 129.3, 129.5 (d, $^3J_{\text{C-F}} = 8.6$ Hz), 134.5, 136.4 (d, $^3J_{\text{C-P}} = 6.1$ Hz), 144.9 (d, $^3J_{\text{C-F}} = 7.7$ Hz), 162.8 (d,

$^1J_{C-F}$ = 244.7 Hz), 173.25. ^{31}P -NMR (121.5 MHz, $CDCl_3$): δ_P ppm = 33.43. HRMS (ESI): calculated for $C_{35}H_{40}FNO_5P$ [(M+H) $^+$], 604.2623; found 604.2656.

Dibenzyl (2-(2-((benzyloxy)(methyl)amino)-2-oxoethyl)-5-(4-(trifluoromethyl)phenyl)pentyl)phosphonate (**5.31g**): Prepared according to general procedure V. Purification 3:1 hexane/acetone v/v; yield 55%. 1H NMR (300 MHz, $CDCl_3$) δ_H ppm 1.34-1.59 (m, 4H, $-CH_2-$), 1.70-2.05 (m, 2H, $-CH_2-$), 2.25-2.64 (m, 5H, $-CH_2-$, $-CH-$), 3.12 (s, 3H, N- CH_3), 4.72 (s, 2H, $-NOCH_2Ph$), 4.87-5.08 (m, 4H, $-POCH_2Ph$), 7.17 (d, J = 8.2 Hz, 2H, Ar-H), 7.32 (m, 15H, Ar-H), 7.48 (d, J = 8.2 Hz, 2H, Ar-H). ^{13}C -NMR (75 MHz, $CDCl_3$) δ_C ppm 28.2, 29.5 (d, $^2J_{C-P}$ = 3.6 Hz), 29.7 (d, $^1J_{C-P}$ = 138.2 Hz), 32.8, 34.4 (d, $^3J_{C-P}$ = 10.1 Hz), 35.5, 36.7 (d, $^3J_{C-P}$ = 9.5 Hz), 66.9 (d, $^2J_{C-P}$ = 6.4 Hz), 67.0 (d, $^2J_{C-P}$ = 6.6 Hz), 76.1, 124.5 (quart., $^1J_{C-F}$ = 272.7 Hz), 125.1 (quart., $^4J_{C-F}$ = 3.8 Hz), 127.9, 128.2 (quart., $^2J_{C-F}$ = 22.1 Hz), 128.3, 128.5, 128.6, 128.9, 129.2, 134.5, 136.4 (d, $^3J_{C-P}$ = 6.3 Hz), 146.4, 173.8. ^{31}P -NMR (121.5 MHz, $CDCl_3$): δ_P ppm = 33.43. HRMS (ESI): calculated for $C_{36}H_{40}F_3NO_5P$ [(M+H) $^+$], 654.2591; found 654.2601.

Dibenzyl (2-(2-((benzyloxy)(methyl)amino)-2-oxoethyl)-5-(naphthalen-1-yl)pentyl)phosphonate (**5.31h**): Prepared according to general procedure V. Purification 98:2 dichloromethane/methanol v/v; yield 44%. 1H NMR (300 MHz, $CDCl_3$) δ_H ppm 1.50-2.04 (m, 6H, $-CH_2-$), 2.29-2.64 (m, 3H, $-CH_2-$, $-CH-$), 2.90-3.00 (m, 2H, $-CH_2-$), 3.12 (s, 3H, N- CH_3), 4.68 (s, 2H, $-NOCH_2Ph$), 4.88-5.05 (m, 4H, $-POCH_2Ph$), 7.19-7.40 (m, 17H, Ar-H), 7.43-7.50 (m, 2H, Ar-H), 7.66-7.72 (m, 1H, Ar-H), 7.80-7.86 (m, 1H, Ar-H), 7.93-7.99 (m, 1H, Ar-H). ^{13}C -NMR (75 MHz, $CDCl_3$) δ_C ppm 28.1, 29.9 (d, $^1J_{C-P}$ = 138.4 Hz), 29.9 (d, $^2J_{C-P}$ = 4.9 Hz), 33.2, 35.2 (d, $^3J_{C-P}$ = 9.8 Hz), 36.9 (d, $^3J_{C-P}$ = 8.5 Hz), 67.2 (d, $^2J_{C-P}$ = 6.7 Hz), 67.3 (d, $^2J_{C-P}$ = 6.7 Hz), 76.3, 124.1, 125.6, 125.8, 125.9, 126.1, 126.7, 128.2, 128.5, 128.8, 128.9, 129.0, 129.1, 129.5, 132.0, 134.1, 134.8, 136.7 (d, $^3J_{C-P}$ = 6.4 Hz), 136.7 (d, $^1J_{C-P}$ = 6.1 Hz), 138.8, 168.0. ^{31}P -NMR (121.5 MHz, $CDCl_3$): δ_P ppm = 33.49. HRMS (ESI): calculated for $C_{39}H_{43}NO_5P$ [(M+H) $^+$], 636.2873; found 636.2880.

Dibenzyl (2-(2-((benzyloxy)(methyl)amino)-2-oxoethyl)-5-(naphthalen-2-yl)pentyl)phosphonate (**5.31i**): Prepared according to general procedure V. Purification 3:1 hexane/acetone v/v; yield 78%. 1H NMR (300 MHz, $CDCl_3$) δ_H ppm 1.37-2.02 (m, 6H, $-CH_2-$), 2.26-2.75 (m, 5H, $-CH-$, $-CH_2-$), 3.11 (s, 1H, N- CH_3), 4.71 (s, 2H, $-NOCH_2Ph$), 4.85-5.08 (m, 4H, $-POCH_2Ph$), 7.21-7.34 (m, 16H, Ar-H), 7.36-7.47 (m, 2H, Ar-H), 7.53 (s, 1H, Ar-H), 7.70-7.81 (m,

3H, Ar-H). ^{13}C -NMR (75 MHz, CDCl_3) δ_{C} ppm 28.7, 29.9 (d, $^2J_{\text{C-P}} = 3.9$ Hz), 30.0 (d, $^1J_{\text{C-P}} = 138.8$ Hz), 32.9, 34.8 (d, $^3J_{\text{C-P}} = 10.4$ Hz), 36.2, 36.9 (d, $^3J_{\text{C-P}} = 9.1$ Hz), 67.2 (d, $^2J_{\text{C-P}} = 6.6$ Hz), 67.3 (d, $^2J_{\text{C-P}} = 6.0$ Hz), 76.3, 125.3, 126.0, 126.6, 127.5, 127.6, 127.8, 128.0, 128.2, 128.5, 128.8, 128.9, 129.1, 129.5, 132.2, 133.8, 134.8, 136.7 (d, $^2J_{\text{C-P}} = 6.6$ Hz), 136.8 (d, $^2J_{\text{C-P}} = 6.2$ Hz), 140.1, 170.4. ^{31}P -NMR (121.5 MHz, CDCl_3): δ_{P} ppm = 33.49. HRMS (ESI): calculated for $\text{C}_{39}\text{H}_{43}\text{NO}_5\text{P}$ [(M+H) $^+$], 636.2873; found 636.2880.

Dibenzyl (5-([1,1'-biphenyl]-4-yl)-2-(2-((benzyloxy)(methyl)amino)-2-oxoethyl)pentyl)phosphonate (**5.31j**). Prepared according to general procedure V. Purification 97:3 dichloromethane/ethyl acetate v/v; yield 68%. ^1H NMR (300 MHz, CDCl_3) δ_{H} ppm 1.38-1.64 (m, 4H, $-\text{CH}_2-$), 1.75-2.04 (m, 2H, $-\text{CH}_2-$), 2.28-2.66 (m, 5H, $-\text{CH}_2-$, $-\text{CH}-$), 3.13 (s, 3H, N- CH_3), 4.72 (s, 2H, NOCH_2Ph), 4.89-5.07 (m, 4H, $-\text{POCH}_2\text{Ph}$), 7.11-7.19 (m, 3H, Ar-H), 7.25-7.60 (m, 21H, Ar-H). ^{13}C -NMR (75 MHz, CDCl_3) δ_{C} ppm 28.5, 29.6 (d, $^2J_{\text{C-P}} = 4.7$ Hz), 30.3, 29.6 (d, $^1J_{\text{C-P}} = 138.2$ Hz), 34.5 (d, $^3J_{\text{C-P}} = 10.2$ Hz), 35.4, 36.6 (d, $^3J_{\text{C-P}} = 10.2$ Hz), 66.9 (d, $^2J_{\text{C-P}} = 6.1$ Hz), 70.0 (d, $^2J_{\text{C-P}} = 6.6$ Hz), 76.0, 126.9, 127.9, 128.2, 128.5, 128.6, 128.7, 128.8, 128.9, 129.2, 134.5, 136.4 (d, $^3J_{\text{C-P}} = 6.4$ Hz), 138.5, 141.0, 141.5, 172.6. ^{31}P -NMR (121.5 MHz, CDCl_3): δ_{P} ppm = 32.33. HRMS (ESI): calculated for $\text{C}_{41}\text{H}_{45}\text{NO}_5\text{P}$ [(M+H) $^+$], 662.3030; found 662.3039.

Sodium hydrogen (2-(2-(hydroxy(methyl)amino)-2-oxoethyl)-5-(*p*-tolyl)pentyl)phosphonate (**5.24a**). White powder. Prepared from compound **5.31a** (150 mg, 0.25 mmol) according to general procedure VI. ^1H NMR (300 MHz, D_2O) δ_{H} ppm 1.29-1.78 (m, 6H, $-\text{CH}_2-$), 1.94-2.41 (m, 4H, $-\text{CH}-$, Ph- CH_3), 2.45-2.70 (m, 4H, $-\text{CH}_2-$), 3.01 (s, 5/6 of N- CH_3), 3.23 (s, 1/6 of N- CH_3), 6.89-7.23 (m, 4H, Ar-H). ^{13}C -NMR (75 MHz, D_2O) δ_{C} ppm 20.0, 27.6, 30.5 (d, $^2J_{\text{C-P}} = 4.3$ Hz), 31.6 (d, $^1J_{\text{C-P}} = 130.7$ Hz), 34.1 (d, $^3J_{\text{C-P}} = 12.7$ Hz), 34.5, 37.0, 39.2 (d, $^1J_{\text{C-P}} = 7.1$ Hz), 128.4, 128.9, 135.4, 139.8, 177.8. ^{31}P -NMR (121.5 MHz, D_2O): δ_{P} ppm 25.97. HRMS (ESI): calculated for $\text{C}_{15}\text{H}_{23}\text{NO}_5\text{P}$ [(M-H) $^-$], 328.1319; found 328.1320.

Sodium hydrogen (2-(2-(hydroxy(methyl)amino)-2-oxoethyl)-5-(*m*-tolyl)pentyl)phosphonate (**5.24b**). White powder. Prepared from compound **5.31b** (150 mg, 0.25 mmol) according to general procedure VI. ^1H NMR (300 MHz, D_2O) δ_{H} ppm 1.22-1.69 (m, 6H, $-\text{CH}_2-$), 1.99-2.23 (m, 1H, $-\text{CH}-$), 2.28 (s, 3H, Ph- CH_3), 2.49-2.68 (m, 4H, $-\text{CH}_2-$), 3.18 (s, 5/6 of N- CH_3), 3.35 (s, 1/6 of N- CH_3), 7.02-7.15 (m, 3H, Ar-H), 7.23 (app. t, $J = 7.4$ Hz, 1H, Ar-H). ^{13}C -NMR (75 MHz,

D₂O) δ_C ppm 20.5, 28.4, 32.2 (d, $^2J_{C-P}$ = 4.1 Hz), 33.4 (d, $^1J_{C-P}$ = 130.7 Hz), 35.3, 35.4 (d, $^3J_{C-P}$ = 9.8 Hz), 36.2, 36.3 (d, $^3J_{C-P}$ = 5.9 Hz), 125.8, 126.5, 128.7, 129.4, 138.7, 143.8, 174.4. ^{31}P -NMR (121.5 MHz, D₂O): rotamers at δ_P ppm 22.14 and 22.25. HRMS (ESI): calculated for C₁₅H₂₃NO₅P [(M-H)⁻], 328.1319; found 328.1318.

Sodium hydrogen (2-(2-(hydroxy(methyl)amino)-2-oxoethyl)-5-(4-methoxyphenyl)pentyl)phosphonate (5.24c). White powder. Prepared from compound **5.31c** (125 mg, 0.20 mmol) according to general procedure VI. 1H NMR (300 MHz, D₂O) δ_H ppm 1.23-1.66 (m, 6H, -CH₂-), 2.01-2.26 (m, 1H, -CH-), 2.47-2.67 (m, 4H, -CH₂-), 3.17 (s, 5/6 of N-CH₃), 3.34 (s, 1/6 of N-CH₃), 3.78 (s, 3H, PhOCH₃), 6.91 (m, 2H, Ar-H), 7.21 (m, 2H, Ar-H). ^{13}C -NMR (75 MHz, D₂O) δ_C ppm 28.3, 32.0 (d, $^2J_{C-P}$ = 4.0 Hz), 33.3 (d, $^1J_{C-P}$ = 129.9 Hz), 34.4, 35.1 (d, $^3J_{C-P}$ = 10.7 Hz), 36.1, 36.4 (d, $^3J_{C-P}$ = 6.2 Hz), 55.6, 114.1, 129.9, 136.2, 156.9, 175.0. ^{31}P -NMR (121.5 MHz, D₂O): δ_P ppm = 22.48. HRMS (ESI): calculated for C₁₅H₂₃NO₆P [(M-H)⁻], 344.1268; found 344.1269.

Sodium hydrogen (2-(2-(hydroxy(methyl)amino)-2-oxoethyl)-5-(3-methoxyphenyl)pentyl)phosphonate (5.24d). White powder. Prepared from compound **5.31d** (150 mg, 0.24 mmol) according to general procedure VI. 1H NMR (300 MHz, D₂O) δ_H ppm 1.24-1.69 (m, 6H, -CH₂-), 2.02-2.26 (m, 1H, -CH-), 2.51-2.66 (m, 4H, -CH₂-), 3.17 (s, 5/6 of N-CH₃), 3.34 (s, 1/6 of N-CH₃), 3.79 (s, 3H, Ph-OCH₃), 6.77-6.93 (m, 3H, Ar-H), 7.26 (app. t, J = 7.9 Hz, 1H, Ar-H). ^{13}C -NMR (75 MHz, D₂O) δ_C ppm 28.0, 31.8 (d, $^2J_{C-P}$ = 4.1 Hz), 33.1 (d, $^1J_{C-P}$ = 130.2 Hz), 35.1 (d, $^3J_{C-P}$ = 10.6 Hz), 35.4, 36.1, 36.5 (d, $^3J_{C-P}$ = 7.3 Hz), 55.4, 111.5, 114.2, 121.7, 129.8, 145.5, 159.0, 175.2. ^{31}P -NMR (121.5 MHz, D₂O): δ_P ppm = 21.72. HRMS (ESI): calculated for C₁₅H₂₃NO₆P [(M-H)⁻], 344.1268; found 344.1269.

Sodium hydrogen (5-(4-fluorophenyl)-2-(2-(hydroxy(methyl)amino)-2-oxoethyl)pentyl)phosphonate (5.24e). White powder. Prepared from compound **5.31e** (100 mg, 0.17 mmol) according to general procedure VI. 1H NMR (300 MHz, D₂O) δ_H ppm 1.14-1.68 (m, 6H, -CH₂-), 1.92-2.20 (m, 1H, -CH-), 2.42-2.66 (m, 4H, P-CH₂-, CH₂-CON-), 3.14 (s, 5/6 of N-CH₃), 3.27 (s, 1/6 of N-CH₃), 6.97-7.09 (m, 2H, Ar-H), 7.20-7.33 (m, 2H, Ar-H). ^{13}C -NMR (75 MHz, D₂O) δ_C ppm 28.0, 31.4 (d, $^2J_{C-P}$ = 4.5 Hz), 33.9 (d, $^1J_{C-P}$ = 139.3 Hz), 34.6 (d, $^3J_{C-P}$ = 8.1 Hz), 34.7, 36.3 (d, $^3J_{C-P}$ = 8.3 Hz), 37.1, 114.7 (d, $^2J_{C-F}$ = 21.2 Hz), 129.9 (d, $^3J_{C-F}$ = 8.3 Hz), 139.2 (d, $^4J_{C-F}$ = 3.7 Hz), 160.7 (d, $^1J_{C-F}$ = 239.1 Hz), 169.0. ^{31}P -NMR (121.5 MHz, D₂O): rotamers at δ_P

ppm 21.40, 21.50. HRMS (ESI): calculated for $C_{14}H_{21}FNO_5P$ [(M-H)⁻], 332.1069; found 332.1088.

Sodium hydrogen (5-(3-fluorophenyl)-2-(2-(hydroxy(methyl)amino)-2-oxoethyl)pentyl)phosphonate (5.24f). White powder. Prepared from compound **5.31f** (130 mg, 0.22 mmol) according to general procedure VI. ¹H NMR (300 MHz, D₂O) δ_H ppm 1.23-1.68 (m, 6H, -CH₂-), 2.02-2.23 (m, 1H, -CH-), 2.50-2.69 (m, 4H, -CH₂-), 3.17 (s, 5/6 of N-CH₃), 3.35 (s, 1/6 of N-CH₃), 6.88-7.10 (m, 3H, Ar-H), 7.25-7.34 (m, 1H, Ar-H). ¹³C-NMR (75 MHz, D₂O) δ_C ppm 27.9, 31.9 (d, ²J_{C-P} = 4.1 Hz), 33.1 (d, ¹J_{C-P} = 129.1 Hz), 35.0 (d, ³J_{C-P} = 8.2 Hz), 35.1, 36.1, 36.4 (d, ³J_{C-P} = 7.0 Hz), 112.5 (d, ²J_{C-F} = 23.32 Hz), 115.3 (d, ²J_{C-F} = 21.9 Hz), 124.6 (d, ⁴J_{C-F} = 2.7 Hz), 130.1 (d, ³J_{C-F} = 8.7 Hz), 146.2 (d, ³J_{C-F} = 8.7 Hz), 162.9 (d, ¹J_{C-F} = 247.1 Hz), 175.0. ³¹P-NMR (121.5 MHz, D₂O): δ_P ppm = 22.75. HRMS (ESI): calculated for $C_{14}H_{20}FNO_5P$ [(M-H)⁻], 332.1069; found 332.1067.

Sodium hydrogen (2-(2-(hydroxy(methyl)amino)-2-oxoethyl)-5-(4-(trifluoromethyl)phenyl)pentyl)phosphonate (5.24g). White powder. Prepared from compound **5.31g** (150 mg, 0.25 mmol) according to general procedure VI. ¹H NMR (300 MHz, D₂O) δ_H ppm 1.27-1.71 (m, 6H, -CH₂-), 2.00-2.26 (m, 1H, -CH-), 2.50-2.61 (m, 2H, -CH₂-), 2.66 (t, *J* = 7.4 Hz, 2H, -CH₂-), 3.16 (s, 5/6 of N-CH₃), 3.34 (s, 1/6 of N-CH₃), 3.79, 7.40 (d, *J* = 7.9 Hz, 2H, Ar-H), 7.61 (d, *J* = 7.9 Hz, 2H, Ar-H). ¹³C-NMR (75 MHz, D₂O) δ_C ppm 27.5, 29.5, 31.5 (d, ²J_{C-P} = 4.1 Hz), 32.8 (d, ¹J_{C-P} = 130.7 Hz), 34.5 (d, ³J_{C-P} = 11.0 Hz), 34.9, 35.8, 36.3 (d, ³J_{C-P} = 6.8 Hz), 124.4 (quart., ¹J_{C-F} = 270.5 Hz), 125.0 (quart., ³J_{C-F} = 4.1 Hz), 128.9 (app. s), 147.6, 174.9. ³¹P-NMR (121.5 MHz, D₂O): δ_P ppm = 21.49. HRMS (ESI): calculated for $C_{15}H_{20}F_3NO_5P$ [(M-H)⁻], 382.1037; found 382.1039.

Sodium hydrogen (2-(2-(hydroxy(methyl)amino)-2-oxoethyl)-5-(naphthalen-1-yl)pentyl)phosphonate (5.24h). White powder. Prepared from compound **5.31h** (150 mg, 0.24 mmol) according to general procedure VI. ¹H NMR (300 MHz, D₂O) δ_H ppm 1.38-1.84 (m, 6H, -CH₂-), 2.02-2.27 (m, 1H, -CH-), 2.46-2.65 (m, 2H, -CH₂-), 3.07 (t, *J* = 7.6 Hz, 2H, -CH₂-), 3.13 (s, 5/6 of N-CH₃), 3.24 (s, 1/6 of N-CH₃), 7.39-7.62 (m, 4H, Ar-H), 7.78 (dd, *J* = 2.4 Hz, 7.4 Hz, 1H, Ar-H), 7.92 (dd, *J* = 2.4 Hz, 8.1 Hz, 1H, Ar-H), 8.18 (d, *J* = 8.1 Hz, 1H, Ar-H). ¹³C-NMR (75 MHz, D₂O) δ_C ppm 27.8, 32.1 (d, ²J_{C-P} = 4.5 Hz), 32.7, 33.8 (d, ¹J_{C-P} = 129.3 Hz), 34.5, 35.7 (d, ³J_{C-P} = 10.8 Hz), 36.4 (d, ³J_{C-P} = 7.6 Hz), 36.6, 124.4, 126.1, 126.2, 126.3, 126.4, 128.8,

131.6, 133.7, 139.7, 172.7. ^{31}P -NMR (121.5 MHz, D_2O): rotamers at δ_{P} ppm 21.94, 22.18. HRMS (ESI): calculated for $\text{C}_{18}\text{H}_{23}\text{NO}_5\text{P}$ [(M-H) $^-$], 364.1319; found 364.1315.

Sodium hydrogen (2-(2-(hydroxy(methyl)amino)-2-oxoethyl)-5-(naphthalen-2-yl)pentyl)phosphonate (5.24i). White powder. Prepared from compound **5.31i** (150 mg, 0.24 mmol) according to general procedure VI. ^1H NMR (300 MHz, D_2O) δ_{H} ppm 1.23-1.80 (m, 6H, $-\text{CH}_2-$), 2.01-2.29 (m, 1H, $-\text{CH}-$), 2.46-2.65 (m, 2H, $-\text{CH}_2-$), 2.78 (t, $J = 7.8$ Hz, 2H, $-\text{CH}_2-$), 3.12 (s, 5/6 of $\text{N}-\text{CH}_3$), 3.30 (s, 1/6 of $\text{N}-\text{CH}_3$), 7.44-7.55 (m, 3H, Ar-H), 7.77 (s, 1H, Ar-H), 7.84-7.92 (m, 3H, Ar-H). ^{13}C -NMR (75 MHz, D_2O) δ_{C} ppm 29.8, 31.8 (d, $^2J_{\text{C-P}} = 3.7$ Hz), 34.1 (d, $^1J_{\text{C-P}} = 130.8$ Hz), 35.0 (d, $^3J_{\text{C-P}} = 10.9$ Hz), 35.8, 36.5 (d, $^3J_{\text{C-P}} = 8.0$ Hz), 37.3, 125.5, 126.3, 126.4, 127.5, 127.7, 127.9, 128.1, 131.7, 133.5, 141.6, 169.7. ^{31}P -NMR (121.5 MHz, D_2O): δ_{P} ppm = 22.48. HRMS (ESI): calculated for $\text{C}_{18}\text{H}_{23}\text{NO}_5\text{P}$ [(M-H) $^-$], 364.1319; found 364.1315.

Sodium hydrogen (5-([1,1'-biphenyl]-4-yl)-2-(2-(hydroxy(methyl)amino)-2-oxoethyl)pentyl)phosphonate (5.24j). White powder. Prepared from compound **5.31j** (200 mg, 0.30 mmol) according to general procedure VI. ^1H NMR (300 MHz, D_2O) δ_{H} ppm 1.23-1.73 (m, 6H, $-\text{CH}_2-$), 1.98-2.24 (m, 1H, $-\text{CH}-$), 2.42-2.70 (m, 4H, $-\text{CH}_2-$), 3.14 (s, 5/6 of $\text{N}-\text{CH}_3$), 3.30 (s, 1/6 of $\text{N}-\text{CH}_3$), 7.35-7.53 (m, 5H, Ar-H), 7.58-7.71 (m, 4H, Ar-H). ^{13}C -NMR (75 MHz, D_2O) δ_{C} ppm 27.9, 31.5 (d, $^2J_{\text{C-P}} = 4.1$ Hz), 33.0 (d, $^1J_{\text{C-P}} = 130.1$ Hz), 34.5 (d, $^2J_{\text{C-P}} = 10.1$ Hz), 35.0, 36.3 (d, $^3J_{\text{C-P}} = 8.38$ Hz), 37.1, 126.7, 126.8, 127.4, 129.0, 129.3, 137.8, 140.4, 143.1, 169.2. ^{31}P -NMR (121.5 MHz, D_2O): rotamers at δ_{P} ppm 21.37, 21.54. HRMS (ESI): calculated for $\text{C}_{20}\text{H}_{25}\text{NO}_5\text{P}$ [(M-H) $^-$], 390.1476; found 390.1479.

REFERENCES

1. Haemers, T.; Wiesner, J.; Gießmann, D.; Verbrugghen, T.; Hillaert, U.; Ortmann, R.; Jomaa, H.; Link, A.; Schlitzer, M.; Van Calenbergh, S. Synthesis of β - and γ -oxa isosteres of fosmidomycin and FR900098 as antimalarial candidates. *Bioorg. Med. Chem.* **2008**, *16*, 3361–3371.
2. Brucher, K.; Illarionov, B.; Held, J.; Tschan, S.; Kunfermann, A.; Pein, M. K.; Bacher, A.; Gräwert, T.; Maes, L.; Mordmüller, B.; Fischer, M.; Kurz, T. α -Substituted β -oxa isosteres of fosmidomycin: synthesis and biological evaluation. *J. Med. Chem.* **2012**, *55*, 6566–6575.
3. Kunfermann, A.; Lienau, C.; Illarionov, B.; Held, J.; Gräwert, T.; Behrendt, C. T.; Werner, P.; Hähn, S.; Eisenreich, W.; Riederer, U.; Mordmüller, B.; Bacher, A.; Fischer, M.; Groll, M.; Kurz, T. IspC as target for antiinfective drug discovery: Synthesis, enantiomeric separation, and structural biology of fosmidomycin thia isosters. *J. Med. Chem.* **2013**, *56*, 8151–8162.
4. Andaloussi, M.; Henriksson, L. M.; Wieckowska, A.; Lindh, M.; Bjorkelid, C.; Larsson, A. M.; Suresh, S.; Iyer, H.; Srinivasa, B. R.; Bergfors, T.; Unge, T.; Mowbray, S. L.; Larhed, M.; Jones, T. A.; Karlen, A. Design, synthesis, and X-ray crystallographic studies of α -aryl substituted fosmidomycin analogues as inhibitors of *Mycobacterium tuberculosis* 1-deoxy-D xylulose 5-phosphate reductoisomerase. *J. Med. Chem.* **2011**, *54*, 4964–4976.
5. Jansson, A. M.; Wieckowska, A.; Bjorkelid, C.; Yahiaoui, S.; Sooriyaarachchi, S.; Lindh, M.; Bergfors, T.; Dharavath, S.; Desroses, M.; Suresh, S.; Andaloussi, M.; Nikhil, R.; Sreevalli, S.; Srinivasa, B. R.; Larhed, M.; Jones, T. A.; Karlén, A.; Mowbray, S. L. DXR inhibition by potent mono- and disubstituted fosmidomycin analogues. *J. Med. Chem.* **2013**, *56*, 6190–6199.
6. Topliss, J. G. A manual method for applying the Hansch approach to drug design. *J. Med. Chem.* **1977**, *20*, 463–469.
7. Kamiya, T. S.; Hashimoto, M. T.; Hemmi, K. K.; Takeno, H. N. Hydroxyaminohydrocarbonphosphonic acids. US Patent 4, 206, 156, June 3, **1980**.
8. Silber, K.; Heidler, P.; Kurz, T.; Klebe, G. AFMoC enhances predictivity of 3D QSAR: A case study with DOXP-reductoisomerase. *J. Med. Chem.* **2005**, *48*, 3547–3563.

9. Goble, J. L.; Adendorff, M. R.; De Beer, T. A. P.; Stephens, L. L.; Blatch, G. L. The malaria drug target *Plasmodium falciparum* 1-deoxy-D-xylulose-5-phosphate reductoisomerase (PfDxr): development of a 3-D model for identification of novel, structural and functional features and for inhibitor screening. *Protein Pept. Lett.* **2010**, *17*, 109–120.
10. Kuntz, L.; Tritsch, D.; Grosdemange-Billiard, C.; Hemmerlin, A.; Willem, A.; Bacht, T.; Rohmer, M. Isoprenoid biosynthesis as a target for antibacterial and antiparasitic drugs: Phosphonohydroxamic acids as inhibitors of deoxyxylulose phosphate reducto-isomerase. *Biochem. J.* **2005**, *386*, 127–135.
11. Kazuyoshi, T.; Akira, A.; Hiroko, N.; So-ichi, T.; Yoshihisa, M.; Hiroaki, T.; Yoshihiro, H. Dicarbonates: Convenient 4-dimethylaminopyridine catalyzed esterification reagents. *Synthesis* **1994**, 1063–1066.
12. Yamaguchi, M.; Tsukamoto, Y.; Hayashi, A.; Minami, T. A stereoselective Michael addition of α -lithiated phosphonates to α,β -unsaturated esters. *Tetrahedron Lett.* **1990**, *31*, 2423–2424.
13. Nair, S. C.; Brooks, C. F.; Goodman, C. D.; Strurm, A.; McFadden, G. I.; Sundriyal, S.; Anglin, J. L.; Song, Y.; Moreno, S. N. J.; Striepen, B. Apicoplast isoprenoid precursor synthesis and the molecular basis of fosmidomycin resistance in *Toxoplasma gondii*. *J. Exp. Med.* **2011**, *208*, 1547–1559.
14. Zinglé, C.; Kuntz, L.; Tritsch, D.; Grosdemange, C. B.; Rohmer, M. Modifications around the hydroxamic acid chelating group of fosmidomycin, an inhibitor of the metalloenzyme 1-deoxyxylulose 5-phosphate reductoisomerase (DXR). *Bioorg. Med. Chem. Lett.* **2012**, *22*, 6563–6567.
15. Ponaire, S.; Zinglé, C.; Tritsch, D.; Grosdemange-Billiard, C.; Rohmer, M. Growth inhibition of *Mycobacterium smegmatis* by prodrugs of deoxyxylulose phosphate reductoisomerase inhibitors, promising anti-mycobacterial agents. *Eur. J. Med. Chem.* **2012**, *51*, 227–285.
16. Shiloh, M. U.; Champion, P. A. To catch a killer. What can mycobacterial models teach us about *Mycobacterium tuberculosis* pathogenesis? *Curr. Opin Microbiol.* **2010**, 86–92.
17. Verbrugghen, T.; Cos, P.; Maes, L.; Van Calenbergh, S. Synthesis and evaluation of β -halogenated analogues of 3-(acetylhydroxyamino)propylphosphonic acid (FR900098) as antimalarials. *J. Med. Chem.* **2010**, *53*, 5342–5346.

18. Read, R. J. Improved Fourier coefficients for maps using phases from partial structures with errors. *Acta Crystallogr., Sect. A* **1986**, 42, 140–149.
19. Björkelid, C.; Bergfors, T.; Unge, T.; Mowbray, S. L.; Jones, T. A. Structural studies on *Mycobacterium tuberculosis* Dxr in complex with the antibiotic FR-900098. *Acta Crystallogr., Sect. D: Biol. Crystallogr.* **2012**, 68, 134–143.
20. Mohamadi, F.; Richards, N. G. J.; Guida, W. C.; Liskamp, R.; Lipton, M.; Caufield, C.; Chang, G.; Hendrickson, T.; Still, W.C. MacroModel- An integrated software system for modeling organic and bioorganic molecules using molecular mechanics. *J. Comput. Chem.* **1990**, 11, 440–467.
21. European Committee for Antimicrobial Susceptibility Testing (EUCAST) of the European Society of Clinical Microbiology and Infectious Diseases (ESCMID). EUCAST Discussion Document E. Dis 5.1: Determination of minimum inhibitory concentrations (MICs) of antibacterial agents by broth dilution. *Clin. Microbiol. Infec.* **2003**, 9, 1–7.
22. Ming-Kui, Z.; Jun-Feng, Z.; Teck-Peng, L. Palladium-catalyzed C-C bond formation of arylhydrazines with olefins via carbon-nitrogen bond cleavage. *Org. Lett.* **2011**, 13, 6308–6311.
23. Wei-Ting, W.; Jiann-Yih, Y.; Ting-Shen, K.; Hsyueh-Liang, W. Highly enantioselective rhodium-catalyzed asymmetric 1,4-addition reactions of arylboronic acids to acyclic α,β -unsaturated compounds: the formal synthesis of (-)-indatraline. *Chem. Eur. J.* **2011**, 17, 11405–11409.
24. Henriksson, L. M.; Unge, T. Carlsson, J. Aqvist, J. Mowbray, S. L.; Jones, T. A. Structures of *Mycobacterium tuberculosis* 1-deoxy-D-xylulose-5-phosphate reductoisomerase provide new insights into catalysis. *J. Biol. Chem.* **2007**, 282, 27, 19905–19916.
25. Sweeney, A. M.; Lange, R.; Fernandes, R. P. M.; Schulz, H.; Dale, G. E.; Douangamath, A.; Proteau, P. J.; Oefner, C. The crystal structure of *E. coli* 1-deoxy-D-xylulose-5 phosphate reductoisomerase in a ternary complex with the antimalarial compound fosmidomycin and NADPH reveals a tight-binding closed enzyme conformation. *J. Mol. Biol.*, **2005**, 345, 115–127.

26. Umeda, T.; Tanaka, N.; Kusakabe, Y.; Nakanishi, M.; Kitade, Y.; Nakamura, K. T. Molecular basis of fosmidomycin's action on the human malaria parasite *Plasmodium falciparum*. *Sci. Rep.*, **2011**, *1*, 1–8.
27. Xue, J.; Diao, J.; Cai, G.; Deng, L.; Zheng, B.; Yao, Y.; Song, Y. Antimalarial and structural studies of pyridine-containing inhibitors of 1-deoxyxylulose-5-phosphate reductoisomerase. *Med. Chem. Lett.* **2013**, *4*, 278–282.
28. Masini, T.; Kroezen, B. S.; Hirsch, A. K. Druggability of the enzymes of the non mevalonate-pathway. *Drug Discov. Today*, **2013**, *18*: 23–24, 1256–1262.
29. Kholodar, S. A.; Tomblin, G.; Liu, J.; Tan, Z.; Allen, C. L.; Gulick, A. M.; Murkin, A. S. Alteration of the flexible loop in 1-deoxy-D-xylulose-5-phosphate reductoisomerase boosts enthalpy-driven inhibition by fosmidomycin. *Biochemistry* **2014**, *53*, 3423–3431.
30. Deng, L.; Endo, K.; Kato, M.; Cheng, G.; Yajima, S.; Song, Y. Structures of 1-deoxy-D-xylulose-5-phosphate reductoisomerase/lipophilic phosphonate complexes. *Med. Chem. Lett.* **2011**, *2*, 165–170.
31. Giessmann, D.; Heidler, P.; Haemers, T.; Van Calenbergh, S.; Reichenberg, A.; Jomaa, H.; Weidemeyer, C.; Sanderbrand, S.; Wiesner, J.; Link, A. Towards new antimalarial drugs: synthesis of nonhydrolyzable phosphate mimics as feed for a predictive QSAR study on 1 deoxy-D-xylulose-5-phosphate reductoisomerase inhibitors. *Chem. Biodiversity* **2008**, *5*, 643–656.

Chapter VI

PHOSPHORAMIDE

ANALOGUES OF

FOSMIDOMYCIN

VI. PHOSPHORAMIDE ANALOGUES OF FOSMIDOMYCIN

VI.A. Introduction

Phosphoric acid amides and their derivatives constitute an important class of organophosphorus compounds with a wide range of applications. A host of bioactive molecules showing potent antifungal, antitumor, and anti-HIV activities contain the phosphoramidate structural scaffold.^{1,2} Apart from their importance in medicine, they serve in other uses such as flame retardants,³ in agriculture⁴ as pesticides and herbicides as well as in organic chemistry where they afford synthetic intermediates^{5,6} and phosphorylation has also been validated as a protecting strategy for amines.⁷

Due to their wide use, several approaches have been developed towards the synthesis of phosphoramides (Figure VI.1),⁸ including the well-known reaction of an amine with a phosphoryl halide in the presence of a strong base.

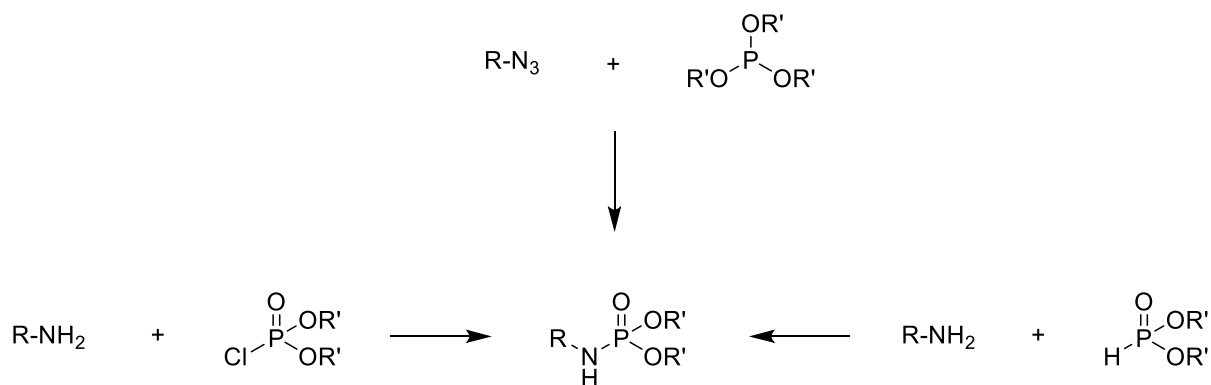


Figure VI.1: Synthetic routes to phosphoramides.

The Atherton-Todd reaction exploits the generation of a reactive phosphoryl halide *in situ* from dibenzyl or dialkyl phosphites and CCl_4 , which then reacts with an amine.⁹ The use of CCl_4 has been circumvented by the Staudinger-phosphite reaction, which allows the use of alkyl azides and phosphites to form phosphorimides followed by hydrolysis to attain the desired phosphoramides.¹⁰ Oxidative cross-coupling reactions between amines and H-phosphonates are popular alternative strategies for the synthesis of phosphoramides.^{11,12,13}

The natural substrate of Dxr (DOXP), is a phosphate monoester. The introduction of electron withdrawing aryl or halogen substituents in α -position of the phosphonate group of fosmidomycin increase the acidity of the phosphonic acid group, thereby leading to a stronger interaction with the phosphate binding site of Dxr. Woo *et al.* modified the polar phosphonate head group of fosmidomycin/FR900098 to a phosphate and showed that fosfoxacin (**1.35**, also a natural antibiotic), and its acetyl congener **1.36** are more potent inhibitors of *Synechocystis sp.* PCC6803 Dxr than fosmidomycin (K_i of 19 nM (**1.35**) and 2 nM (**1.36**) versus 57 nM for fosmidomycin).¹⁴ Such an effect could possibly be achieved by incorporating a nitrogen atom into the α -position of the three-carbon chain of compound **1.6**. With the anticipation that amide derivatives of phosphoric acid are chemically and metabolically more stable than the corresponding esters, we sought to abate the liability associated with the phosphate in fosfoxacin by preparing the phosphoramidic acid analogues **6.1** (Figure VI.2). Furthermore, alkylation at the nitrogen would offer the possibility to construct a small library with various substituents that may elicit further interactions with active site residues.

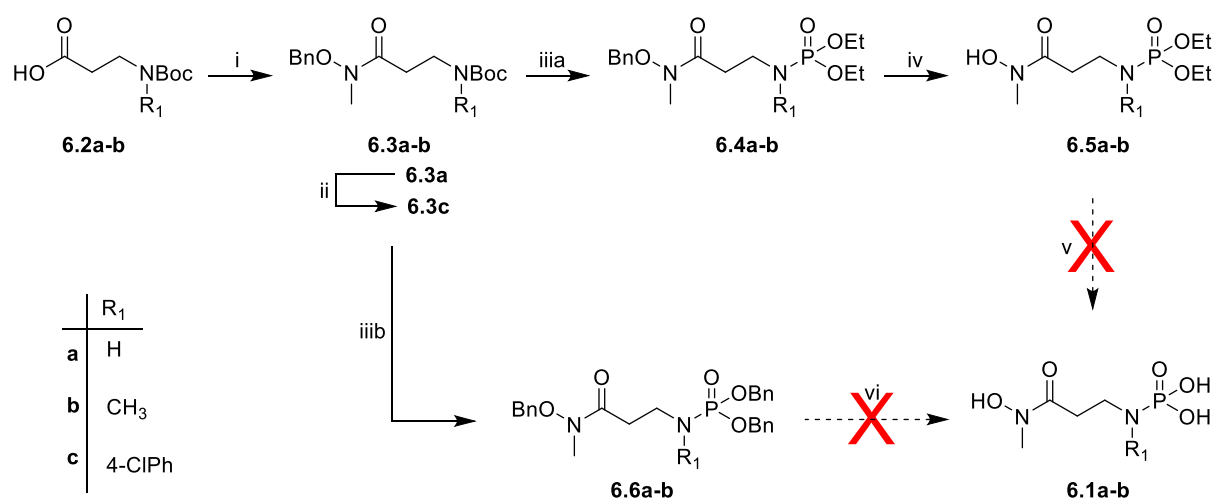


Figure VI.2: Analogues of fosmidomycin/FR900098 bearing a (substituted)heteroatom in the α -position.

VI.B. Synthesis

A synthetic strategy for accessing the envisaged analogues is outlined in Scheme VI.1. Since *N*-arylation would be achievable via a Buchwald-Hartwig cross coupling reaction, commercially available *N*-Boc-protected β -alanine was considered a suitable starting material for synthesis of the phosphoramidic acid **6.1a** and its *N*-aryl derivative. Boc-*N*-methyl- β -alanine meanwhile, served as starting material for the corresponding *N*-methyl analogue. EDC-mediated coupling of these acids with *O*-benzyl-*N*-methyl-hydroxylamine afforded the protected hydroxamates **6.3a-b**. Compound **6.3a** was in turn transformed to

6.3c via a Buchwald-Hartwig coupling with 1-bromo-4-chlorobenzene. Boc group removal and subsequent phosphorylation of **6.3a-b** with diethyl chlorophosphate in the presence of triethylamine yielded the diethylphosphoramides **6.4a-b**, which were subsequently treated with BCl_3 to obtain the hydroxamates **6.5a-b**. TMSBr-mediated deprotection of the ethyl protecting groups of **6.5a-b** proved unsuccessful and led us to convert **6.3a-b** to the dibenzylphosphoramides **6.6a-b** by phosphorylation with dibenzyl phosphite. Unfortunately, attempts to remove the benzyl groups of **6.6a-b** by catalytic hydrogenolysis were also unsuccessful. Reaction monitoring by MS revealed only traces of the target compounds (**6.1a** or **6.1b**). A literature search was conducted to understand the underlying reasons for the fruitless deprotection.



Scheme VI.1 Reagents and conditions: i) $\text{MeNH}(\text{OBn})$, EDC, Et_3N , CH_2Cl_2 , rt, overnight, 81% (**6.3a**), 83% (**6.3b**); ii) 1-bromo-4-chlorobenzene, $\text{Pd}(\text{OAc})_2$, Xantphos, Cs_2CO_3 , 1,4-dioxane, reflux, 48 h, 45%; iii) TFA, Et_3SiH , CH_2Cl_2 , 2 h, 0 °C to rt; (a) $(\text{EtO})_2\text{OPCl}$, Et_3N , CH_2Cl_2 , 2 h, 71% (**6.4a**), 78% (**6.4b**); (b) $(\text{BnO})_2\text{OPH}$, NCS, toluene; Et_3N , CH_2Cl_2 , 2 h, 64% (**6.6a**), 68% (**6.6b**); iv) BCl_3 , CH_2Cl_2 , -78 °C, 1 h, 72% (**6.5a**), 74% (**6.5b**); v) TMSBr, BSTFA, CH_2Cl_2 , 0 °C to rt; vi) H_2 , Pd/C, MeOH, rt.

Different groups have reported that (*N*-substituted) phosphoramidic acids are hydrolyzed in aqueous solution to the corresponding amines and phosphoric acid.^{15,16,17} The anticipation that phosphoramidate analogues of fosmidomycin/FR900098 will be more stable than their phosphate counterparts such as fosfoxacin (which we erstwhile prepared for a collaborative project) turned out to be naive. Halmann and colleagues examined the mechanism of

hydrolysis of phosphoramidic acid and found that the rate follows strict first-order kinetics and rises steadily with increasing acidity.¹⁶ In aqueous solution within the pH 1–7 range, the neutral molecule (which probably exists as a zwitterion) or the conjugate acid appears to react by a unimolecular mechanism to form a transient metaphosphate intermediate, which then rapidly reacts with water to give the products. At alkaline pH however, the compounds lose the positive charge on the nitrogen and resist hydrolysis. Following this analogy, it can be understood that the onset of the deprotection of **6.5** or **6.6** is as expected, with the target compounds **6.1a-b** initially formed, but then subsequently and rapidly degraded as depicted in Figure VI.3.

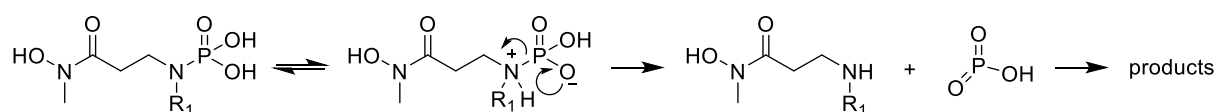


Figure VI.3: Plausible mechanism for the degradation of compounds **6.1a-b**.

An alternative mechanism consistent with a new study¹⁸ on the pH-dependent hydrolysis of phosphoramidates may involve the hydroxamic acid moiety (Figure VI.4). This pathway is also based on the notion that at physiological conditions, phosphoramidates have zwitterionic character. A proton transfer to the phosphoramidate, which results in a more electrophilic phosphorus center, facilitates nucleophilic attack by water.

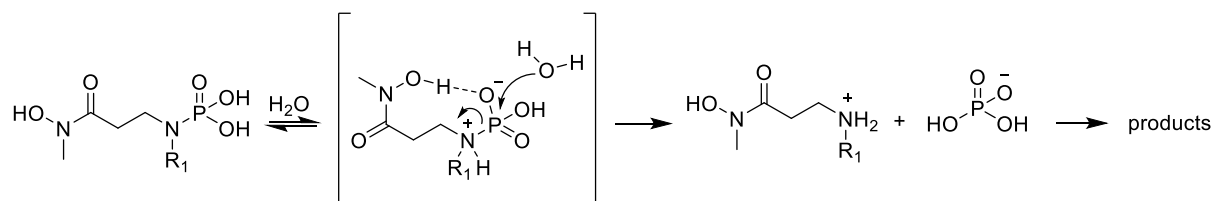


Figure VI.4: Intramolecular acid mechanism of phosphoramidate hydrolysis.

VI.C. Conclusions

Tandem degradation of the target compounds upon deprotection of their respective precursors made that the synthesis of the target compounds could not be realized due to decomposition during the final deprotection step. The lability of these compounds is probably due to the combination of the positively charged nitrogen and the tendency of the phosphoryl group towards resonating forms with a positive charge on the phosphorus atom.

VI.D. Experimental details

General Methods and Materials. See section III.E.

General procedure I: EDC-mediated formation of protected hydroxamate.

To a solution of the acid (1.0 equiv, 0.15 M) in CH₂Cl₂ was added triethylamine (5.0 equiv) and EDC (1.2 equiv). *O*-Benzyl-*N*-methylhydroxylamine TFA salt (1.2 equiv) was added as a 0.5 M solution in CH₂Cl₂ and the mixture stirred overnight at room temperature. Upon completion of the reaction, the mixture was quenched with sat. aq NaHCO₃, extracted three times with CH₂Cl₂, washed with brine, and dried over Na₂SO₄. Column chromatography produced the protected hydroxamic acids **6.3a-b**.

General procedure II: Acidic cleavage of Boc protecting group and phosphorylation of 6.3a-b.

A 0.1 M solution of the *N*-Boc-protected compound **6.3a-b** (1.0 equiv) in CH₂Cl₂/TFA (70:30) and triethylsilane (2 equiv) at 0 °C was stirred for 2 hours, after which an excess of toluene was added to the reaction mixture which was then reduced *in vacuo*. The crude amine was redissolved in CH₂Cl₂ and the pH adjusted to 9 by addition of KOH before washing with water and *in vacuo* concentration. To the 'free' base in CH₂Cl₂ (0.1 M), was added the chlorophosphate (1.3 equiv) and triethylamine (3 equiv) dropwise at 0 °C before warming the mixture to room temperature and stirring for 2 hours. The reaction was quenched with NH₄Cl and after separation, the aqueous layer was extracted three times with CH₂Cl₂, washed once with brine, dried over Na₂SO₄, filtered and concentrated *in vacuo*. Column chromatography gave to access the phosphorylated compounds (**6.4** and **6.6**).

Dibenzyl chlorophosphate (for the preparation of **6.6**) was prepared by dissolving dibenzyl phosphite (1.3 equiv) in dry toluene (0.3 M) followed by the addition of *N*-chlorosuccinimide (1.4 equiv). The mixture was then stirred for 2 hours, filtered and concentrated to obtain an oil, which was immediately used for phosphorylation.

General procedure III: Boron trichloride mediated selective debenylation of 6.4a-b.

A 0.1 M solution of the benzylation hydroxamate in dichloromethane was cooled to -75 °C. BCl₃ (1 M solution in CH₂Cl₂, 3.0 equiv) was added dropwise, and the mixture allowed to stir

at this temperature for 45 min. Next, the reaction mixture was poured into aqueous NaHCO_3 and extracted 4 times with CH_2Cl_2 . The organic fractions were combined, washed with brine, dried (Na_2SO_4), filtered, and concentrated *in vacuo*. The residue was purified by silica gel column chromatography to obtain the free hydroxamate.

General procedure IV: Trimethylbromosilane mediated deprotection of diethyl phosphonates 6.5a-b.

To a 0.1 M solution of starting material in dichloromethane was added BSTFA (4.0 equiv). The mixture was allowed to stir at room temperature for 15 min before an ice bath was installed, and TMSBr (10.0 equiv) was added. The ice bath was removed after 10 min, and the reaction allowed to stir while being monitored by MS and phosphorus NMR. Unexpectedly, several peaks emerged on the MS spectrum, which did not represent the product (or species related to the 'normal' deprotection pathway) and this coincided with a cluster of phosphorus peaks observed on the ^{31}P NMR. Different attempts using a lower concentration of TMSBr and/or keeping the reaction in an ice bath throughout monitoring were futile, as a similar pattern was observed in each case.

General procedure V: Catalytic hydrogenolysis of benzyl protective groups.

The benzyl protected compound (**6.6a-b**) was dissolved in MeOH (10 mg/mL) under a nitrogen atmosphere, and a catalytic amount of Pd/C (10%) was added. The resulting mixture was then stirred under a hydrogen atmosphere while monitoring by MS and ^{31}P NMR. Unfortunately, the unusual deprotection findings described above (general procedure IV) were again the outcome in this case, so that compounds **6.1a-b** were ultimately inaccessible.

Tert-butyl (3-((benzyloxy)(methyl)amino)-3-oxopropyl)carbamate (6.3a). Prepared from compound **6.2a** (1.4 g, 7.40 mmol) according to general procedure I. Clear wax; purification 2:1 Hex/EtOAc v/v; yield 81%. ^1H NMR (300 MHz, CDCl_3) δ_{H} ppm 1.43 (br s, 9H, *t*-Bu), 2.51-2.68 (m, 2H, $-\text{CH}_2-\text{CO}$), 3.20 (s, 3H, $\text{N}-(\text{CH}_3)\text{CO}$), 3.29-3.48 (m, 2H, $\text{N}(\text{Boc})-\text{CH}_2-$), 4.81 (s, 2H, $-\text{CH}_2\text{Ph}$), 7.29-7.47 (m, 5H, Ar-H). ^{13}C -NMR (75 MHz, CDCl_3) δ_{C} ppm 28.4, 32.6, 33.4, 35.8, 76.2, 79.0, 128.7, 129.0, 129.3, 134.2, 155.9, 173.9. HRMS (ESI): calculated for $\text{C}_{16}\text{H}_{25}\text{N}_2\text{O}_4$ $[(\text{M}+\text{H})^+]$, 309.1809; found 309.1827.

Tert-butyl (3-((benzyloxy)(methyl)amino)-3-oxopropyl)(methyl)carbamate (6.3b). Prepared from compound **6.2b** (1.4 g, 6.89 mmol) according to general procedure I. Clear wax; purification 2:1 Hex/EtOAc v/v; yield 83%. ^1H NMR (300 MHz, CDCl_3) δ_{H} ppm 1.44 (br s, 9H, *t*-Bu), 2.52-2.74 (m, 2H, $-\text{CH}_2\text{-CO}$), 2.84 (s, 3H, $\text{N-}(\underline{\text{C}}\text{H}_3)\text{CO}$), 3.20 (s, 3H, $\text{N}(\underline{\text{C}}\text{H}_3)\text{Boc}$), 3.39-3.58 (m, 2H, $\text{N}(\text{Boc})\text{-}\underline{\text{C}}\text{H}_2\text{-}$), 4.83 (s, 2H, $-\text{CH}_2\text{Ph}$), 7.31-7.47 (m, 5H, Ar-H). ^{13}C -NMR (75 MHz, CDCl_3) δ_{C} ppm 28.4, 30.9, 44.9, 76.3, 79.3, 128.6, 128.9, 129.3, 134.2, 155.5. HRMS (ESI): calculated for $\text{C}_{17}\text{H}_{27}\text{N}_2\text{O}_4$ [(M+H) $^+$], 323.1965; found 323.1941.

Tert-butyl (3-((benzyloxy)(methyl)amino)-3-oxopropyl)(4-chlorophenyl)carbamate (6.3c). Compound **6.3a** (740 mg, 2.40 mmol) was dissolved in degassed 1,4-dioxane (5.0 mL) at room temperature, followed by addition of 1-bromo-4-chlorobenzene (515 mg, 2.64 mmol), palladium (II) diacetate (22 mg, 0.10 mmol), Xantphos (186 mg, 13 mole%) and cesium carbonate (1.11 g, 3.4 mmol). The reaction mixture was heated to 110 °C over 48 hours, after which it was cooled to room temperature, sorped on celite and purified by column chromatography (2:1 Hex/EtOAc v/v) to produce 452 mg of the title compound (45%) as a white wax. ^1H NMR (300 MHz, CDCl_3) δ_{H} ppm 1.42 (br s, 9H, *t*-Bu), 2.59-2.74 (m, 2H, $-\text{CH}_2\text{-CO}$), 3.15 (s, 3H, N-CH_3), 3.85-3.98 (m, 2H, $\text{N}(4\text{-ClPh})\text{-}\underline{\text{C}}\text{H}_2\text{-}$), 4.98 (s, 2H, $-\text{CH}_2\text{Ph}$), 7.06-7.41 (m, 9H, Ar-H). ^{13}C -NMR (75 MHz, CDCl_3) δ_{C} ppm 28.3, 31.4, 33.4, 46.2, 76.4, 80.3, 126.1, 127.1, 128.3, 128.7, 134.4, 140.9, 142.3, 154.2, 154.5. HRMS (ESI): calculated for $\text{C}_{22}\text{H}_{28}\text{ClN}_2\text{O}_4$ [(M+H) $^+$], 419.1732; found 419.1749.

Diethyl (3-((benzyloxy)(methyl)amino)-3-oxopropyl)phosphoramidate (6.4a). Prepared from compound **6.3a** (1.1 g, 3.57 mmol) according to general procedure II. Colorless oil; purification 97.5: 2.5 $\text{CH}_2\text{Cl}_2/\text{MeOH}$ v/v; yield 71%. ^1H NMR (300 MHz, CDCl_3) δ_{H} ppm 1.30 (t, $J = 7.1$ Hz, 3H, $-\text{CH}_2\text{-}\underline{\text{C}}\text{H}_3$), 1.31 (t, $J = 7.1$ Hz, 3H, $-\text{CH}_2\text{-}\underline{\text{C}}\text{H}_3$), 2.59 (t, $J = 5.7$ Hz, 2H, $-\text{CH}_2\text{-CO}$), 3.09-3.24 (m, 5H, N-CH_3 , $-\text{NH-}\underline{\text{C}}\text{H}_2\text{-}$), 3.96-4.12 (m, 4H, $\text{P-O-}\underline{\text{C}}\text{H}_2\text{-CH}_3$), 4.83 (s, 2H, $-\text{CH}_2\text{Ph}$), 7.31-7.46 (m, 5H, Ar-H). ^{13}C -NMR (75 MHz, CDCl_3) δ_{C} ppm 16.9 (d, $^3J_{\text{C-P}} = 7.1$ Hz), 31.8, 34.0, 45.0 (d, $^3J_{\text{C-P}} = 4.6$ Hz), 62.4 (d, $^2J_{\text{C-P}} = 6.7$ Hz), 76.4, 128.7, 128.9, 129.2, 129.5, 136.1, 168.1. ^{31}P -NMR (121.5 MHz, CDCl_3): δ_{P} ppm = 8.90. HRMS (ESI): calculated for $\text{C}_{15}\text{H}_{26}\text{N}_2\text{O}_5\text{P}$ [(M+H) $^+$], 345.1574; found 345.1501.

Diethyl (3-((benzyloxy)(methyl)amino)-3-oxopropyl)(methyl)phosphoramidate (6.4b). Prepared from compound **6.3b** (900 mg, 2.79 mmol) according to general procedure II.

Colorless oil; 98:2 CH₂Cl₂/MeOH; yield 78%. ¹H NMR (300 MHz, CDCl₃) δ_H ppm 1.28 (t, *J* = 7.3 Hz, 3H, -CH₂-CH₃), 1.29 (t, *J* = 7.0 Hz, 3H, -CH₂-CH₃), 2.58-2.69 (m, 5H, N-CH₃, -CH₂-CO), 3.21 (s, 3H, N-CH₃), 3.26-3.39 (m, 2H, -N(CH₃)-CH₂-), 3.91-4.10 (m, 4H, P-O-CH₂-CH₃), 4.86 (s, 2H, -CH₂Ph), 7.34-7.45 (m, 5H, Ar-H). ¹³C-NMR (75 MHz, CDCl₃) δ_C ppm 16.1 (d, ³*J*_{C-P} = 7.3 Hz), 31.5, 33.9, (d, ²*J*_{C-P} = 4.1 Hz), 45.0 (d, ³*J*_{C-P} = 4.8 Hz), 62.0 (d, ²*J*_{C-P} = 6.9 Hz), 76.3, 128.6, 128.9, 129.2, 134.3, 164.1. ³¹P-NMR (121.5 MHz, CDCl₃): δ_P ppm = 10.0. HRMS (ESI): calculated for C₁₆H₂₈N₂O₅P [(M+H)⁺], 359.1730; found 359.1748.

Diethyl (3-(hydroxy(methyl)amino)-3-oxopropyl)phosphoramidate (6.5a). Prepared from compound **6.4a** (500 mg, 1.45 mmol) according to general procedure III. Pale yellow oil; purification 94:6 CH₂Cl₂/MeOH v/v; yield 72%. ¹H NMR (300 MHz, CDCl₃) δ_H ppm 1.31 (t, *J* = 6.9 Hz, 3H, -CH₂-CH₃), 1.32 (t, *J* = 7.1 Hz, 3H, -CH₂-CH₃), 2.67 (t, *J* = 7.36 Hz, 2H, -CH₂-CO), 3.08-3.23 (m, 5H, N-CH₃, -NH-CH₂-), 3.96-4.09 (m, 4H, P-O-CH₂-CH₃). ¹³C-NMR (75 MHz, CDCl₃) δ_C ppm 15.1 (d, ³*J*_{C-P} = 7.7 Hz), 33.9 (d, ³*J*_{C-P} = 6.2 Hz), 34.7, 36.7, 62.3 (d, ²*J*_{C-P} = 5.8 Hz), 172.6. ³¹P-NMR (121.5 MHz, CDCl₃): δ_P ppm = 10.01. HRMS (ESI): calculated for C₈H₂₀N₂O₅P [(M+H)⁺], 255.1104; found 255.1201.

Diethyl (3-(hydroxy(methyl)amino)-3-oxopropyl)(methyl)phosphoramidate (6.5b). Prepared from compound **6.4b** (450 mg, 1.26 mmol) according to general procedure III. Pale yellow oil; purification 95:5 CH₂Cl₂/MeOH v/v; yield 74%. ¹H NMR (300 MHz, CDCl₃) δ_H ppm 1.25-1.44 (m, 6H, -CH₂-CH₃), 2.60-2.83 (m, 5H, N-CH₃, -CH₂-CO), 3.23 (s, 3H, N-CH₃), 3.31-3.49 (m, 2H, -N(CH₃)-CH₂-), 3.91-4.09 (m, 4H, -CH₂CH₃). ¹³C-NMR (75 MHz, CDCl₃) δ_C ppm 16.0 (d, ³*J*_{C-P} = 7.64 Hz), 33.4 (d, ³*J*_{C-P} = 4.9 Hz), 33.6 (d, ²*J*_{C-P} = 3.5 Hz), 35.91, 45.2 (d, ²*J*_{C-P} = 6.3 Hz), 62.6 (d, ²*J*_{C-P} = 6.3 Hz), 171.2. ³¹P-NMR (121.5 MHz, CDCl₃): δ_P ppm = 10.70. HRMS (ESI): calculated for C₉H₂₂N₂O₅P [(M+H)⁺], 269.1261; found 269.1280.

Dibenzyl (3-((benzyloxy)(methyl)amino)-3-oxopropyl)phosphoramidate (6.6a). Prepared from compound **6.3a** (650 mg, 2.11 mmol) according to general procedure II. Colorless oil; purification 97:3 CH₂Cl₂/MeOH v/v; yield 64%. ¹H NMR (300 MHz, CDCl₃) δ_H ppm 2.52 (t, *J* = 6.3 Hz, 2H, -CH₂-CO), 3.07-3.25 (m, 5H, N-CH₃, N(CH₃)-CH₂-), 4.71 (s, 2H, -CH₂Ph), 4.97-5.21 (m, 4H, P-O-CH₂-Ph), 7.23-7.42 (m, 15H, Ar-H). ¹³C-NMR (75 MHz, CDCl₃) δ_C ppm 29.5, 33.7 (d, ²*J*_{C-P} = 4.8 Hz), 36.7, 67.9, 76.1, 127.7, 128.1, 128.4, 128.6, 129.0, 129.2, 136.4, 136.5 (d,

$^3J_{C-P} = 8.1$ Hz), 178.0. ^{31}P -NMR (121.5 MHz, CDCl_3): δ_P ppm = 9.50. HRMS (ESI): calculated for $\text{C}_{25}\text{H}_{30}\text{N}_2\text{O}_5\text{P}$ [(M+H) $^+$], 469.1887; found 469.1881.

Dibenzyl (3-((benzyloxy)(methyl)amino)-3-oxopropyl)(methyl)phosphoramidate (6.6b).

Prepared from compound **6.3a** (630 mg, 1.95 mmol) according to general procedure II. Colorless oil; purification 97:3 $\text{CH}_2\text{Cl}_2/\text{MeOH}$ v/v; yield 68%. ^1H NMR (300 MHz, CDCl_3) δ_H ppm 2.50-2.74 (m, 5H, N- CH_3 , $-\text{CH}_2\text{-CO}$), 3.14 (s, 3H, N- CH_3), 3.22-3.40 (m, 2H, N(CH_3)- CH_2 -), 4.75 (s, 2H, $-\text{CH}_2\text{Ph}$), 4.89-5.09 (m, 4H, P-O- CH_2 -Ph), 7.27-7.41 (m, 15H, Ar-H). ^{13}C -NMR (75 MHz, CDCl_3) δ_C ppm 28.1, 29.4, 33.1 (d, $^2J_{C-P} = 5.1$ Hz), 35.4, 67.9 (d, $^2J_{C-P} = 4.8$ Hz), 75.9, 127.0, 127.9, 128.3, 128.5, 129.0, 129.2, 135.8, 136.1 (d, $^3J_{C-P} = 8.4$ Hz), 176.2. ^{31}P -NMR (121.5 MHz, CDCl_3): δ_P ppm = 10.39. HRMS (ESI): calculated for $\text{C}_{26}\text{H}_{32}\text{N}_2\text{O}_5\text{P}$ [(M+H) $^+$], 483.2043; found 483.2056.

REFERENCES

1. Li, Z. Han, J. Jiang, Y.; Browne, P. Knox, R. J. Hua, L. Nitrobenzocyclophosphamides as potential prodrugs for bioreductive activation: synthesis, stability, enzymatic reduction, and antiproliferative activity in cell culture. *Bioorg. Med. Chem.* **2003**, *11*, 4171–4178.
2. Baldwin, A.; Huang, Z.; Jounaidi, Y.; Waxman, D. J. Identification of novel enzyme prodrug combinations for use in cytochrome P450-based gene therapy for cancer. *Arch. Biochem. Biophys.* **2003**, *409*, 197–206.
3. Nguyen, T. M. D.; Chang, S.; Condon, B.; Uchimiya, M.; Fortier, C. Development of an environmentally friendly halogen-free phosphorus-nitrogen bond flame retardant for cotton fabrics. *Polym. Adv. Technol.* **2012**, *23*, 1555–1563.
4. Grapov, A. F. and Mel'nikov, N. N. Organophosphorus fungicides. *Russ. Chem. Rev.* **1973**, *42*, 9, 772–781.
5. Denmark, S. E.; Beutner, G. L. Lewis base catalysis in organic synthesis. *Angew. Chem., Int. Ed.* **2008**, *47*, 1560–1638.
6. Focken, T.; Hanessian, S. Application of cyclic phosphoramidate reagents in the total synthesis of natural products and biologically active molecules. *Beilstein J. Org. Chem.* **2014**, *10*, 1848–1877.
7. Zwierzak, A.; Brylikowska-Piotrowicz, J. Alkylation of diethyl phosphoramidates - a simple route from primary to secondary amines. *J. Angew. Chem., Int. Ed.* **1977**, *16*, 2, 107.
8. Kim, H.; Park, J.; Kim, J. G.; Chang, S. Synthesis of phosphoramidates: a facile approach based on the C-N bond formation via Ir-catalyzed direct C-H amidation. *Org. Lett.* **2014**, *16*, 5466–5469.
9. Le Corre, S. S.; Berchel, M.; Couthon-Gourvès, H.; Haelters, J. P.; Jaffrès, P. A. Atherton-Todd reaction: mechanism, scope and applications. *Beilstein J. Org. Chem.* **2014**, *10*, 1166–1196.
10. Serwa, R.; Wilkening, I.; Del Signore, G.; Muhlberg, M.; Claußnitzer, I.; Weise, C.; Gerrits, M.; Hackenberger, C. P. R. Chemoselective Staudinger-Phosphite reaction of azides for the phosphorylation of proteins. *Angew. Chem. Int. Ed.* **2009**, *48*, 8234–8239.

11. Wang, G.; Yu, Q. Y.; Chen, S. Y.; Yu, X. Q. Copper-catalyzed aerobic oxidative cross coupling of arylamines and dialkylphosphites leading to *N*-arylphosphoramidates. *Tetrahedron Lett.* **2013**, 54, 6230–6232.
12. Dhineshkumar, J. and Prabhu, K. R. Cross-hetero-dehydrogenative coupling reaction of phosphites: A catalytic metal-free phosphorylation of amines and alcohols. *Org. Lett.* **2013**, 15 23, 6062–6065.
13. Dar, B. A.; Dangroo, N. A.; Gupta, A.; Wali, A.; Khuroo, M. A.; Vishwakarma, R. A.; Singh, B. Iodine catalyzed solvent-free cross-dehydrogenative coupling of arylamines and H-phosphonates for the synthesis of *N*-arylphosphoramidates under atmospheric conditions. *Tetrahedron Lett.* **2014**, 55, 1544–1548.
14. Woo, Y.; Fernandes, R. P. M.; Proteau, P. J. Evaluation of fosmidomycin analogs as inhibitors of the *Synechocystis* sp. PCC6803 1-deoxy-D-xylulose 5-phosphate reductoisomerase. *Bioorg. Med. Chem.* **2006**, 14, 2375–2385.
15. Chanley, J. D. and Feageson, E. A study of the hydrolysis of phosphoramides. II. Solvolysis of phosphoramidic acid and comparison with phosphate esters. *J. Am. Chem. Soc.* **1963**, 85, 1181–1190.
16. Halmann, M.; Lapidot, A.; Samuel, D. The mechanism of hydrolysis of phosphoramidic acid. *J. Chem. Soc.* **1963**, 242, 1299–1303.
17. Maiti, M.; Michielssens, S.; Dyubankova, N.; Mohitosh, M.; Lescrinier, E.; Ceulemans, A.; Herdewijn, P. Influence of the nucleobase and anchimeric assistance of the carboxyl acid groups in the hydrolysis of amino acid nucleoside phosphoramidates. *Chem. Eur. J.* **2012**, 18, 857–868.
18. Choy, C. J.; Geruntho, J. J.; Davis, A. L.; Berkman, C. E. Tunable pH-Sensitive Linker for Controlled Release. *Bioconjug. Chem.* **2016**, Mar 2: DOI:10.1021/acs.bioconjchem.6b00027.

Chapter VII

CYCLIC PHOSPHONATE

PRODRUGS OF FR900098

VII. CYCLIC PHOSPHONATE PRODRUGS OF FR900098

VII.A. Introduction

As a result of extensive efforts to overcome the moderate bioavailability of fosmidomycin which mainly stems from the polarity of its phosphonate group, several prodrugs of this lead have been developed (see I.E.3.2). In this regard, the acyloxymethyl- and alkoxycarbonyloxymethyl esters are amongst the most explored groups and have resulted in analogues that inhibit the multiplication of *P. falciparum* blood stages with IC₅₀ values in the single-digit nanomolar range. Such phosphonate prodrug moieties are established in marketed antiviral drugs, e.g., the bis-pivaloyloxymethyl ester of adefovir (Hepsera, **7.1**, Figure VII.1) and the diisopropylloxycarbonyloxymethyl ester of tenofovir fumarate (Viread, **7.2**). These acyclic nucleoside phosphonates are used for the treatment of hepatitis B and HIV infections.¹ Despite their successful development, *in vivo* decomposition-related toxicity is a current concern especially during long term treatment.^{2,3}

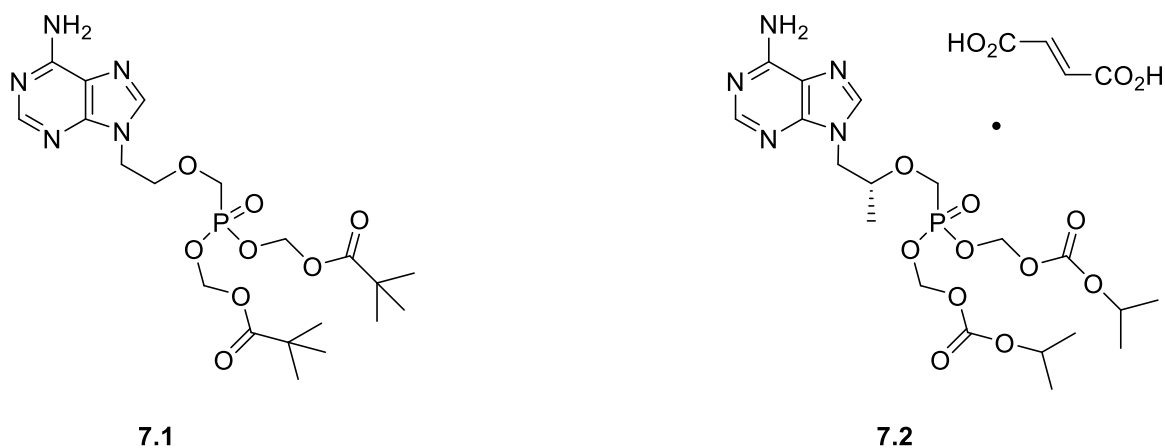
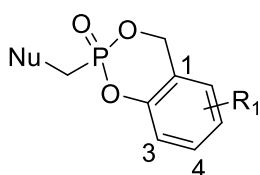


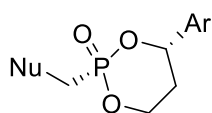
Figure VII.1: Structures of Hepsera (**7.1**) and Viread (**7.2**).

Reducing the amount of debris generated from the *in vivo* hydrolysis of known effective prodrug moieties through a cyclic prodrug technology is an interesting challenge. In this strategy, only one of the phosphonate O is connected to the prodrug moiety, while the second O is temporarily locked in a cyclic structure with an integral part of the parent compound. The concept of cyclic phosphonate masks has been studied before.

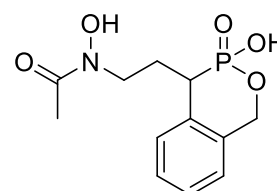
Cyclosaligenyl phosphonate prodrugs^{4,5}, which present a salicyl alcohol (**7.3**, Figure VII.2) as the only masking unit for both hydroxyl moieties of the phosphonic acid, have been successfully applied for the intracellular delivery of a number of antiviral nucleotides (e.g., azidothymidine).³ The HepDirect prodrugs, which contain a cyclic 1-aryl-1,3-propanyl ester (**7.4**), target phosph(on)ate-containing drugs to the liver for antiviral therapy, due to their selective activation by a liver specific cytochrome P450 isozyme, CYP3A4.⁶ In the context of antimalarials, HepDirect prodrugs will be relevant for targeting hypnozooids or for prophylactic use. A more effective plan, however, would be the development of such cyclic prodrug entities that neutralize the disease-causing erythrocytic stage of the malaria parasite or that access and kill Mtb cells since these do not concentrate in hepatocytes.



7.3



7.4

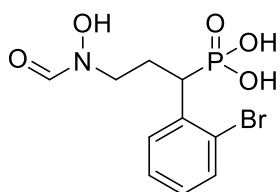


7.5

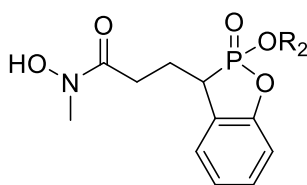
R₁ = H, 6-F, 3-Me, 3-tBu...

Nu = nucleoside; Ar = aryl

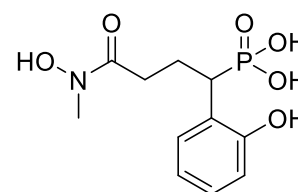
R₂ = H, acyloxy, alkoxy carbonyl,
alkyl, aryl, alkylaryl...



7.6



7.7



7.8

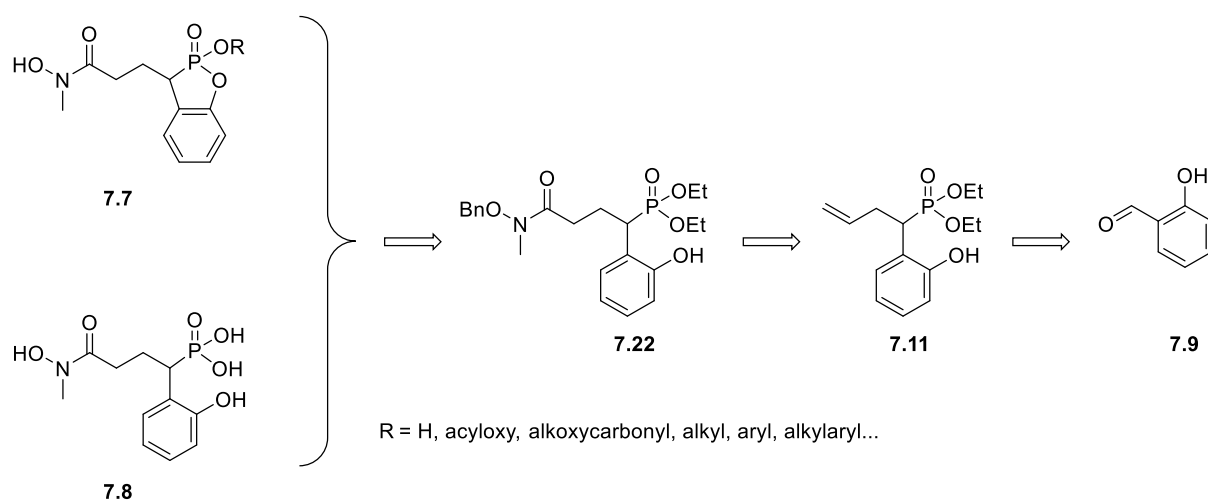
Figure VII.2: Structures of known cyclic phosphonate prodrug moieties (**7.3** and **7.4**), reported α -aryl fosmidomycin analogues (**7.5** and **7.6**) and planned derivatives (**7.7** and **7.8**).

Several fosmidomycin/FR900098 analogues bearing a (substituted) phenyl ring in α -position have been reported to elicit promising inhibitory activity both at the levels of isolated PfDxr or in parasite growth assays (see I.E.2.2). Andaloussi *et al.* reported on the ability of α -aryl-substituted fosmidomycin analogues to inhibit MtbDxr and intact *Mycobacteria* cells.⁷ This study featured the bicyclic compound **7.5**, which unfortunately, lacked activity against the

enzyme and was also shown to have MIC > 32 µg/mL. However, the IC₅₀ value of the bromo derivative **7.6** (5.6 µM) indicates that substitution in *ortho* position is tolerated by the enzyme. While steric constraints (stemming from the ring architecture in **7.5**) may unfavorably influence binding to the enzyme, the (possibly) unliberated phosphonate hydroxyl may have sacrificed a part of the crucial H-bonding that is necessary to anchor the analogue to the active site. The synthesis of compounds **7.7**, would be a good starting point to investigate the potential of new cyclic prodrug derivatives. We envisioned that upon entry into the pathogen cells, the compounds would hydrolyze to the *α-ortho*-hydroxyphenyl analogue **7.8**, while releasing halve as much side products as the corresponding 'bis-' prodrug analogues. Preparation of compound **7.8** was also planned, to serve as a control in the assessment of this cyclic prodrug paradigm.

VII.B. Synthesis

A retrosynthesis for the preparation of **7.7** and **7.8** is shown in Scheme VII.1. We planned to access compounds **7.7** by cyclizing intermediate **7.22** via a Michaelis-Arbusov reaction and then substituting the phosphonate ethyl group with various prodrug moieties before final debenzoylation of the hydroxamate function.

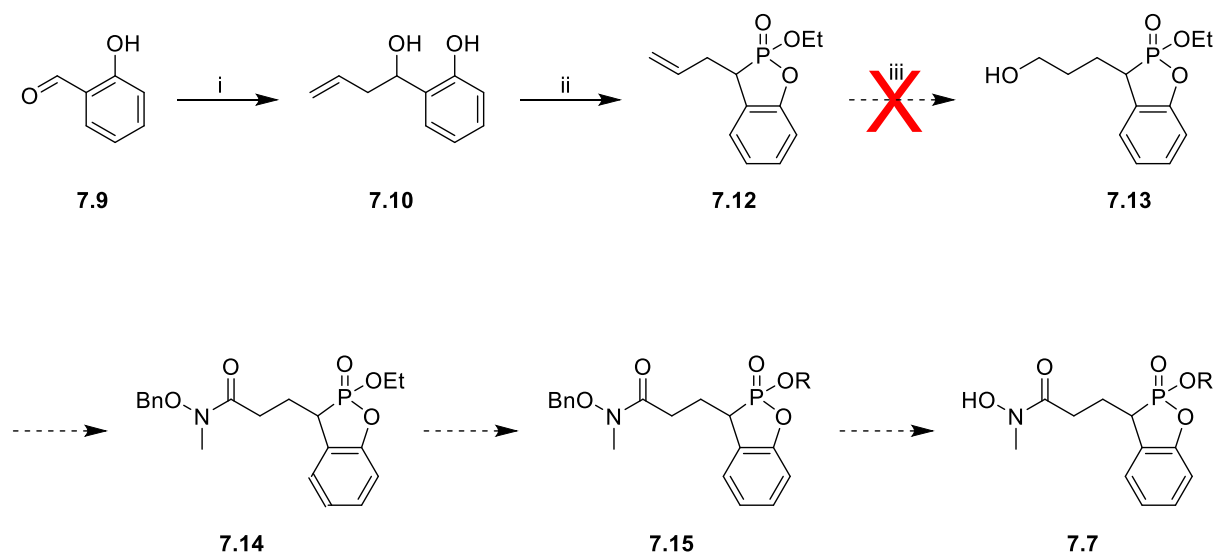


Scheme VII.1: Retrosynthesis of the cyclic prodrug derivatives (**7.7**) and *α-ortho*-hydroxyphenyl FR900098 analogue (**7.8**) starting from salicylaldehyde.

The uncyclized parent compound **7.8** would be obtained from debenzoylation and cleavage of the ethyl groups in **7.22**. Hydroboration of **7.11**, followed by Dess-Martin periodinane

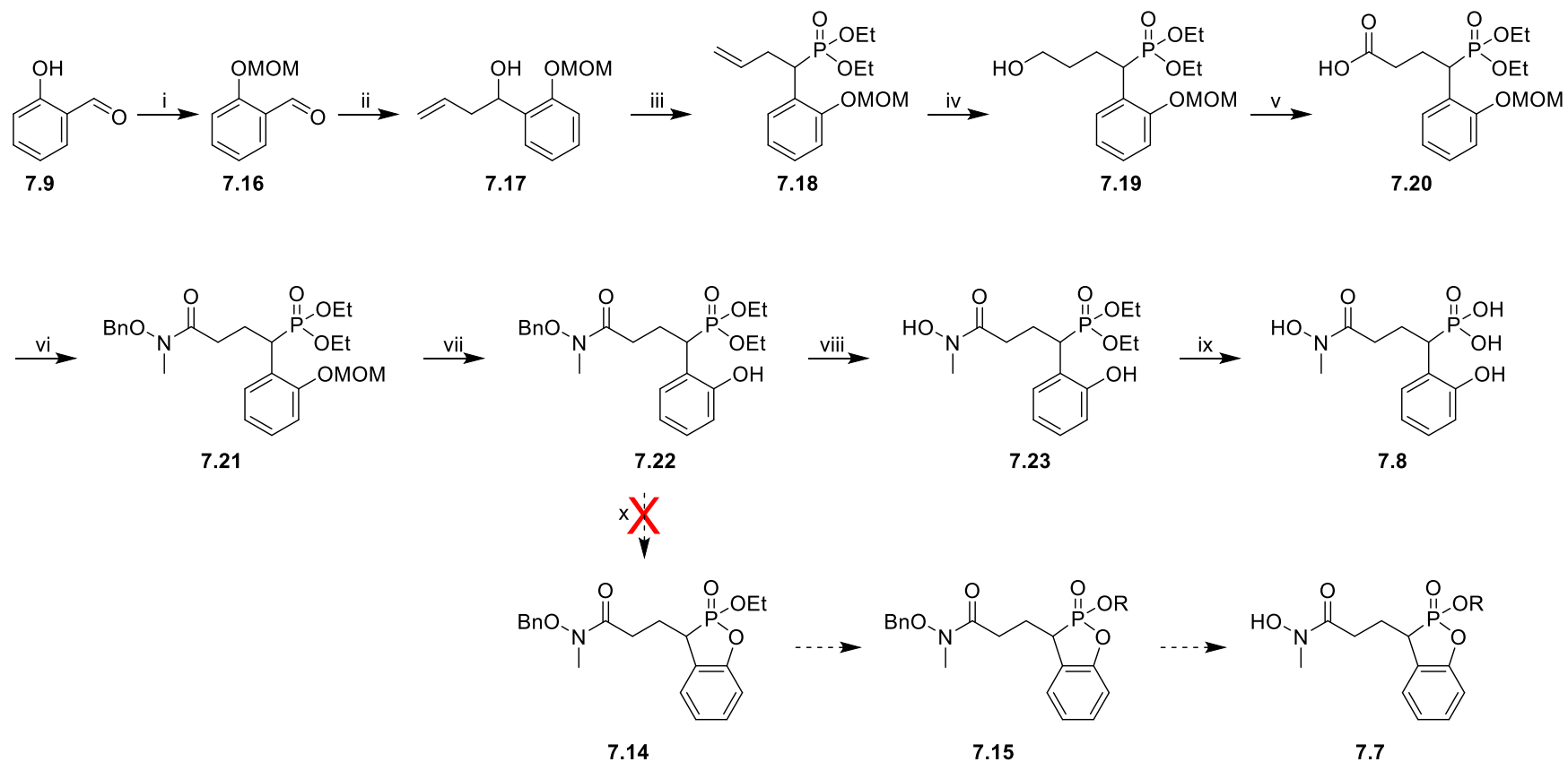
oxidation of the resulting primary alcohol and hydroxamate formation affords compound **7.22**. Intermediate **7.11** is attainable through zinc-mediated addition of allyl bromide to commercially available salicylaldehyde (**7.9**) and subsequent Arbusov reaction.

The synthesis of **7.7** (Scheme VII.2) commenced, as envisioned, with the allylation of purchased salicylaldehyde (**7.9**) according to the procedure described by Einhorn and Luche.⁸ Phosphorylation of the resulting allyl diol **7.10** was accomplished by refluxing it in dry toluene in the presence of triethyl phosphite to obtain **7.12**, albeit in low yield. Attempts to transform **7.12** into **7.13** by hydroboration did not afford the desired compound, rather, yielding a reaction mixture fraught with polar constituents that remain on the base-line during thin layer chromatography (TLC) analysis and accordingly do not elute when loaded on a silica gel column. This failure, barely two steps into the synthesis, together with a low yield recorded for the previous step led to the suspicion that the five membered ring in **7.12** is susceptible to reaction conditions, necessitating a switch to a synthetic approach that allows late stage ring formation.



Scheme VII.2 Reagents and conditions: (i) Zn, allyl bromide, THF, NH₄Cl, rt, 1.5 h, 92%; (ii) (EtO)₃P, dry toluene, 130 °C, 48 h, 21%; (iii) BH₃, THF, NaBO₃·H₂O, H₂O, 0 °C to rt, 4 h.

Thus an alternative route (Scheme VII.3) was explored, starting still from salicylaldehyde. Treatment of **7.9** with methoxymethyl chloride afforded **7.16** which was then allylated to obtain **7.17**.

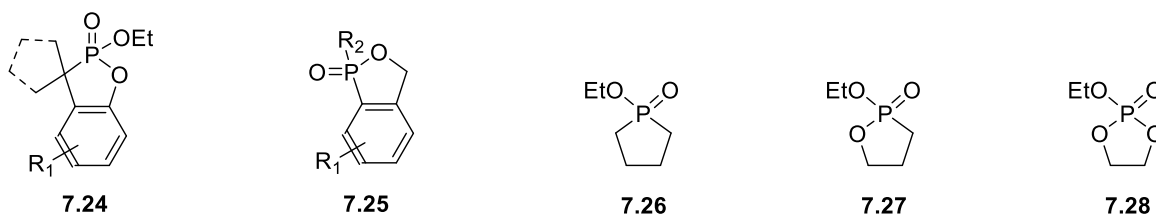


Scheme VII.3 Reagents and conditions: (i) CH_2Cl_2 , DIPEA, MOMCl, rt, 8 h, 94%; (ii) $\text{CH}_2=\text{CHCH}_2\text{Br}$, Zn, THF, NH_4Cl , rt, 2 h, 91%; (iii) $\text{P}(\text{OEt})_3$, ZnBr_2 , rt, 1.5 h, 89%; (iv) BH_3 , THF, $\text{NaBO}_3 \cdot \text{H}_2\text{O}$, H_2O , 0 °C to rt, 4.5 h, 93%; (v) TEMPO, BAIB, MeCN, H_2O , rt, 18 h, 73%; (vi) $\text{CH}_3\text{N}(\text{OH})\text{H}$, EDC.HCl, Et_3N , CH_2Cl_2 , rt, 18 h, 74%; (vii) PTSA. H_2O , MeOH, H_2O , rt, 42 h, 87%; (viii) H_2 , Pd/C, MeOH, 25 °C, 15 min, 62%; (ix) TMSBr, CH_2Cl_2 , H_2O , $\text{NH}_4\text{OHaq.}$, 48 h, quant.; (x) dry toluene, 130 °C, 36 h.

Phosphorylation with triethyl phosphite produced **7.18**, which was easily hydroborated to obtain **7.19**. Oxidation of **7.19** with catalytic 2,2,6,6-tetramethyl-1-piperidinyloxy (TEMPO) in the presence of (diacetoxyiodo)benzene (BAIB) generated the corresponding carboxylic acid **7.20**, which was then coupled with *N*-methyl *O*-benzyl hydroxyl amine to afford the fully protected intermediate **7.21**. Acidic cleavage of the methoxymethyl ether in **7.21** yielded **7.22**, an intermediate from where divergence could be exploited to arrive at both **7.7** and **7.8**. Thus intermediate **7.22** was debenzylated to **7.23**. Bromotrimethyl silane mediated removal of the phosphonate esters of **7.23** followed by basic workup gave access to the target **7.8** as the bisammonium salt.

Attempts to obtain the cyclized precursor **7.14** were, however, unsuccessful. We observed that at the end of the reaction, TLC analysis typically indicated a major product spot but unfortunately, after filtration of the reaction mixture and *in vacuo* concentration, mass spectrometry analysis revealed a mixture of the target product, starting material and a product derived from hydrolysis of the five membered ring in **7.14**. Efforts to resolve this mixture by column chromatography failed as only a small amount of the product was recovered, which in turn generated multiple ^{31}P signals and cumbersome ^1H and ^{13}C NMR spectra. In a subsequent attempt, mass spectrometry analysis of the crude reaction mixture and the residue after filtration showed that **7.14** was indeed formed during the reaction, but contaminated with the mono-protected phosphonate form, responsible for the baseline spot on the TLC.

Remarkably, Eom and collaborators did not report any decay problems during the synthesis of related benzoxaphosphole 1- and 2-oxides (Figure VII.3, **7.24** and **7.25** respectively) from phosphonic and phosphinic acids.⁹ However, an earlier investigation by Aksnes and Bergesen¹⁰ revealed that there is an enormous increase (factor of 5×10^4) in hydrolysis rate when moving from the phospholan **7.26** to the oxaphospholan **7.27** ester and also a strong increase when moving from the latter to the dioxaphospholan ester **7.28**.



R₁ = Me, OMe, F₃Me....; R₂ = Me, OMe, OEt, Ph

Figure VII.3: Structures of cyclic phosphoryl esters.

The authors observed that hydrolysis in water or water-alcohol mixtures is exclusively by ring opening and attributed the high rate to a release of ring strain during hydrolysis, as well as a favorable entropy of activation. These findings, together with our experience in handling compound **7.14**, make clear that the target cyclic prodrugs **7.7** are not attainable according to our synthetic plan and/or probably too labile to serve as useful prodrugs.

VII.C. Conclusion

In conclusion, the objective of preparing cyclic phosphonate prodrugs with one phosphonate O masked by a substituent on the molecule is theoretically attractive, but the synthesis and purification of such entities proved problematic. The 3H-benzo [α][1,2]oxaphosphole 2-oxide system shows to be prone to cleavage, making mono-protection of the other phosphonate O a serious challenge, and undermining the envisaged prodrug initiative.

VII.D. Experimental procedures

General Methods and Materials. See section III.E.

2-(1-Hydroxybut-3-en-1-yl)phenol (7.10). To a solvent mixture of THF and NH₄Cl (50 mL, 1:3), was added salicylaldehyde (2.67 mL, 25 mmol), followed by zinc granules (3.3 g, 50 mmol) and allyl bromide (1.4 mL, 50 mmol) at room temperature. An exothermic reaction ensued with disappearance of the zinc granules, and the mixture was stirred for 1.5 hours after which TLC analysis confirmed a completed reaction. Transfer of the mixture to a separation funnel was followed by aqueous layer extraction (three times with 75 mL EtOAc). The organic fractions were pooled, dried over Na₂SO₄, filtered and concentrated under reduced pressure before purification by silica gel chromatography (gradient of 0 to 20% EtOAc in toluene) to obtain 3.78 g of **7.10** as a colorless oil (yield 92%). ¹H NMR (300 MHz, CDCl₃) δ _H

ppm 2.46-2.70 (m, 2H, -CH₂-), 3.07 (s, 1H, -CH(CH₂)-OH), 4.83 (t, $J = 6.3$ Hz, -CH(CH₂)-OH), 5.17 (app. d, $J = 12.7$ Hz, 2H, CH₂=CH-), 5.73-5.89 (m, 1H, CH₂=CH-), 6.78-6.87 (m, 2H, Ar-H), 6.95 (dd, $J = 1.8$ Hz, 7.4 Hz, 1H, Ar-H), 7.15 (td, $J = 1.8$ Hz, 7.3 Hz, 1H, Ar-H), 8.05 (s, 1H, Ar-OH). ¹³C-NMR (75 MHz, CDCl₃) δ_C ppm 42.1, 74.6, 117.1, 119.2, 119.9, 126.5, 127.2, 128.9, 133.9, 155.3. HRMS (ESI): calculated for C₁₀H₁₃O₂ [(M+H)⁺], 165.0910; found 165.0918.

3-Allyl-2-ethoxy-3H-benzo[d][1,2]oxaphosphole 2-oxide (7.12). In the presence of powdered 4 Å molecular sieves, a solution of **7.10** (500 mg, 3.05 mmol) and triethyl phosphite (0.53 mL, 3.05 mmol) in dry toluene (15 mL) and was stirred under reflux for 36 hours. Solvent evaporation under vacuum and column chromatography (0 to 20% EtOAc in toluene) afforded 158 mg of **7.12** (yield 21%) as a brown oil. ¹H NMR (300 MHz, CDCl₃) δ_H ppm 1.37 (t, $J = 6.9$ Hz, 3H, -CH₂CH₃), 2.47-2.84 (m, 2H, -CH₂-), 3.29-3.43 (m, 1H, P-CH(Ar)-), 4.20-4.38 (m, 2H, -CH₂CH₃), 5.11-5.34 (m, 2H, CH₂=CH-), 5.91-6.07 (m, 1H, CH₂=CH-), 6.96-7.09 (m, 2H, Ar-H), 7.19-7.28 (m, 2H, Ar-H). ¹³C-NMR (75 MHz, CDCl₃) δ_C ppm 16.4 (d, ³J_{C-P} = 6.1 Hz), 32.9 (d, ²J_{C-P} = 6.1 Hz), 35.5 (d, ¹J_{C-P} = 124.2 Hz), 63.7 (d, ²J_{C-P} = 6.9 Hz), 117.8, 123.3, 125.68, 127.2 (d, ²J_{C-P} = 6.5 Hz), 128.8, 129.0 (d, ³J_{C-P} = 7.7 Hz), 134.6 (d, ³J_{C-P} = 8.7 Hz), 152.0 (d, ³J_{C-P} = 9.2 Hz). ³¹P-NMR (121.5 MHz, CDCl₃): δ_P ppm = 47.1. HRMS (ESI): calculated for C₁₂H₁₆O₃P [(M+H)⁺], 239.0832; found 239.0810.

2-Ethoxy-3-(3-hydroxypropyl)-3H-benzo[d][1,2]oxaphosphole 2-oxide (7.13). Compound **7.12** (432 mg, 1.81 mmol) was dissolved in 18 mL of THF and BH₃ (1 M solution in THF, 2 mL) was added at 0 °C. After 10 minutes, the ice bath was removed and the reaction mixture allowed to slowly rise to room temperature while stirring over 2 hours. Water (18 mL) and NaBO₃·H₂O (199 mg) was added and the mixture stirred for another 2 hours after which, it was diluted with EtOAc, the organic phase collected and the aqueous layer extracted three times with EtOAc. The combined organic fractions were washed with water and brine, dried over Na₂SO₄, filtered and concentrated *in vacuo* and TLC analysis showed the product to remain at the baseline, and would not elute at eluent polarities higher than expected. Attempts to purify this by silica gel chromatography failed, as the product did not elute.

2-(Methoxymethoxy)benzaldehyde (7.16). Methoxymethyl chloride (2.38 mL, 30.71 mL) was added dropwise to a solution of salicylaldehyde (**7.9**; 2.5 g, 20.47 mmol) and DIPEA (15 mL, 81.87 mmol) in CH₂Cl₂ (102 mL) at room temperature. After stirring for 4 h, water was added

and the organic layer separated. The aqueous layer was further extracted with CH₂Cl₂, (3 X 150 mL), the combined organic extracts were dried (Na₂SO₄) and the solvent was removed *in vacuo*. The crude product was purified by flash chromatography (hexane/EtOAc, 9:1) to give **7.16** (3.20 g, 94 %) as a pale brownish oil. ¹H NMR (300 MHz, CDCl₃) δ_H 3.53 (s, 3 H, CH₃-O-CH₂-), 5.34 (s, 2H, CH₃-O-CH₂-), 7.04 (t, *J* = 7.4 Hz, 1 H, Ar-H), 7.21 (d, *J* = 8.4 Hz, 1 H, Ar-H), 7.50–7.57 (m, 1 H, Ar-H), 7.83 (dd, *J* = 2.1, 8.0 Hz, 1 H, Ar-H), 10.51 (d, *J* = 1.0 Hz, 1 H, CHO). ¹³C-NMR (75 MHz, CDCl₃) δ_C ppm = 56.3, 95.1, 114.9, 121.5, 125.5, 128.8, 135.5, 160.1, 190.0.

1-(2-(Methoxymethoxy)phenyl)but-3-en-1-ol (7.17). To a solution of compound **7.16** (3 g, 18.05 mmol) in a solvent mixture of THF and NH₄Cl (40 mL, 1:3) was added zinc granules (2.36 g, 36.12 mmol) and allyl bromide (3.20 mL, 36.12 mmol) at room temperature. An exothermic reaction proceeded with disappearance of the zinc granules, and the mixture was stirred for 2 hours after which TLC analysis confirmed a completed reaction. The mixture was transferred to a separation funnel and the organic phase was separated from the aqueous layer which was then extracted with EtOAc (3 X 70 mL). The combined organic fractions were pooled, dried over Na₂SO₄, filtered and concentrated under reduced pressure. Purification by silica gel chromatography afforded 3.42 g of **7.17** as a yellow oil (yield 91%). ¹H NMR (300 MHz, CDCl₃) δ_H ppm 2.56–2.93 (m, 2H, -CH₂-), 3.34 (s, 3 H, CH₃-O-CH₂-), 5.10 (t, *J* = 5.9 Hz, -CH(CH₂)-OH), 5.20 (m, 2H, CH₂=CH-), 5.34 (s, 2H, CH₃-O-CH₂-), 5.41–5.90 (m, 1H, CH₂=CH-), 6.78–6.86 (m, 2H, Ar-H), 6.90 (m, 1H, Ar-H), 7.22 (td, *J* = 1.9 Hz, 7.1 Hz, 1H, Ar-H). ¹³C-NMR (75 MHz, CDCl₃) δ_C ppm 42.2, 53.1, 69.9, 91.4, 117.2, 119.7, 119.8, 126.7, 127.2, 128.9, 133.9, 154.9. HRMS (ESI): calculated for C₁₂H₁₇O₃ [(M+H)⁺], 209.1172; found 209.0991.

Diethyl (1-(2-(methoxymethoxy)phenyl)but-3-en-1-yl)phosphonate (7.18). To a solution of compound **7.17** (634 mg, 3.04 mmol) and triethylphosphite (2.65 mL, 15.23 mmol) at room temperature, zinc bromide (760 mg, 3.35 mmol) was added and the mixture allowed to stir for 1.5 hours. After consumption of the starting material (monitored by TLC), the reaction mixture was transferred to a separation funnel containing ice and 2N HCl solution. The organic layer was separated and the aqueous layer extracted with EtOAc (3 X 50 mL), dried (Na₂SO₄), filtered and the solvent removed under *vacuo*. Flash column chromatography (toluene/EtOAc; 1:1) afforded 889 mg of **7.18** as a colorless oil (yield 89%). ¹H NMR (300

MHz, CDCl₃) δ_{H} ppm 1.09 (t, $J = 7.0$ Hz, 3H, -CH₂CH₃), 1.28 (t, $J = 7.3$ Hz, 3H, -CH₂CH₃), 2.58-2.93 (m, 2H, -CH(Ar)-CH₂CH=C), 3.48 (s, 3H, CH₃-O-CH₂-), 3.70-4.15 (m, 5H, P-CH(Ar)-CH₂-, -CH₂CH₃), 4.85-5.02 (m, 2H, CH₂=CH-), 5.20 (s, 2H, CH₃-O-CH₂-), 5.54-5.71 (m, 1H, CH=CH₂-), 6.97-7.11 (m, 2H, Ar-H), 7.14-7.22 (m, 1H, Ar-H), 7.48 (dt, $J = 2.1$ Hz, 7.7 Hz, 1H, Ar-H). ¹³C-NMR (75 MHz, CDCl₃) δ_{C} ppm 16.20 (d, ³J_{C-P} = 5.7 Hz), 16.4 (d, ³J_{C-P} = 6.0 Hz), 34.2 (d, ²J_{C-P} = 2.3 Hz), 34.9 (d, ¹J_{C-P} = 138.0 Hz), 56.0, 61.7 (d, ²J_{C-P} = 7.6 Hz), 62.3 (d, ²J_{C-P} = 7.1 Hz), 94.6, 114.1 (d, ⁴J_{C-P} = 2.3 Hz), 116.4, 121.8 (d, ⁴J_{C-P} = 3.6 Hz), 125.0 (d, ²J_{C-P} = 6.9 Hz), 127.9 (d, ⁵J_{C-P} = 3.5 Hz), 129.2 (d, ³J_{C-P} = 4.6 Hz), 135.4 (d, ³J_{C-P} = 16.3 Hz), 155.1 (d, ³J_{C-P} = 8.2 Hz). ³¹P-NMR (121.5 MHz, CDCl₃): δ_{P} ppm = 29.1. HRMS (ESI): calculated for C₁₆H₂₆O₅P [(M+H)⁺], 329.1512; found 329.1499.

Diethyl (4-hydroxy-1-(2-(methoxymethoxy)phenyl)butyl)phosphonate (7.19). Compound **7.18** (2.97 g, 9.05 mmol) was dissolved in 90 mL of THF and BH₃ (1 M solution in THF, 10 mL) was added at 0 °C. After 10 minutes, the ice bath was removed and the reaction mixture allowed to slowly rise to room temperature while stirring over 2.5 hours. Water (90 mL) and NaBO₃·H₂O (1.04 g, 10 mmol) was added and the mixture stirred for another 2 hours after which, it was diluted with EtOAc, the organic phase collected and the aqueous layer extracted three times with EtOAc. The combined organic fractions were washed with water and brine, dried over Na₂SO₄, filtered and column chromatography (CH₂Cl₂/MeOH; 97:3) gave access to **7.19** (2.92 g, 93% yield). ¹H NMR (300 MHz, CDCl₃) δ_{H} ppm 1.08 (t, $J = 7.4$ Hz, 3H, -CH₂CH₃), 1.26 (t, $J = 7.0$ Hz, 3H, -CH₂CH₃), 1.47 (app. quint. $J = 7.8$ Hz, 2H, C(Ar)H-CH₂-CH₂-), 1.84-2.29 (m, 2H, C(Ar)H-CH₂-CH₂-), 2.64 (s, 1H, OH), 3.48 (s, 3H, CH₃-O-CH₂-), 3.56 (t, $J = 6.5$ Hz, 2H, -CH₂-CH₂-OH), 3.67-4.15 (m, 5H, P-CH(Ar)-CH₂-, -CH₂CH₃), 5.18 (s, 2H, CH₃-O-CH₂-), 7.00 (t, $J = 5.6$ Hz, 1H, Ar-H), 7.06-7.22 (m, 2H, Ar-H), 7.47 (app. dt, $J = 2.2$ Hz, 7.7 Hz, Ar-H). ¹³C-NMR (75 MHz, CDCl₃) δ_{C} ppm 16.1 (d, ³J_{C-P} = 5.6 Hz), 16.3 (d, ³J_{C-P} = 6.5 Hz), 26.2 (d, ²J_{C-P} = 2.5 Hz), 30.5 (d, ³J_{C-P} = 14.9 Hz), 34.4 (d, ¹J_{C-P} = 139.3 Hz), 56.0, 61.6 (d, ²J_{C-P} = 7.5 Hz), 61.9, 62.3 (d, ²J_{C-P} = 7.5 Hz), 94.5, 114.0 (d, ⁴J_{C-P} = 2.5 Hz), 121.9 (d, ³J_{C-P} = 3.5 Hz), 125.2 (d, ²J_{C-P} = 6.3 Hz), 127.9 (d, ⁴J_{C-P} = 3.7 Hz), 128.9 (d, ³J_{C-P} = 5.47 Hz), 155.2 (d, ³J_{C-P} = 8.3 Hz). ³¹P-NMR (121.5 MHz, CDCl₃): δ_{P} ppm = 29.7. HRMS (ESI): calculated for C₁₆H₂₈O₆P [(M+H)⁺], 347.1618; found 347.1619.

4-(Diethoxyphosphoryl)-4-(2-(methoxymethoxy)phenyl)butanoic acid (7.20). TEMPO (0.32 g, 2.07 mmol) and BAIB (7.36 g, 22.85 mmol) were added to a solution of **7.19** in a mixture of

water and acetonitrile (50 mL, 1:1). The reaction mixture was stirred at room temperature until TLC analysis indicated a complete reaction. The reaction then quenched with a 5% aqueous Na₂S₂O₃, the organic layer separated and the aqueous layer extracted with EtOAc (3 X 100 mL). Column chromatography (7% MeOH in CH₂Cl₂ and 0.5 mL CH₃COOH) yielded **7.20** as an oil. ¹H NMR (300 MHz, CDCl₃) δ_H ppm 1.09 (t, *J* = 7.1 Hz, 3H, -CH₂CH₃), 1.28 (t, *J* = 7.1 Hz, 3H, -CH₂CH₃), 2.01-2.50 (m, 4H, -CH₂-CH₂-CO), 3.47 (s, 3H, CH₃-O-CH₂-), 3.70-4.15 (m, 5H, P-CH(Ar)-CH₂-, -CH₂CH₃), 5.17 (s, 3H, CH₃-O-CH₂-), 6.96-7.24 (m, 3H, Ar-H), 7.47 (dt, *J* = 1.9 Hz, 7.8 Hz, 1H, Ar-H). ¹³C-NMR (75 MHz, CDCl₃) δ_C ppm 16.1 (d, ³J_{C-P} = 5.8 Hz), 16.3 (d, ³J_{C-P} = 6.0 Hz), 25.2, 31.9 (d, ³J_{C-P} = 16.6 Hz), 34.1 (d, ¹J_{C-P} = 139.5 Hz), 56.0, 62.0 (d, ²J_{C-P} = 7.9 Hz), 62.7 (d, ²J_{C-P} = 7.4 Hz), 94.6, 114.1, 122.1 (d, ⁴J_{C-P} = 3.9 Hz), 124.3 (d, ²J_{C-P} = 6.9 Hz), 128.4 (d, ⁵J_{C-P} = 2.4 Hz), 129.0 (d, ³J_{C-P} = 4.6 Hz), 155.4 (d, ²J_{C-P} = 8.6 Hz), 176.9. ³¹P-NMR (121.5 MHz, CDCl₃): δ_P ppm = 28.9. HRMS (ESI): calculated for C₁₆H₂₆O₇P [(M+H)⁺], 361.1411; found 361.1362.

Diethyl (4-((benzyloxy)(methyl)amino)-1-(2-(methoxymethoxy)phenyl)-4-oxobutyl)phosphonate (7.21). To a solution of the acid **7.20** (3.50 g, 9.71 mmol) and EDC.HCl (2.23 g, 11.66 mmol) in CH₂Cl₂ (77 mL) was added *O*-Benzyl-*N*-methylhydroxylamine (1.60 g, 11.66 mmol) and Et₃N (8 mL, 58.28 mmol). After stirring overnight at room temperature, water was added and the mixture was extracted with CH₂Cl₂ (3 X 150 mL). The organic layer was washed with brine, dried over Na₂SO₄ and after evaporation of the solvent, the residue was purified by column chromatography (CH₂Cl₂/MeOH; 97:3) affording compound **7.21** (3.45 g, 74%) as a yellow oil. ¹H NMR (300 MHz, CDCl₃) δ_H ppm 1.09 (t, *J* = 7.0 Hz, 3H, -CH₂CH₃), 1.28 (t, *J* = 7.0 Hz, 3H, -CH₂CH₃), 2.08-2.56 (m, 4H, -CH₂-CH₂-CO), 3.13 (s, 3H, N-CH₃), 3.43 (s, 3H, CH₃-O-CH₂-), 3.73-4.16 (m, 5H, -CH₂CH₃, P-CH(Ar)-CH₂-), 4.59 (s, 2H, -CH₂Ph), 5.15 (s, 2H, CH₃-O-CH₂-), 6.96-7.35 (m, 8H, Ar-H), 7.50 (dt, *J* = 2.2 Hz, 7.81 Hz, 1H, Ar-H). ¹³C-NMR (75 MHz, CDCl₃) δ_C ppm 16.1 (d, ³J_{C-P} = 5.7 Hz), 16.3 (d, ³J_{C-P} = 7.0 Hz), 24.7, 30.0 (d, ³J_{C-P} = 16.5 Hz), 34.3 (d, ¹J_{C-P} = 140.1 Hz), 55.9, 61.7 (d, ²J_{C-P} = 8.3 Hz), 62.2 (d, ²J_{C-P} = 8.3 Hz), 76.04, 94.6, 114.2, 114.2, 124.85 (d, ²J_{C-P} = 5.9 Hz), 128.0 (d, ³J_{C-P} = 3.7 Hz), 128.5, 128.8, 129.1, 129.1 (d, ³J_{C-P} = 4.8 Hz), 134.1, 155.4 (d, ³J_{C-P} = 8.3 Hz). ³¹P-NMR (121.5 MHz, CDCl₃): δ_P ppm = 32.9. HRMS (ESI): calculated for C₂₄H₃₅NO₇P [(M+H)⁺], 480.2146; found 480.2150.

Diethyl (4-((benzyloxy)(methyl)amino)-1-(2-hydroxyphenyl)-4-oxobutyl)phosphonate (7.22). Compound **7.21** (660 mg, 1.38 mmol) and *p*-toluenesulfonic acid (PTSA) monohydrate (147 mg, 0.77 mmol) were dissolved in methanol (14 mL) and H₂O (1 mL) at room temperature.

After stirring the mixture overnight, TLC analysis revealed little progress in the deprotection. An additional amount of PTSA.H₂O (800 mg, 4.13 mmol) and 24 h more of reaction time at room temperature, eventually led to a completed reaction. The reaction mixture was quenched with sat. aq. NaHCO₃ (30 ml), and MeOH was evaporated. The organic layer was washed with brine, dried over Na₂SO₄, filtered and concentrated *in vacuo*. Silica gel chromatography (4% MeOH in CH₂Cl₂) of the residue gave **7.22** (523 mg, 87%). ¹H NMR (300 MHz, CDCl₃) δ_H ppm 1.11 (t, *J* = 6.9 Hz, 3H, -CH₂CH₃), 1.32 (t, *J* = 7.4 Hz, 3H, -CH₂CH₃), 2.11-2.49 (m, 4H, -CH₂-CH₂-CO), 3.15 (s, 3H, N-CH₃), 3.48 (dt, *J* = 7.6 Hz, 23.2 Hz, 1H, P-CH(Ar)-CH₂-), 3.74-4.21 (m, 4H, -CH₂CH₃), 4.54 (s, 2H, -CH₂Ph), 6.86 (t, *J* = 7.0 Hz, 1H, Ar-H), 6.96 (d, *J* = 8.1 Hz, 1H, Ar-H), 7.05-7.36 (m, 7H, Ar-H), 8.91 (s, 1H, Ar-OH). ¹³C-NMR (75 MHz, CDCl₃) δ_C ppm 16.1 (d, ³*J*_{C-P} = 6.0 Hz), 16.3 (d, ³*J*_{C-P} = 6.5 Hz), 22.1 (d, ²*J*_{C-P} = 6.5 Hz), 29.3 (d, ³*J*_{C-P} = 15.2 Hz), 36.6 (d, ¹*J*_{C-P} = 135.0 Hz), 62.9 (d, ²*J*_{C-P} = 7.0 Hz), 63.4 (d, ²*J*_{C-P} = 7.1 Hz), 76.2, 119.1, 120.7, 121.4, 128.6, 128.9, 129.0, 129.1, 129.3, 131.0 (d, ³*J*_{C-P} = 6.8 Hz), 134.0, 156.0 (d, ³*J*_{C-P} = 5.7 Hz), 174.26. ³¹P-NMR (121.5 MHz, CDCl₃): δ_P ppm = 31.3. HRMS (ESI): calculated for C₂₂H₃₁NO₆P [(M+H)⁺], 436.1884; found 436.1902.

Diethyl (4-(hydroxy(methyl)amino)-1-(2-hydroxyphenyl)-4-oxobutyl)phosphonate (7.23). The benzyl-protected hydroxamate **7.22** (500 mg, 1.15 mmol) was dissolved in MeOH (10 mL) and Pd/C (10% wt. on activated carbon, 100 mg) was added under inert atmosphere. The resulting mixture was then stirred under hydrogen atmosphere for 15 minutes and the progress monitored by mass spectrometry. At completion, the reaction mixture was filtered, concentrated *in vacuo*, and flash column chromatography (5% MeOH in CH₂Cl₂) afforded **7.23** (245 mg, 62%) as a golden brown oil. ¹H NMR (300 MHz, CDCl₃) δ_H ppm 1.12 (t, *J* = 7.3 Hz, 3H, -CH₂CH₃), 1.30 (t, *J* = 7.3 Hz, 3H, -CH₂CH₃), 2.03-2.47 (m, 4H, -CH₂-CH₂-CO), 3.14 (s, 3H, N-CH₃), 3.30 (quint. *J* = 1.8 Hz, 1H, -CH(Ar)-CH₂-), 3.74-4.17 (m, 4H, -CH₂CH₃), 6.78-6.87 (m, 2H, Ar-H), 7.09 (tt, *J* = 1.9 Hz, 7.5 Hz, 1H, Ar-H), 7.34 (dt, *J* = 1.9 Hz, 7.7 Hz, 1H, Ar-H). ¹³C-NMR (75 MHz, CDCl₃) δ_C ppm 16.2 (d, ³*J*_{C-P} = 5.7 Hz), 16.3 (d, ³*J*_{C-P} = 6.0 Hz), 23.6 (d, ¹*J*_{C-P} = 125.4 Hz), 28.1 (d, ³*J*_{C-P} = 16.6 Hz), 29.4 (d, ²*J*_{C-P} = 14.9 Hz), 36.0, 62.8 (d, ²*J*_{C-P} = 7.2 Hz), 63.0 (d, ²*J*_{C-P} = 7.3 Hz), 118.7, 120.6, 128.7, 129.2, 129.8 (d, ²*J*_{C-P} = 7.2 Hz), 155.3 (d, ³*J*_{C-P} = 8.8 Hz), 173.7. ³¹P-NMR (121.5 MHz, CDCl₃): δ_P ppm = 30.6. HRMS (ESI): calculated for C₁₅H₂₅NO₆P [(M+H)⁺], 346.1414; found 346.1493.

Ammonium 4-(hydroxy(methyl)amino)-1-(2-hydroxyphenyl)-4-oxobutyl)phosphonate (7.8). **7.23** (150 mg, 0.43 mmol) was dissolved in dry CH₂Cl₂ (4 mL) under inert atmosphere and cooled to 0 °C. TMSBr (0.6 mL, 4.3 mmol) was added dropwise while stirring after which, the ice bath was removed and the reaction was stirred at room temperature. After 24 hours another 0.4 mL of TMSBr was added and the reaction was further stirred for 24 h. All volatiles were then removed *in vacuo*, the crude material was dissolved in 5% aqueous ammonia and washed with diethyl ether. Lyophilization of the solution yielded the **7.8** as a brown solid in quantitative yield. ¹H NMR (300 MHz, D₂O) δ_H ppm 2.07-2.42 (m, 4H, -CH₂-CH₂-CO), 3.01-3.28 (s, 3H, N-CH₃), 3.12-3.30 (m, 1H, P-CH(Ar)-CH₂-), 6.85-7.00 (m, 2H, Ar-H), 7.13-7.27 (m, 2H, Ar-H), 8.40 (s, 1H, Ar-OH). ¹³C-NMR (75 MHz, D₂O) δ_C ppm 24.0, (d, ²J_{C-P} = 4.8 Hz), 30.3 (d, ³J_{C-P} = 16.9 Hz), 35.8, 45.1 (d, ¹J_{C-P} = 129.4 Hz), 117.0, 121.0, 125.2 (d, ²J_{C-P} = 9.1 Hz), 128.0, 130.5, 154.1 (d, ³J_{C-P} = 7.8 Hz), 175.2. ³¹P-NMR (121.5 MHz, D₂O): δ_P ppm = 22.0. HRMS (ESI): calculated for C₁₁H₁₅NO₆P [(M-H)⁻], 288.0642; found 288.0579.

N-(Benzyloxy)-3-(2-ethoxy-2-oxido-3H-benzo[d][1,2]oxaphosphol-3-yl)-N-methylpropanamide (7.14). In the presence of powdered activated 4 Å molecular sieves, a solution of **7.22** (800 mg, 1.84 mmol) in dry toluene (10 mL) was stirred under reflux for 36 hours. Solvent evaporation under vacuum afforded a residue which upon analysis by TLC and mass spectrometry, was found to contain traces of the target product (**7.14**) and a significant amount of a contaminant corresponding to hydrolysis of the five membered ring in **7.14**, together with unspent starting material. Attempts to purify this by column chromatography failed.

REFERENCES

1. Pertusati, F.; Serpi, M.; McGuigan, C. Medicinal chemistry of nucleoside phosphonate prodrugs for antiviral therapy. *Antivir. Chem. Chemother.* **2012**, *22*, 181–203.
2. Zídek, Z.; Kmoníčková, E.; Holý, A. Cytotoxicity of pivoxil esters of antiviral acyclic nucleoside phosphonates: adefovir dipivoxil versus adefovir. *Biomed Pap Med Fac Univ Palacky Olomouc Czech Repub.* **2005**, *149*, 2, 315–319.
3. Pradere, U.; Garnier-Amblard, E. C.; Coats, S. J.; Amblard, F.; Schinazi, R. F. Synthesis of nucleoside phosphate and phosphonate prodrugs. *Chem. Rev.* **2014**, *114*, 9154–9218.
4. Meier, C.; Görbig, U.; Müller, C.; Balzarini, J. cycloSal-PMEA and cycloAmb-PMEA: potentially new phosphonate prodrugs based on the cycloSal-pronucleotide approach. *J. Med. Chem.* **2005**, *48*, 25, 8079–8086.
5. Meier, C. CycloSal phosphates as chemical trojan horses for intracellular nucleotide and glycosylmonophosphate delivery - Chemistry meets Biology. *Eur. J. Org. Chem.* **2006**, *5*, 1081–1102.
6. Erion, M. D.; Reddy, K. R.; Boyer, S. H.; Matelich, M. C.; Gomez-Galeno, J.; Lemus, R. H.; Ugarkar, B. G.; Colby, T. J.; Schanzer, J.; Van Poelje, P. D. Design, synthesis and characterization of a series of cytochrome P450 3A-activated prodrugs (HepDirect prodrugs) useful for targeting phosph(on)ate-based drugs to the liver. *J. Am. Chem. Soc.* **2004**, *126*, 16, 5154–5163.
7. Andaloussi, M.; Henriksson, L. M.; Wieckowska, A. *et al.* Design, synthesis, and X-ray crystallographic studies of α -aryl substituted fosmidomycin analogues as inhibitors of *Mycobacterium tuberculosis* 1-deoxy-D-xylulose 5-phosphate reductoisomerase. *J. Med. Chem.* **2011**, *54*, 4964–4976.
8. Einhorn, C. and Luche, J. L. Selective allylation of carbonyl compounds in aqueous media. *J. Organomet. Chem.* **1987**, *322*, 177–183.
9. Eom, D.; Jeong, Y.; Kim, Y. R.; Lee, E.; Choi, W. Lee, P. H. Palladium-catalyzed C(sp^2 and sp^3)-H activation/C-O bond formation: synthesis of benzoxaphosphole 1- and 2-oxides. *Org. Lett.* **2013**, *15*, 20, 5210–5213.

10. Aksnes, G. and Bergesen, K. Rate studies of cyclic phosphinates, phosphonates and phosphates. *Acta Chem. Scand.* **1966**, 20, 9, 2508–2514.

Chapter VIII

BROADER INTERNATIONAL
CONTEXT, RELEVANCE AND
FUTURE PERSPECTIVES

VIII. BROADER INTERNATIONAL CONTEXT, RELEVANCE AND FUTURE PERSPECTIVES

VIII.A. Global socio-economic impact of malaria

With the end still out of sight, the World Health Organization's plan of having reduced the number of new malaria infections by 75% (from levels registered in 2000) and deaths to near zero by the end of 2015 has shown to be a monumental challenge. Since the year 2000, a tremendous expansion in the financing and coverage of malaria control programs has led to a wide-scale reduction in malaria incidence and mortality. Global data in 2015 show that 57 of 106 countries that had ongoing transmission in 2000 have reduced malaria incidence by >75%.¹ Malaria mortality decreased by 60% globally between 2000 and 2015 and malaria is no longer the leading cause of death among children in sub-Saharan Africa, the region most affected by the disease. The WHO trends (Figure VIII.1)² reveal wide ranging progress in averting malaria deaths: zero deaths, more than 75% reduction and less than 50% decrease in some regions although unfortunately, increased rates were observed in parts of Guyana and Venezuela.

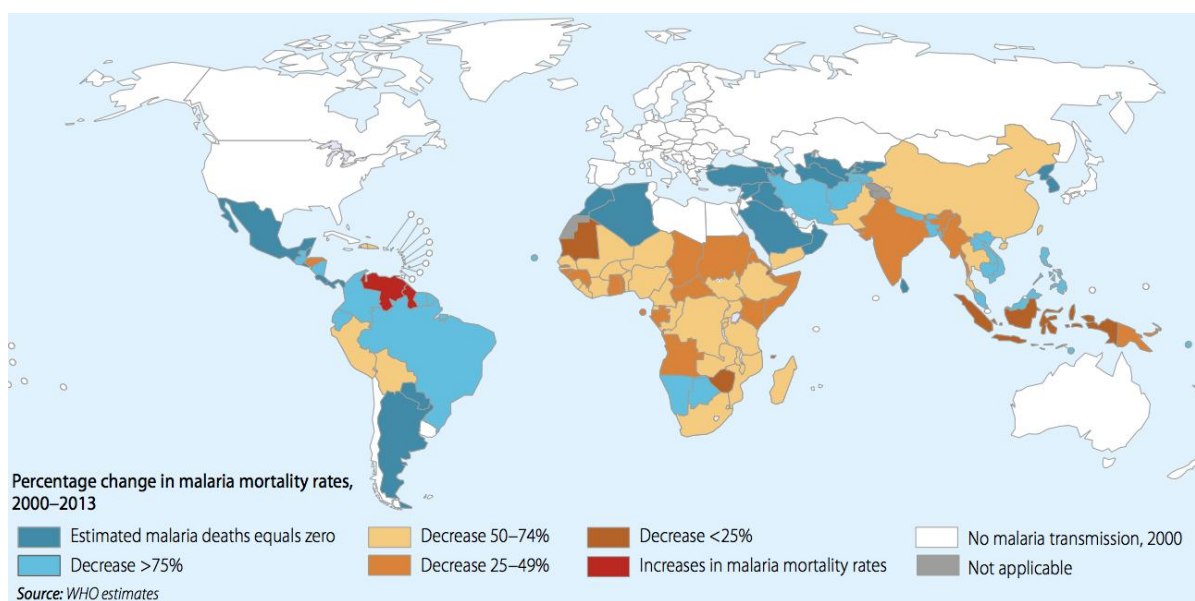


Figure VIII.1: Percentage change in malaria mortality rate between 2000 and 2013.²

Malaria received heightened attention in 1998 with the launching of the Roll Back Malaria Partnership and global financing for control of this disease increased from an estimated US\$ 960 million in 2005 to US\$ 2.5 billion in 2014.¹ The optimistic reports about a progressive decrease of malaria mortality and/or increase in antimalarial campaign financing should be put in perspective given the stubbornly high annual death toll due to malaria and the fact that it remains a major global health threat. In 2015 only, there were some 214 million malaria cases and about half a million deaths, an estimated 90% of these from Africa. Lapses in data collection and reporting suggest that these figures are underestimated. The emergence and spread of antimalarial drug resistance which is now established for commonly used antimalarials has substantial implications for malaria control and global public health.³ Not only does it lead to an increase in treatment failures and mortality, it also augments the risk of anaemia, low birth weight, increased transmission and malaria epidemics, repeated consultations at health facilities and the associated costs.

An effective malaria containment strategy will (besides vector control and improved diagnostics), hinge especially on a radical treatment of infected individuals, which would directly curb mortality, and offset transmission patterns. In this regard, deployment of new and safe drugs acting on unexplored targets is invaluable, to replace moribund antimalarial medicines.

VIII.B. The global burden of tuberculosis

Tuberculosis ranks amongst the world's most deadly communicable diseases and unlike malaria, is a major health problem not only for developing countries, but all regions of the world. Accordingly, the annual death toll from TB surpasses that due to malaria. Since declaration of a global emergency in 1993, the incidence rate was relatively stable up until around 2000. It then started falling by an average of 1.5% per year and is now 18% lower than the level of 2000. However, in 2014, an estimated 9.6 million people developed TB and 1.5 million died from the disease (1.1 million HIV-negative and 0.4 million HIV-positive), the majority in poor countries (Figure VIII.2).⁴ Most cases of tuberculosis are found in the Western Pacific regions, Africa and South East Asia. Poverty and tuberculosis are closely interwoven: malnutrition, crowded unhygienic quarters with poor air circulation and improper sanitation are poverty indicators that increase both the probability of becoming

infected and of developing clinical disease. Co-infection with the human immunodeficiency virus, which is highly prevalent in developing countries, leads to myriad consequences including increased susceptibility to TB, reactivation of latent TB and rapid TB progression to active disease.⁵ The global burden of tuberculosis amounts to approximately \$12 billion annually.⁶

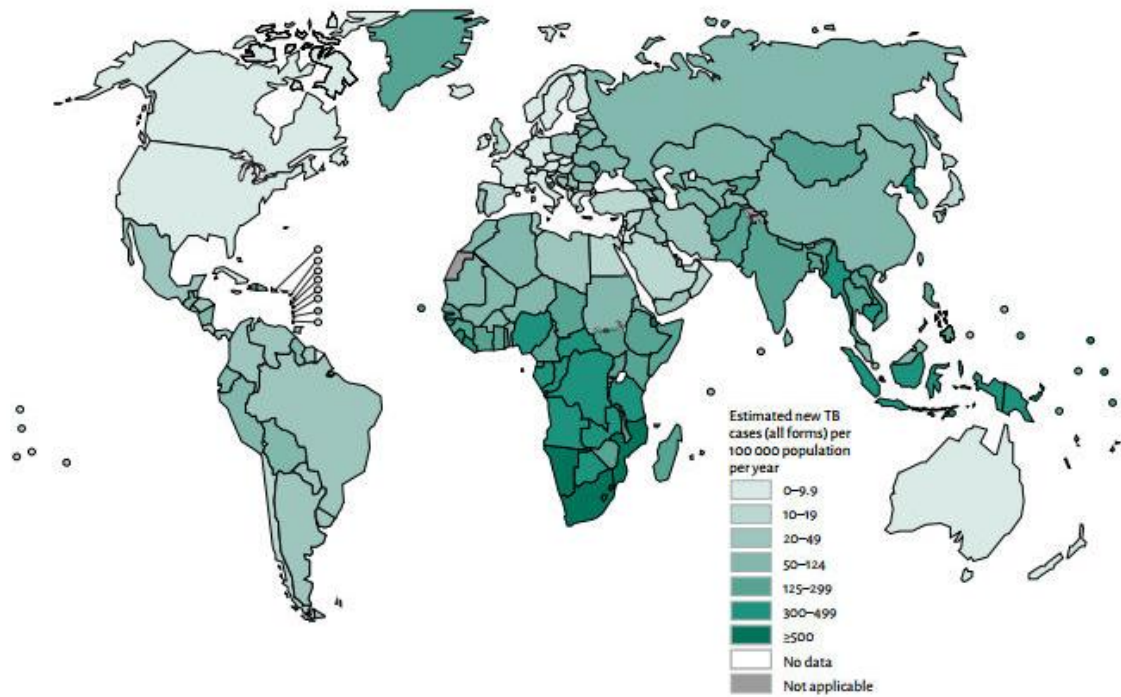


Figure VIII.2: Estimated tuberculosis incidence rates, 2014.⁴

Multidrug-resistance, which started in the early 1990s as an emerging torpedo to antituberculosis efforts, occurs when a *Mycobacterium tuberculosis* (Mtb, the causative agent of human tuberculosis) strain has become resistant to isoniazid (INH) and rifampicin (RIF), the two mainstays of first-line TB therapy.^{7,8} More TB patients were tested for drug resistance in 2014 than ever before: Worldwide, an estimated 480,000 cases of MDR-TB occurred, resulting in about 190,000 fatalities.⁴ These data heap pressure on the push for upgrading of the antituberculosis arsenal, including the development of novel chemical entities with unique modes of action that effectively neutralize all forms of TB infection.

VIII.C. The potential for Dxr inhibitors to contribute to the global antimalarial and/or antituberculosis armamentarium

Having presented an overview of the pathways for modern drug discovery and development (section I.C.), it is essential to bring the case of antimalarial and antituberculosis drug discovery into context, with a critical examination of the prospects in pursuing these goals through the NMP. Whether by the target-based or phenotypic-based high-throughput (HTS) screening approach, the *modus operandi*, which is generally characterized by well-delineated milestones that include selection of the drug target (for the target-based approach), identification of a lead compound, its optimization to a compound suitable for testing in animals, and advancement of candidate(s) to clinical trials, culminates in a new drug for the treatment of a human disease.

With a high quality lead (fosmidomycin) in hand, the work covered in this thesis focuses on structural modification of this compound, aimed at broadening its SAR and ameliorating its druglike character. From a synthetic medicinal chemistry vantage point, the Lipinski rule of five⁹ serves as a necessary but not exhaustive guideline for structural optimization towards molecules with improved drug-like properties, although some molecules that violate this rule have still trickled to the clinical level.¹⁰ Do the phosphonate group, the propyl spacer and the hydroxamate moiety of fosmidomycin, all of which offer diverse routes for multiple structural modifications, guarantee the successful development of a drug from this lead? Potential pitfalls including severe side effects, inability to create an acceptable dosage form (after obtaining a promising candidate) and the formation of reactive metabolites (e.g., from prodrugs) only intensify the downstream attrition debate.

VIII.C.1. Desired qualities for new antimalarial drugs

VIII.C.1.1. Advancing the concept of combination therapy

The current WHO guidelines for malaria treatment recommend that drugs should be deployed mainly as combination therapy, aiming at primarily preventing or slowing the onset and spread of resistance.¹¹ According to these guidelines, the three key criteria that members of a combination therapy should fulfill are: different modes of action, different biochemical targets and exhibition of independent blood schizonticidal activity. Although the

development of a fosmidomycin-clindamycin combination therapy recently stalled due to inadequate efficacy in clearing uncomplicated malaria in Mozambican children less than three years old,¹² fosmidomycin remains in the spotlight with new, ongoing combination therapy initiatives. Notably, a fosmidomycin-piperaquine combination therapy is currently under Phase II clinical investigation by Jomaa Pharma GmbH.¹³ Like the artemisinins, fosmidomycin is a fast-acting antimalarial. It operates by Dxr inhibition, has a remarkably good human safety record and is active against existing drug-resistant parasites. Piperaquine, which is believed to accumulate within the parasite food vacuole where it prevents haem detoxification, is a member of the 'quine' family of antimalarials, with a longer half life than fosmidomycin (2 to 3 weeks, against 1.6 hours for fosmidomycin).^{14,15,16} The rationale for combining these drugs is that besides their respective schizonticidal prowess, the difference in half life between the two is beneficial for mutual protection against parasite resistance and that piperaquine will additionally provide post-treatment prophylaxis. The above-mentioned WHO exigencies on the properties of combination therapy entities imply that multiple-drug therapies that include a nonantimalarial drug to enhance the antimalarial effect of a blood schizonticidal drug are not considered combination therapy. Thus, fosmidomycin-derived compounds stand a good chance to be used in combination therapies if the pharmacokinetic attributes of this lead are ameliorated such that as a single entity, the derived analogue(s) elicit(s) fast parasite clearance with high bioavailability, high human tolerance and a longer residence time.

Thomson Reuters Life Science Consulting demonstrated that two-thirds of the Phase III clinical trial failures across all therapeutic areas, initial indications and major new indications, between 2007 and 2010 were attributable to inadequate efficacy.¹⁷ They concluded from this analysis that large numbers of failures are occurring with drugs that have novel mechanisms of action. As a mitigation plan, they suggested a reliance on high-quality scientific evidence by fully testing mechanisms against each target indication, beginning at the earlier levels of the drug discovery process. This revelation highlights the fact that promising drug targets with a likelihood of clinical efficacy, as shown in predictive *in vitro* and *in vivo* models, are key for drug discovery success. In this regard, the success rates in feeding the antimalarial/antituberculosis pipeline with drugs acting on the NMP will not only depend on the synthetic medicinal chemistry effort in deriving analogues of promising lead

compounds, but much more on the quality of the drug target(s). All the enzymes involved in the NMP have been genetically validated as drug targets¹⁸ and the X-ray structure of each of the enzymes has been solved.^{19,20} Recently, a systematic druggability assessment of the NMP enzymes conducted by Hirsch and co-workers, revealed that all substrate- or cofactor-binding pockets are druggable.²¹ A 'druggable' target is a protein, peptide or nucleic acid with activity that can be modulated by a drug, which can consist of a small molecular weight chemical compound or a biologic such as an antibody or a recombinant protein.²² Of all the NMP enzymes, Dxr is the only one for which inhibitors with antimicrobial activity at pharmaceutically relevant concentrations are known²³ and it is also the most widely investigated of these potential drug targets.

VIII.C.1.2. Ease of administration; regimens that are appropriate for outpatient use

Another desirable quality for an antimalarial drug is the possibility for regimens that are appropriate for outpatient use. The most hard hit malaria endemic areas of the world are unfortunately also the poorest; with relatively few standard medical facilities, qualified medical personnel and the inability of patients (especially in rural areas), to afford expensive health care by hospitalization. This means that oral formulations, which most closely meet the needs of these communities, should be promoted in antimalarial drug discovery ventures. Since all the enzymes of the NMP are well characterized, target-based drug discovery is the favored approach to arrive at clinical candidates. However, the high polarity of NMP intermediates, which are all phosphorylated and the corresponding polar enzyme active sites make the structure-based design of drug-like inhibitors for these enzymes challenging. An immediate consequence of this liability is that fosmidomycin-derived inhibitors of Dxr are highly polar, with the likelihood of poor oral bioavailability and short plasma half-life. This shortcoming is responsible for the recrudescence malaria infections associated with fosmidomycin use, even though this compound is a specific and highly potent inhibitor of Dxr.

Even with the abundance of crystallographic information about Dxr from several organisms, its dramatic conformational change upon ligand binding also undermines the structure-based design of improved inhibitors. Given difficulties arriving at novel and potent entities via the target-based drug discovery approach, a switch to the phenotypic-based paradigm

may uncover novel inhibitors with significantly better pharmacokinetic data than that of the currently known compounds. Fosmidomycin was actually discovered by a phenotypic-based drug discovery effort,²⁴ and this approach is reportedly making a comeback in drug discovery, as some researchers have concluded that alternative strategies such as target-based screening are useful but may also limit the breadth of new findings.²⁵

VIII.C.1.3. Radical treatment and chemoprevention

A radical antimalarial campaign should involve not only the killing of the blood stage merozoites, but also inhibition of the liver stage (pre-erythrocytic) development and obstruction of the transmission stages (killing gametocytes and inactivating sporozoites), which would prevent re-infection or protect other humans.²⁶ The pipeline for the blood stage is arguably the best in history, and has indeed been recently expanded by several potent new chemotypes. However, the current challenge is to translate the potential of these chemotypes into an agent that addresses all the qualities of an ideal antimalarial drug, notably: address drug-resistance issues, have a rapid onset of action, be safe especially in children and pregnant women and cure malaria in a single dose. The potential for drugs that target the transmission stages to revolutionize malaria eradication efforts is enormous, but research efforts in this direction have been hampered by the absence of high-throughput screens.²⁷ Drug discovery endeavors directed towards the liver and transmission stages are still premature but slowly gaining traction. Fosmidomycin and related compounds act on the intra-erythrocytic parasites, and therefore cannot confer a full cure (especially for *P. vivax* infections), or serve as chemoprophylaxis. This shortcoming resonates with the WHO call for combination therapy as partner drugs may assure the destruction of the (fosmidomycin)-insensitive parasite forms.

Intermittent preventive treatment of malaria in pregnancy (IPTp), which entails a full therapeutic course of antimalarial medicine given to pregnant women at routine prenatal visits, regardless of whether the recipient is infected with malaria, reduces maternal malaria episodes, maternal and fetal anaemia, placental parasitaemia, intra-uterine growth retardation, preterm birth, low birth weight, and neonatal mortality. Given that pregnant women are at an increased risk for malaria infection and that great caution should be exercised when any drug is given during pregnancy, the lowest possible risk of clinical failure

and a satisfactory safety profile are sought after qualities for drugs used in IPTp. Unfortunately, most antimalarials have not been studied in pregnant women, restricting the options for treatment in this group of patients due to the unknown effects of these agents on the foetus.²⁸ Noteworthy is the fact that the pharmacokinetic profile of most antimalarial drugs is modified in pregnancy and dosages will need to be adapted. Currently, a sulfadoxine-pyrimethamine combination (Fansidar) is the standard of care for IPTp.²⁹ Data on the use of fosmidomycin for the treatment of malaria in pregnant women is scarce but some patents^{30,31} covering pharmaceutical preparations/compositions of fosmidomycin derivatives in combination with other antimalarial active ingredients, aim to widen the range or therapeutic application of these compounds, to include the treatment of 'problematic' groups such as children and pregnant women. The promising safety record^{14,32} of fosmidomycin, even in young children,³³ is an advantage to be exploited as derivatives with improved efficacy may find a place for use during gestation or for neonatal care.

Plasmodium species belong to the phylum apicomplexa: parasitic protists, which harbor a plastid-like organelle called apicoplast. The machinery within the apicoplast appears to serve two distinct but related functions, identified to be "self-sustenance" and the "sustenance of the parasite" as a whole. Ramya and collaborators demonstrated that although drugs which interfere with the processes of apicoplast replication, transcription, and translation lead to apicoplast loss, they do not kill the malaria parasite rapidly, as they permit other apicoplast biochemical processes essential to the survival of the parasite to proceed, thereby enabling it to survive a cycle of growth.³⁴ Thus, such drugs do not affect the doubling frequency of these parasites in the first host cell; however, division is slowed upon subsequent invasion of new host cells as the consequence of the generation of daughter cells devoid of an apicoplast, which fail to complete erythrocytic development. This phenomenon, termed 'the delayed death phenotype', is a severe limitation in malaria treatment since a single cycle of asexual reproduction in *Plasmodium falciparum* takes 48 h to complete and a delay of 48 h or more in treating malaria could have severe consequences for the patient. The essential biochemical processes taking place inside the apicoplast, which if obliterated, would lead to rapid parasite death include fatty acid synthesis, heme biosynthesis, and isoprenoid synthesis. Fosmidomycin is a known exception to the delayed death phenotype shown by most antibiotics (e.g., clindamycin) that are active against *Plasmodium* parasites.^{35,36}

VIII.C.2. Desired characteristics of new antituberculosis drugs

A new treatment for drug sensitive, active tuberculosis, should address the following preferences over existing regimens:

- Shorten treatment duration to preferably less than two months (potency greater than the most active first-line drug, isoniazid).
- A novel mechanism of action against Mtb.
- Possibility for oral dosing.
- A pharmacokinetic-pharmacodynamic profile that allows for a once-daily or less frequent dosing.
- Minimal or no interactions with hepatic cytochrome P450 enzymes, thereby reducing the likelihood of drug-drug interaction, especially with antiretroviral therapy.
- Financially affordable.

Currently available drugs for the treatment of drug-resistant TB forms are less effective (compared with drugs for first-line treatment), have more associated adverse side effects, and are significantly more expensive. Therefore, a new drug for this category might not be subjected to the same stringent criteria as for new first-line therapy, but will still generally fulfill the conditions stated above as an improvement on the current second-line TB drugs. The need to completely eliminate tuberculosis will mean that new TB drugs should be more effective for the treatment of latent TB infection.

The WHO treatment policy for tuberculosis is similar to that of malaria, with a call for the broad use of combination therapy.³⁷ The development of fosmidomycin derivatives as drugs for Mtb infection is still in its infancy but ongoing research conducted by the Dowd group and others on inhibition of the NMP as a potential treatment for tuberculosis indicate that there is a way forward.^{38,39} Fosmidomycin and associated compounds show minimal activity against intact Mtb cells even though some of these compounds effectively inhibit purified recombinant MtbDxr. The important challenges posed by the thick complex lipophilic cellular barrier shielding *Mycobacteria*, together with the lack of the essential glycerol-3-phosphate

transporter, which actively moves fosmidomycin across *Plasmodium species* membranes, need to be addressed in a systematic way, alongside reinforcement of interactions between MtbDxr and fosmidomycin derivatives. It has been shown that interference with the integrity of the thick mycobacterial cell wall improves the efficacy of fosmidomycin.⁴⁰ The headway made already with prodrugs, which yield rather promising activity in killing intact pathogen cells, is impetus for further exploration of this option as a way to offset the intracellular delivery obstacles associated with both the phosphonate group of fosmidomycin and the mycobacterial cell barrier.

VIII.D. Future perspectives

The future of fosmidomycin-based therapeutics has to take account of what is currently available or possible. Investigations into the intravenous administration of potent fosmidomycin-type compounds for the treatment of severe malaria, which is often characterized by frequent vomiting (that precludes oral drug dosing), should be promoted. As a long-term goal, the development of a synergistic drug combination targeting Dxr and any other downstream enzyme of the NMP will be an ideal implementation of combination therapy, which is the standard in both malaria and TB therapy. Good combination therapy partners will also include drugs that interfere with the integrity of the cell barrier in these pathogens thereby facilitating cellular access.

Substituting the polar phosphonate or the hydroxamate of fosmidomycin (which limit cellular entry) with less polar isosteres has widely proven deleterious to the activity of the derived analogues, leaving just the option of keeping these functionalities and dealing with the challenges they pose. Masking the phosphonate with prodrug moieties has on the other hand, shown to offer a promising leeway in going around the compound polarity issues. Recently, the Kurz group published⁴¹ a systematic comparison of phosphonate and phosphonate-hydroxamate double prodrugs of reverse fosmidomycin derivatives. According to the study, there was no outstanding advantage in blocking both functionalities with prodrug groups. This means that focusing on phosphonate-only prodrugs, may be a beneficial way forward while the challenges associated with the hydroxamate (so far the best metal complexing group in fosmidomycin-like compounds), may be addressed alternatively. The fact that hydroxamate prodrugs would have to be bioactivated by

esterase-like enzymes of the host or parasite cells, for which details are not known and that fosmidomycin derivatives with exclusive hydroxamate prodrug moieties have not been studied, reinforces this view.

Inspiration can be borrowed from established and currently marketed antiviral phosphonate prodrugs, for the design of more effective and clinically relevant fosmidomycin prodrug derivatives. Both an oral antimalarial and an oral antiviral drug must be capable of gastrointestinal absorption, but the pathway thereafter differs for the two drug types. In order to access the apicoplast and obstruct isoprenoid synthesis in an intra-erythrocytic parasite form, the antimalarial drug must (following gastrointestinal absorption) cross multiple cellular membrane barriers notably, the erythrocyte membrane, the parasitophorous vacuole membrane, the *Plasmodium* cell membrane, and the four membrane layers of the apicoplast (Figure VIII.3).⁴²

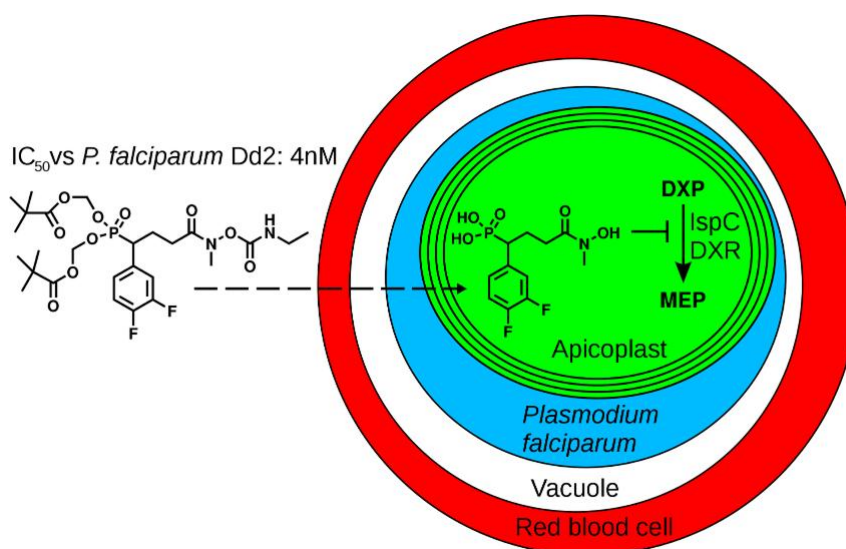


Figure VIII.3: Passage of a Dxr inhibitor across membrane barriers in *Plasmodium*-infected red blood cells.⁴¹

The antiviral drug on the other hand, needs permeation into the nuclear and/or cytoplasmic compartments of target cells, the site of viral replication and assembly. There is therefore more membranes to be crossed by the antimalarial than the antiviral drug, with the complication that partial or terminal prodrug hydrolysis could be proceeding in any or all of the following compartments: (i) the erythrocyte cytoplasm, (ii) the parasitophorous vacuole, (iii) the parasite cytoplasm, and/or (iv) inside the apicoplast. The Kurz report⁴¹ states that at

least a significant fraction of the prodrugs access the parasites without prior hydrolysis although it remains unknown whether hydrolysis then proceeds in the parasite cytoplasm and/or inside the apicoplast. This understanding clarifies the precaution that must be taken in importing prodrug knowledge from other therapeutic areas, or when designing prodrug moieties against different Dxr-dependent species such as falciparum and Mtb.

Deprez-Poulain and coworkers showed that substituents in the neighborhood of the hydroxamate, such as methylation of the α position to the electrophilic carbonyl increases plasma stability/half-life of this group.⁴³ In the context of fosmidomycin derivatives, this will mean introduction of hydroxamate-stabilizing substituents in the β -position to the phosphonate group (since a propyl spacer is the optimal linkage for the phosphonate and hydroxamate),³⁹ with an extra effort to identify substituents that will also reinforce interactions with Dxr active site residues. Alternatively, some effort can be dedicated to the investigation of hydroxamate prodrugs. Any breakthroughs in modification of the propyl linker and/or the hydroxamate function of fosmidomycin will amount to no real milestone progress in an *in vivo* context, if the drug delivery obstacles associated with the phosphonate are not properly addressed.

VIII.E. The broader malaria prevention outlook: Vector control

The work covered in this thesis focuses on antimalarial chemotherapy. However, an effective malaria eradication plan would also involve targeting the mosquitoes, which are responsible for transmitting the parasite from one individual to another. Clearing of marshes in residential neighborhoods deprive mosquitoes of their breeding sites, thereby limiting their numbers and the likelihood of coming in contact with and biting humans. Biological methods involving the use of natural enemies of targeted mosquitoes and of biological toxins, achieve effective vector management.⁴⁴ Such agents include larvivorous fish, invertebrate predators, bacteria and nematodes which are capable of thriving identifiable mosquito breeding places.

Since mosquitoes bite mostly during the night when people are at rest, sleeping under long-lasting insecticidal nets has been promoted as a way to significantly reduce the chances of being bitten by a mosquito. Currently, the WHO recommends that insecticidal nets contain pyrethroid insecticides only.⁴⁵ Such nets are designed for a minimum lifespan of 20 standard

washes or 3 years of usage under field conditions although their physical and chemical performance can vary greatly depending on the setting. The decline in malaria mortality in children under 5 years between 2000 and 2015 coincides with an increased use of this inexpensive protective means; the proportion of children of this age group sleeping under a net increased from under 2% in 2000 to an estimated 68% in 2015.

Indoor residual spraying, which involves spraying (on indoor walls and ceilings) an effective dose of insecticide with a long residual activity, typically once or twice per year, is also recommended by the WHO. In this regard, dichlorodiphenyltrichloroethane (which played an important role in malaria eradication efforts in Europe) continues to be used in limited situations alongside other modern synthetic and more durable analogues of natural pyrethrum.⁴⁶ The emerging challenge to this strategy however, is the development of resistance in all major vector species and to all classes of insecticides.

In a nutshell, an effective deployment of all vector control technologies, combined with a scale-up on the advances in antimalarial chemotherapy will deliver the knock-out blow necessary to attain the ambitious *Global Technical Strategy for Malaria 2016-2030* (reducing malaria case incidence by at least 90% and reducing malaria mortality rates by at least 90% of the current rate), formulated by the WHO.

REFERENCES

1. World Health Organization. WHO World Malaria Report **2015**; <http://www.who.int/malaria/publications/world-malaria-report-2015/wmr2015-without-profiles.pdf?ua=1> (accessed on December 16, 2015).
2. World Health Organization. WHO World Malaria Report **2014**; http://www.who.int/malaria/publications/world_malaria_report_2014/en/ (accessed on February 11, 2015).
3. Sachs, J. and Malaney, P. The economic and social burden of malaria. *Nature* **2002**, 415, 680–685.
4. World Health Organization. Global tuberculosis report **2015**; http://www.who.int/tb/publications/global_report/gtbr2015_executive_summary.pdf?ua=1 (accessed on December 18, 2015).
5. Shenoj, S.; Heysell, S.; Moll, A.; Friedland, G. Multidrug-resistant and extensively drug-resistant tuberculosis: consequences for the global HIV community. *Curr. Opin. Infect. Dis.* **2009**, 22, 1, 11–17.
6. World Health Organization. Tuberculosis control; http://www.who.int/trade/distance_learning/gpgh/gpgh3/en/index7.html (accessed on December 16, 2015).
7. Mitchison, D. A. Role of individual drugs in the chemotherapy of tuberculosis. *Int. J. Tuberc. Lung Dis.* **2000**, 4, 9, 796–806.
8. Sandhu, G. K. Tuberculosis: Current situation, challenges and overview of its control programs in India. *J. Glob. Infect. Dis.* **2011**, 3, 2, 143–150.
9. Lipinski C. A.; Lombardo, F.; Dominy, B. W.; Feeney, P. J. Experimental and computational approaches to estimate solubility and permeability in drug discovery and development settings. *Adv. Drug. Deliv. Rev.* **1997**, 23, 3–25.
10. Keserü, G. M. and Makara, G. M. The influence of lead discovery strategies on the properties of drug candidates. *Nat. Rev. Drug Discovery* **2009**, 8, 203–212.

11. World Health Organization. Antimalarial drug combination therapy; Report of a WHO technical consultation. Geneva, 4–5 April 2001; http://apps.who.int/iris/bitstream/10665/66952/1/WHO_CDS_RBM_2001.35.pdf.
12. Lanaspá, M.; Moraleda, C.; Machevo, S. *et al.* Inadequate efficacy of a new formulation of fosmidomycin-clindamycin combination in Mozambican children less than three years old with uncomplicated *Plasmodium falciparum* malaria. *Antimicrob. Agents Chemother.* **2012**, 56, 6, 2923–2928.
13. International Clinical Trials Registry Platform. World Health Organization. Evaluation of fosmidomycin and piperazine in the treatment of acute *falciparum* malaria (FOSPIP) <http://apps.who.int/trialsearch/Trial2.aspx?TrialID=NCT02198807>. (Last accessed February 28, 2016).
14. Kuemmerle, H. P.; Murakawa, T.; Sakamoto, H.; Sato, N.; Konishi, T.; De Santis, F. Fosmidomycin, a new phosphonic acid antibiotic. Part II: 1. Human pharmacokinetics. 2. Preliminary early phase IIa clinical studies. *Int. J. Clin. Pharmacol. Ther. Toxicol.* **1985**, 23, 521–528.
15. Kuemmerle, H. P.; Murakawa, T.; De Santis, F. Pharmacokinetic evaluation of fosmidomycin, a new phosphonic acid antibiotic. *Chemioterapia* **1987**, 6, 2, 113–119.
16. Hung, T. Y.; Davis, T. M. E.; Ilett, K. F.; Karunajeewa, H.; Hewitt, S.; Denis, M. B.; Lim, C.; Socheat, D. Population pharmacokinetics of piperazine in adults and children with uncomplicated *falciparum* or *vivax* malaria. *Br. J. Clin. Pharmacol.* **2003**, 57, 3, 253–262.
17. Arrowsmith, J. Trial watch: phase III and submission failures: 2007–2010. *Nat. Rev. Drug Discov.* **2011**, 10, 2, 87.
18. Hirsch, A. K. H.; Diederich, F. The non-mevalonate pathway to isoprenoids biosynthesis: A potential source of new drug targets. *Chimia* **2008**, 62, 4, 226–230.
19. Hale, I.; O'Neill, P. M.; Berry, N. G.; Odom, A.; Sharma, R. The MEP pathway and the development of inhibitors as potential anti-infective agents. *MedChemComm* **2012**, 3, 418–433.
20. Hunter, W. N. The non-mevalonate pathway of isoprenoid precursor biosynthesis. *J. Biol. Chem.* **2007**, 282, 21573–21577.
21. Masini, T.; Kroezen, B. S.; Hirsch, A. K. H. Druggability of the enzymes of the non mevalonate-pathway. *Drug Discov. Today* **2013**, 18, 23/24, 1256–1262.

22. Gashaw, I.; Ellinghaus, P.; Sommer, A.; Asadullah, K. What makes a good drug target? *Drug Disc. Today* **2012**, 17S, S24–S30.
23. De Ruyck, J.; Wouters, J.; Poulter, C. D. Inhibition studies on enzymes involved in isoprenoid biosynthesis: Focus on two potential drug targets: DXR and IDI-2 Enzymes. *Curr. Enzym. Inhib.* **2011**, 7, 2.
24. Neu, H. C.; Kamimura, T. In vitro and in vivo antibacterial activity of FR-31564, a phosphonic acid antimicrobial agent. *Antimicrob. Agents Chemother.* **1981**, 19, 6, 1013–1023.
25. Kotz, J. Phenotypic screening, take two. *SciBX* **2012**, 5, 15.
26. Wells, T. N. C.; Alonso, P. L.; Gutteridge, W. E. New medicines to improve control and contribute to the eradication of malaria. *Nat. Rev. Drug Discov.* **2009**, 8, 879–891.
27. Biamonte, M. A.; Wanner, J.; Le Roch, K. G. Recent advances in malaria drug discovery. *Bioorg. Med. Chem. Lett.* **2013**, 23, 2829–2843.
28. Nosten, F.; McGready, R.; d'Alessandro, U.; Bonell, A.; Verhoeff, F.; Menendez, C.; Mutabingwa, T.; Brabin, B. Antimalarial drugs in pregnancy: a review. *Curr. Drug Saf.* **2006**, 1, 1, 1–15.
29. World Health Organization. Updated WHO Policy Recommendation: Intermittent preventive treatment of malaria in pregnancy using sulfadoxine-pyrimethamine (IPTp-SP), October, **2012**; http://www.who.int/malaria/iptp_sp_updated_policy_recommendation_en_102012.pdf?ua=1.
30. Hutchinson, D.; Gutteridge, W. New drug combinations for the treatment of malaria. EP2590651 A1, May 15, 2013.
31. Hassan Jomaa, H.; Wiesner, J. Combination preparations of 3-n-formyl hydroxy amino propyl phosphonic acid derivatives or 3-n-acetyl hydroxy amino propyl phosphonic acid derivatives together with special pharmaceutical active ingredients. US20150190418 A1, 9 Jul 2015.
32. Kuemmerle, H. P.; Murakawa, T.; Soneoka, K.; Konishi, T. Fosmidomycin: a new phosphonic acid antibiotic. Part I: Phase I tolerance studies. *Int. J. Clin. Pharmacol. Ther. Toxicol.* **1985**, 23, 10, 515–20.

33. Borrmann, S.; Lundgren, I.; Oyakhirome, S. et al. Fosmidomycin plus clindamycin for treatment of pediatric patients aged 1 to 14 years with *Plasmodium falciparum* malaria. *Antimicrob. Agents Chemother.* **2006**, 50, 8, 2713–2718.
34. Ramya, T. N. C.; Mishra, S.; Karmodiya, K.; Surolia, N.; Surolia, A. Inhibitors of nonhousekeeping functions of the apicoplast defy delayed death in *Plasmodium falciparum*. *Antimicrob. Agents Chemother* **2007**, 51, 1, 307–316.
35. Dahl, E. L.; Rosenthal, P. J. Multiple antibiotics exert delayed effects against the *Plasmodium falciparum* apicoplast. *Antimicrob. Agents Chemother.* **2007**, 51, 10, 3485–3490.
36. Fernández-Álvaro, E.; Hong, W. D.; Nixon, G. L.; O'Neill, P. M.; Calderon, F. Antimalarial chemotherapy: natural product inspired development of pre-clinical and clinical candidates with diverse mechanisms of action. *J. Med. Chem.* **2016**, Article ASAP.
37. World Health Organization. Treatment of tuberculosis: guidelines – 4th ed. **2010**: http://apps.who.int/iris/bitstream/10665/44165/1/9789241547833_eng.pdf?ua=1&ua=1.
38. San Jose, G.; Jackson, E. R.; Uh, E.; Johnny, C.; Haymond, A.; Lundberg, L.; Pinkham, C.; Kehn-Hall, K.; Boshoff, H. I.; Couch, R. D.; Dowd C. S. Design of potential bisubstrate inhibitors against *Mycobacterium tuberculosis* (Mtb) 1-deoxy-D-xylulose 5-phosphate reductoisomerase (Dxr)-evidence of a novel binding mode. *Med. Chem. Commun.* **2013**, 4, 1099–1104.
39. Jackson, E. R.; San Jose, G.; Brothers, R. C.; Edelstein, E. K.; Sheldon, Z.; Haymond, A.; Johnny, C.; Boshoff, H. I.; Couch, R. D.; Dowd, C. S. The effect of chain length and unsaturation on Mtb Dxr inhibition and antitubercular killing activity of FR9000098 analogs. *Bioorg. Med. Chem. Lett.* **2014**, 24, 2, 649–653.
40. Sparr, C.; Purkayastha, N.; Kolesinska, B.; Gengenbacher, M.; Amulic, B.; Matuschewski, K.; Seebach, D.; Kamenaf, F. Improved efficacy of fosmidomycin against *Plasmodium* and *Mycobacterium* species by combination with the cell-penetrating peptide octaarginine. *Antimicrob. Agents Chemother.* **2013**, 57, 10, 4689–4698.
41. Brücher, K.; Gräwert, T.; Konzuch, S.; Held, J.; Lienau, C. Behrendt, C.; Illarionov, B.; Maes, L.; Bacher, A.; Wittlin, S.; Mordmüller, B.; Fischer, M.; Kurz, T. Prodrugs of reverse fosmidomycin analogues. *J. Med. Chem.* **2015**, 58, 2025–2035.
42. Botté, C. Y.; Dubar, F.; McFadden, G. I.; Maréchal, E.; Biot, C. *Plasmodium falciparum* apicoplast drugs: targets or off-targets? *Chem. Rev.* **2011**, 112, 1269–1283.

43. Flipo, M.; Charton, J.; Hocine, A.; Dassonneville, S.; Deprez, B.; Deprez-Poulain, R. Hydroxamates: relationships between structure and plasma stability. *J. Med. Chem.* **2009**, *52*, 6790–6802.
44. Walker, K. Environmental Health Project: A review of control methods for African malaria vectors. Activity Report 108, April **2002**.
45. World Health Organization. Core vector control methods; http://www.who.int/malaria/areas/vector_control/core_methods/en/ (accessed on May 26, 2016).
46. Curtis, C. F. and Townson, H. Malaria: Existing methods of vector control and molecular entomology. *Br. Med. Bull.* **1998**, *54*, 2, 311–325.

APPENDIX

CURRICULUM VITAE

PERSONAL

Surname and name: Chofofor René
Male/female: Male
Date of birth: January 8, 1979
Nationality: Cameroonian
E-mail: srrchofofor@yahoo.com

EDUCATION

Doctorate (2010 – present)

University/College of Higher Education: Ghent University, Belgium
Title: Synthesis and Evaluation of 1-Deoxy-D-xylulose 5-phosphate reductoisomerase inhibitors as Antimalarial and Antituberculosis Agents
Doctoral promoter: Prof. dr. Van Calenbergh S.
Degree: **Ph.D. in Pharmaceutical Sciences**

Subsequent Master's Degree (2008-2009)

University/College of Higher Education: Ghent University, Belgium
Date: June, 2009
Master's subject: Master of Applied Pharmaceutical Sciences
Thesis topic: Synthesis of α -Galactosylceramide Analogues with Amino Groups in the Phytosphingosine Chain
Promoter: Prof. dr. Van Calenbergh S.
Grade: Great distinction

Master's Degree (2006-2008)

University/College of Higher Education: Ghent University, Belgium
Date: June, 2008
Master's subject: Master of Science in Environmental Sanitation
Thesis topic: Behavior of Antibiotics in the Aqueous Environment: Sorption on Suspended Particulate Matter
Promoter: Prof. dr. Demeestere K.
Grade: Distinction

Bachelor's Degree (1998-2001)

University/College of Higher Education: Buea University, Cameroon
Date: September, 2001
Bachelor's degree: Bachelor of Science degree in Chemistry, and Chemical Process Technology
Grade: Honors

TEACHING EXPERIENCE

October 2010 – present

Function: - Supervisor of master thesis students

1) Veronica Micozzi (Synthesis of fosmidomycin analogues with altered chelating moieties, academic year 2013/14).

2) Laura Carlini (Synthesis of β -aryl analogues of fosmidomycin as antimalarials, academic year 2014/15).

- Tutor of practical course in organic synthesis for 3rd year Bachelor of Pharmaceutical Sciences

September 2002 – June 2006

Function: Secondary/high school chemistry teacher. Supervisor of chemistry laboratory sessions for the General Certificate of Education exam

Institution: Mervick Bilingual Grammar School, Yaoundé, Cameroon

LIST OF PUBLICATIONS

A1-articles

Chofor, R.; Sooriyaarachchi, S.; Risseeuw, M.D.P.; Bergfors T.; Pouyez, J.; Johnny, C.; Haymond, A.; Everaert, Dowd, C.S.; A.; Maes L.; Coenye, T.; Alex, A.; Couch, R.D.; Jones, T. A.; Wouters, J.; Mowbray, S. L.; Van Calenbergh, S. Synthesis and bioactivity of β -aryl-substituted fosmidomycin analogues targeting *Plasmodia* and *Mycobacteria*. *J. Med. Chem.*, **2015**, 58 (7), 2988–3001.

Chofor, R.; Risseeuw, M.D.P.; Pouyez, J.; Johnny, C.; Wouters, J.; Dowd, C.S.; Couch, R.D.; Van Calenbergh, S. Synthetic fosmidomycin analogues with altered chelating moieties do not inhibit 1-deoxy-D-xylulose 5-phosphate reductoisomerase or *Plasmodium falciparum* growth in vitro. *Molecules*, **2014**, 19, 2571–2587.

Trappeniers, M.; Chofor, R.; Aspeslagh, S.; Li, Y.; Linclau, B.; Zajonc, D. M.; Elewaut, D.; Van Calenbergh, S. Synthesis and evaluation of amino-modified α -GalCer analogues. *Org. Lett.*, **2010**, 12 (13), 2928–2931.

Chofor, R.; Sooriyaarachchi, S.; Risseeuw, M.D.P.; Matheussen, A.; Pouyez, J.; Wouters, J.; Maes L.; Dowd, C.S.; Couch, R.D. Mowbray, S. L.; Van Calenbergh, S. β -Phenpropyl derivatized analogues of FR900098 as inhibitors of 1-deoxy-D-xylulose 5-phosphate reductoisomerase. Manuscript submitted for review.

CONFERENCES AND PRESENTATIONS

Actively participated in several conferences and workshops including (but not limited) to the following:

Conference: Frontiers in Medicinal Chemistry
Date: September, 2015
Location: Antwerp, Belgium
Kind of contribution: Poster presentation
Title : Synthesis and Evaluation of β -substituted Fosmidomycin Analogues as Inhibitors of 1-deoxy-D-xylulose 5-phosphate Reductoisomerase

Conference: Chemistry Conference for Young Scientists (ChemCYS 2014)
Date: February, 2014
Location: Blankenberge, Belgium
Kind of contribution: Poster presentation
Title: Synthesis and Evaluation of Fosmidomycin Analogues with Altered Chelating Moieties as Inhibitors of 1-deoxy-D-xylulose 5-phosphate Reductoisomerase

Conference: European School of Medicinal Chemistry
Date: July, 2012
Location: Urbino, Italy
Kind of contribution: Oral presentation
Title: Synthesis of β -aryl Analogs of FR900098 as New Antimalarials

Conference: Chemistry Conference for Young Scientists (ChemCYS 2012)
Date: March, 2012
Location: Blankenberge, Belgium
Kind of contribution: Poster presentation
Title : Synthesis of β -aryl Analogues of FR900098 as Possible Antimalarials

Conference: Annual One-Day Meeting on Medicinal Chemistry of SRC & KVCV
Date: November, 2011
Location: Ghent, Belgium
Conference: 1st Glycolipid European Network Congress
Date: November 2010
Location: Reims, France
Kind of contribution: Poster presentation
Title: Synthesis of α -GalCer Analogues Characterized by a Truncated Sphingosine Backbone and Bearing a Terminal Phenyl ring

AWARD AND RESEARCH FELLOWSHIP

- Special Research Fund - Doctoral Scholarships for Candidates from Developing Countries, 2010-present
- Obtained the European School of Medicinal Chemistry (ESMEC) scholarship for foreign students attending PhD courses in European Universities, 2012.
- Received the Minister of Higher Education Awards for outstanding academic performance, Buea University, Cameroon, 1999/2000.

SKILLS AND PERSONAL INFORMATION

Language	Speaking	Understanding	Reading	Writing
English	1 st language	1 st language	1 st language	1 st language
French	Advanced	Advanced	Advanced	Advanced
Dutch	Basic	Basic	Basic	Basic

Personal competences: Conscientious, sociable, enthusiastic, eager to learn,
Excellent knowledge of all usual Microsoft office tools

Hobbies: Web surfing, making new friends and learning new cultures, music.

ACKNOWLEDGEMENT

The financial drive for accomplishment of this research work came from the Special Research Fund (BOF) of the University of Ghent, an offer for which I feel highly honored and will always remain thankful. A word of acknowledgement is now, more than ever before, insufficient to express the deep and sincere appreciation that I wish to render to a host of people who have engineered my way up to this achievement.

With much gratitude, I will forever remember the day I met my promoter Professor Serge Van Calenbergh, for discussions on conducting research in his group, within the framework of my master's degree thesis. That meeting marked the onset of an ambitious career in Medicinal Chemistry, which I will embrace throughout life. Professor Van Calenbergh, you offered me the opportunity to start in your group as a master's degree student and your unrelenting professional coaching and tenacious emphasis on quality over the years has yielded fruits; taking me beyond my initial goal in your lab, unto a PhD in Pharmaceutical Sciences. You have always been there for me, with the rich scientific mentoring, fast and highly critical correction of manuscripts and open doors for discussions on the way forward. Even when things seemed so tough, you taught me the art of transforming challenges into opportunities for a showcase of excellence. Your tact in keeping a healthy balance between the scientific and social spheres of the group definitely makes being your student, a unique experience. Besides your solid scientific knowledge, the extensive network of collaborations that you host, offers the opportunity to learn much within a short time with you.

I take this opportunity to appreciate the college of partners who have contributed in different ways to bring this thesis to a valuable closure. Thank you Professor Cynthia S. Dowd, Professor Robin D. Couch, Chinchu Johny and Amanda Haymond, for the fruitful collaboration on antituberculosis screening and brainstorming for the analogues pipeline. Professor Sherry L. Mowbray, Professor Thomas A. Jones, Sanjeevani Sooriyaarachchi, and Terese Bergfors, your data on *P. falciparum* Dxr inhibition together with the beautiful outcome of the X-ray crystallography studies has been quite invaluable. I salute your commitment Professor Johan Wouters and Jenny Pouyez and appreciate the wealth of data

from the *E. coli* works. Professor Tom Coenye and Annelien Everaert, you joined the effort with the important *M. smegmatis* inhibition tests thereby, broadening our portfolio of NMP-dependent pathogens under investigation and increasing our SAR knowledge on the robust *Mycobacterium species*. Professor Louis Maes and An Matheussen, I truly appreciate your unrelenting effort in ensuring that we get the crucial *P. falciparum* inhibition data. Alexander Alex, your predictions from the modeling studies pointed to the right direction.

And now to my (former) colleagues of the Laboratory for Medicinal Chemistry, you have been a tremendous asset. Our time together has been characterized by a cooperative and teamwork spirit, which is vital for proper operation of the intellectual machinery. Matthias, Thomas, Sarah, Nora, Martijn, Kiran, Joren, Jolien, Annelies, Shari, Dries, Lijun, Fabian, Mingcheng and Jonas, you are all great people to work with. If I would mention your names one after the other to give specific credits, several pages will not suffice, but you certainly do remember all the good times we spent together; the ideas we shared regarding our work, be it on a private basis or at group meetings, the social outings, 't Blauw Kotje, Frahan etc. Martijn, I will dare to mention that working next to you has led to a trove of ideas to foster my career in chemistry. Charlotte, I wish you the best as you continue to seek a solution for the malaria and tuberculosis community. Veronica, Laura and Francesca, I do acknowledge the contribution you brought as exchange students under my supervision. Annelies and Izet, besides your role in keeping a convivial working atmosphere, you have been very effective in supporting the group through your administrative and technical efforts.

Ok, it's getting long now, but I must appreciate all brethren and friends that have been by me throughout these years, in happy moments as well as in difficult times; I am highly indebted to you for your support. I rest this trophy before you my parents and family, as a display of the unwavering encouragement that you have given me throughout life.

Nadège, you and Gabriel have endured the brunt of the busy years. You have stood the test of time! Your love and support has seen me through. Sing for joy for we have finally made it; rejoice and remember that my deep endearment for you is evermore.

TO GOD BE THE GLORY

